

DATA ACQUISITION AND REDUCTION OF
HIGH RESOLUTION GAMMA-RAY SPECTRA

By

DAVID BALDWIN COTTRELL

A DISSERTATION PRESENTED TO THE GRADUATE COUNCIL OF
THE UNIVERSITY OF FLORIDA IN PARTIAL
FULFILLMENT OF THE REQUIREMENTS FOR THE DEGREE OF
DOCTOR OF PHILOSOPHY

UNIVERSITY OF FLORIDA
1973

TO MY WIFE
FOR HER PATIENCE
AND ENCOURAGEMENT

ACKNOWLEDGEMENTS

The author wishes to express his gratitude to the many people who contributed to the success of this project. First and foremost is his research director, Dr. Stuart P. Cram, whose continued guidance, encouragement, and enthusiastic support made this work possible. The author is also grateful to the other members of his committee, Dr. Roger G. Bates, Dr. James D. Winefordner, Dr. William H. Ellis, and Dr. Frank G. Martin, for their help and cooperation during the course of this study. Finally, the helpful discussions with fellow members of the research group are gratefully acknowledged.

Special thanks go to Jack E. Leitner for his unselfish cooperation and time during the early months of this work. His many helpful discussions concerning computer operation contributed greatly to the success of this project.

The design of the electronic components used in this work was contributed by Mr. Bob Dugan and his able staff in the electronics lab of the Chemistry Department.

The author wishes to acknowledge the financial support which he has received. This research was supported in part by NSF Research Grant No. GP-14754, and in part by a Traineeship from the National Science Foundation.

The author's deep appreciation goes to Mrs. Edna Roberts, his typist, for her expert work.

Finally, the author wishes to express his gratitude to his

parents, Mr. and Mrs. R. E. Cottrell, for their faith and encouragement, and to his wife, Liz, for her patience and understanding throughout the duration of this work.

TABLE OF CONTENTS

	Page
ACKNOWLEDGEMENTS	iii
LIST OF TABLES	vii
LIST OF FIGURES	viii
ABSTRACT	xiv
INTRODUCTION	1
Research Objectives	1
Historical Review	2
THEORETICAL	8
Data Smoothing	8
Peak Detection	9
Peak Quantitation	14
Curve Fitting	18
Method of Standard Addition	27
EXPERIMENTAL	30
Hardware	33
Interface	33
Timing System	36
Software	39
Data Acquisition	40
Data Printout	46
Display	46
Data Smoothing	53

	Page
Peak Detection	53
Preparation of FOCAL Compatible Data	69
RESULTS AND DISCUSSION	75
System Evaluation	75
Data Smoothing	88
Peak Detection	94
Curve Fitting	109
Peak Areas	194
Liver Analysis	198
APPENDICES.	227
APPENDIX I. CORE RESIDENT SOFTWARE	228
APPENDIX II. FOCAL PROGRAMS	287
1. Photopeak Fitting Routine	288
2. Baseline Fitting Routine	291
3. Calculation of the Total Fitted Curve	294
4. Numerical Integration by the Trapezoid Method	296
5. Linear Least Squares	298
BIBLIOGRAPHY	300
BIOGRAPHICAL SKETCH	305

LIST OF TABLES

TABLE		Page
I	EXPERIMENTAL CONDITIONS FOR THE SAMPLE SPECTRA	76
II	COMBINED RESULTS OF THE AUTOMATED PEAK SEARCHES	96
III	NUMBER OF PEAKS FOUND BY THE AUTOMATED PEAK SEARCHES	102
IV	PERCENT CHANGE IN THE RESIDUAL OF THE CURVE FITTING FUNCTION.	115
V	DESCRIPTION OF PEAKS SELECTED FOR CURVE FITTING	116
VI	INITIAL AND FINAL VALUES FROM THE CURVE FITTING CALCULATIONS	117
VII	INITIAL AND FINAL VALUES FROM THE CURVE FITTING CALCULATIONS	120
VIII	CURVE FITTING RESULTS	196
IX	CURVE FITTING RESULTS	197
X	CURVE FITTING RESULTS	199
XI	SIGNIFICANT PEAKS IN AN IRRADIATED LIVER SAMPLE	205
XII	EXPERIMENTAL CONDITIONS FOR THE LIVER ANALYSIS	207
XIII	RESULTS OF THE LIVER ANALYSIS	209
XIV	RESULTS OF THE LIVER ANALYSIS	210
XV	EXPERIMENTAL AND NATIONAL BUREAU OF STANDARDS RESULTS OF THE ANALYSIS OF STANDARD REFERENCE MATERIAL 1577 (BOVINE LIVER)	223

LIST OF FIGURES

Figure		Page
1.	Two possible peak shapes in a digital, gamma-ray spectrum	11
2.	Quantitative peak areas from three different methods	17
3.	Physical interpretations of the eight parameters in a photopeak fitting function	22
4.	Block diagram of the experimental system	31
5.	Interface between an analog to digital converter and a PDP-8/L computer	35
6.	Timing system for accurate and precise timing control of the data acquisition software. A push button switch is engaged from time T_A to T_B . The timing pulse is generated from T_{B+} to T_0 and corresponds in length to the time preset on the thumbwheel switch	37
7.	Flowchart of the data acquisition software	42
8.	Timing relations between the computer and analog to digital converter	43
9.	Flowchart of the data printout software	48
10.	Sample page from the computer printout of a stored spectrum	50
11.	Flowchart of the display software	52
12.	Flowchart of the data smoothing software	54
13.	Flowchart of the peak detection (method one) software	57
14.	Flowchart of the software which tests for peak validity and permanently stores valid peak locations and boundaries	59

Figure	Page
15. Flowchart of the peak detection (method two) software	63
16. Flowchart of the software which determines the first differences and prints the final results of the peak searches	66
17. Flowchart of the software which calculates the average height of the noise over 40 channels	68
18. Flowchart of the software which calculates and prints the peak areas by the total peak area and Wasson methods	71
19. Flowchart of the software which converts the integer data to floating point and stores the results in core locations accessible by the FOCAL subroutine FNEW	73
20. Plot of spectrum 6, attenuated by a factor of (x 8). The full energy range of the spectrum is 0-1.378 MeV (0.624 KeV/channel)	78
21. Plot of spectrum 6, unattenuated. The full energy range of the spectrum is 0-1.378 MeV (0.624 KeV/channel)	80
22. Plot of spectrum 6, attenuated by a factor of (x 1/2). The full energy range of the spectrum is 0-1.378 MeV (0.624 KeV/channel)	82
23. Plot of channel number vs. photopeak energy for the full energy range used in the research (data obtained from spectrum 6).	84
24. Plot of channel number vs. photopeak energy for the low energy region (data obtained from spectrum 10)	87
25. Plot of the resolution of the experimental system vs. photopeak energy for the full energy range used in the research (data obtained from all eleven sample spectra)	90
26. Effects of the statistical scatter on the total peak area, resulting in too large (peak A) or too small (peak B) a quantitative area	92

Figure	Page
27. Plot of spectrum 9, unattenuated. The full energy range of the spectrum is 0-965 KeV (0.471 KeV/channel)	99
28. Plot of spectrum 7, unattenuated. The full energy range of the spectrum is 0-557 KeV (0.165 KeV/channel)	101
29. Plot of spectrum 11, attenuated by a factor of (x 1/2). The full energy range of the spectrum is 477-955 KeV (0.253 KeV/channel)	105
30. Plot of spectrum 4, unattenuated. The full energy range of the spectrum is 0.1.378 MeV (0.624 KeV/channel)	108
31. Plot of the percent change in the residual sum of squares vs. the number of iterations performed in the curve fitting process	113
32. Raw data and fitted curve (offset) for the 1115.51 KeV Zn - 65 peak taken from spectrum 2	122
33. Raw data and fitted curve (offset) for the 884.5 KeV Ag - 110m peak taken from spectrum 1	124
34. Raw data and fitted curve (offset) for the 884.5 KeV Ag - 110m peak taken from spectrum 9	126
35. Raw data and fitted curve (offset) for the 937.3 KeV Ag - 110m peak taken from spectrum 1	128
36. Raw data and fitted curve (offset) for the 937.3 KeV Ag - 110m peak taken from spectrum 9	130
37. Raw data and fitted curve (offset) for the 884.5 KeV Ag-110m peak taken from spectrum 11	132
38. Raw data and fitted curve (offset) for the 320.08 KeV Cr - 51 peak taken from spectrum 7	134
39. Raw data and fitted curve (offset) for the 1099.27 KeV Fe - 59 peak taken from spectrum 3	137

Figure	Page
40. Raw data and fitted curve (offset) for the 937.3 KeV Ag - 110m peak taken from spectrum 4	139
41. Raw data and fitted curve (offset) for the 884.5 KeV Ag - 110m peak taken from spectrum 4	141
42. Raw data and fitted curve (offset) for the 121.13 KeV Se - 75 peak taken from spectrum 7	143
43. Raw data and fitted curve (offset) for the 511 KeV annihilation peak taken from spectrum 8	145
44. Raw data and fitted curve (offset) for the 817.9 KeV Ag - 110m peak taken from spectrum 1	147
45. Raw data and fitted curve (offset) for the 817.9 KeV Ag - 110m peak taken from spectrum 9	149
46. Raw data and fitted curve (offset) for the 446.2 KeV Ag - 110m peak taken from spectrum 1	151
47. Raw data and fitted curve (offset) for the 400.64 KeV Se - 75 peak taken from spectrum 10	153
48. Raw data and fitted curve (offset) for the 817.9 KeV Ag - 110m peak taken from spectrum 4	155
49. Raw data and fitted curve (offset) for the 446.2 KeV Ag - 110m peak taken from spectrum 10	157
50. Raw data and fitted curve (offset) for the 620.1 KeV Ag - 110m peak taken from spectrum 9	159
51. Raw data and fitted curve (offset) for the 96.73 KeV Se - 75 peak taken from spectrum 7	162
52. Raw data and fitted curve (offset) for the 96.73 KeV Se - 75 peak taken from spectrum 10	164

Figure	Page
53. Raw data and fitted curve (offset) for the 817.9 KeV Ag - 110m peak taken from spectrum 11	167
54. Raw data and fitted curve (offset) for the 620.1 KeV Ag - 110m peak taken from spectrum 11	169
55. Raw data and fitted curve (offset) for the 303.89 KeV Se - 75 peak taken from spectrum 7	171
56. Raw data and fitted curve (offset) for the 303.89 KeV Se - 75 peak taken from spectrum 10	173
57. Raw data and fitted curve (offset) for the 1173.2 KeV Co - 60 peak taken from spectrum 6	175
58. Raw data and fitted curve (offset) for the 1173.2 KeV Co - 60 peak taken from spectrum 5	177
59. Raw data and fitted curve (offset) for the 744.2 KeV Ag - 110m peak taken from spectrum 11	179
60. Raw data and fitted curve (offset) for the 657.6 KeV Ag - 110m peak taken from spectrum 6	181
61. Raw data and fitted curve (offset) for the 1173.2 KeV Co - 60 peak taken from spectrum 3	183
62. Raw data and fitted curve (offset) for the 1173.2 KeV Co - 60 peak taken from spectrum 3. The data was smoothed before the fit was obtained	185
63. Raw data and fitted curve (offset) for the 657.6 KeV Ag - 110m peak taken from spectrum 8. The data was smoothed before the fit was obtained.	188
64. Raw data and fitted curve (offset) for the 884.5 KeV Ag - 110m peak taken from spectrum 6. The data was smoothed before the fit was obtained.	190

Figure	Page
65. Raw data and fitted curve (offset) for the 677.5 and 686.8 KeV Ag - 110m peaks taken from spectrum 1	193
66. Plot of an irradiated liver spectrum, unattenuated. The full energy range of the spectrum is 2.383 MeV (1.164 KeV/channel)	202
67. Plot of an irradiated liver spectrum, attenuated by a factor of (x 0.208). The full energy range of the spectrum is 2.383 MeV (1.164 KeV/channel).	204
68. Plot of the total peak area (open circles) and Wasson area (closed circles) vs. the amount of standard added to the liver samples for the analysis of chlorine. The peak areas were obtained from the 1.643 MeV Cl - 38 peak . .	212
69. Plot of the total peak area (open circles) and Wasson area (closed circles) vs. the amount of standard added to the liver samples for the analysis of chlorine. The peak areas were obtained from the 2.168 MeV Cl - 38 peak . .	214
70. Plot of the total peak area (open circles) and Wasson area (closed circles) vs. the amount of standard added to the liver samples for the analysis of manganese. The peak areas were obtained from the 0.847 MeV Mn - 56 peak . .	216
71. Plot of the total peak area (open circles) and Wasson area (closed circles) vs. the amount of standard added to the liver samples for the analysis of manganese. The peak areas were obtained from the 1.811 MeV Mn - 56 peak	218
72. Plot of the total peak area (open circles) and Wasson area (closed circles) vs. the amount of standard added to the liver samples for the analysis of potassium. The peak areas were obtained from the 1.525 MeV K - 42 peak	220
73. Plot of the total peak area (open circles) and Wasson area (closed circles) vs. the amount of standard added to the liver samples for the analysis of sodium. The peak areas were obtained from the 1.368 MeV Na - 24 peak	222

Abstract of Dissertation Presented to the Graduate Council
of the University of Florida in Partial Fulfillment of the
Requirements for the Degree of Doctor of Philosophy

DATA ACQUISITION AND REDUCTION OF
HIGH RESOLUTION GAMMA-RAY SPECTRA

By

David Baldwin Cottrell

March, 1973

Chairman: Dr. Stuart P. Cram
Major Department: Chemistry

A versatile, mini-computer based laboratory system was developed for the collection and reduction of high resolution gamma-ray spectra. A dedicated mini-computer served as both a control and memory for the data acquisition, and a central processing unit for the automated data reduction.

An interface and timing system were designed and constructed to allow computer control of the data acquisition. A complete software package was written to perform all aspects of the data acquisition and reduction. The application of the total analytical system to the analysis of a complex biological material was studied.

A new peak detection algorithm, sensitive to small signal-to-noise peaks, was developed to automatically search the digital data and determine the locations and boundaries of photopeaks in a gamma-ray spectra. A technique was devised to perform curve fitting by the method of nonlinear least squares on a mini-computer. A new function, which defines the shape of a photopeak in a Ge(Li) spectrum, was developed and tested. Photopeak areas calculated from the fitted functions were compared to the peak areas determined by conventional methods directly from the digital data.

INTRODUCTION

The principles of activation analysis, which have been reviewed by Lynn (1), were first introduced by Hevesy and Levi (2,3) in 1936 and Seaborg and Livingood (4) in 1938. Little was done with this technique, however, until the dawn of the nuclear age, following World War II, brought about an increasing availability of nuclear reactors. Since then the development of sophisticated radiation detectors and additional sources of nuclear particles has contributed to the remarkable growth of this technique. The sensitivity and accuracy of activation analysis have made it an extremely useful method of trace element determination in almost every scientific field.

Neutron activation analysis has proven to be an extremely sensitive analytical technique for most elements in a diversity of matrices, from distilled water to biological tissues. The development of high resolution, lithium-drifted germanium detectors has made possible the instrumental analysis of complex samples by gamma-ray spectrometry. The digital computer has proven essential to the rapid, accurate reduction of the large volume of data required by this technique.

Research Objectives

This research was directed toward the development of a versatile, mini-computer based laboratory system for the collection and reduction of high resolution gamma-ray spectra. A real time system for collecting

data under the control of a dedicated mini-computer was developed to maintain the high resolution of the detector and the integrity of the pulse-height. New concepts in direct data reduction by the laboratory computer were developed and compared to existing methods, with special emphasis placed upon small signal-to-noise peaks in the pulse-height spectrum from Ge(Li) detectors. The application of such a system to the analysis of biological materials was examined.

Historical Review

Early researchers in neutron activation analysis could measure only total activity and were forced to use some form of chemical separation to isolate the radioactive element of interest. Development of the early pulse-height discriminators and the sodium iodide scintillation detector, however, contributed to the increasing popularity of instrumental activation analysis by gamma-ray spectrometry. Connally and Leboeuf (5) were among the first to demonstrate the value of this new analytical technique. Morrison and Cosgrove (6,7) demonstrated the usefulness of gamma-ray spectrometry in the determination of trace impurities in a bulk component, and several researchers proved the practicality of totally instrumental neutron activation analysis (8-10). With the development of the Ge(Li) detector (11), high resolution gamma-ray spectrometry is today the accepted method of data collection in neutron activation analysis.

By the early sixties many scientists realized that the method of data reduction was equally as important as that of data collection. The volume of data required in gamma-ray spectrometry was more than could be handled by manual reduction. Covell (12) attempted to solve this problem

by developing a new, simplified method of data reduction. His new technique used only the data from a fixed number of channels immediately to the left and right of the peak center. Most laboratories, however, realized that a better solution was to take advantage of the computational power and speed of the digital computer.

Guinn and Lasch (13) noted that comparison of photopeak areas with those in standard spectra was still the easiest and most practical quantitative approach. Computer routines were written to obtain this information by fitting a mathematical function to the experimental data (14, 15), or by simply analyzing the raw digital data (16-18). Often, however, the limited resolution of the NaI(Tl) scintillation detector failed to produce resolved photopeaks. Heath (19) discussed the value of the computer for the analysis of these complicated spectra.

Lee (20) reported on the instrumental technique of complement subtraction. The theory of spectrum stripping was quickly expanded and computerized (13,21-23). Standard spectra of pure elements were collected and stored in the computer memory. Sequential subtraction of the spectra corresponding to the highest energy photopeak was then performed until only the background remained.

This method was often unsuccessful for low energy peaks uncovered after several subtractions. A more complex approach, based on the theory of least squares, sought to overcome this problem (9,24-28). An assumption was made that contributions from the various elements in any channel were independent and additive. By the method of least squares, standard spectra were combined until the best fit to the entire experimental spectrum was obtained. Another approach, based on the same

assumptions, attempted to solve a set of simultaneous linear equations using data from only selected channels of the standard and experimental spectra (29-32).

Other special methods were reported (33,34), but the above were by far the most commonly used methods for the analysis of complex scintillation gamma-ray spectra. Because of resolution problems, most of these computerized techniques required some form of qualitative input before accurate quantitative calculations could be performed.

The development of the high resolution, semiconductor Ge(Li) detector (35) caused a rapid change in the field of activation analysis. The superior resolution required bigger and better pulse-height analyzers and resulted in a tremendous increase in the volume of digital data to be reduced. It also produced a distinctly different form of gamma-ray spectra, with photopeaks more numerous but now resolved and available for direct quantitation. Prussin and co-workers (36,37) quickly demonstrated the value of this new detector for instrumental analysis of complex mixtures. The fully resolved photopeaks easily furnished both qualitative and quantitative information.

The increased resolution also increased the problem of statistical scatter of the digital data. Several methods were proposed to smooth the spectra, to remove the undesired scatter without destroying the analytical information lying underneath (38-40). A least squares technique particularly suited for computer adaptation was reported by Savitsky and Golay (41). Yule (16,42) successfully applied this technique to gamma-ray spectra and determined that the number of points in the smoothing should be as large as possible without exceeding the full width at half maximum of the photopeaks. Tominaga and co-workers (43) studied the

effects of smoothing on peak area determinations and reported that smoothing was often unnecessary for curve fitting methods but beneficial for other quantitative techniques. Yule (44) showed that one smoothing by the Savitsky and Golay method did not distort the analytical information contained in the spectra, as long as the correct smoothing interval was used.

Several methods were developed for automatically locating peaks in a Ge(Li) gamma-ray spectrum. Connelly and Black (45,46) described the technique of cross-correlation for both peak detection and area determination. Dooley and co-workers (47) looked for significant count increases in adjacent channel groups to indicate the presence of a peak. Gunnink and Niday (48) examined the changes in slope between data points. Ralston and Wilcox (49) developed a special method for defining the baseline from which to begin and end peak integration.

An automated peak detection method particularly suitable for efficient software execution involved the numerical approximation of the derivatives of the digital spectrum. Morrey (50) described in detail the utilization of the second, third, and fourth derivatives to locate peaks. Yule (16,51) applied the convolution technique of Savitsky and Golay (41) to obtain the smoothed derivatives in one rapid, efficient, computational operation. He demonstrated the use of both the first derivative alone (51), and of higher derivatives (52), to locate peaks. Barnes (53) reported a slightly different form of calculating the smoothed derivatives, but obtained essentially the same results as the Savitsky and Golay method.

Several authors (54-56) chose to use the second differences, similar to the second derivatives, to locate peaks. Mills (54) pointed out that the smoothed spectra gave better estimates of the initial parameters for peak fitting. Subtraction of adjacent data points then gave a good approximation of the smoothed derivative.

Once the photopeaks were located, some measure of their area was necessary to obtain quantitative information about the contributing element. The area could be calculated either directly from the digital data or from the integration of an analytical function which was fitted to the peak.

Several methods were developed to obtain quantitative information directly from the digital data. The most commonly used technique was the total peak area (TPA) method, successfully employed by several workers (33,38,51,57). This method assumed a linear baseline beneath the peak and subtracted a trapezoid background correction from the summed total area to obtain the quantitative area.

The previously mentioned method of Covell (12) was also utilized (43). In this method a linear baseline was again assumed, but only the data from a fixed number of channels immediately to the left and right of the peak center were used in the area computation. Sterlinski (58,59) modified Covell's method to give increasingly greater weight to those channels nearer to the peak center.

Quittner (60,61) proposed a method for estimating the actual baseline contribution to the total peak area. He first fitted a second or third degree polynomial to several channels on either side of the peak. He then constructed a baseline beneath the peak in such a way that, at the peak boundaries, it had the same magnitudes and slopes as the fitted polynomials.

Baedecker (62) described a modification of the TPA method suggested by Wasson in a private communication. This technique combined the principles of the TPA and Covell methods in that it constructed the same baseline as the TPA method but only used data from a fixed number of

channels immediately surrounding the peak center. The author then examined the precision obtainable by the methods described above.

Baedecker's experiments showed that the more complex methods did not provide a significantly greater precision than the simple ones. He therefore recommended the Wasson technique, except for cases where there were large deadtime differences between samples or where changes in resolution created a problem. For these latter cases he recommended the TPA method.

More complex approaches to photopeak quantitation, such as curve fitting, were also reported. The least squares technique for fitting a function to a set of data points, discussed by Roberts, Wilkinson, and Walker (63), was the usual method of choice, although Ciampi and co-workers (34) used a maximum probability technique.

Early authors (55,64,65) used a pure Gaussian fitting function to approximate the photopeak shape in Ge(Li) spectra. However it soon became clear that this function did not give a satisfactory fit to the peak shape. Routti and Prussin (56) discussed the physical properties of a Ge(Li) detector system which gave rise to the basic photopeak shape and noted that there was often severe tailing of the basic Gaussian on the low energy side. Additional tailing was also observed under conditions of high counting rates.

Many functional forms were suggested to account for the tailing of the main Gaussian shape. Sanders and Holm (66) pointed out that the only criterion for the selection of the analytical fitting function was an adequate representation of the data points. They, among others (56, 67,68), used a functional form which combined a Gaussian with an exponential contribution for tailing. Kern (69) and Pratt and Luther (70)

suggested methods of skewing the Gaussian with a polynomial. Robinson (71) combined two offset Gaussians and an arctangent to represent the photopeak shape. The background slope was usually represented by either a polynomial or an exponential.

On-line computer control of data acquisition was reported by a few workers (72-76). DerMateosian (77) described an experimental system which interfaced a laboratory computer to a pulse-height analyzer. He then described the advantages of direct data reduction by the small computer. Norbeck and Mancusi (78) described the more common approach, which involved the transfer of the digital data to a large computer for reduction.

Neutron activation analysis has been used for the analysis of biological materials since shortly after its introduction to the scientific world. Much of this work involved the chemical separation and isolation of the desired element (79,80) or the removal of large interferences, such as sodium (81). Recently, however, instrumental analysis, using Ge(Li) detectors, was used for the multielement analysis of biological materials (82). Linekin and co-workers (83), however, indicated that the majority of this research used data reduction techniques developed by researchers in other fields. Therefore, it is the purpose of this research to demonstrate the applicability of the dedicated laboratory computer to both the acquisition and reduction of gamma-ray spectra of complex biological samples.

THEORETICAL

Modern activation analysis experiments usually involve the acquisition of large amounts of digital data. The computer can therefore relieve the analyst of many hours of tedious, time-consuming data reduction. Correctly programmed the computer can quickly search the data, locate valid peaks, and determine their energies and peak areas.

Data reduction is easily done on a large computer, where the programs may be complex, lengthy, and written in a conversational language such as FORTRAN, without significantly increasing the computation time. On a mini-computer, however, the data reduction methods should be programmed in assembly language and decoded into machine language to conserve core space and keep the turn around time compatible with laboratory operation.

Data Smoothing

Due to the statistical nature of the spectra obtained in gamma-ray spectrometry, it is often desirable to smooth the digital data before attempting automated data reduction. This is done to remove much of the random noise without unduely degrading the underlying analytical information.

The smoothing technique used in this research was described by Savitsky and Golay (41). This method uses a data convolution process to obtain the least squares fit of a polynomial function to the center point of a block of raw data. The convoluting integers are the same for either

a cubic or a quadratic function.

With the correct set of convoluting integers and normalization factor the smoothed data value is calculated from

$$Y_j^* = \left(\sum_{i=-m}^{i=+m} C_i Y_{j+i} \right) / N \quad (1)$$

where

- Y_j^* = smoothed data value, in counts
- i = running index for the data block
- m = (number of points in the block - 1)/2
- C_i = convoluting integer for the i th point
in the block
- Y_{j+i} = raw data for the i th point in the block,
in counts
- j = index for the channel number
- N = normalization factor, a scaler

Yule (42,44) has shown that a single smoothing does not degrade the analytical information if the number of points in the smoothing interval does not exceed the average peak width at half maximum. It will be shown in a later section, however, that the smoothed data produce more accurate results from the automated data reduction routines.

Peak Detection

Figure 1 illustrates the two possible peak shapes found in digital spectra. The first has a positive first derivative from the left boundary minimum to the peak maximum, and a negative first derivative from the maximum to the right boundary minimum. The second peak, however,

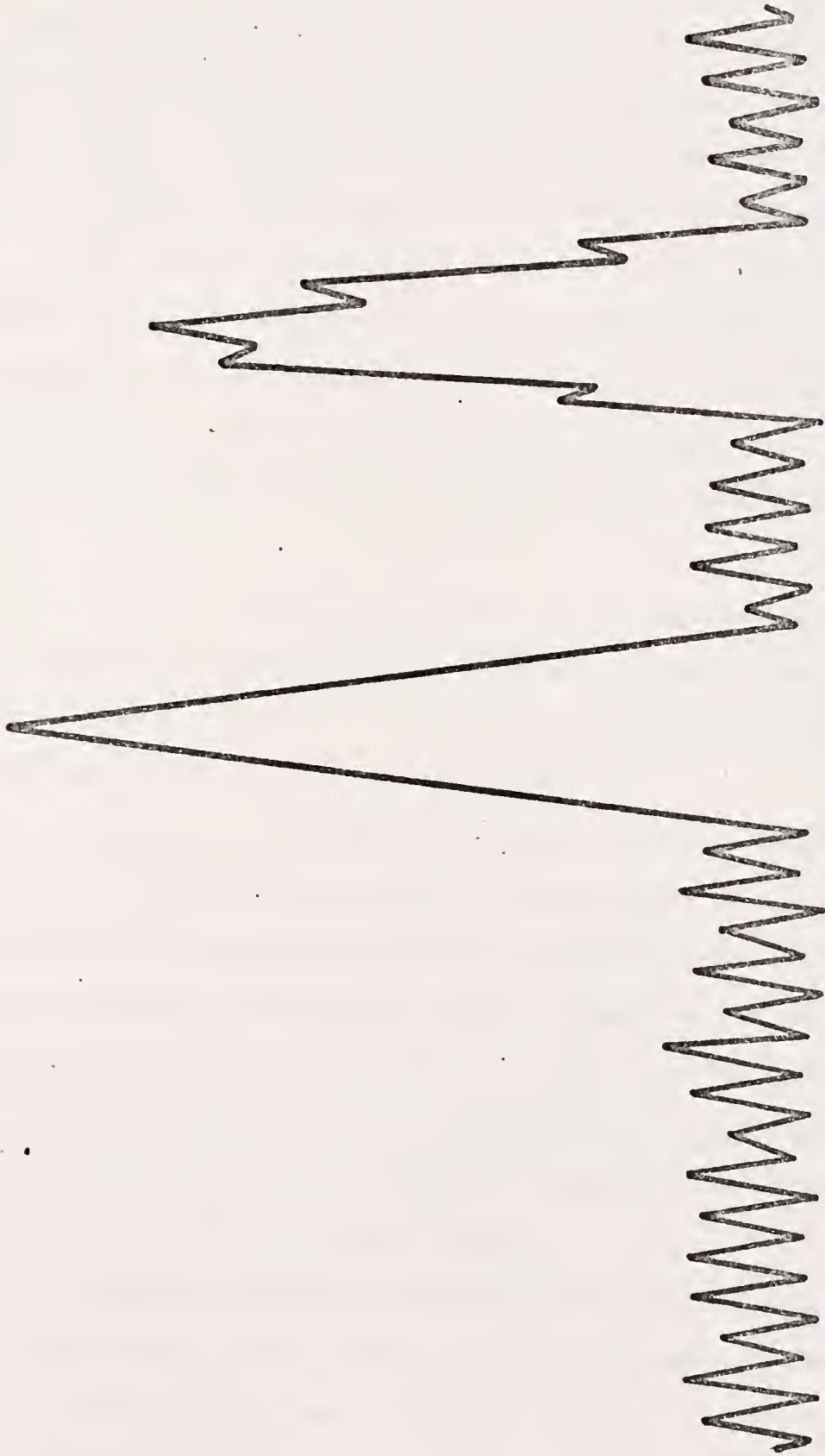


Figure 1. Two possible peak shapes in a digital, gamma-ray spectrum

has several minima superimposed on the basic peak shape. This problem is common in spectra which cover a narrow energy range, resulting in a greater number of channels within the peak boundaries. It is also common to peaks with small peak-to-noise ratios. The first derivative will change signs several times within the true peak boundaries.

In order to limit the size and complexity of the peak detection software, and still locate both types of valid peak shapes, two detection routines are used. Together they occupy less than 12% of the available 4K of core and require only two to eight minutes to search a 2048 channel spectrum and print all qualitative and quantitative information.

Both of the peak detection routines use the sign change of the first derivative to locate minima and maxima. However, since neither routine requires the absolute value of the derivative, the sign changes may be determined from the first differences.

The first routine searches for a minimum to maximum height which is greater than a multiple (usually one) of the baseline noise. The noise is determined by averaging the minimum to maximum heights over the forty channels immediately preceding the height in question. If two peaks are separated by less than forty channels, as illustrated by Figure 1, the same value of the noise is used to test both peaks. Each time a satisfactory height is detected, the integral channel location of the minimum is stored as a possible left peak boundary.

The right peak boundary is determined by the channel location of the next minimum whose height, relative to the left boundary minimum, is less than the average noise value. As shown by Figure 1, one or more maxima

may be detected within the boundary minima. The peak maximum is determined by the channel location of the highest maxima.

Valid peaks must exceed a minimum width, which is determined by the resolution of the system. The peak height, relative to both boundaries, must also exceed a minimum peak-to-noise ratio, which may be assigned a value as low as two. If any of these requirements are not satisfied, the region defined by the boundary channels is assumed to be a noise spike.

The second peak detection routine assumes that all valid peaks have only one maximum, located at the channel where the sign of the first derivative changes from positive to negative. The left and right boundaries are then located at the first minimum to either side of the peak maximum.

Valid peaks must also have a minimum number of channels between each boundary minimum and the peak maximum. This number is determined from the resolution of the system and may be as small as two. The peak height, relative to both boundaries, must also exceed the minimum peak-to-noise ratio.

The two peak detection routines are complementary to each other. While both methods will locate the first peak in Figure 1, method two is faster and less sensitive to changes in the slope of the baseline. Only method one will detect the second peak in Figure 1, but, as will be shown in a later section, this method of detection may select erroneous boundary channels. A complete search of the spectrum by both routines is therefore necessary to insure a complete and accurate analysis.

Peak Quantitation

Once the peak boundaries are determined, a quantitative measure of the peak area, and thus of the activity of the decaying isotope, is calculated. Several techniques have been suggested for obtaining this area directly from the digital data. Two of these, the total peak area (TPA) method and a modification of this, devised by Wasson and cited by Baedeker (62), are used in this research.

The total peak area method yields the largest value for the peak area within the selected boundaries. The area is calculated from

$$A_{\text{TPA}} = \sum_{i=L}^{i=R} C_i - (C_L + C_R)(R - L + 1)/2 \quad (2)$$

where

- A_{TPA} = total peak area, in counts
- C_i = number of counts in channel i , $L \leq i \leq R$
- L = channel number of the left boundary
- R = channel number of the right boundary

An alternative method, devised by Covell (12), uses only a portion of this total peak area. The usable area is calculated from

$$A_C = \sum_{i=M-N}^{i=M+N} C_i - (N + 1/2)(C_{M+N} + C_{M-N}) \quad (3)$$

where

- A_C = Covell's peak area in counts
 M = the channel number of the peak maximum
 N = the number of channels included to the
left and right of the peak maximum

The Wasson modification is a combination of the above two methods. The usable Wasson area is calculated from

$$A_W = \sum_{i=M-N}^{i=M+N} C_i - (N + \frac{1}{2})(B_{M+N} + B_{M-N}) \quad (4)$$

where

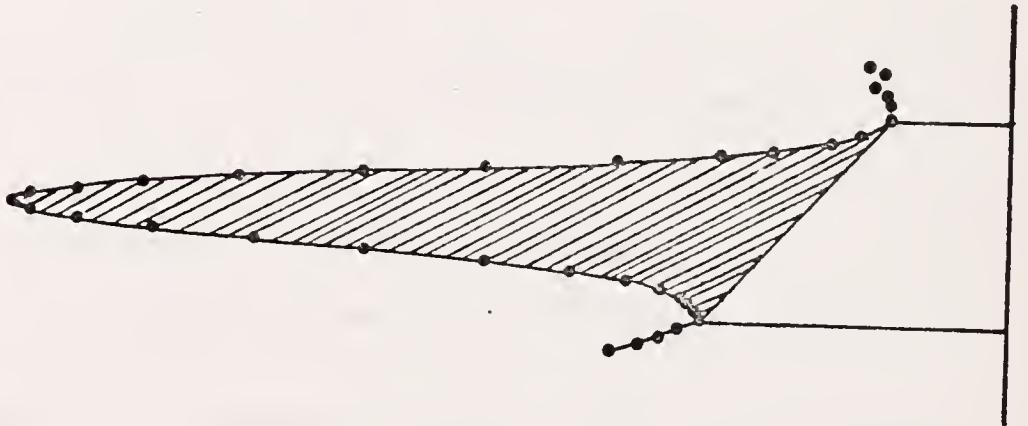
- A_W = Wasson's peak area in counts
 B_j = the background in channel j determined from
a straight line between channels L and R

These three methods are graphically illustrated in Figure 2.

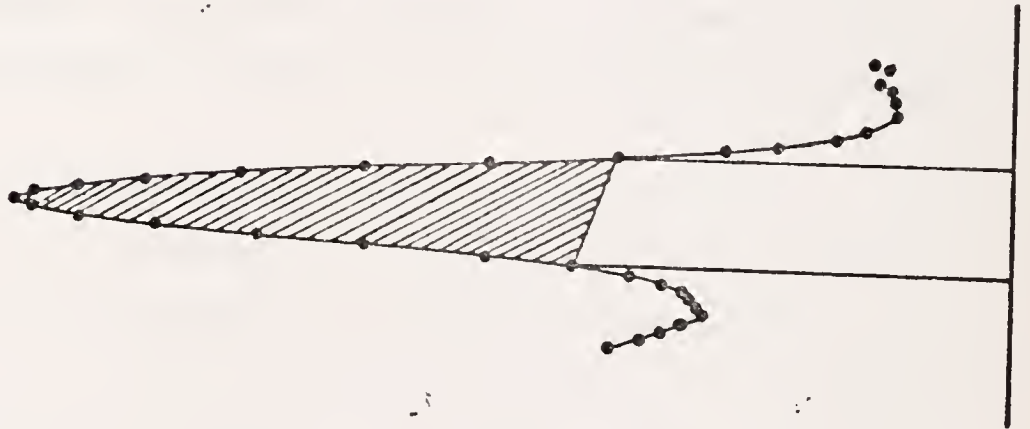
Baedecker (62) has shown that the Wasson area yields a more precise measure of the peak area. The total peak area includes contributions from the extremities of the peak, where the statistical fluctuations are greater. The Covell method excludes these regions but yields a much smaller absolute area than the Wasson method. This research includes both the TPA and the Wasson methods in an attempt to obtain the best results in all cases.

Figure 2. Quantitative peak areas from three different methods

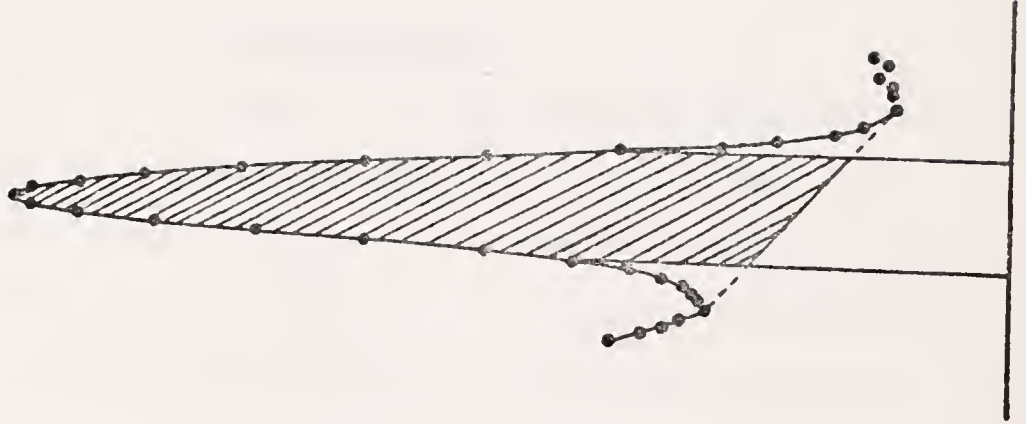
TOTAL
PEAK AREA



COVELL



WASSON



Curve Fitting

The method of curve fitting is used to obtain an estimate of the total peak area not obtainable directly from the digital data. The final functional parameter estimates can be used to calculate the area beneath the fitted curve by integration. This method is independent of peak boundaries and yields an excellent estimate of the true area of the peak.

The method of least squares, which has been successfully applied to chromatographic data by Roberts, Wilkinson, and Walker (63) and Chesler and Cram (84), is used to fit a suitable function to the digital data. If

X_i = the independent variable, $i = 1, 2, \dots, N$

Y_i = the experimentally observed data, $i = 1, 2, \dots, N$

P_j = the parameters in the theoretical function F_i ,
 $j = 1, 2, \dots, m$

P_j^k = the estimated value of P_j for the k th iteration

ΔP_j^k = the correction to the estimate P_j^k

W_i = a weighting factor, a scaler, $i = 1, 2, \dots, N$

$F_i = F(P_1, P_2, \dots, P_m, X_i)$ = the theoretical function
 evaluated at point X_i

N = the number of experimental data points

m = the number of parameters in the function

then the nonlinear least squares technique is an iterative process that fits the function F to a set of N data points.

The residual sum of squares

$$S = \sum_{i=1}^N W_i (F_i - Y_i)^2 \quad (5)$$

is minimized through the choice of values of the m parameters.

This leads to equation (6), a set of m equations in the m unknowns $\Delta P_1^k, \Delta P_2^k, \dots, \Delta P_m^k$. For the k th iteration the function F_i is given by F_i^k and new estimates of the parameters are calculated from

$$P_j^{k+1} = P_j^k + \Delta P_j^k, \quad j = 1, 2, \dots, m \quad (7)$$

The process converges when

$$\lim_{k \rightarrow \infty} P_j^k \rightarrow P_j, \quad j = 1, 2, \dots, m \quad (8)$$

In this research all values of W_i are set equal to one.

The full energy peak in a Ge(Li) spectrum may be estimated by a basic Gaussian shape which has a low energy tail. The width of the Gaussian is determined by both the electronic noise of the system and by statistical processes connected with energy absorption in the detector. The tail on the leading edge of the Gaussian is caused by the incomplete charge collection of hole-electron pairs, due to recombination and trapping. Several researchers, including Routti and Prussin (56), Varnell and Trischuk (67), and Head (68), have shown that the basic peak shape may be accurately approximated by a Gaussian function which has been joined to some form of leading exponential edge.

The fitting function used in this research is a modification of the empirical function successfully used by Chesler and Cram (84) to

$$\left[\begin{array}{c}
 \sum_{i=1}^N W_i \left(\frac{\partial F_i}{\partial P_1} \right), \sum_{i=1}^N W_i \left(\frac{\partial F_i}{\partial P_2} \right), \dots, \sum_{i=1}^N W_i \left(\frac{\partial F_i}{\partial P_m} \right) \\
 \sum_{i=1}^N W_i \left(\frac{\partial F_i}{\partial P_1} \right), \sum_{i=1}^N W_i \left(\frac{\partial F_i}{\partial P_2} \right), \dots, \sum_{i=1}^N W_i \left(\frac{\partial F_i}{\partial P_m} \right) \\
 \cdot \\
 \cdot \\
 \cdot \\
 \sum_{i=1}^N W_i \left(\frac{\partial F_i}{\partial P_1} \right), \sum_{i=1}^N W_i \left(\frac{\partial F_i}{\partial P_2} \right), \dots, \sum_{i=1}^N W_i \left(\frac{\partial F_i}{\partial P_m} \right)
 \end{array} \right]$$

$$\left(\begin{array}{c}
 \Delta P_1 \\
 \Delta P_2 \\
 \cdot \\
 \cdot \\
 \cdot \\
 \Delta P_m
 \end{array} \right) = \left(\begin{array}{c}
 \sum_{i=1}^N W_i (Y_i - F_i) \frac{\partial F_i}{\partial P_1} \\
 \sum_{i=1}^N W_i (Y_i - F_i) \frac{\partial F_i}{\partial P_2} \\
 \cdot \\
 \cdot \\
 \cdot \\
 \sum_{i=1}^N W_i (Y_i - F_i) \frac{\partial F_i}{\partial P_m}
 \end{array} \right)$$

(6)

fit chromatographic peaks. It is composed of a leading exponential edge, a hyperbolic tangent joining function, and a central Gaussian. The functional form is

$$F_i = P_1 \left(\exp\left[\frac{-(X_i - P_4)^2}{2P_5}\right] + 0.5 [1 - \text{Tanh}[P_2(X_i - P_3)]] \right) \times$$

$$\times [P_6 \exp(-P_7[\{(P_8 - X_i)^2\}^{1/2} + \{P_8 - X_i\}])] \quad (9)$$

where

- P_1 = the height of the Gaussian, in counts
- P_2 = the rate of change of the joining function
- P_3 = the center of change of the joining function,
in sigma units
- P_4 = the center of the Gaussian, in sigma units
- P_5 = σ^2 of the Gaussian
- P_6 = the initial height of the exponential, in counts
- P_7 = the rate of decrease of the exponential
- P_8 = the position of the start of the exponential, in
sigma units
- X_i = the independent variable, in sigma units

The physical interpretations of these parameters are graphically illustrated in Figure 3.

Several constraints should be placed on the parameter estimates to aid in the correct convergence of the fitting process. These constraints are suggested by the physical interpretation of the empirical fitting function. The heights of both the Gaussian and the exponential tail should always remain positive. The change of the joining function and the

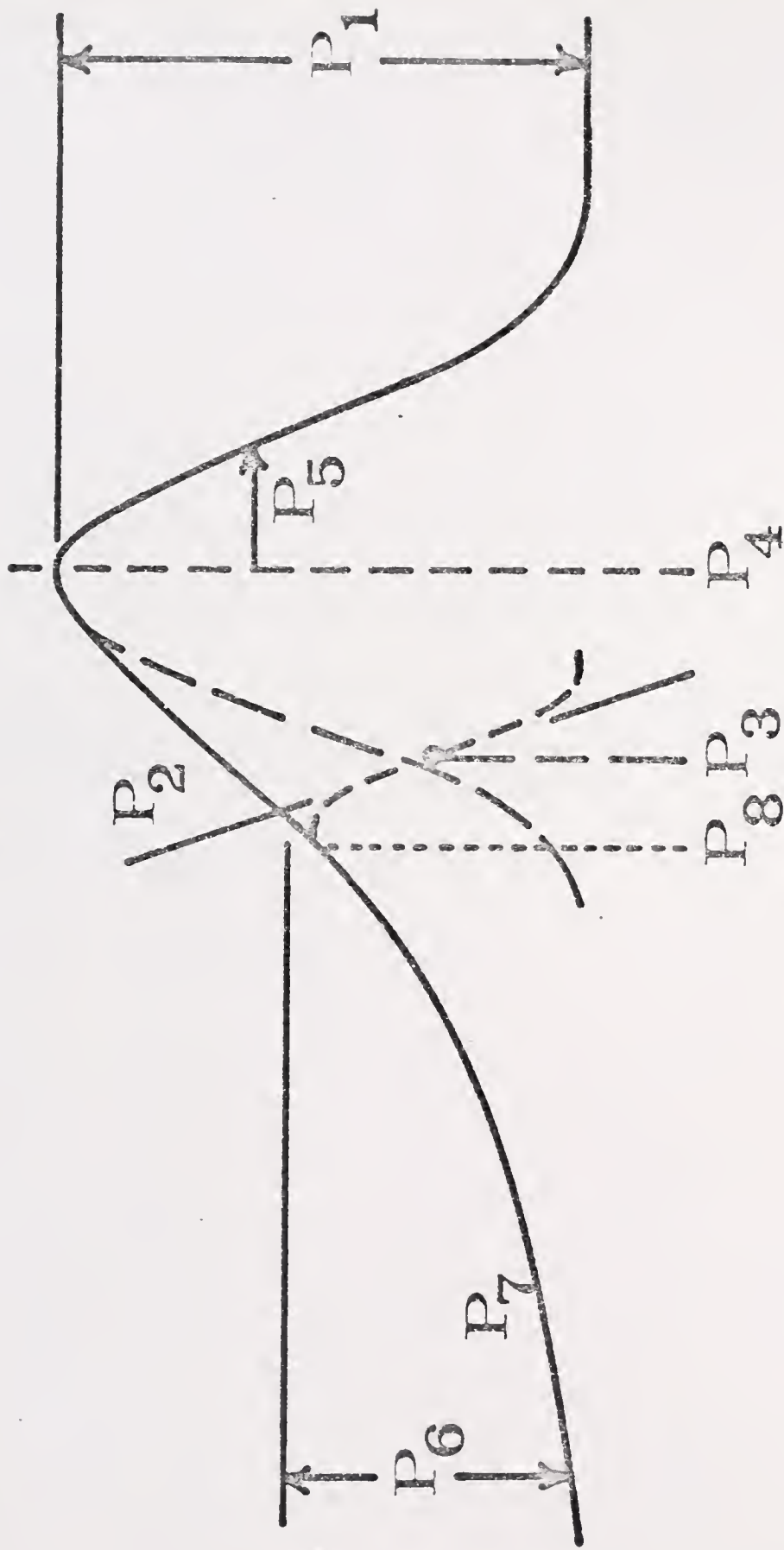


Figure 3. Physical interpretations of the eight parameters in a photopeak fitting function

exponential should proceed in only one direction. The value of σ^2 should always be positive. The positions of the joining function and the start of the exponential should always be to the left of the peak maximum. Therefore the signs of P_1^k , P_2^k , P_5^k , P_6^k , and P_7^k should always be positive, while those of P_3^k and P_8^k should remain negative. Only the sign of P_4^k should be allowed to vary.

The signs of the parameter estimates are checked following the solutions of equation (7) but before the beginning of the next iteration. If any sign is found to be incorrect the value of the parameter estimate is changed to one-half of the last accepted value.

To simplify the partial derivatives let

$$A_i = \exp\left[\frac{-(X_i - P_4)^2}{2P_5}\right] \quad (10)$$

$$B_i = 0.5 \{1 - \text{Tanh}[P_2(X_i - P_3)]\} \quad (11)$$

$$C_i = P_6 \exp(-P_7 \{ (P_8 - X_i)^2 \}^{1/2} + \{P_8 - X_i\}) \quad (12)$$

and therefore

$$F_i = P_1 (A_i + B_i C_i) \quad (13)$$

The partial derivatives may then be calculated from

$$\frac{\partial F_i}{\partial P_1} = A_i + B_i C_i \quad (14)$$

$$\frac{\partial F_i}{\partial P_2} = P_1 C_i \left(\frac{\partial B_i}{\partial P_2} \right) \quad (15)$$

$$\frac{\partial F_i}{\partial P_3} = P_1 C_i \left(\frac{\partial B_i}{\partial P_3} \right) \quad (16)$$

$$\frac{\partial F_i}{\partial P_4} = P_1 \left(\frac{\partial A_i}{\partial P_4} \right) \quad (17)$$

$$\frac{\partial F_i}{\partial P_5} = P_1 \left(\frac{\partial A_i}{\partial P_5} \right) \quad (18)$$

$$\frac{\partial F_i}{\partial P_6} = P_1 B_i \left(\frac{\partial C_i}{\partial P_6} \right) \quad (19)$$

$$\frac{\partial F_i}{\partial P_7} = P_1 B_i \left(\frac{\partial C_i}{\partial P_7} \right) \quad (20)$$

$$\frac{\partial F_i}{\partial P_8} = P_1 B_i \left(\frac{\partial C_i}{\partial P_8} \right) \quad (21)$$

where

$$\frac{\partial A_i}{\partial P_4} = \frac{-(P_4 - X_i) A_i}{P_5} = \frac{(X_i - P_4) A_i}{P_5} \quad (22)$$

$$\frac{\partial A_i}{\partial P_5} = \frac{(X_i - P_4)^2 A_i}{2P_5^2} \quad (23)$$

$$\frac{\partial B_i}{\partial P_2} = \frac{-2(X_i - P_3)}{\{\exp[P_2(X_i - P_3)] + \exp[-P_2(X_i - P_3)]\}^2} \quad (24)$$

$$\frac{\partial B_i}{\partial P_3} = \frac{2P_2}{\{\exp[P_2(X_i - P_3)] + \exp[-P_2(X_i - P_3)]\}^2} \quad (25)$$

$$\frac{\partial C_i}{\partial P_6} = \frac{C_i}{P_6} \quad (26)$$

$$\frac{\partial C_i}{\partial P_7} = -C_i \{ [(P_8 - X_i)^2]^{1/2} + (P_8 - X_i) \} \quad (27)$$

$$\frac{\partial C_i}{\partial P_8} = C_i P_7 \left\{ \frac{(P_8 - X_i)}{[(P_8 - X_i)^2]^{1/2}} + 1 \right\} \quad (28)$$

The baseline on either side of the peak is approximated by the polynomial

$$D_i = P_9 + P_{10} X_i + P_{11} X_i^2 + P_{12} X_i^3 \quad (29)$$

where X_i is expressed in channel units. The same nonlinear least squares process is used to fit this four parameter function. The partial derivatives are calculated from

$$\frac{\partial D_i}{\partial P_9} = 1 \quad (30)$$

$$\frac{\partial D_i}{\partial P_{10}} = X_i \quad (31)$$

$$\frac{\partial D_i}{\partial P_{11}} = x_i^2 \quad (32)$$

$$\frac{\partial D_i}{\partial P_{12}} = x_i^3 \quad (33)$$

The total fitting function which approximates the combined peak and baseline shape is therefore

$$T_i = F_i + D_i, \quad i = 1, 2, \dots, N \quad (34)$$

The solution of this total function, however, requires the filling of a twelve by twelve matrix, and the solving of twelve equations in twelve unknowns. The computation time for each iteration can be greatly reduced by fitting the polynomial baseline separately. Equation (29) is then evaluated for all points and subtracted from the experimental data. The resulting corrected data are then fitted with the eight parameter function F_i .

The success of the curve fitting process depends greatly on the accuracy of the initial parameter estimates. The digital data are often used to obtain these estimates. The initial value of P_9^1 is determined from the value of the baseline at the left peak boundary. The initial values of P_{10}^1 , P_{11}^1 , and P_{12}^1 are set to zero. The values of the eight peak parameters may be estimated from the corrected digital data, following the baseline subtraction. The estimate of P_1^1 is obtained directly from the corrected data. The values of P_2^1 , P_3^1 , P_4^1 , P_5^1 , and P_8^1 are usually estimated by 3.0, -1.5, 0, 1.0, and -1.5 respectively. The initial estimates of P_6^1 and P_7^1 depend upon the actual shape of the leading edge of the peak, but are usually between zero and one.

To obtain the X_i values in the fitting interval, expressed in sigma units, the right side of the peak is assumed to be pure Gaussian. The number of abscissa points from the peak maximum to the right boundary is therefore assumed to be equal to three sigma units. From this assumption the values of the increment and the initial abscissa point in the fitting interval are determined. It will be shown later that the peak function can be successfully fitted to as few as ten data points.

Method of Standard Addition

In the method of standard addition quantitative peak areas are determined for samples to which known amounts of standard have been added. This gives

$$A_i = k(W_i + S_i) \quad (35)$$

where

A_i = peak area for sample i , in counts

k = a constant

W_i = the amount of element in sample i , in grams

S_i = the amount of element added to sample i , in micrograms

and

$$A_p = k(W_p) \quad (36)$$

where

A_p = peak area of a pure sample, in counts

W_p = the amount of element in a pure sample, in grams

Before they can be compared, however, all results must be normalized to a standard sample weight. The normalization factor is given by

$$CF_i = \frac{\text{desired standard weight}}{\text{sample weight in grams}} = \frac{1.00 \text{ grams}}{\text{sample weight in grams}} \quad (37)$$

After normalization, equations (35) and (36) become

$$A_i CF_i = k(W_i CF_i + S_i CF_i) \quad (38)$$

and

$$A_P CF_P = k(W_P CF_P) \quad (39)$$

Since

$$W_i CF_i = W_P CF_P \quad (40)$$

then subtraction of equation (39) from equation (38) yields

$$A_i CF_i = k(S_i CF_i) + A_P CF_P \quad (41)$$

The X-intercept of a plot of $A_i CF_i$ as a function of $S_i CF_i$ is therefore

$$\text{X-intercept} = \frac{-A_P CF_P}{k} = -W_P CF_P \quad (42)$$

which is the negative of the desired experimental value.

The method of standard addition is used to insure a constant matrix effect from the complex sample. The data points are fitted by the method of linear least squares, which assumes that all of the error is in the calculated peak areas, and the measured amounts of standard

solution added to the samples are exact. The resulting mean square deviation (MSD), calculated by the least squares method, is used to estimate the error in the X-intercept from

$$\pm \text{Error} = \pm \text{MSD}/k \quad (43)$$

EXPERIMENTAL

The hardware and software developed for this research were designed and constructed to yield a completely flexible multichannel pulse-height spectrometer. The experimental system, shown in Figure 4, was capable of both high resolution, high precision data acquisition, and rapid, comprehensive data reduction. The central, dedicated computer served as both a control and memory for the collection process, and a central processing unit for the data reduction.

The elements up to and including the analog to digital converter (ADC) are common to all pulse-height analyzer systems. They include a detector, a pre-amplifier, a linear pulse-height amplifier, and an ADC.

The experimental system developed for this research utilized a 50 cc lithium-drifted germanium detector made by Nuclear Diodes. The detector was a wrap-around coaxial design which was rated at 8% efficiency, relative to a 3×3 NaI(Tl) detector. The resolution of the Ge(Li) detector was rated at 2.3 KeV, measured at the 1.33 MeV cobalt peak, and the peak-to-compton ratio was rated at 23:1.

The detector was biased at 2500 volts by an Ortec Model 456 high-voltage power supply. A Nuclear Diodes Model 103 pre-amplifier was connected to an Ortec Model 451 spectroscopy amplifier. An Ortec Model 444 biased amplifier was available as an option.

The 0-10V output of the linear amplifier was digitized by a Northern Scientific Model NS-629 analog to digital converter. The Wilkinson type ADC was capable of 8192 channels of resolution and used a 50 MHz

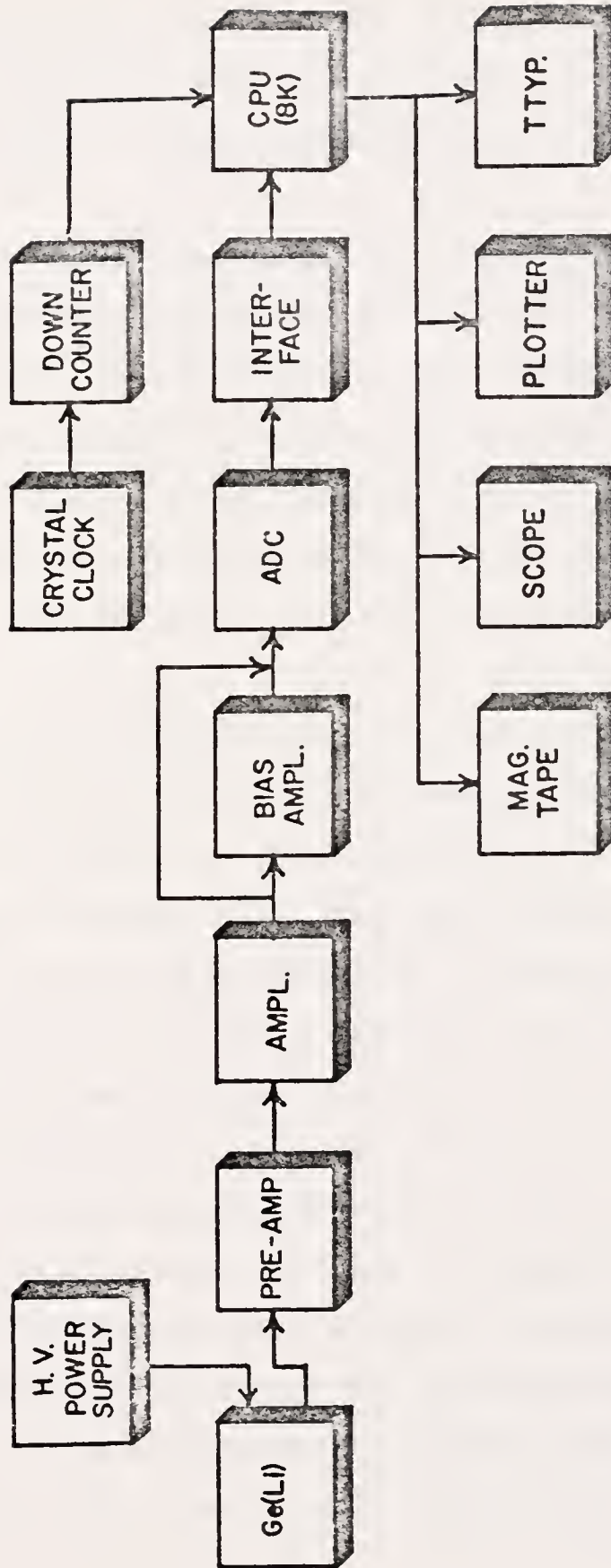


Figure 4. Block diagram of the experimental system

clock rate for the digitization process. The dead time of the ADC was rated at $3 + 0.02N$ μ sec per event, where N is the channel address of the converted signal. The maximum dead time of the system was therefore 167 μ sec.

All signals necessary for the transfer of the digital data and the control of the ADC operation were 0-5V positive logic, and were accessible through pins at the back panel of the ADC. Thirteen bits of address data were available for parallel transfer, as well as a ready signal, a clear line, and a dead time signal. The ADC performed most of the functions of a biased amplifier and, when desired, allowed a full 8192 channels of resolution to be used with the 2048 channels of available memory.

The non-flexible nature of most commercially available pulse-height analyzers was overcome by the use of a programmable mini-computer as the basic control and memory unit. The versatile nature of the software allowed complete flexibility in all functions, including data acquisition, printout, display, and data reduction. The computer was a PDP-8/L from Digital Equipment Corporation. With 8K of available core, 4K was used for memory storage and 4K was allotted for core resident software. The PDP-8/L used 12-bit words, had a cycle time of 1.6 μ sec, contained one common bus, and had one level of program interrupt.

All major input and output was achieved through a Model ASR 33 Teletype, which typed ten characters a second. The spectra were displayed on an ITT Model 1935D fifteen-inch display oscilloscope, and were plotted on a Model 7127A strip chart recorder from Hewlett-Packard. A Tri-Data Model 4096 magnetic tape unit, capable of trans-

fering 462 12-bit words a second, was used for all bulk storage.

Hardware

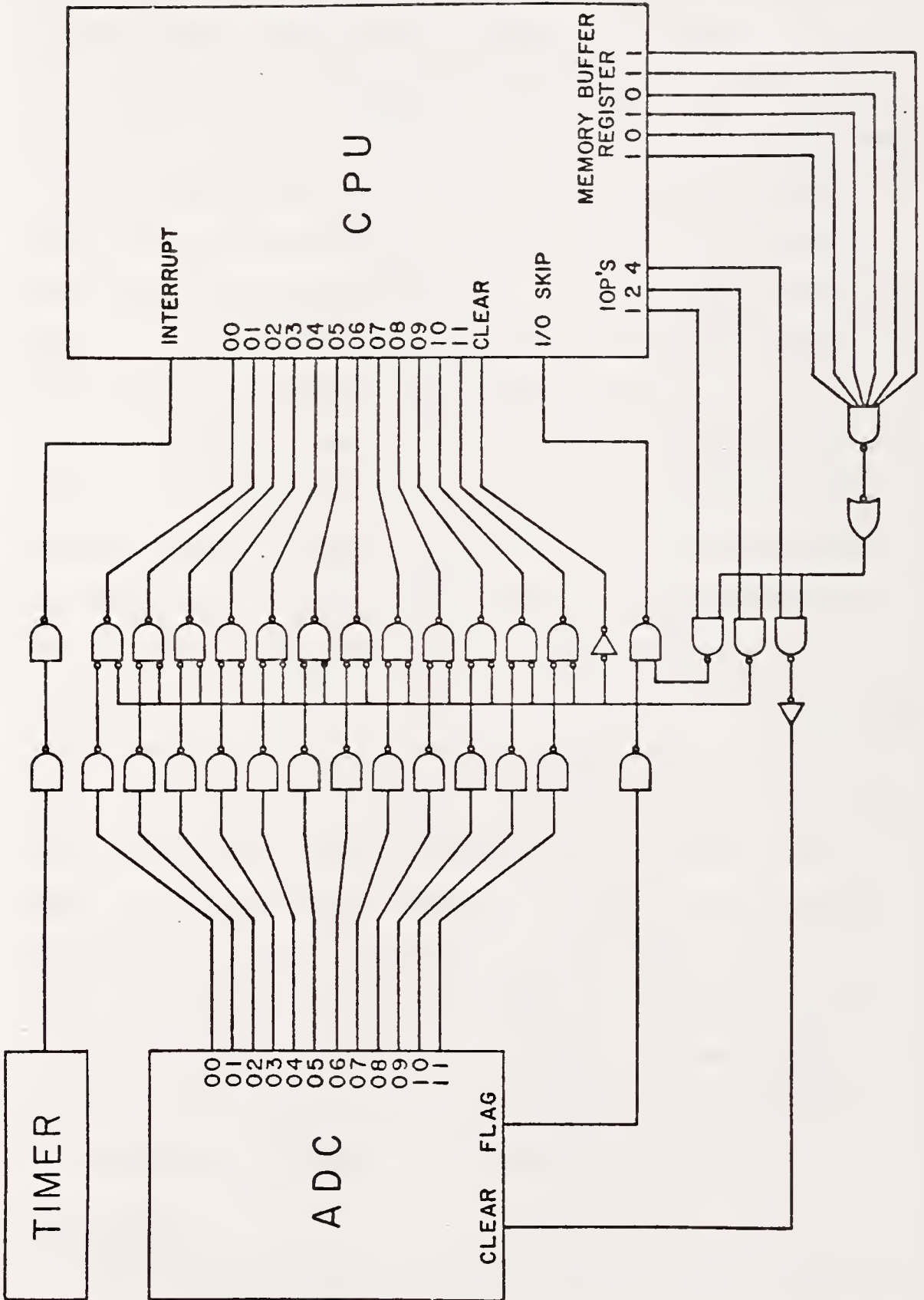
The computer based pulse-height analyzer system, described above, required the design and construction of two critical hardware components. An interface was built to allow computer control of the data acquisition by the ADC, and to provide a means for transferring the digital address data to the computer. A high precision digital clock was built to accurately control all count times. These two components are discussed in detail below.

Interface

The logic interface shown in Figure 5 was designed and developed to allow computer control of the ADC, and to provide a means for parallel transfer of digital data from the 13-bit ADC output register to the 12-bit accumulator register of the computer. Since only 2048 channels of memory storage were available, the twelve least significant bits of the ADC output were connected to the computer.

Since all computer peripherals were connected to one common bus, individual devices were controlled by means of a 6-bit binary code generated through the memory buffer register (MBR). The execution of an input-output transfer (IOT), software command ($6XXY_8$), caused a logical "1" to be generated for 4.25 μ sec on the six memory buffer lines indicated by the two octal digits XX (56 for the ADC interface). Therefore, by connecting a six-input nand gate to the appropriate MBR lines, a specific device, such as the interface, was individually controlled.

Figure 5. Interface between an analog to digital converter and a PDP-8/L computer



The same $6XXY_8$ command caused the computer to generate any combination of three input-output pulses (IOP's), each 600 nsec in duration. The octal digit Y designated which combination of IOP's were generated. If more than one IOP was designated by the software command, the order of generation was IOP1, IOP2, and IOP4, with each pulse separated by a 100 nsec delay. As shown in Figure 5, only when the correct device code (XX) was called were the IOP's passed through the logic of the device selector. This prevented the IOP's intended for other peripherals from activating the ADC interface.

Each of the three IOP's performed a specific function in the ADC interface. The IOP1 was used to check the status of the ready flag of the ADC. When the flag was set to a logical "1", indicating that the current gamma-ray pulse had been digitized and the address data were available at the output register, the IOP1 was passed to the input-output skip gate of the computer. This pulse caused the computer to skip execution of the next software command, and is discussed in more detail in the software section. The IOP2 was used to open a 12-bit bus driver network, which allowed a parallel transfer of the address data from the output register of the ADC to the accumulator register of the computer. The IOP4 was used to send a pulse to the clear input of the ADC. This pulse caused the ADC to clear the output register, reset the ready flag to a logical "0", and accept a new input signal for digitization. The timing of these signals will be discussed more thoroughly in the software section.

Timing System

The timing system shown in Figure 6 was designed and constructed

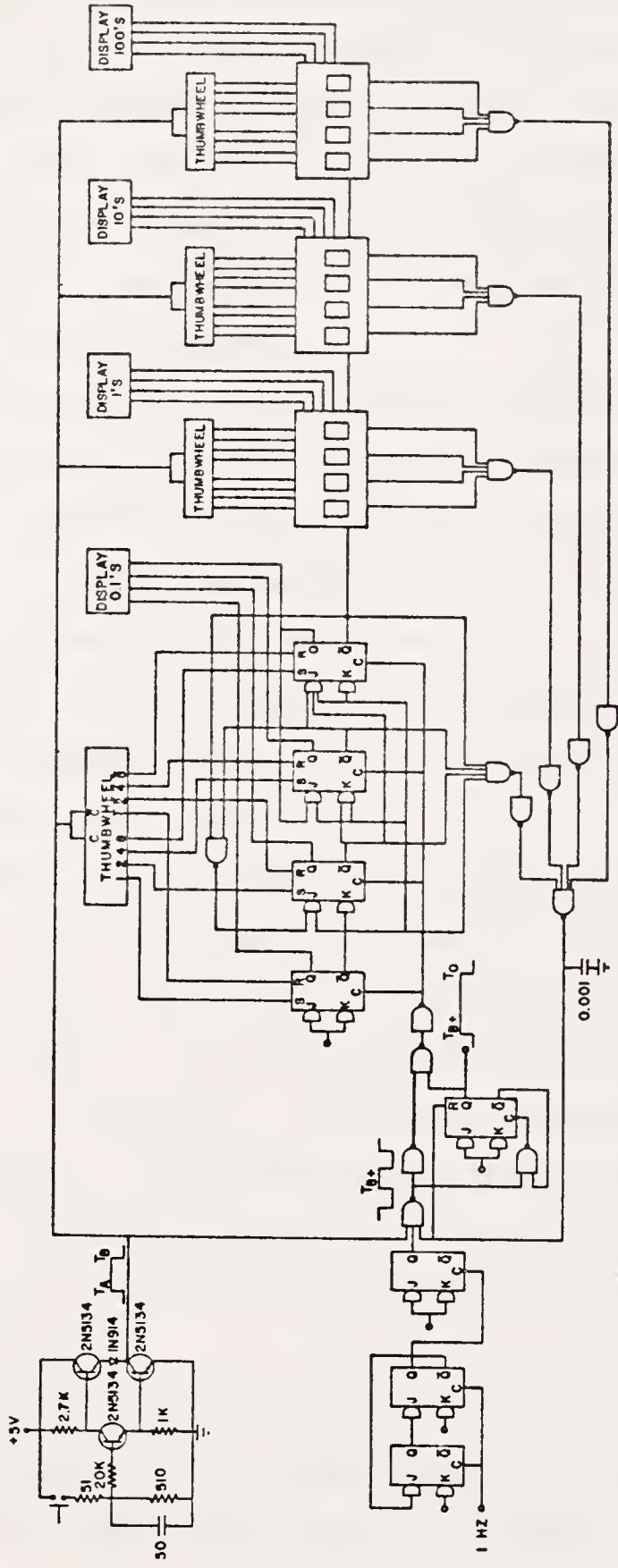


Figure 6. Timing system for accurate and precise timing control of the data acquisition software. A push button switch is engaged from time T_A to T_B . The timing pulse is generated from time T_{B+} to T_O and corresponds in length to the time preset on the thumbwheel switch

to allow the highly precise and accurate control of experimental count times required by this research. A 1 MHz crystal clock, accurate to three parts in 10^6 , was passed through a series of logic networks to yield a 1 Hz output. The 1 Hz clock rate was passed through the divide-by-six network shown in Figure 6 to yield a 1/6 Hz input to the four decade, presettable down counter. The 1/6 Hz pulse train clocked the counter every tenth of a minute.

When the counter was at zero, the gated output from the four decades was a logical "1", which held the input nand gate closed to the clock pulses. A push button switch, connected to the contact bounce eliminating network shown in Figure 6, produced a short logic pulse from time T_A to time T_B . This enabled the contents of a four decade thumbwheel switch to be transferred to the four decades of the down counter. The contents of the counter were continuously shown on a four digit, LED, decimal display.

The gated output of the four decades caused the input nand gate to open at time T_B , which allowed the passage of the 1/6 Hz clock pulses. The leading edge of the first pulse through the input gate (at time T_{B+}) caused the Q output of the control flip-flop to go from a logical "0" to a logical "1". This output was connected to both the interrupt facility of the computer and the remaining input nand gate. The logical "1" therefore served to both initiate the computer interrupt and to open the input nand gates and allow the clock pulses to drive the counter.

As the 1/6 Hz clock pulses triggered the counter, the time remaining for data acquisition was constantly shown on the lighted display. When the counter reached zero, at time T_0 , the gated output of the

four decades reset the control flip-flop, causing the Q output to return to a logical "0". The input nand gate was also closed, preventing any more clock pulses from reaching the counter.

In this manner a logical pulse, extending from time T_{B+} to time T_0 , was transferred to the interrupt facility of the computer, as illustrated in Figure 6. Since this pulse was initiated by the leading edge of a clock pulse, the length of the logical pulse corresponded to the time period originally set on the thumbwheel switch. The effect of this timing pulse is discussed further in the software section.

A single pole, double throw switch allowed a choice between counting in live time or clock time. When the live time position was chosen, the 1 MHz clock rate, directly out of the crystal, was gated with the dead time signal of the ADC. Clock pulses were therefore allowed to pass to the counter only when the ADC was clear to accept an input pulse from the linear amplifier. When the clock time position was chosen all clock pulses were passed to the counter.

Software

The complex mathematical calculations required by the curve fitting and linear least squares processes were performed using the conversational computer language FOCAL, developed by Digital Equipment Corporation. The FOCAL programs written to perform these mathematical calculations are listed in Appendix II.

All other software used in this research was written in assembly language and decoded into machine language. The final software package was completely resident in the 4K of core allotted for that purpose, and included all routines necessary for the operation of the

experimental system and all data reduction routines except those involving curve fitting. Also present in core was Digital Equipment Corporation's floating point package, DEC-08-YQ2B-PB, designed to perform basic mathematical operations and to provide a means for obtaining formatted digital input and output through a Teletype. A complete program listing, excluding the floating point package, is found in Appendix I. The following section discusses the methods of operation of this software.

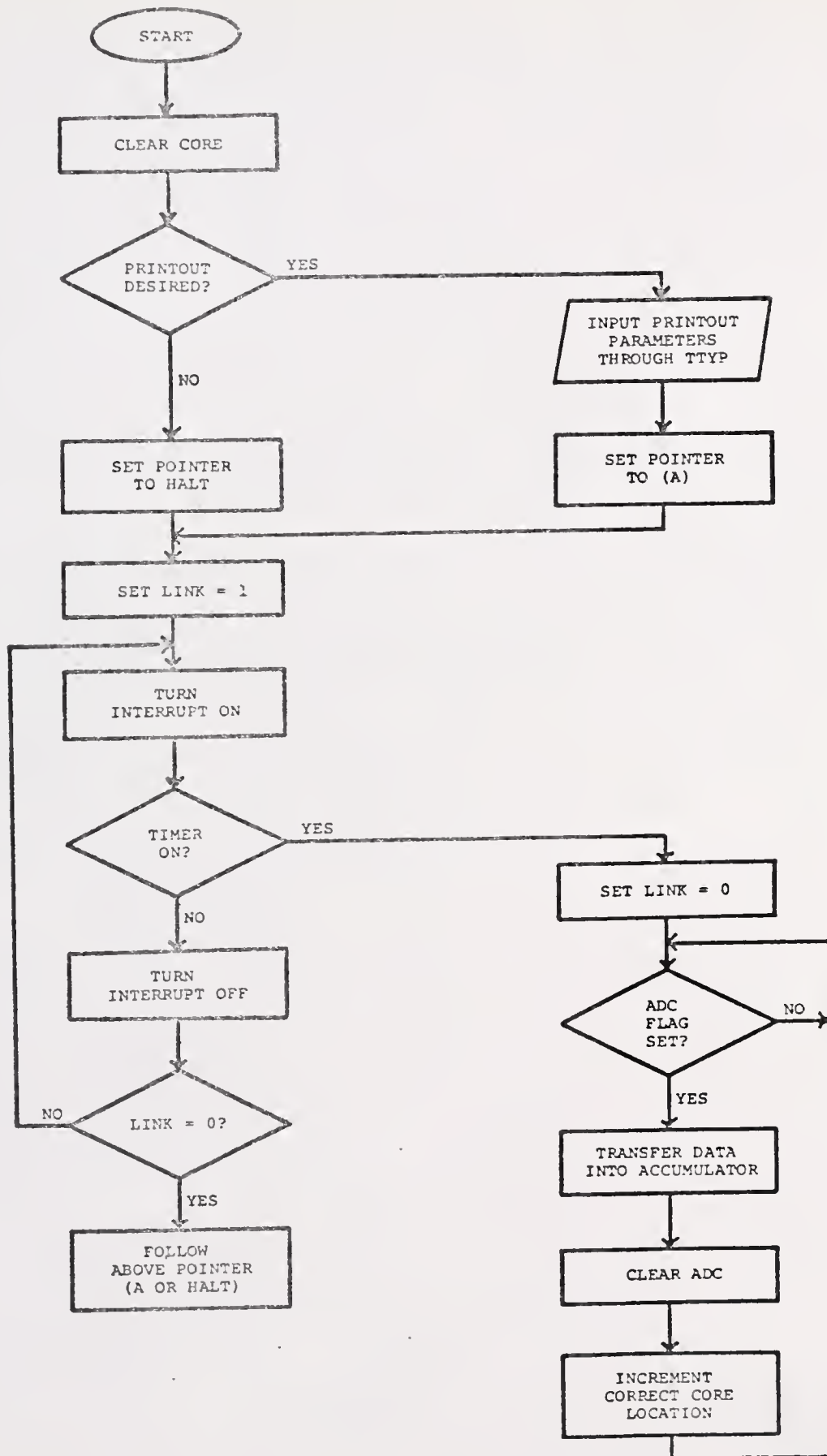
Data Acquisition

In order to maintain the resolution of the detector and ADC, a pulse-height analyzer system must be capable of high speed data acquisition and have an adequate memory. To satisfy these requirements with a PDP-8/L computer, the data were stored as 24-bit, double precision words in one 4K block of core, and the computer was devoted full time to the data collection process. This yielded the shortest possible software execution time and created a 2048 channel analyzer, with a memory storage capacity of over 16 million counts per channel.

Figure 7 illustrates the software sequence for the data collection process, and Figure 8 shows the timing relations between the computer and the ADC. The software was written to interact with the ADC interface and timer described earlier in the hardware section. The following discussion uses ideas introduced in this earlier section.

The software routine first cleared the entire 4K of memory. Then, using Teletype interaction, a pointer was set to allow an exit to either a printout routine or a program halt. If a printout was desired, the specific parameters (first and last desired channels) were entered

Figure 7. Flowchart of the data acquisition software



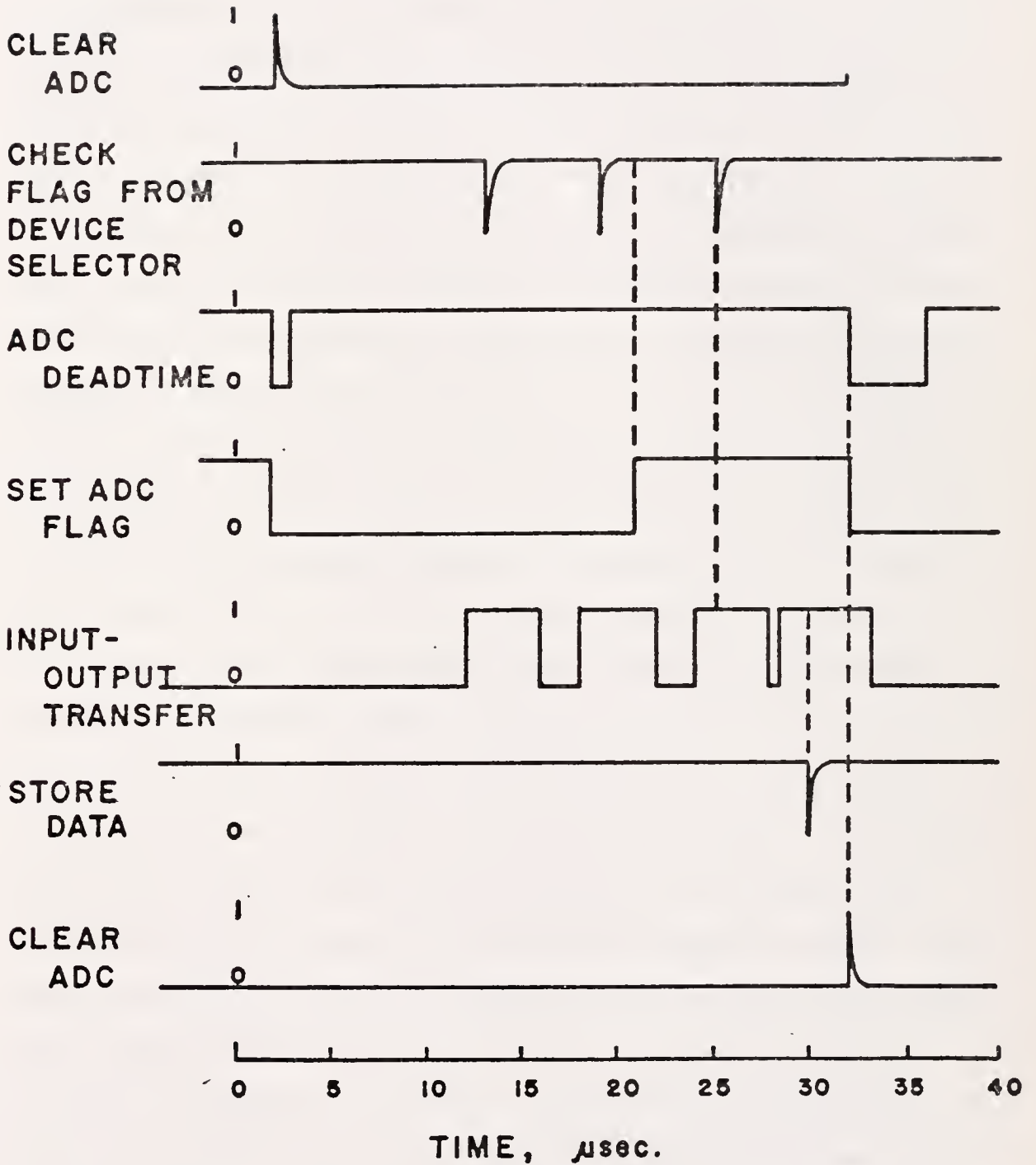


Figure 8. Timing relations between the computer and analog to digital converter

through the Teletype. The link, a 1-bit register also used as a pointer, was then set to one, to indicate that no data collection had occurred.

The heart of the data acquisition routine consisted of two software loops. The outer loop was a service routine for the interrupt facility of the PDP-8/L. When the interrupt was on, the computer continually monitored the Q output of the control flip-flop of the timer. If the output of the timer was ever a logical "0", indicating that the timer was off, the computer immediately transferred software execution to location zero and turned the interrupt off. The software sequence beginning at location zero checked the link and, if no data had been collected, turned the interrupt on again. Thus the computer waited in a software loop until the timer was initiated, indicating the start of a count. When the timer output went to a logical "1" the computer set the link to zero and entered the inner, data acquisition loop.

An input-output transfer (IOT) command, 6561_8 , called the ADC interface and generated an IOP1 to check the status of the ADC ready flag. If the flag was not set, a repeat command caused the sequence to be repeated every $5.85 \mu\text{sec}$, as illustrated in Figure 8. Once the flag was set, however, the next IOP1 was passed to the input-output skip facility of the computer, and the repeat command was skipped. The skipped instruction allowed the execution of another IOT, 6566_8 , which again called the ADC interface, and generated an IOP2 and an IOP4. As Figure 8 illustrates, the IOP2 was generated first and caused the twelve bits of address data to be parallel transferred from the ADC to the accumulator register of the computer. The IOP4, 100 nsec later, cleared the ADC output register and ready flag, which allowed the ADC

to accept a new signal for conversion.

While the ADC was converting the new signal, the computer performed the proper data storage by incrementing the memory location designated by the contents of the accumulator. Only the lower 12-bit word of the channel address was incremented, unless the incrementation caused an overflow into the second twelve bits. The storage process required 11.2 μ sec, and the overflow, which occurred only once every 4096 counts in any given channel, required an additional 8 μ sec. This time period constituted the entire dead time of the computer and was independent of the ADC dead time. When the data storage was completed, the computer returned to the flag checking sequence.

During the entire data collection process the interrupt remained on. When the count time expired, and the timer output returned to a logical "0", the computer immediately transferred control from the data acquisition loop back to the interrupt service loop. Since the link had been set to zero, the software execution sequence followed the exit pointer to either the data printout routine or a program halt.

For the general case of incrementation of only the lower 12-bit word, there was an 11.2 μ sec computer dead time between the clearing of the ADC and the generation of the first IOP1 to check the ready flag. The conversion time for the ADC was rated at $3 + 0.02N$ μ sec, where N was the channel number. Therefore, during the computer dead time the ADC could complete conversion only on pulses which occurred in the first 410 channels. For these lower energy pulses the flag was set before the first IOP1 was generated. For all channels above 410, however, the computer had to wait in a 5.85 μ sec loop until the ADC conversion was completed.

In Figure 8 the latter case is illustrated. A sequence of IOT's, each 4.25 μ sec in length, generated the IOP1's to check the ADC ready flag. These pulses were separated by a 1.6 μ sec repeat command until the flag was set, at which time a second IOT immediately followed the first. This IOT generated both the IOP2 and the IOP4, which initiated the storage process and cleared the ADC respectively. The only variable time in the sequence was the length of the ADC dead time, which depended upon the channel address of the digitized signal.

Data Printout

Figure 9 shows the flow chart for the data printout process. The printout software was entered either directly from the data acquisition routine (point A) or as an individual routine (point B). Using the printout parameters (first and last desired channels), obtained by direct input through the Teletype, the computer initialized all necessary counters and variables. Then the desired block of data was printed by the Teletype in a format shown in Figure 10. The printout was terminated whenever channel 2047, or the last desired channel was passed.

As Figure 10 illustrates, the first number in each line of data was the channel address of the first data point in the line. The remaining five numbers were the contents of the five channels designated by the line number. The number of digits in the output was variable, and all leading zeroes were replaced by spaces. The page header included the spectrum number, the magnetic tape number, and the date of the data collection. Each page of the printout was eleven inches in length and contained 50 lines of data.

Display

Another requirement of a pulse-height analyzer system, a means of

Figure 9. Flowchart of the data printout software

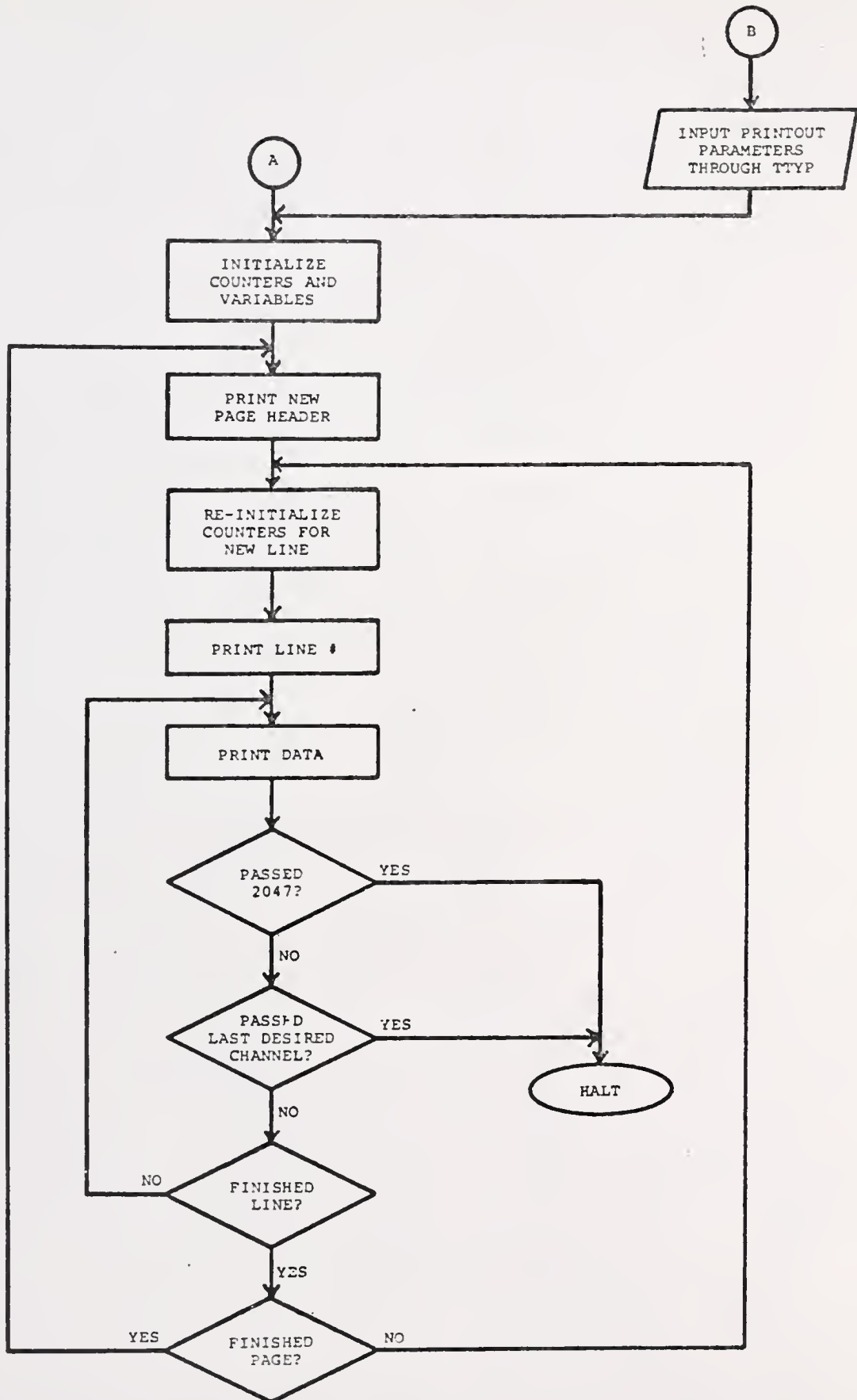


Figure 10. Sample page from the computer printout of a stored spectrum

SPECTRUM = 5 TAPE = 2 DATE : 6/ 4/ 72

1500	448	450	477	444	397
1505	418	424	476	457	395
1510	454	466	431	458	461
1515	453	477	460	477	468
1520	471	483	414	444	445
1525	479	479	444	466	400
1530	452	432	425	474	445
1535	501	463	477	442	411
1540	448	460	458	466	469
1545	476	455	435	462	483
1550	441	472	458	474	479
1555	475	443	533	479	471
1560	458	502	487	485	469
1565	517	455	513	489	509
1570	476	511	514	490	517
1575	487	523	502	479	537
1580	473	477	467	503	529
1585	475	537	489	511	522
1590	499	584	479	531	488
1595	475	502	459	440	469
1600	430	427	385	413	406
1605	408	397	369	376	389
1610	403	368	401	434	403
1615	438	459	443	510	553
1620	598	630	757	811	1124
1625	1436	1821	2419	3147	4240
1630	5714	7479	9018	9714	8944
1635	6953	4193	2252	1049	591
1640	450	368	431	461	494
1645	511	651	783	914	1196
1650	1471	2054	2680	3606	4733
1655	6319	7735	8789	8193	6583
1660	4057	2216	1009	407	274
1665	229	201	194	172	155
1670	191	167	181	182	169
1675	183	167	165	170	144
1680	148	162	134	160	148
1685	160	145	148	142	157
1690	144	162	157	145	145
1695	124	138	131	142	149
1700	129	152	141	133	120
1705	145	139	126	135	125
1710	124	129	135	140	127
1715	101	113	119	116	100
1720	113	123	141	109	105
1725	99	102	114	107	111
1730	126	123	119	95	122
1735	114	143	121	158	171
1740	100	214	216	269	224
1745	177	139	96	87	88

visual display of the data contained in memory, was achieved through the software illustrated in Figure 11. The digital data were converted to analog voltages by a 10-bit digital to analog converter (DAC). The analog output of the DAC was fed to either an oscilloscope or a strip chart recorder. The method of display was selected by setting bit two on the PDP-8/L switch register to a one for a plotter and to a zero for a scope.

Since the DAC converted only the ten most significant bits of the low order word of each channel, the spectrum had to first be treated to yield a meaningful display. This was achieved in two ways. If the initialization routine was entered at the start, the spectrum was searched for any data greater than 4095_{10} (larger than twelve bits). If any were found, the entire spectrum was rotated to the right one bit (divided by two). This process was repeated until all data had been fully rotated into the lower twelve bits of each channel address. The second method of display set the low order word of each channel whose contents exceeded twelve bits to 4095_{10} (to yield a full scale display). The initialization routine was then entered at point C. When all data were ready for display, the first and last desired channels were entered directly through the Teletype, and the display subroutine (beginning at point E) was called.

The subroutine first checked the switch register to determine the desired display device. When a scope was indicated, the subroutine was returned, if necessary, to its basic form. After initializing all counters, the data were sequentially displayed through the DAC. Each point was retained by the DAC for as short a time as possible (18.65 sec). At the end of the desired data block the subroutine checked bit

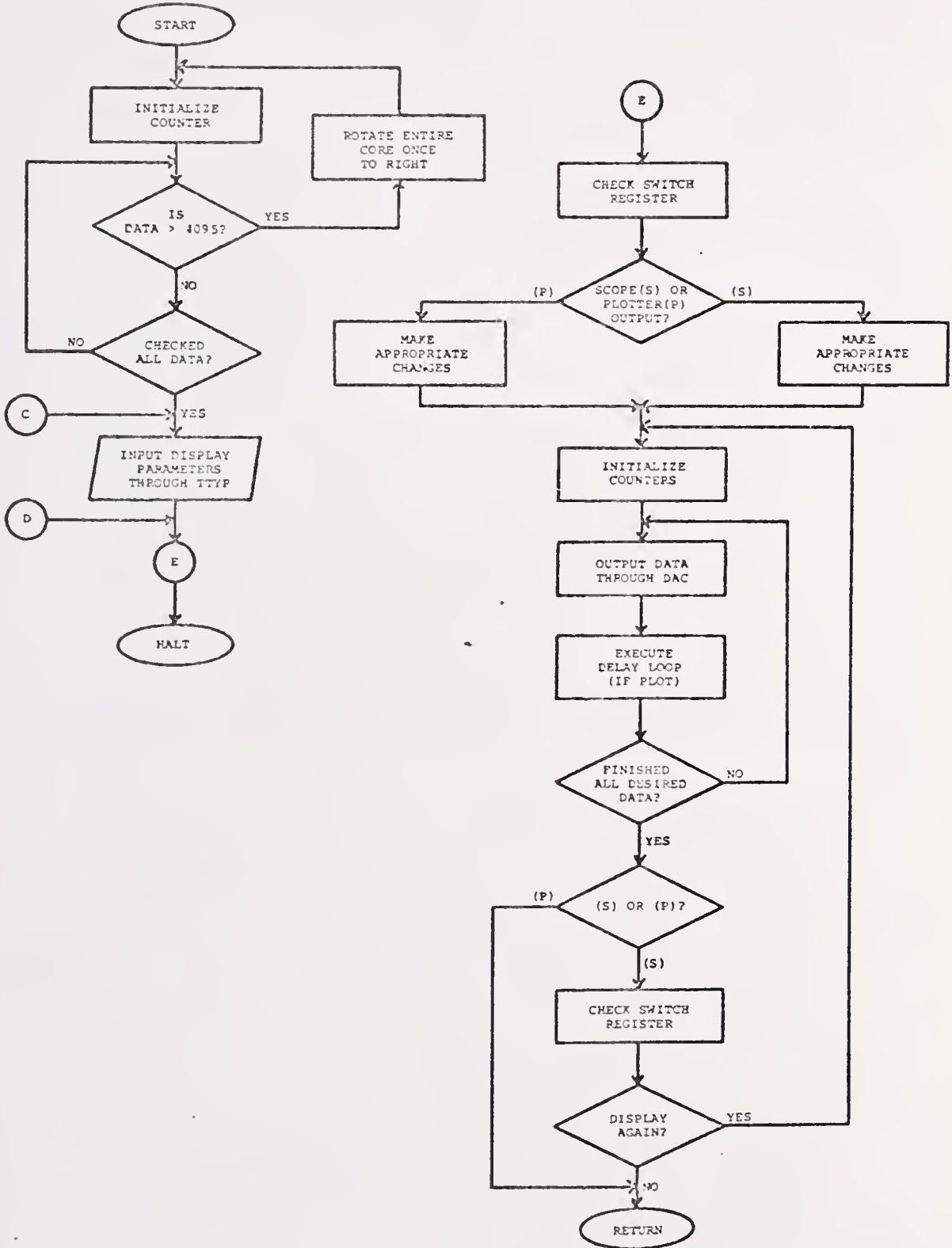


Figure 11. Flowchart of the display software

one of the switch register. The display sequence was repeated until this bit was set to 1, at which time it was terminated.

When a plotter display was desired several changes were made in the subroutine. A delay loop of approximately 64 msec was executed between the display of each data point to allow the plotter pen time to respond to the signal. At the end of the desired data block the display was terminated. Once terminated, however, the identical display could be repeated by entering the routine at point D.

Data Smoothing

The software shown in Figure 12 used the method of Savitsky and Golay (41) to smooth the digital data stored in the computer memory. The original spectrum of raw data was replaced in core by the smoothed data. The concepts and equations for this method were discussed earlier in the theory section.

All values required by equation (1) were entered directly through the Teletype. This input included the number of points in the smooth and all smoothing constants. Then the required number of raw data points were stacked in a string in lower core. Each point in the string was multiplied by appropriate smoothing constant and added to a subtotal. The smoothed data value was obtained by dividing the final subtotal by the appropriate normalization factor. The smoothed value was then stored in upper core in place of the original raw value. The raw string was advanced, the next raw data point was added to the end of the string, and the process was repeated. This sequence was repeated until the entire spectrum had been replaced by smoothed data.

Peak Detection

The two peak detection routines were discussed earlier in the

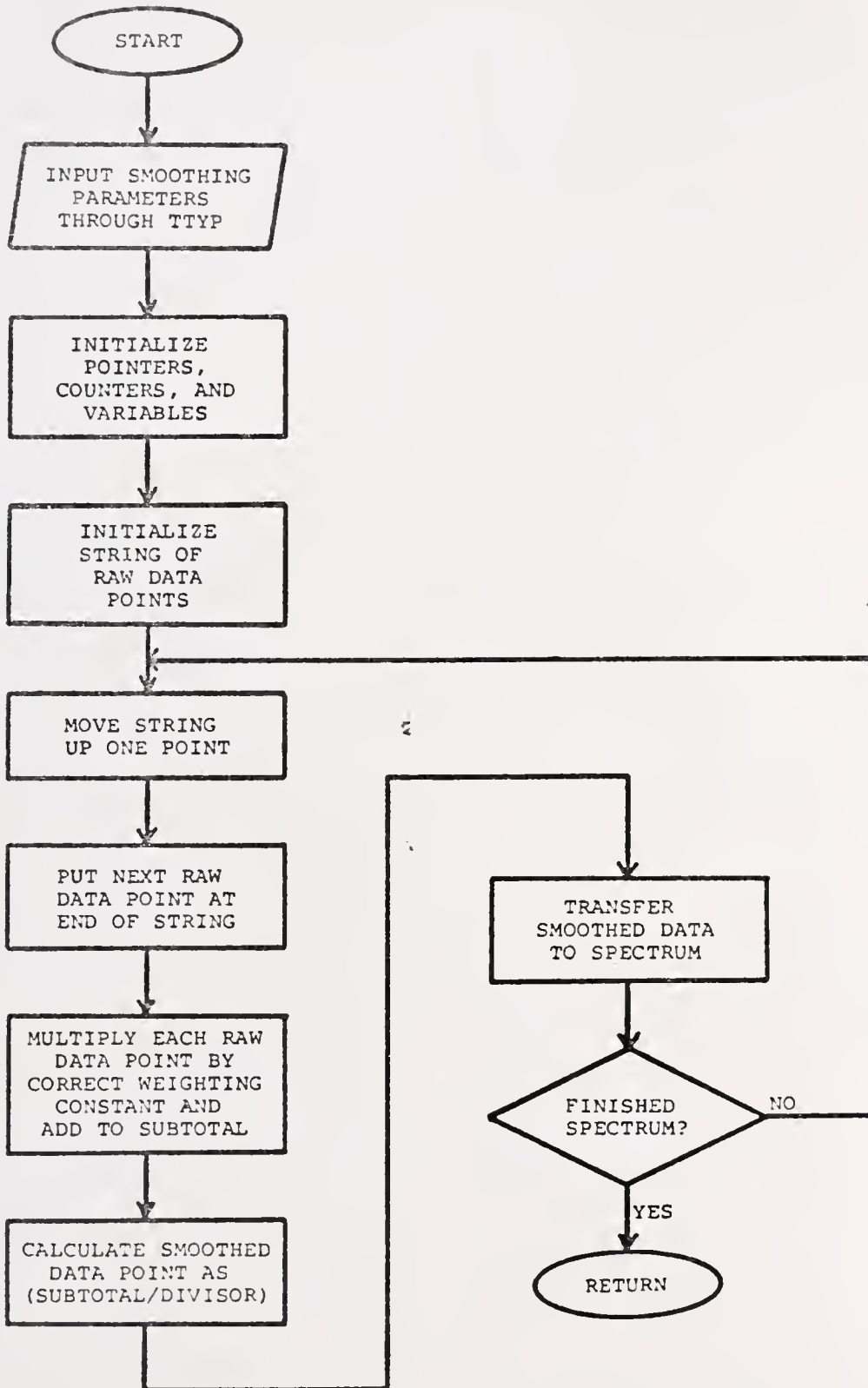


Figure 12. Flowchart of the data smoothing software

theory section. Together the two routines were designed to locate and determine boundaries for the two peak shapes illustrated in Figure 1. The first method of detection, described in Figures 13 and 14, was specifically developed to locate the second peak shape in Figure 1. This peak shape, which has several statistical minima superimposed on the peak, was commonly found in spectra which had not been previously smoothed, and with peaks which had a small peak-to-noise ratio. Peaks of this type were also commonly found in spectra which covered a narrow energy range, even after these spectra had been smoothed.

After setting the printout pointer to the second detection routine, and initializing the required pointers, counters, and variables, the first detection method began the search for a positive first derivative, which indicated the location of a statistical minimum in the digital data. After saving the integral channel location of the minimum as a possible left peak boundary, the routine located the next maximum by the derivative sign change from positive to negative. A subroutine, which was entered at point N and will be discussed later, was then called to calculate the average minimum to maximum height of the noise over the 40 channels immediately preceding the possible left boundary. The height from the boundary minimum to the maximum was then compared to a multiple (designated by the variable MINHT, usually one) of the average noise. Unless the height exceeded this noise value, the routine began the search for a new left boundary. If the minimum to maximum height was larger than the noise, the possibility of a peak was recognized and the routine continued the search for a right peak boundary.

As Figure 1 illustrates, however, more than one statistical minima

Figure 13. Flowchart of the peak detection (method one) software

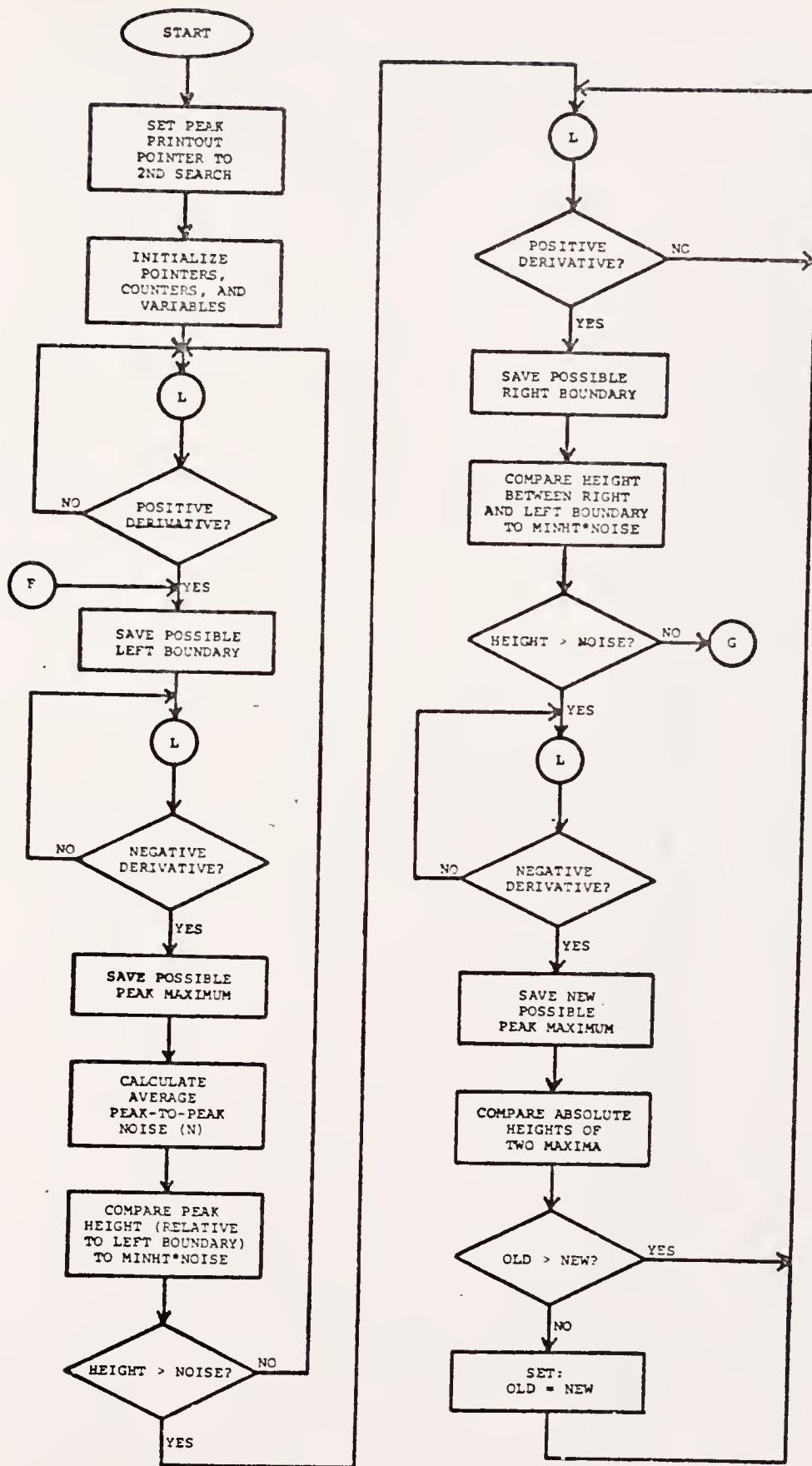
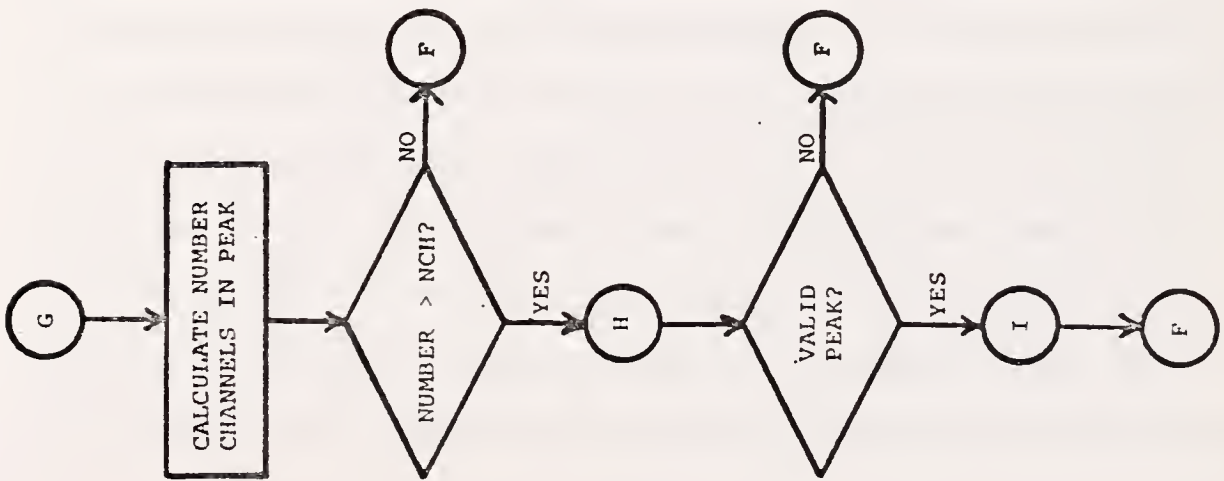
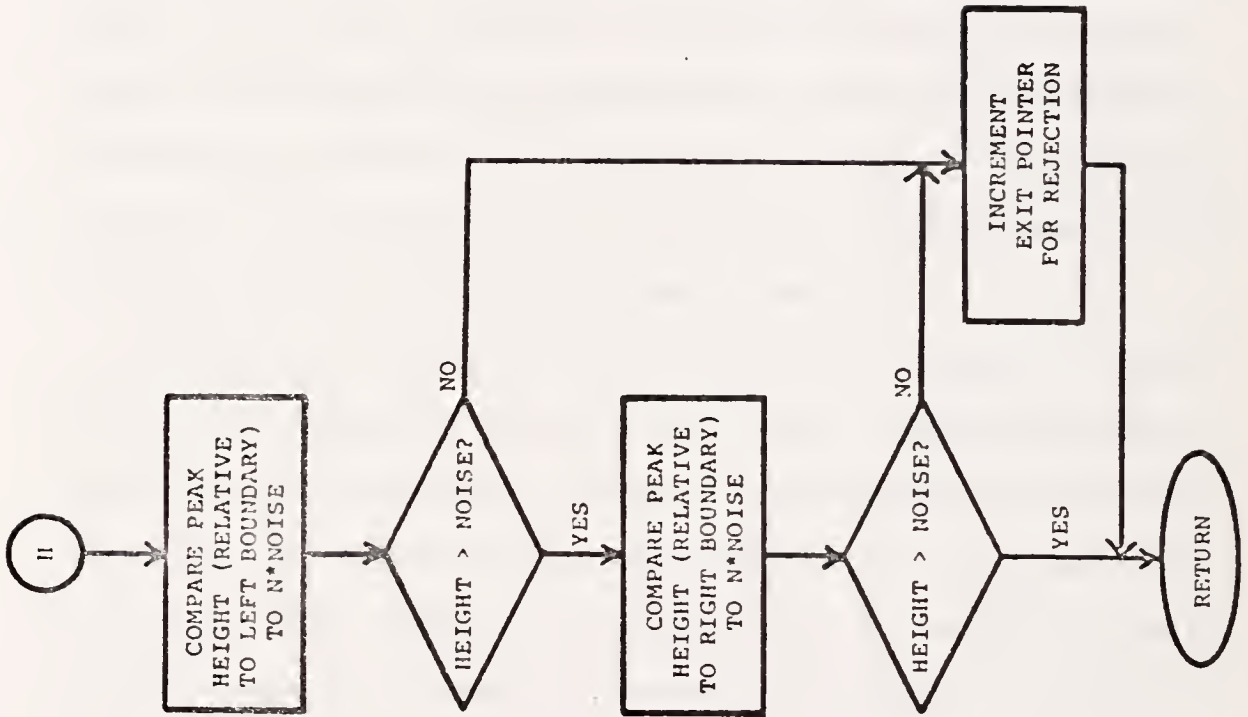


Figure 14. Flowchart of the software which tests for peak validity and permanently stores valid peak locations and boundaries



were often detected within the true peak boundaries. The routine located the next minimum and saved the channel location as a possible right boundary. The height of this minimum, relative to the left boundary minimum, was then compared to the value of the average noise times the variable MINHT. If the height exceeded the noise value, the right boundary was rejected, and the routine determined the location of the next maximum. The absolute heights of the maxima were then compared, and the channel location of the higher was saved as the peak maximum. The search was then continued for a right boundary minimum whose height, relative to the left boundary minimum, was less than the noise value. When this boundary was found, the routine jumped to point G, shown in Figure 14, to test for peak validity.

Beginning at point G the routine calculated the number of channels between the two boundary minima. If the number of channels was less than the required peak width, designated by the variable NCH and determined by the resolution of the system, the peak was rejected as a noise spike. The routine then returned to point F, where the channel location of the last minimum was saved as a possible left boundary and the search was continued. If the peak was wide enough, however, the subroutine beginning at point H was called to test the peak height, relative to both the left and right boundaries. If either height was less than the required peak-to-noise value, designated by the variable N, the routine rejected the peak by returning to point F in the peak detection routine. If all peak criteria were satisfied, however, the subroutine beginning at point I was called to permanently store the peak parameters in a string. A counter for the number of peaks was also incremented, and the routine returned to point F to search for the

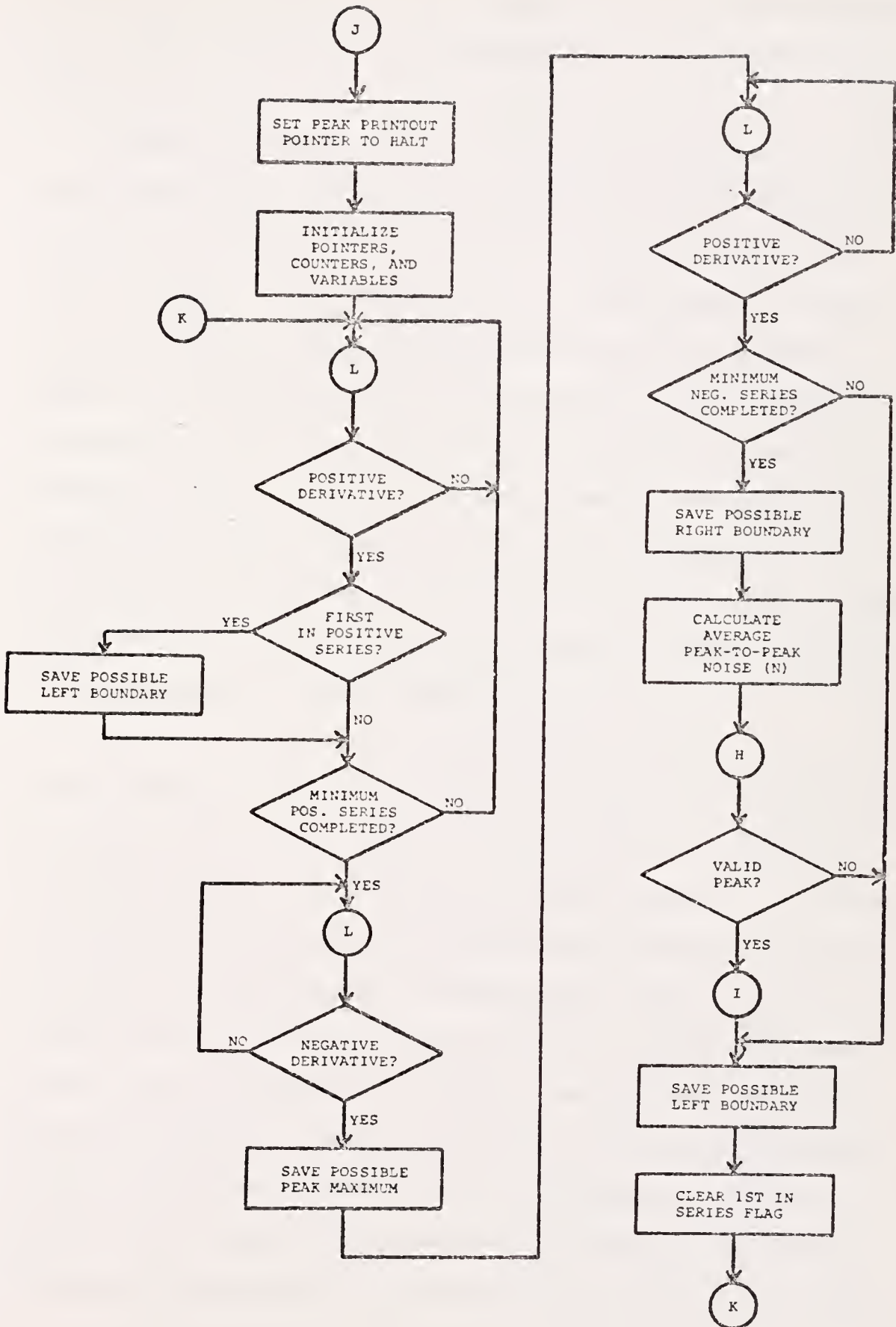
next peak.

The second peak detection method, described in Figure 15, was designed to locate major peaks in a spectrum and assumed that all valid peaks contained only one maximum. After setting the printout pointer to a program halt and initializing all required pointers, counters, and variables, the routine began the search for a positive first derivative. If the positive derivative was the first in a series, indicating the location of a statistical minimum, the channel location of the minimum was saved as a possible left peak boundary. The routine then continued the search until the required number of consecutive positive derivatives, designated by the variable MNUM and determined by the resolution of the system, had been detected.

If the required number was reached the channel location of the next negative derivative was saved as the location of the peak maximum. The routine then searched for the next minimum, indicated by the channel location of the next positive derivative. If the required number of consecutive negative derivatives, again designated by the variable MNUM, were detected, the location of the minimum was saved as a possible right peak boundary. If either series of derivatives were too small, the peak was rejected as noise.

Once the boundary channels were located, the routine called the noise evaluation subroutine to calculate the average noise height over the 40 channels immediately preceding the left peak boundary. The same subroutine used by the first peak detection routine, beginning at point H, was then called to validate the peak height. If the peak-to-noise ratio exceeded the value designated by the variable N, the subroutine beginning at point I was called to permanently store the peak

Figure 15. Flowchart of the peak detection (method two) software



parameters. The routine then saved the location of the last minimum as a possible left boundary and began the search for the next peak at point K.

Whenever the sign of the first derivative was requested by the peak search routines, the derivative subroutine, entered at point L and described in Figure 16, was called to calculate the sign of the first difference. When channel 2047 was reached, however, the peak search was terminated, and the peak printout routine, described in Figure 16, was entered at point M. This routine printed the number of peaks located by the search and typed a header for the remaining printout. Then, for each peak, the peak parameters were printed and a subroutine, which was entered at point Q and is discussed later, was called to calculate and print the peak areas. When all peaks were completed the peak printout pointer was followed to either the second peak detection routine or to a program halt.

Whenever the value of the average noise was required, the subroutine entered at point N and described in Figure 17 was called by the peak search routines. First the channel counter was moved back 40 channels from the left boundary of the peak in question. If this starting channel address was less than the right boundary of the last valid peak, as illustrated by the second peak in Figure 1, the subroutine restored the channel counter and exited with the last noise value. If not, the subroutine proceeded to locate minima and maxima by the sign changes in the first derivative. After locating each extremity, the minimum to maximum height was calculated and added to a subtotal, and a counter was incremented for a divisor. When the 40 channels were evaluated, the average noise was calculated by dividing

Figure 16. Flowchart of the software which determines the first differences and prints the final results of the peak searches

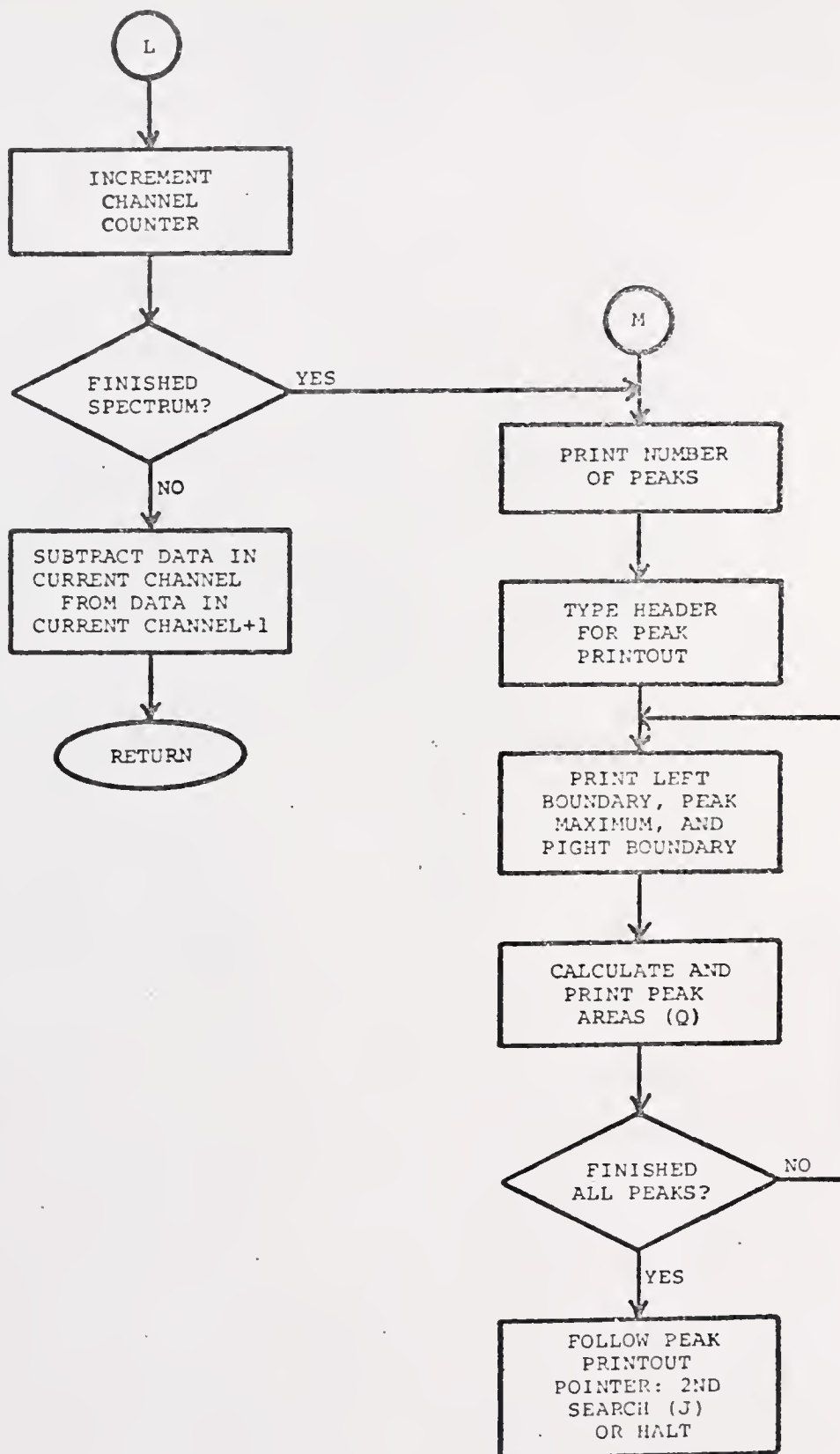
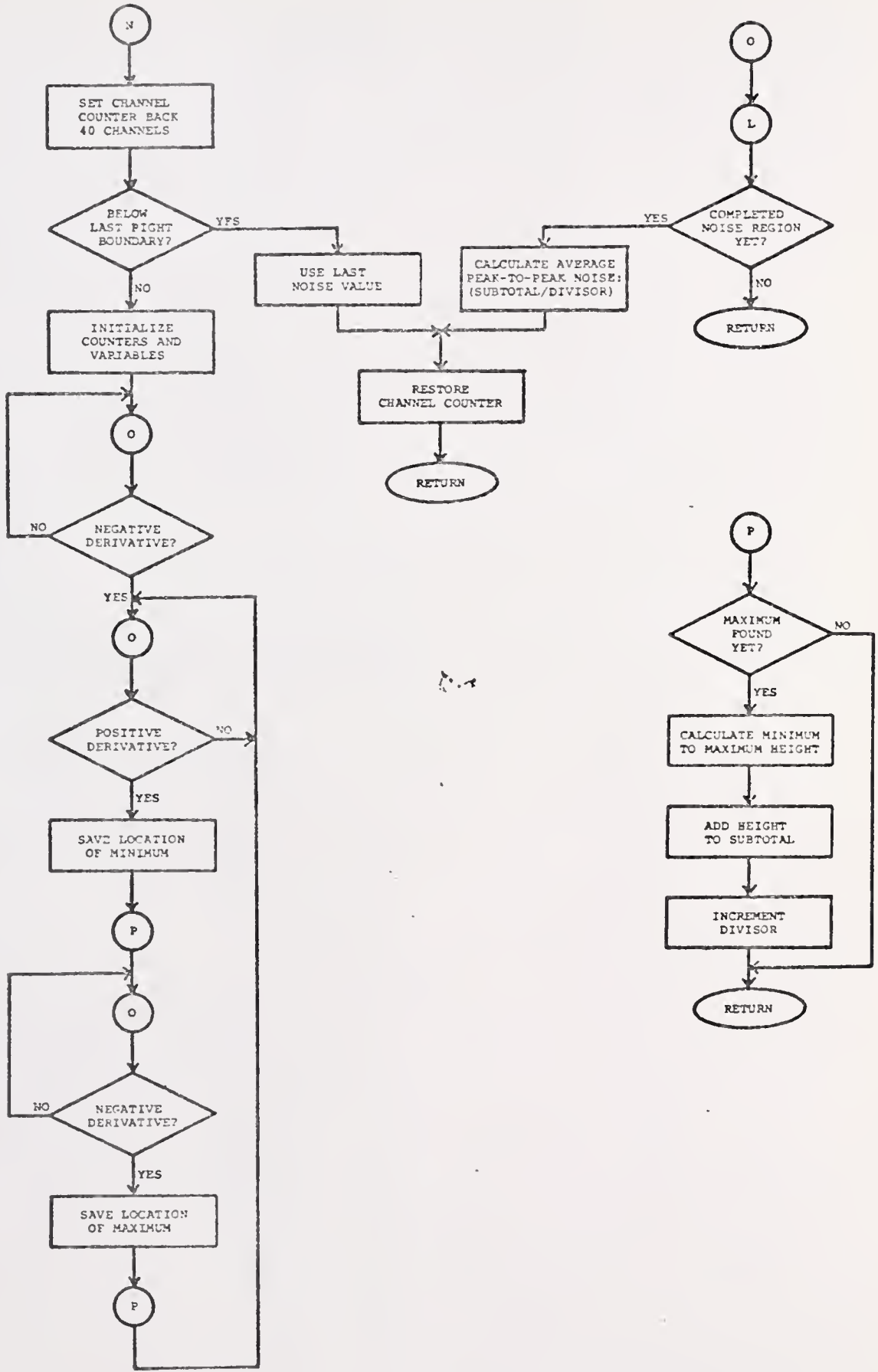


Figure 17. Flowchart of the software which calculates the average height of the noise over 40 channels



the subtotal by the divisor. The subroutine then restored the channel counter and exited with the new noise value.

The software required to calculate and print the peak areas is described in Figure 18. The subroutine, which was called by the peak printout routine and was entered at point Q, first used the peak parameters to calculate a total, trapezoid, and quantitative area according to equation (2). The areas were then printed as total peak area values. The peak parameters were then altered according to the Wasson peak area method. The number of channels to the left and right of the peak maximum included in the Wasson calculation were designated by the variable NWASON. If either of the original peak boundaries were inside the Wasson boundaries, the subroutine was exited without further printout. If the peak was wide enough, however, the slope of the total peak baseline was calculated and used to determine the absolute heights of the Wasson peak boundaries. These new boundary values were then used to calculate new total, trapezoid, and quantitative areas, which were printed as Wasson area values.

Preparation of FOCAL Compatible Data

All curve fitting calculations were performed using the FOCAL programs listed in Appendix II. These programs required that the digital data be converted to floating point and stored in core locations accessible by the FOCAL subroutine FNEW. The software described in Figure 19 was written to perform the conversion and relocation of the digital data.

The first and last channels of the desired data block were entered directly through the Teletype. After initializing the required counters and variables, the data block was relocated in integer form

Figure 18. Flowchart of the software which calculates and prints the peak areas by the total peak area and Wasson methods

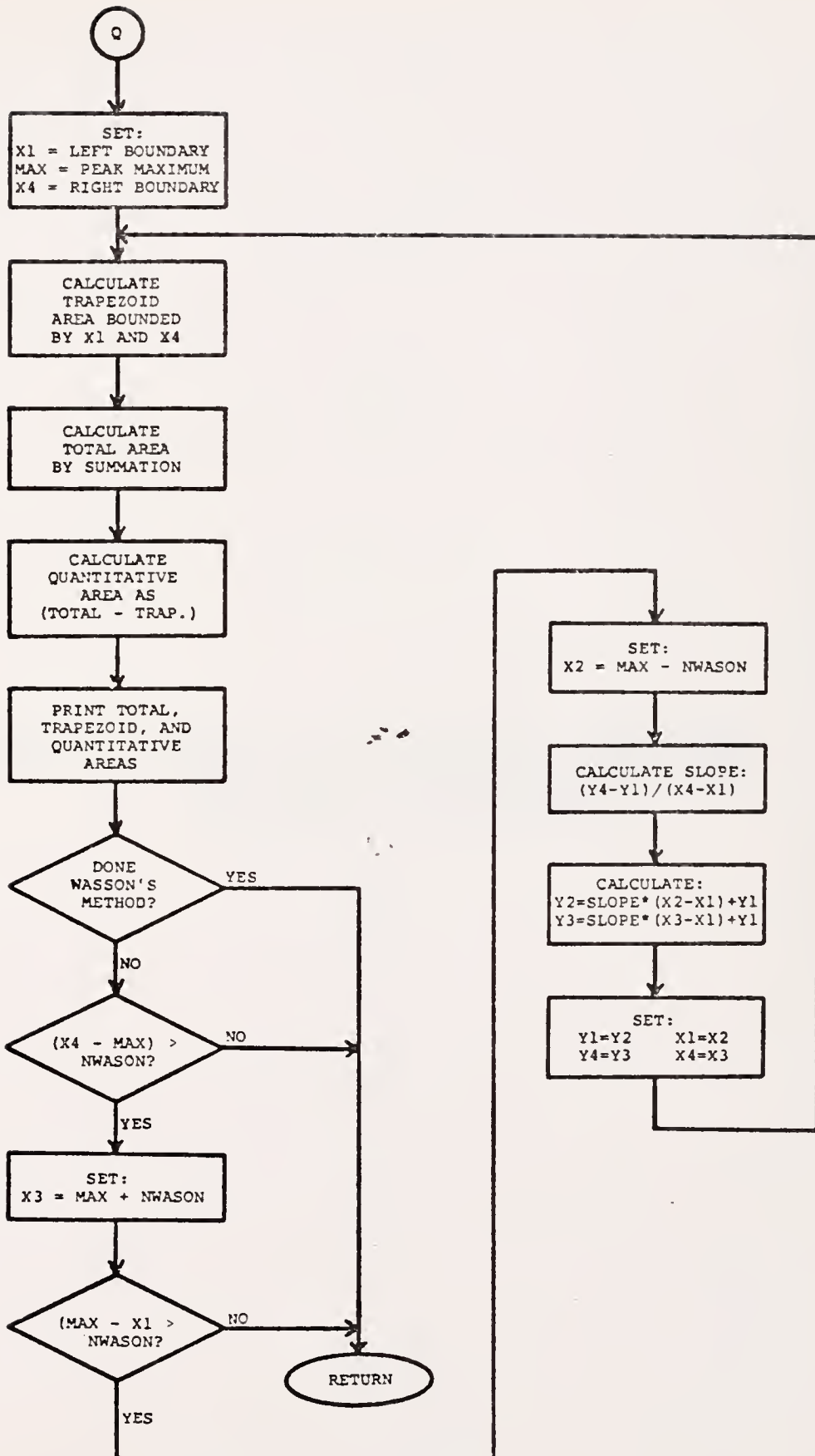
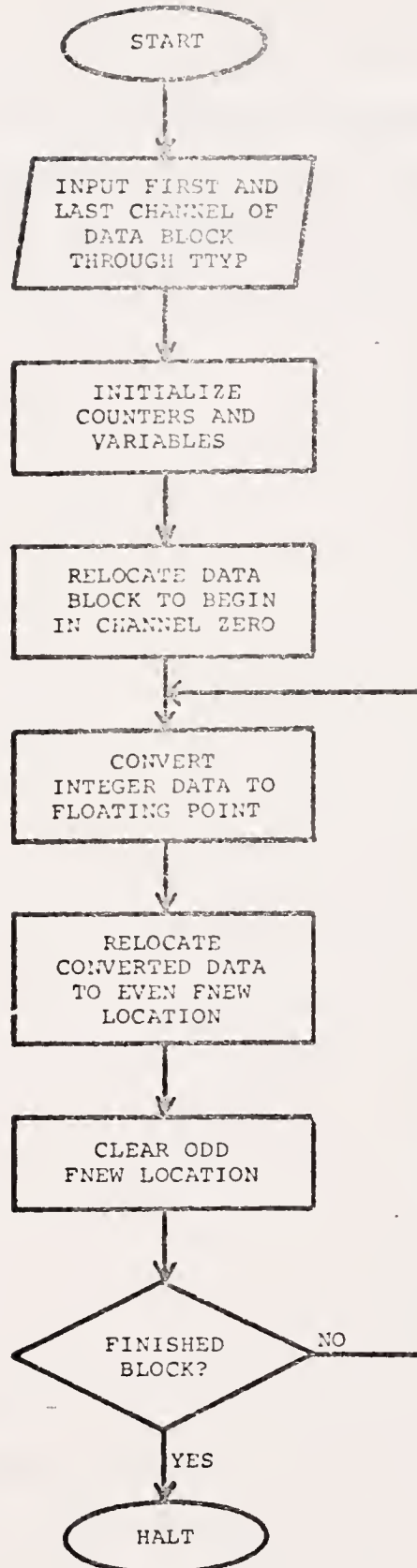


Figure 19. Flowchart of the software which converts the integer data to floating point and stores the results in core locations accessible by the FOCAL subroutine FNEW



to begin in location zero. The data relocation insured that the final converted data were not stored in core locations occupied by the data block. The data were then sequentially converted to a three-word floating point form and relocated in the core locations corresponding to the even FNEW locations. The odd FNEW locations were cleared for later use as storage locations for the fitted data.

RESULTS AND DISCUSSION

System Evaluation

In order to thoroughly test the performance of the analytical data system, eleven different sample spectra were collected and stored on magnetic tape. Pure isotopes of $^{51}_{24}\text{Cr}$, $^{59}_{26}\text{Fe}$, $^{65}_{30}\text{Zn}$, $^{75}_{34}\text{Se}$, $^{86}_{37}\text{Rb}$, and $^{110\text{m}}_{47}\text{Ag}$, obtained from New England Nuclear, were used to prepare the radioactive samples, thus insuring that spectra of known composition were experimentally generated. Table I lists the experimental conditions under which the spectra were collected. The same isotopic samples were used to generate spectra 6-8 and spectra 9-11.

Figures 20-22 illustrate the display capability of a strip chart recorder under control of the display software. The output to the recorder was generated by a 10-bit digital to analog converter. The display routine easily rotated the stored spectrum to the left or right one bit at a time, thereby multiplying or dividing the contents by two. This allowed the operator to display the spectrum completely on scale (Figure 20) or to highlight the regions of interest (Figures 21,22).

Data from spectra 6 and 10 were used to measure the linearity of the data acquisition system. Figure 23 illustrates the linearity between gamma-ray energy and photopeak location over the total energy range used in these studies. The data were obtained from spectra 6, and the method of linear least squares was used to obtain the slope of 1.48 channel/KeV, the zero energy intercept of 0.37, and the standard deviation of 0.72 channel. The peak locations were determined by the

TABLE I

EXPERIMENTAL CONDITIONS FOR THE SAMPLE SPECTRA

<u>SPECTRUM NUMBER</u>	<u>ISOTOPIIC CONTENTS</u>	<u>HALF-LIFE (DAYS)</u>	<u>SPECTRUM ENERGY RANGE (KeV)</u>
1	Ag - 110m	255	0 - 1378
2	Zn - 65	243	0 - 1378
3	Fe - 59	45.6	0 - 1378
4	Zn - 65 Ag - 110m	243 255	0 - 1378
5	Fe - 59 Zn - 65	45.6 243	0 - 1378
6	Cr - 51 Fe - 59 Zn - 65 Se - 75 Rb - 86 Ag - 110m	27.8 45.6 243 120 18.7 255	0 - 1378
7	Cr - 51 Fe - 59 Zn - 65 Se - 75 Rb - 86 Ag - 110m	27.8 45.6 243 120 18.7 255	0 - 337
8	Cr - 51 Fe - 59 Zn - 65 Se - 75 Rb - 86 Ag - 110m	27.8 45.6 243 120 18.7 255	337 - 672
9	Se - 75 Ag - 110m	120 255	0 - 965
10	Se - 75 Ag - 110m	120 255	0 - 477
11	Se - 75 Ag - 110m	120 255	477 - 955

Figure 20. Plot of spectrum 6, attenuated by a factor of (x 8). The full energy range of the spectrum is 0-1.378 MeV (0.624 KeV/channel)

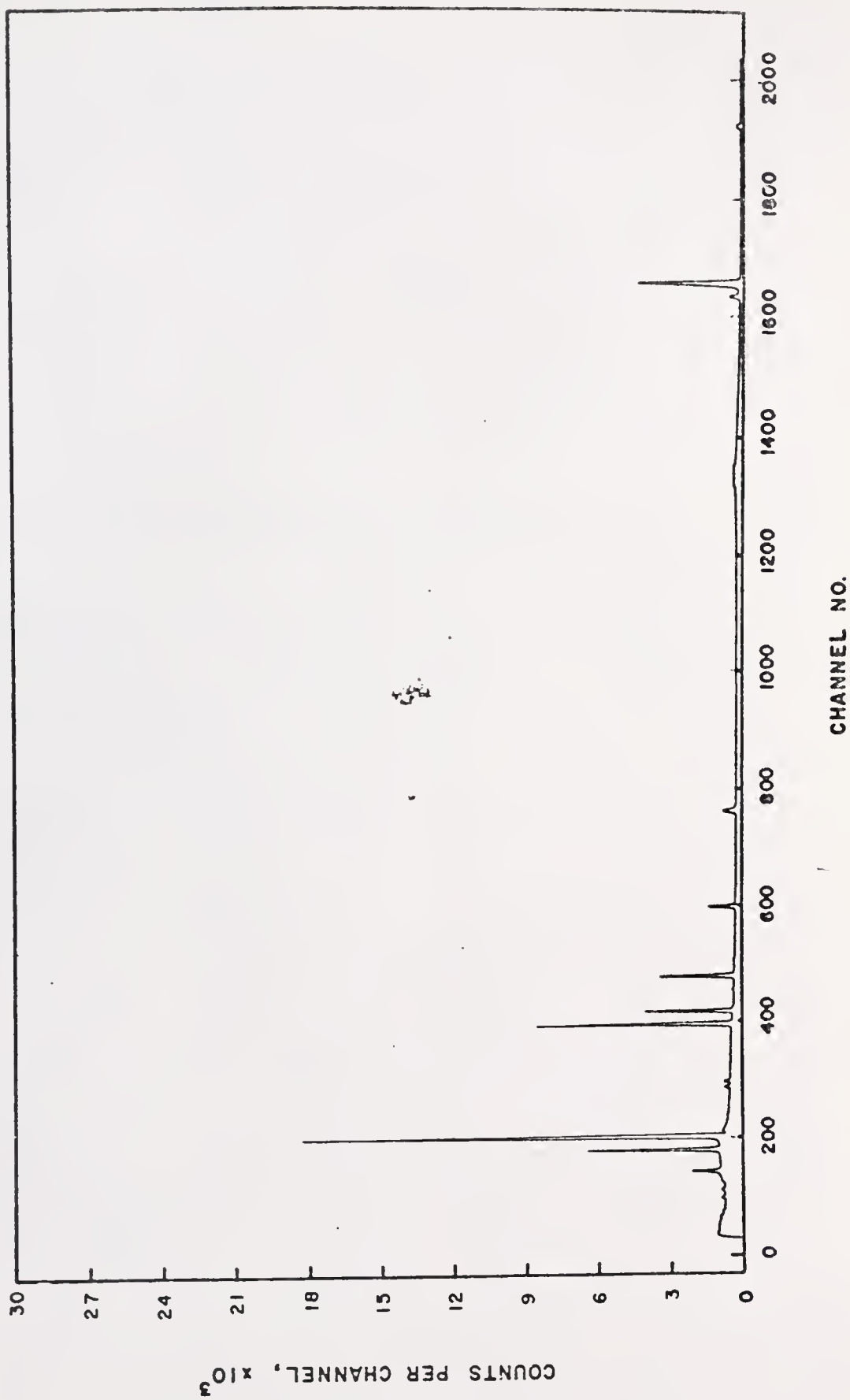
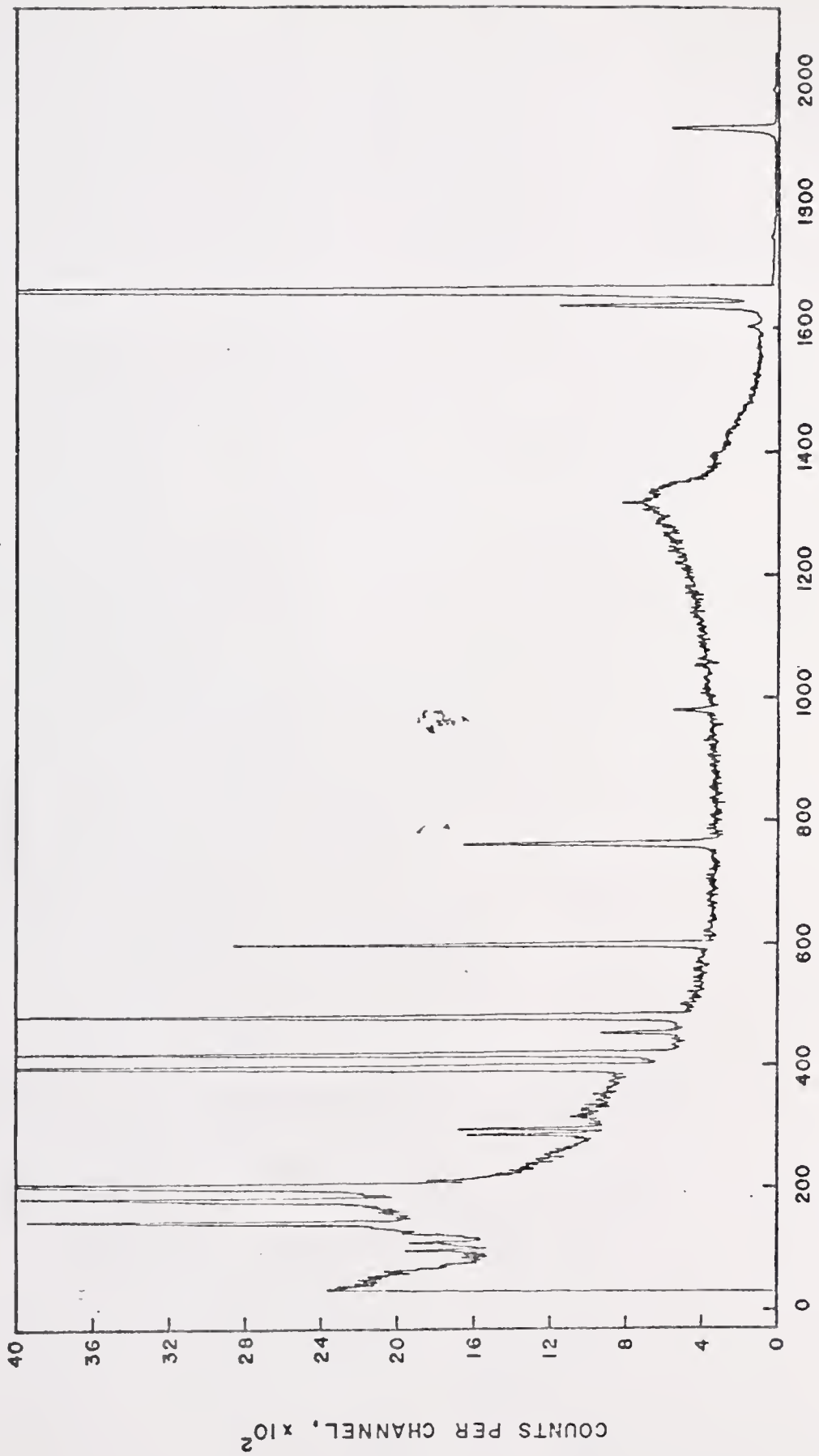
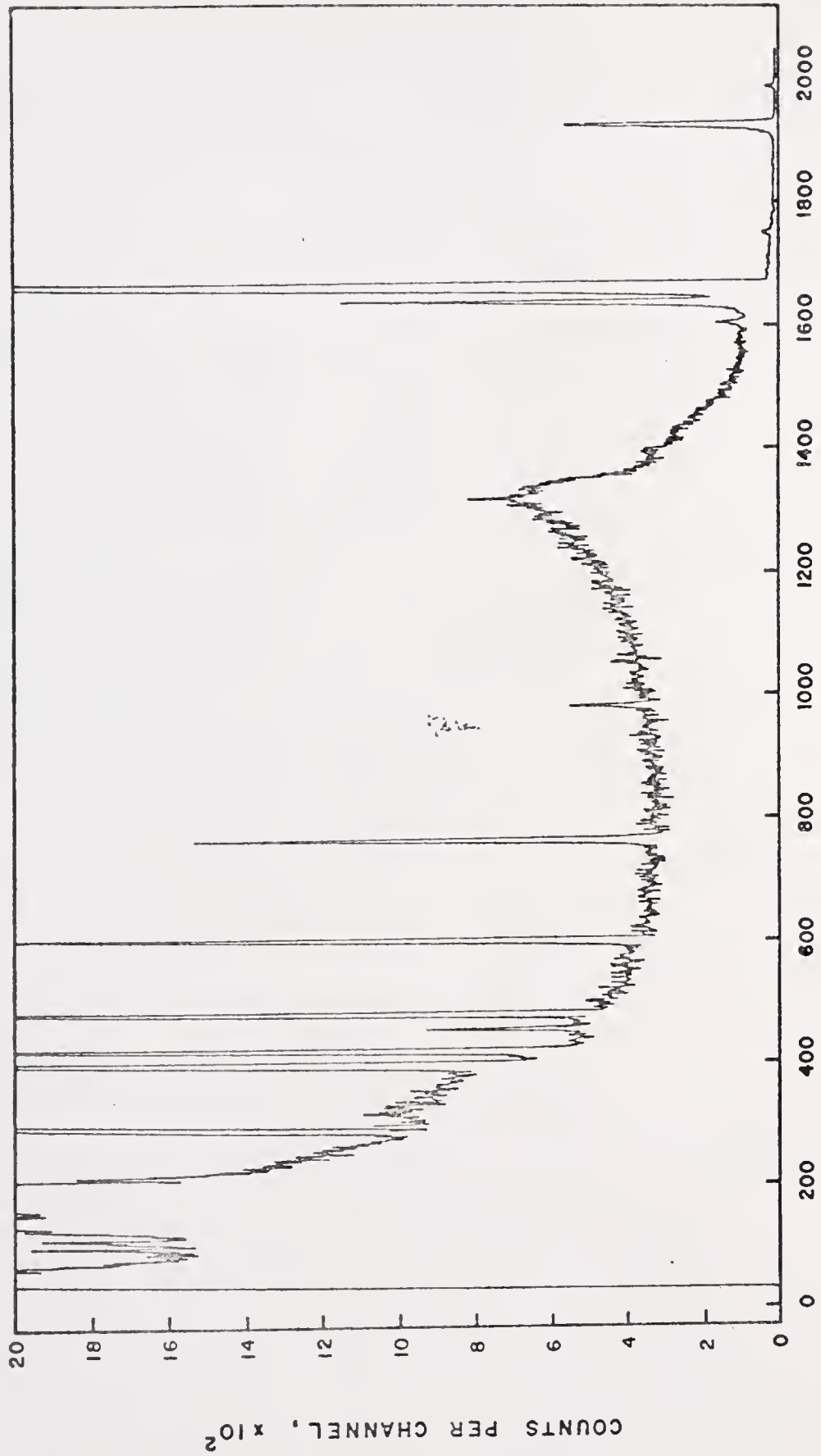


Figure 21. Plot of spectrum 6, unattenuated. The full energy range of the spectrum is 0-1.378 MeV (0.624 KeV/channel)



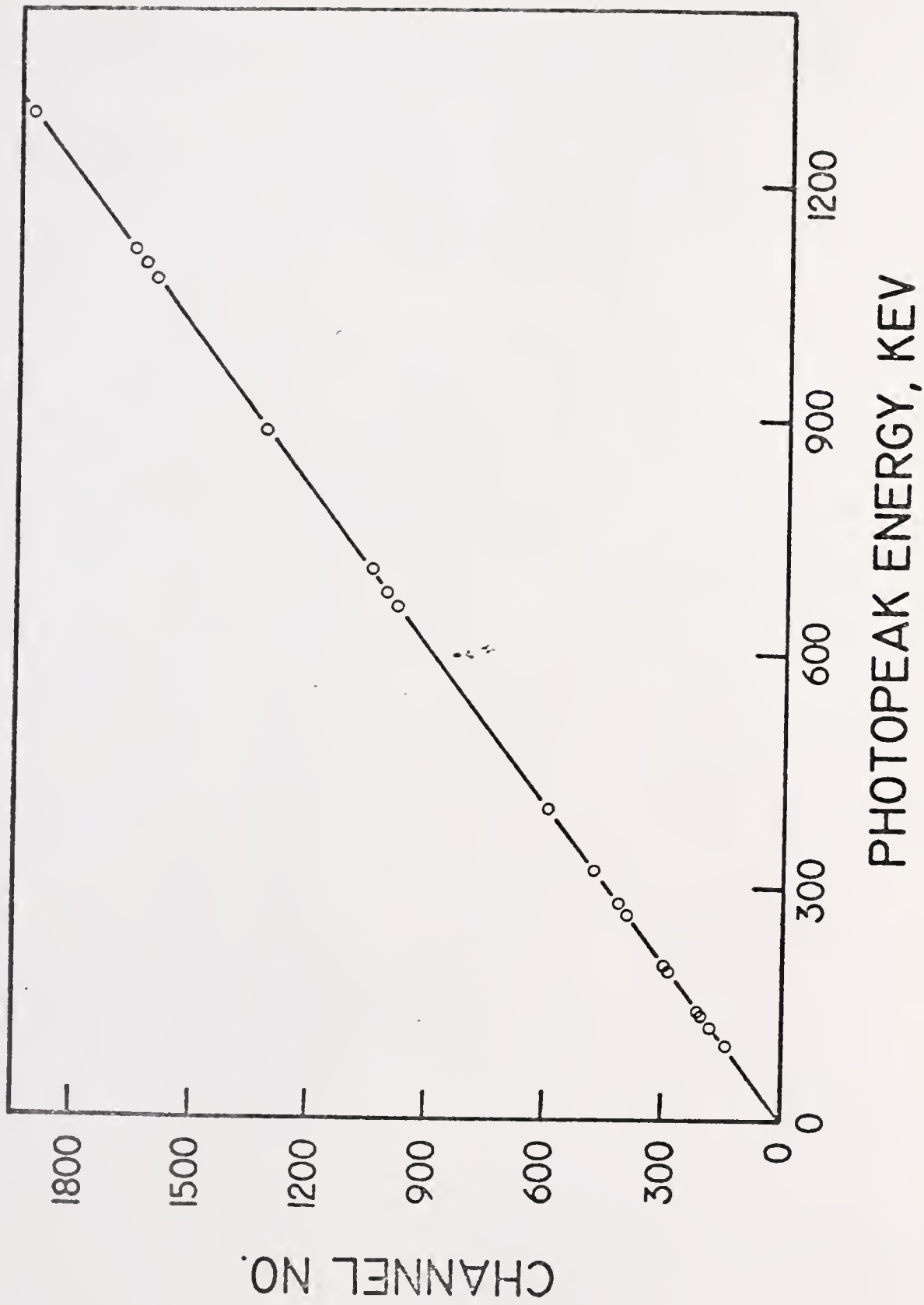
CHANNEL NO.

Figure 22. Plot of spectrum 6, attenuated by a factor of $(x 1/2)$. The full energy range of the spectrum is 0-1.378 MeV (0.624 KeV/channel)



CHANNEL NO.

Figure 23. Plot of channel number vs. photopeak energy for the full energy range used in the research (data obtained from spectrum 6)



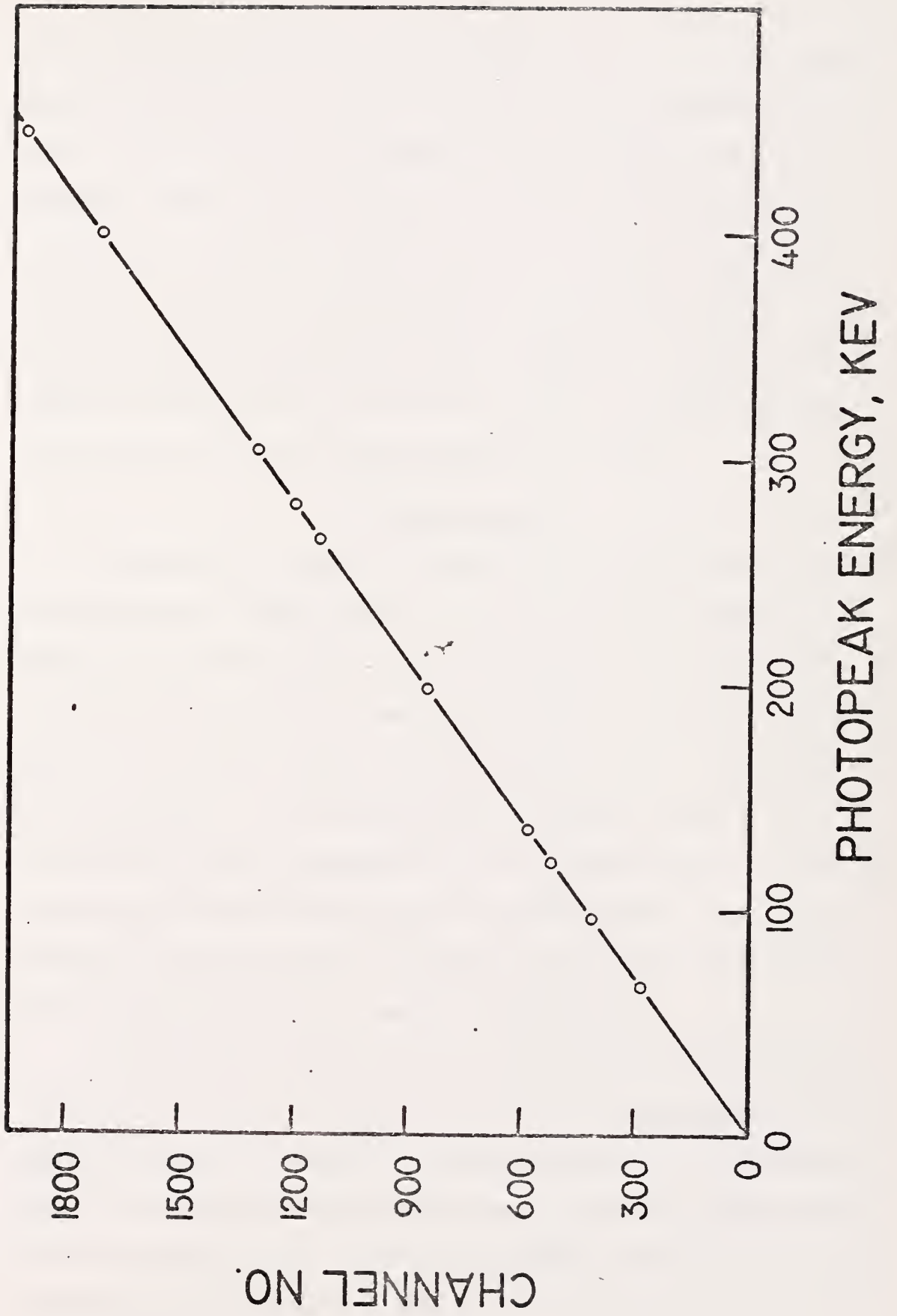
peak detection software and were given by the integral channel location of the peak maxima. The possible error in these values was therefore on the order of ± 1 channel. For this reason the standard deviation of 0.72 channel represented an excellent verification of the linearity of the data acquisition system over the total energy range, while channel zero was well within the error limits of the zero energy intercept, 0.37 ± 0.72 .

Figure 24 shows that this linearity was retained even when the spectrum energy range was decreased and the resolution of the ADC was increased by a factor of two. The least squares slope, zero energy intercept, and standard deviation were 4.30 channel/KeV, -5.47, and 1.27 channels respectively. The increased standard deviation was expected since the number of channels per unit of energy was increased by a factor of almost three. Therefore the measured error of only ± 1.27 channels again demonstrated the excellent linearity of the system. The non-zero value of the zero energy intercept was not significant since it represented only a relative point from which the ADC measured the pulse-height. The zero intercept setting of the ADC was adjustable electronically and was set as close to zero as possible. Once set, however, further adjustment proved unnecessary, even when the resolution was changed, as shown by the results above.

The system stability was demonstrated by comparing the slopes of the linearity curves calculated from the first six spectra. These spectra were collected on six different days, but under identical experimental conditions. The six spectra had a mean slope of 1.48 channel/KeV and a standard deviation of 0.001 channel/KeV, only ± 0.07 of the mean.

The resolution of the Ge(Li) detector was shown to be a linear

Figure 24. Plot of channel number vs. photopeak energy for the low energy region
(data obtained from spectrum 10)



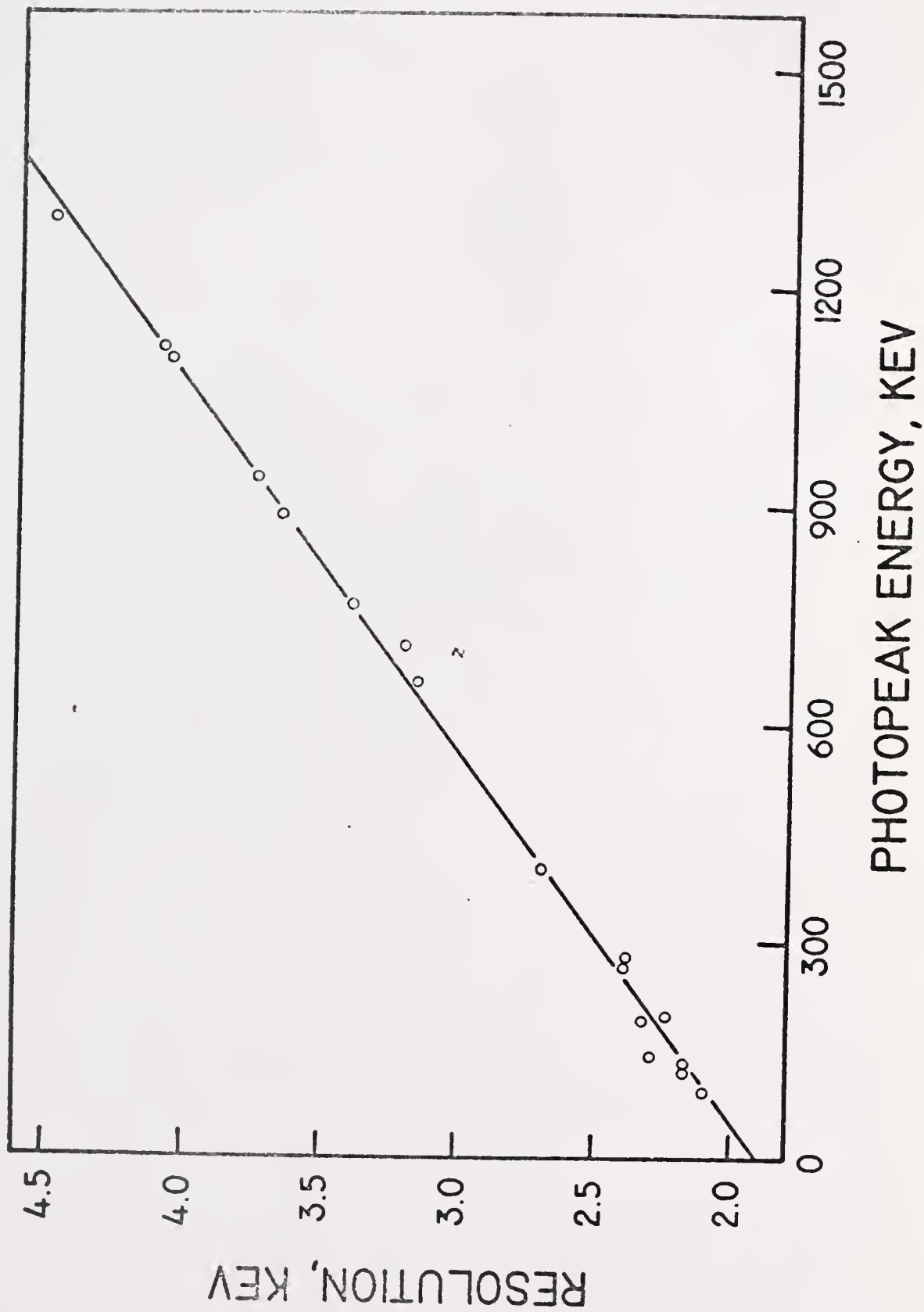
function of gamma-ray energy over the region of interest. The resolution values were calculated from the digital data. The peak height was measured relative to the left peak boundary and the value of the full width at half maximum was obtained by interpolating between two data points on either side of the peak. The width, in channels, was then converted to an energy value by using the channel/KeV value of the spectrum. Data from all eleven spectra were used to evaluate the linear function, with the results shown in Figure 25. The linear least squares analysis yielded a slope of 2.0×10^{-3} , a standard deviation of 0.05 KeV, and a zero energy intercept of 1.9 KeV.

Data Smoothing

To evaluate the effect of smoothing on the digital data, the eleven spectra were smoothed by the method of Savitsky and Golay (41), using the weighting constants for a quadratic-cubic polynomial fit. As Yule (44) suggested, the number of points in the smooth was determined by the number of data points in the full width at half maximum of the photopeaks. Since this number, as shown by Figure 25, was essentially constant throughout any of the sample spectra, the smoothing interval was held constant over the entire spectra. Spectra 1-6 required a five point smooth; spectrum 10, nine points; spectrum 11, eleven points; and spectra 7 and 8, thirteen points.

From the eleven sample spectra listed in Table I, ninety-seven photopeaks, ranging in peak area (corrected for background) from 115 to 142,202 counts, were selected to evaluate the effect of the smoothing. Using the photopeak boundaries determined by the peak search routines, the total spectrum areas beneath the smoothed photopeaks (including the background contribution) were compared to the total areas in the raw

Figure 25. Plot of the resolution of the experimental system vs. photopeak energy for the full energy range used in the research (data obtained from all eleven sample spectra)



data. These ninety-seven values had a mean of 100.08% and a standard deviation of only 0.39%. This clearly indicated that the total areas beneath the photopeaks were not degraded by the smoothing process, when the above smoothing criteria were used.

In the regions between photopeaks, however, the effectiveness of the smoothing was clearly evident. Using spectrum 6 as an example, several of these baseline regions were compared before and after smoothing. As expected the average minimum to maximum height of the statistical fluctuations was reduced 25-50%. The total areas beneath the baseline regions were relatively unchanged by the smooth, with results similar to the total areas above.

The difference in the total spectrum area and the peak area was due to the trapezoidal area representing the Compton and background contributions. The trapezoid area was determined exclusively by the location and contents of the boundary channels, as shown by Figure 2. Therefore the choice of the boundary channels was critical for accurate calculations.

Peak detection method two, previously described in the theory section, was designed to locate the integral channel locations of the minima on either side of the peak maximum. As the two peaks in Figure 26 illustrate, selection of the boundary channels was often influenced more by statistical scatter than by the true spectral minima created by the photopeak. Since this scatter was more pronounced in the wings of a peak, the boundary locations in unsmoothed data were strongly influenced by the statistical nature of a gamma-ray spectrum.

The sharp minima created by the "noise" spikes were generally at a lower activity than the true value of the spectral curve at that channel.

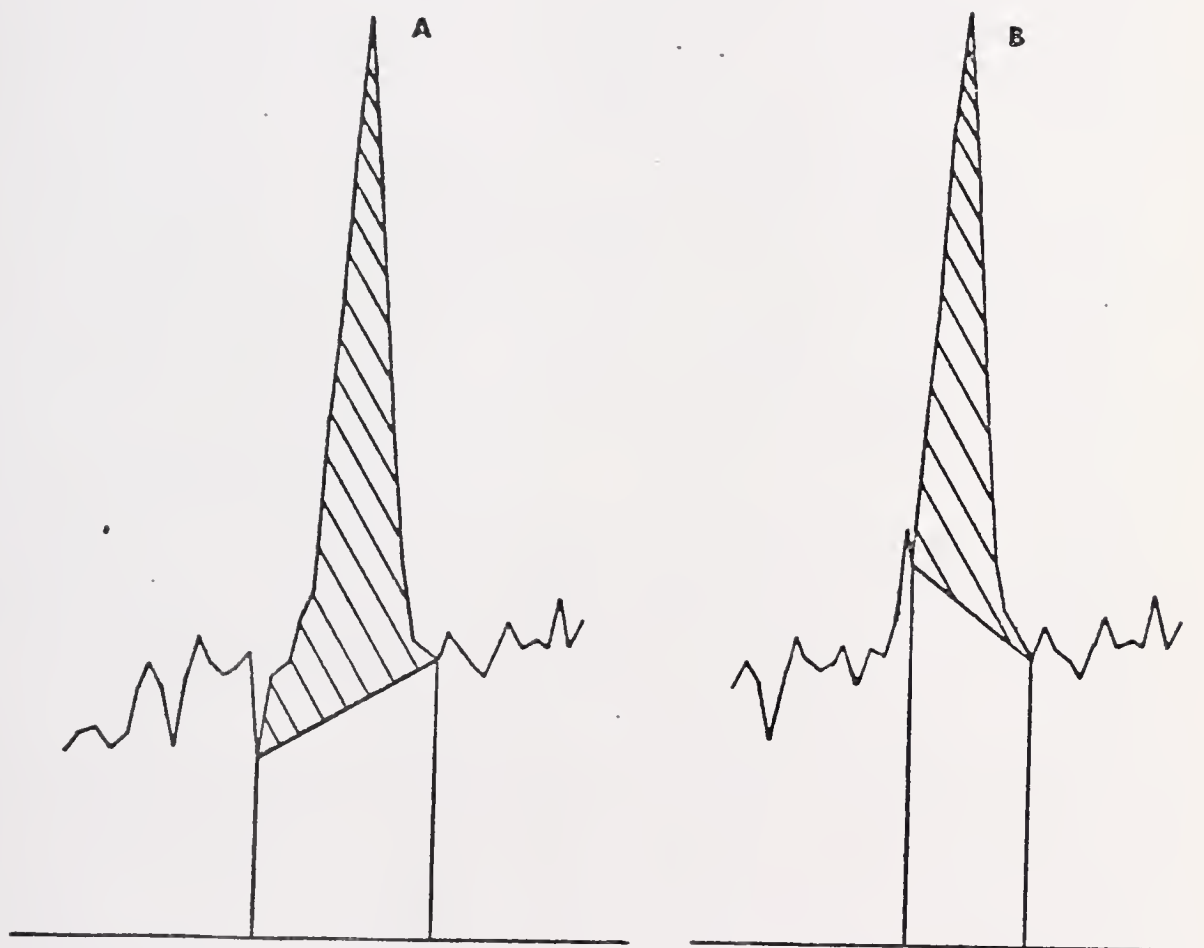


Figure 26. Effects of the statistical scatter on the total peak area, resulting in too large (peak A) or too small (peak B) a quantitative area

Peak A in Figure 26 illustrates the problem encountered when the boundary location, as determined by a digital minimum, corresponded closely to the channel location of the true photopeak minimum. Since the activity in this left boundary channel was lower than the true spectral curve, the trapezoid area was too small, resulting in too large a peak area.

Peak B in Figure 26 illustrates a more frequently occurring problem. A false minimum, due to counting statistics, was detected between the true photopeak minimum and the peak maximum. The activity in this channel was therefore too high, resulting in too large a background correction and too small a peak area.

In either of the above cases smoothing contributed to more accurate peak areas. The suppression of noise spikes helped eliminate undesired minima in the digital data. This led to the selection of boundary channels which were closer to the true photopeak minima and helped to bring the activity in these channels closer to the true spectral curve.

In order to examine the two problems illustrated in Figure 26, 67 of the original 97 peaks were again analyzed. These peaks were located by the second peak detection method in both the smoothed and unsmoothed sample spectra, and were wide enough to allow quantitation by a nine-point Wasson method. The 67 peak areas were first determined from the original, unsmoothed spectra by both the total peak area (TPA) method and the Wasson method. A second set of areas was determined from the smoothed spectra. Each smoothed peak area was then compared to the corresponding raw peak area.

The 67 comparative values from the TPA method ranged from 87% to 128%, with a mean of 105.26% and a standard deviation of 19.71%. The 67 Wasson values had a range of 90% to 112%, a mean of 102.42%,

and a standard deviation of 9.83%. The TPA method yielded a wider range, a higher mean, and a larger standard deviation. This was expected since the Wasson method did not include an area contribution from the wings of the peak, where the statistical scatter was greatest. High mean values from both methods indicated that the scatter in the unsmoothed spectra contributed to high baselines, as illustrated by peak B in Figure 26, and therefore to lost quantitative information.

Based on the above results it was concluded that smoothing of the digital data before searching the spectra and analyzing the photopeaks was highly advantageous. The total spectrum area was unaffected, but the accuracy of the final peak area was improved by as much as 28%. These conclusions were based on the assumption that the correct smooth was performed.

Peak Detection

The peak detection software developed for this research was designed to locate all valid peaks, even when the peak-to-noise ratio was small. The detection routines were also written to operate on a small, laboratory computer, with limited core space and a relatively long cycle time. For these reasons the peak recognition criteria were kept to a minimum. As Mills (54) suggested, the operator could easily reject undesired information when the routines located an invalid pseudo-peak.

Method two, the major detection routine, was based on the first derivative technique described by Yule (51), and was discussed in the theory section. This method assumed that the first derivative was continuous throughout the peak and successfully located most peaks in a smoothed spectrum. However the routine failed to locate peaks which

contained false minima, caused by statistical scatter, in the central peak region.

To aid in locating these peak shapes, illustrated by the second peak in Figure 1, method one was developed. This peak detection method required that the first minimum to maximum height in a peak exceed the average height of the noise in the 40 channels preceding the peak. Except for this requirement all other peak detection criteria, such as a minimum peak-to-noise ratio, were similar to method two.

Table II lists the results of the computer searches performed on the eleven sample spectra. All possible photopeak energies emitted by the six pure isotopes mentioned earlier were obtained from the literature (85-87). Each search routine was performed on both smoothed and raw spectra, and the validity of each peak was verified by a visual check of the data and spectral printouts. The dash signifies the absence of the isotope from the sample. Those photopeaks which were known to exist, but were too weak to form a valid peak in the digital data (as confirmed by the visual check), and therefore were not sensed by the peak detection routines, are designated by the letter A. Valid peaks which were detected by at least one of the search routines are labeled by a letter C, while those which were overlooked by the software, but were actually present in the spectra, are designated by the letter E. The D label indicates that the peak was missed by method two, but was found by method one. The B label refers to peaks which were located by the software searches but were too small to be found by the visual check.

Only three of the 120 possible peaks were not detected by the computer search routines. Two of these, the 303.89 KeV ^{75}Se peak

TABLE II

COMBINED RESULTS OF THE AUTOMATED PEAK SEARCHES

ENERGY (KeV)	ISOTOPE	PERCENT RELATIVE INTENSITY	SPECTRUM NUMBER										
			1	2	3	4	5	6	7	8	9	10	11
66.05	Se - 75	1.4	-	-	-	-	-	C ^c	C	-	C	C	-
96.73	Se - 75	4.8	-	-	-	-	-	C	C	-	C	C	-
121.13	Se - 75	29.2	-	-	-	-	-	C	C	-	C	C	-
136.00	Se - 75	96.0	-	-	-	-	-	C	C	-	C	C	-
142.45	Fe - 59	1.4	-	-	C	-	C	C	E ^e _d	-	-	-	-
192.23	Fe - 59	4.4	-	-	C	-	C	C	D ^d	-	-	-	-
198.60	Se - 75	2.3	-	-	-	-	-	C	C	-	C	C	-
264.65	Se - 75	100.0	-	-	-	-	-	C	C	-	C	C	-
279.52	Se - 75	41.3	-	-	-	-	-	C	C	-	C	C	-
303.89	Se - 75	2.1	-	-	-	-	-	E	D	-	D	C	-
320.08	Cr - 51	100.0	-	-	-	-	-	C ^a	C	-	-	-	-
334.81	Fe - 59	0.4	-	-	C	-	C	A ^a	A	-	-	-	-
400.64	Se - 75	19.2	-	-	-	-	-	C	-	C	C	C	-
446.20	Ag - ^f 110m	3.5	C	-	-	C	-	A	-	A	C	C	-
511.00	- _f	-	-	C	B ^b	C	C	C	-	C	-	-	-
620.10	Ag - 110m	2.9	C	-	-	C	-	A	-	A	C	-	C
657.60	Ag - 110m	100.0	C	-	-	C	-	C	-	C	C	-	C
677.50	Ag - 110m	12.2	C	-	-	C	-	B	-	-	E	-	C
686.80	Ag - 110m	7.4	C	-	-	C	-	A	-	-	C	-	C
706.60	Ag - 110m	17.2	C	-	-	C	-	C	-	-	C	-	C
744.20	Ag - 110m	4.4	C	-	-	C	-	A	-	-	C	-	D
763.80	Ag - 110m	24.0	C	-	-	C	-	A	-	-	C	-	C
817.90	Ag - 110m	7.8	C	-	-	C	-	A	-	-	C	-	C
884.50	Ag - 110m	79.6	C	-	-	C	-	C	-	-	C	-	C
937.30	Ag - 110m	36.5	C	-	-	C	-	A	-	-	C	-	C
1078.00	Rb - 86	100.0	-	-	-	-	-	C	-	-	-	-	-
1099.27	Fe - 59	100.0	-	-	C	-	C	C	-	-	-	-	-
1115.51	Zn - 65	100.0	-	C	-	C	C	C	-	-	-	-	-
1173.20	Co - 60	100.0	-	-	C	-	C	C	-	-	-	-	-
1291.58	Fe - 59	77.0	-	-	C	-	C	C	-	-	-	-	-
1332.50	Co - 60	100.0	-	-	C	-	C	C	-	-	-	-	-

^aThe element was present, but the signal was too weak to form a valid peak

^bA peak was located by the software, but was too small to be detected by a manual check.

^cA valid peak was detected by the software.

^dA valid peak was detected by method one, but was missed by method two.

^eA valid peak was missed by both software routines.

^fAnnihilation peak.

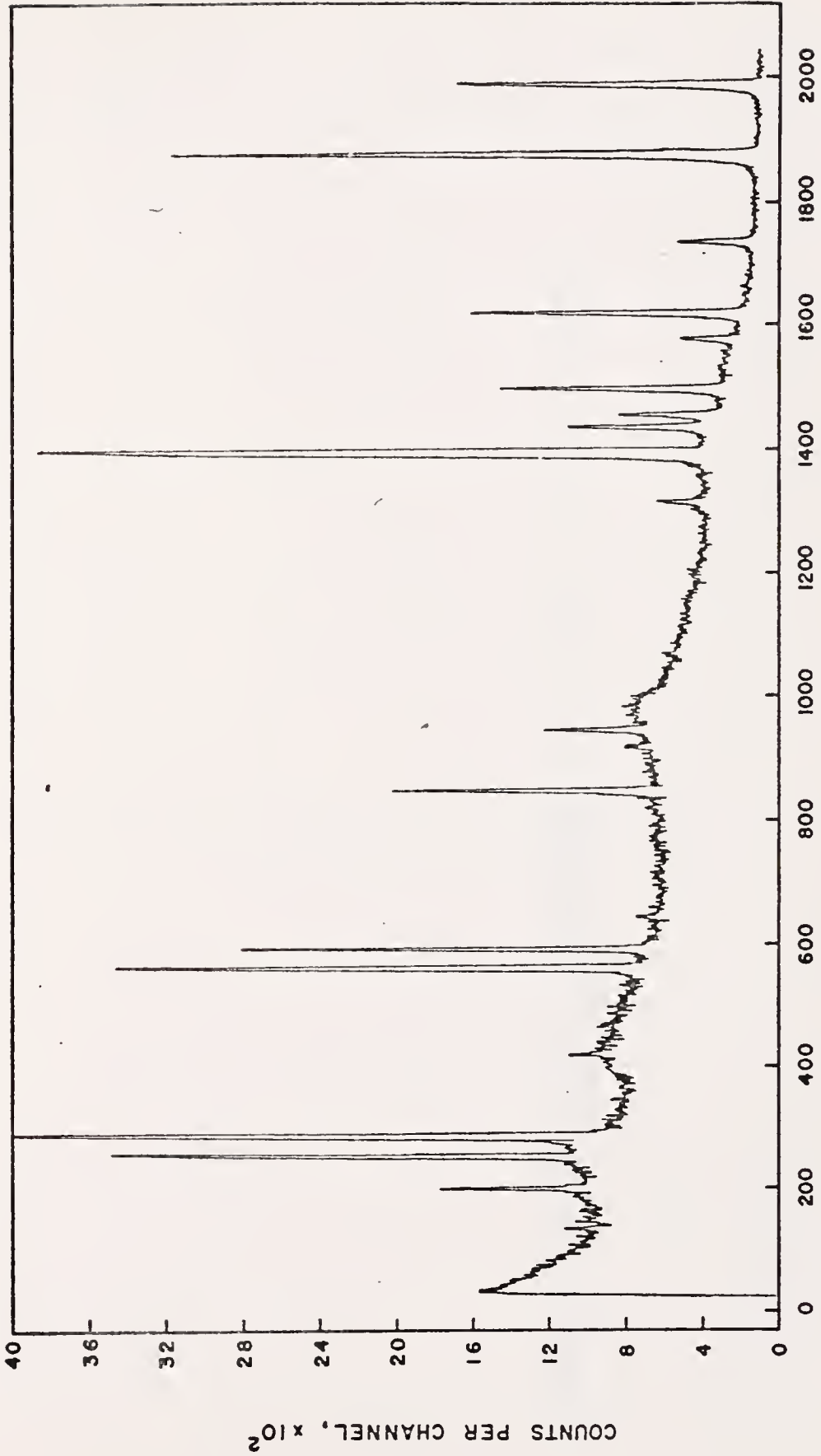
at channel 452 of spectrum 6 (Figure 22) and the 677.5 KeV $\text{Ag}^{110\text{m}}$ peak at channel 1437 of spectrum 9 (Figure 27), were relatively large, but they exhibited extensive scatter throughout. The number of statistical minima superimposed on these peaks was so large that the basic height criterion of method one was never met. The 142.45 KeV Fe^{59} peak at channel 860 of spectrum 7 (Figure 28) was included inside the boundaries of the large 136.00 KeV Se^{75} peak at channel 820 by method one.

Figure 28 also shows two examples of peaks located by method one but missed by method two. The 192.23 KeV Fe^{59} peak at channel 1165 and the 303.89 KeV Se^{75} peak at channel 1846 exhibited statistical minima throughout, even when properly smoothed. Figure 22 shows the apparent absence of a peak at channel 1006, although method one detected the presence of the 677.5 KeV $\text{Ag}^{110\text{m}}$ at that location. This indicated that, in some cases, the detection software was more sensitive to the presence of photopeaks than a visual search.

Although only six pure isotopes were used to prepare the samples, gamma-rays from seven radioisotopes were detected. The two Co^{60} photopeaks were found in all spectra which contained the Fe^{59} photopeaks. This was probably due to the initial β^- decay of the Fe^{59} during irradiation. The resulting stable Co^{59} was then partially irradiated to Co^{60} .

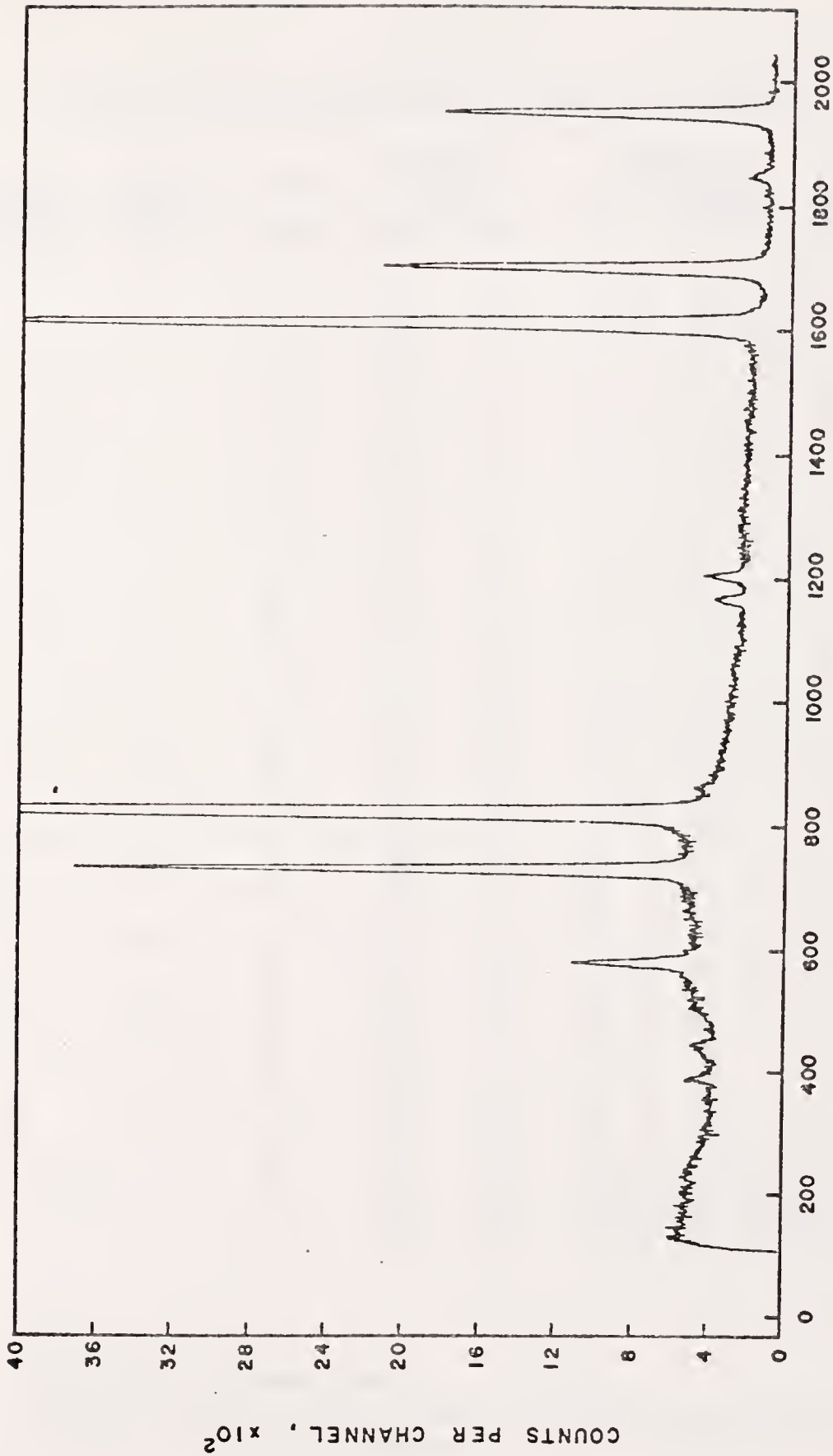
Table III gives the number of peaks detected by each of the search methods. No one method was mutually exclusive of the others. Best results were obtained by performing all four searches. Valid peaks were verified by a visual check of the spectra and a knowledge of the exact sample composition. Table III shows the greatly increased

Figure 27. Plot of spectrum 9, unattenuated. The full energy range of the spectrum is 0-965 KeV (0.471 KeV/channel)



CHANNEL NO.

Figure 28. Plot of spectrum 7, unattenuated. The full energy range of the spectrum is 0-337 KeV (0.165 KeV/channel)



CHANNEL NO.

TABLE III

NUMBERS OF PEAKS FOUND BY THE AUTOMATED PEAK SEARCHES

SPECTRUM NUMBER	NUMBER POSSIBLE PEAKS	MINIMUM (P/N) ^a	COMBINED SEARCHES		METHOD ONE				METHOD TWO			
			TOTAL ^b	VALID ^c	RAW		SMOOTH		RAW		SMOOTH	
					T ^b	V ^c						
1	11	2	34	11	17	11	29	11	13	11	19	11
		3	12	11	12	11	13	11	11	11	12	11
		4	13	11	10	10	12	11	10	10	11	11
2	2	2	18	2	5	2	13	2	4	2	11	2
		3	4	2	2	2	4	2	2	2	2	2
		4	3	2	2	2	3	2	2	2	2	2
3	8	2	29	8	15	8	23	8	7	6	13	6
		3	10	7	8	7	9	7	7	6	6	6
		4	9	7	7	7	9	7	6	6	6	6
4	13	2	35	13	18	13	32	11	10	10	16	13
		3	15	13	13	13	13	11	10	10	12	12
		4	13	12	9	9	12	11	9	9	12	12
5	9	2	29	9	15	9	23	8	11	8	15	8
		3	12	9	9	9	11	8	8	8	8	8
		4	9	8	8	8	8	7	7	7	7	7
6	23	2	27	22	18	17	22	19	20	18	19	19
		3	20	19	17	16	17	16	15	15	17	17
		4	18	18	17	17	14	14	14	14	15	15
7	11	2	51	10	19	9	40	8	6	4	16	8
		3	22	10	11	10	20	8	4	4	8	8
		4	14	10	9	9	12	8	4	4	8	8
8	3	2	32	3	12	3	24	2	2	0	12	3
		3	23	3	3	3	22	2	0	0	4	3
		4	14	3	3	3	14	3	0	0	2	2
9	20	2	33	19	23	18	27	17	19	18	20	17
		3	18	18	17	17	16	16	16	16	17	17
		4	16	16	17	17	16	16	16	16	16	16
10	10	2	38	10	16	9	29	8	5	4	23	10
		3	14	10	9	9	12	8	4	4	11	10
		4	10	9	7	7	8	7	4	4	8	8
11	10	2	47	10	11	10	43	8	3	2	21	9
		3	24	10	9	9	22	8	1	1	11	9
		4	11	10	8	8	9	8	1	1	10	9
Total 120		2	373	117	169	109	305	102	100	83	185	106
		3	174	112	110	106	159	97	78	77	108	103
		4	130	106	97	97	117	94	73	73	97	96

^aPeak-to-noise ratio^bTotal number of peaks found^cNumber of valid peaks found, where the validity was determined by a visual search of the spectrum

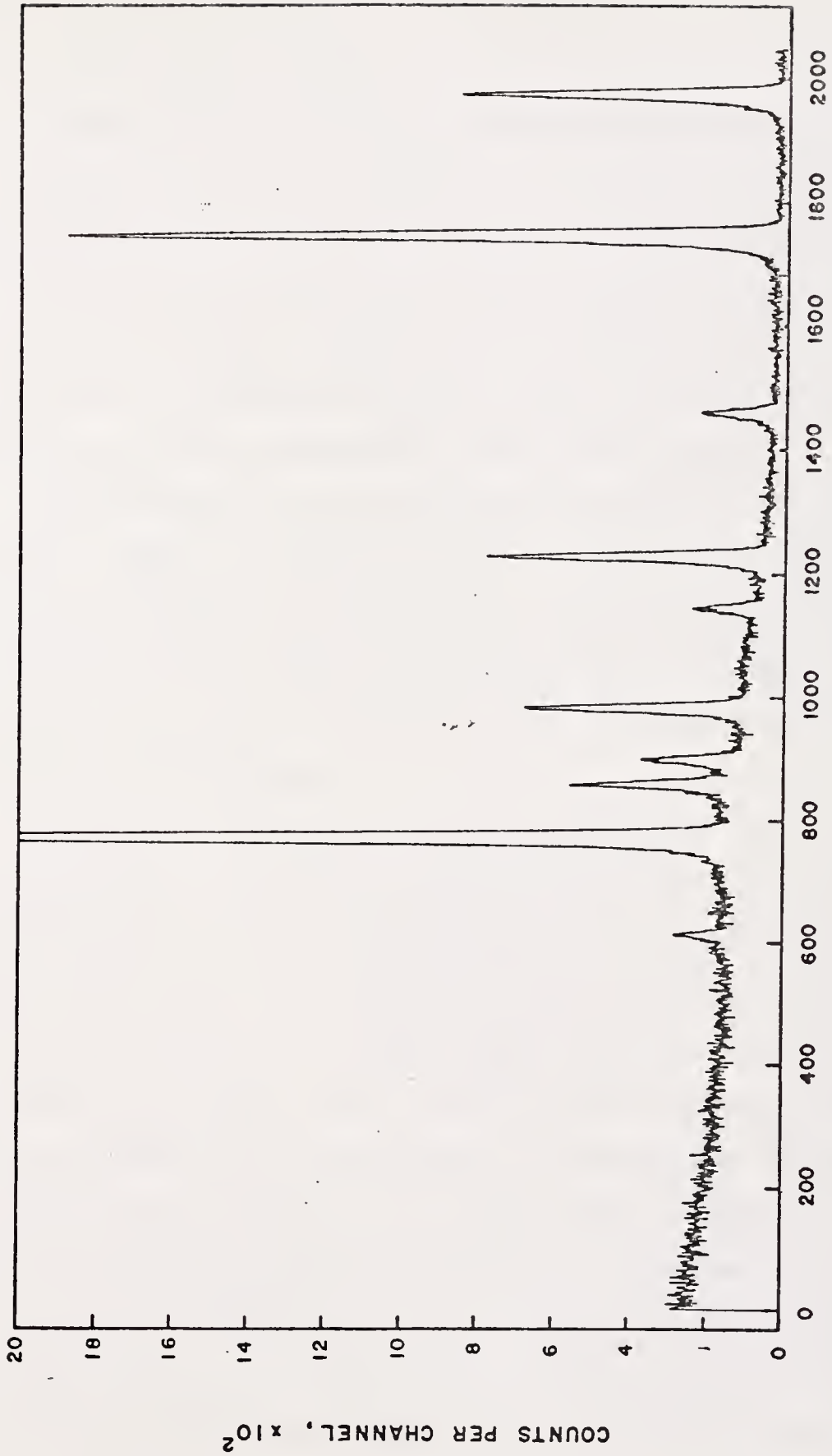
efficiency of method two with the smoothed data. This was especially notable in spectra 7 (Figure 28), 8, 10, and 11 (Figure 29), where the increased ADC resolution and decreased energy range resulted in broader peaks and significantly greater scatter throughout the peak region.

Table III also shows the effect of changing the major peak detection criterion, the minimum allowable peak-to-noise ratio (P/N). As this value was increased from two to four, the number of pseudo-peaks located by the search routines was greatly reduced. This was accomplished, however, by reducing the ability of the computer routine to detect small, valid peaks.

The peak search routines also selected the peak boundary channels. As noted before, these channels played a very important role in the determination of the photopeak area. Method two was designed to select the first minima on either side of the peak maximum. It has been previously shown that, with proper smoothing, these minima were usually relatively close to the true spectral minima, both in location and content. Method one, however, used different detection criteria which often resulted in the selection of different peak boundary channels which were further from the peak maximum.

Ninety-three common peaks were detected in the eleven smoothed spectra by both methods. The two peak detection methods selected different boundaries for 39 (42%) of these 93 peaks. Of the 39 peaks with different boundaries, 37 (95%) had a different left boundary while only 19 (49%) had a different right boundary. As previously discussed the selection of the left boundary by method one was critical to the final choice of the right boundary. This was verified by the fact

Figure 29. Plot of spectrum 11, attenuated by a factor of $(x 1/2)$. The full energy range of the spectrum is 477-955 KeV (0.233 KeV/channel)



CHANNEL NO.

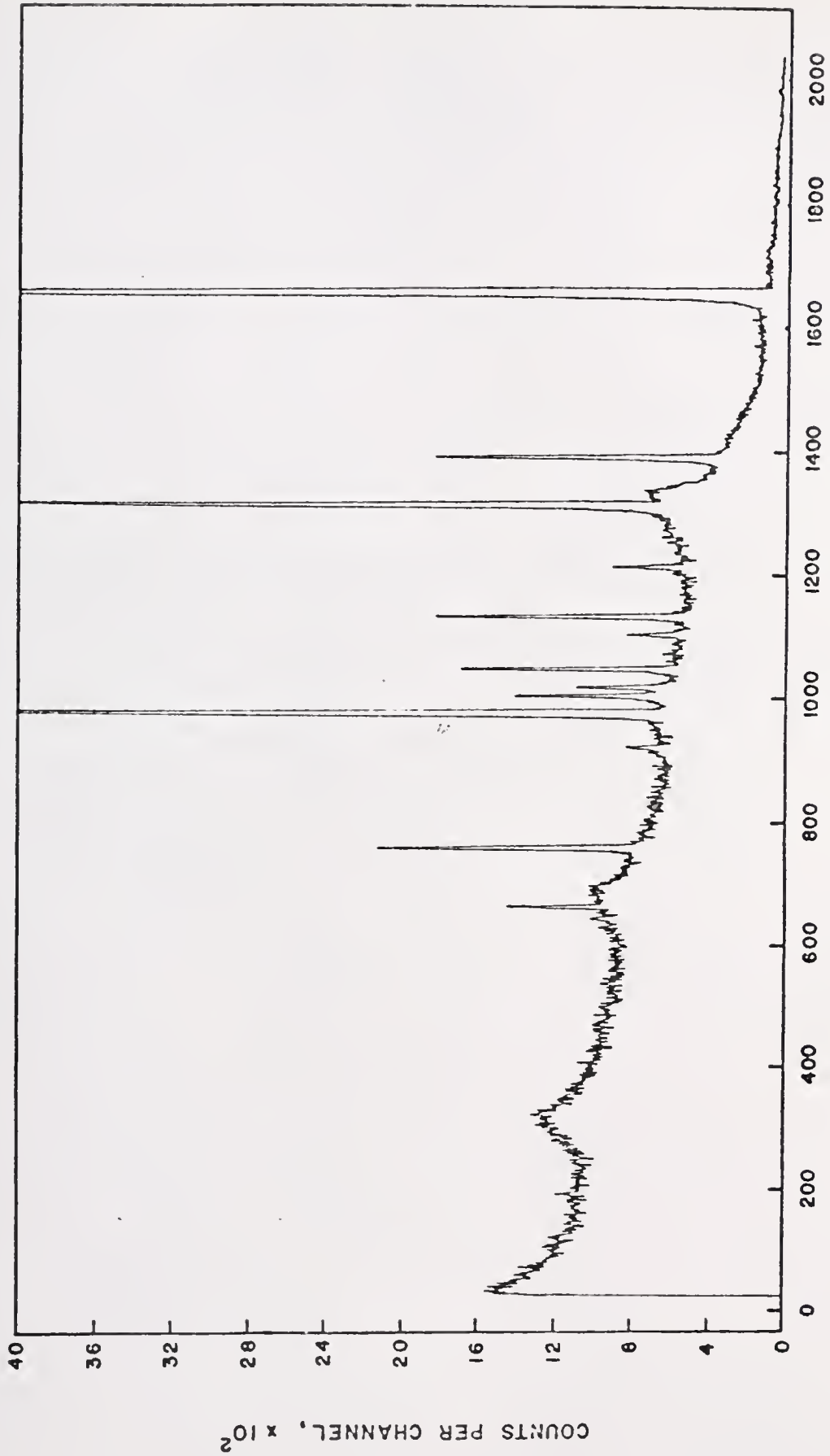
that only two peaks, selected by method one, had the same left boundary but a different right boundary.

Thus the selection of the left boundary by method one was critical to the entire peak detection process. Unfortunately this selection process was strongly influenced both by the slope of the Compton upon which the peaks were located and by overlapping peaks which created large background bases. These problems not only led to the selection of erroneous peak boundaries, but also resulted in the inclusion of more than one peak maximum within a set of peak boundaries.

A few examples of the overlap problem were found in the sample spectra. Method one detected the 136.00 KeV Se⁷⁵ peak at channel 202 of spectrum 6 (Figure 21), but the left boundary at channel 108 included both the 96.73 and 121.13 KeV Se⁷⁵ peaks. In the same spectrum the left boundary of the 1115.51 KeV Zn⁶⁵ peak at channel 1658 included the 1099.27 KeV Fe⁵⁹ peak.

The large positive slopes associated with Compton edges also created problems for method one. The 884.5 KeV Ag^{110m} peak at channel 1315 of spectrum 6 (Figure 22) was assigned a left boundary at channel 1055, near the base of the Compton edge. The slope of the spectral curve was so large that the initial height criterion of method one was satisfied by the Compton edge. Once this occurred, however, a right boundary minimum, whose absolute height was comparable to the left boundary, was not detected until the Compton edge was passed. A similar situation occurred in spectrum 4 (Figure 30). Method one again detected the 884.5 KeV Ag^{110m} peak at channel 1315, with a left boundary at channel 1198. In this case, however, the left boundary included the 817.9 KeV Ag^{110m} peak at channel 1215. In each of the above cases,

Figure 30. Plot of spectrum ^4_2He , unattenuated. The full energy range of the spectrum is 0.1.378 MeV (0.624 KeV/channel)



method two detected all the peaks with reasonable boundaries.

Curve Fitting

The technique of mathematically fitting a function to digital data has been used for many years to determine both the peak maximum and the photopeak area in gamma-ray spectra. The accuracy of this method is greatly influenced by the choice of the functional form. It is common knowledge that the major component of the photopeak shape in a Ge(Li) spectrum is Gaussian, but Routti and Prussin (56) explained that this does not completely describe the total peak shape.

Although many researchers have proposed fitting functions, no two have agreed on an exact form. The majority of the functions, however, have skewed a central Gaussian with an exponential contribution to approximate the low energy tail common to most photopeaks in a Ge(Li) spectrum. Sanders and Holm (66) observed that the only true test of the functional form was how well it approximated the digital data. Tominaga and co-workers (43) stated that smoothing was often unnecessary for curve fitting, but Mills (54) observed that the smoothed spectra gave better estimates of the initial parameters of the fitting function.

The function chosen for this research was an empirical form of a Gaussian skewed by a leading exponential tail. These two major components were smoothly combined by an arctangent joining function. The eight parameters of this three function convolute have been discussed in a previous section. The final functional form was similar to that used by Chesler and Cram (84) in their studies with gas chromatographic peaks. The conversational computer language FOCAL was used to program the fitting function. The mathematical basis for this least squares technique was explained in the theory section, and the FOCAL programs

are listed in Appendix II.

Once a peak was chosen for fitting, an appropriate block of integer data was converted to floating point and stored in memory locations accessible by the FOCAL compiler. Whenever possible at least twenty to forty baseline points were included on either side of the photopeak. The number of data points in the peak ranged from 10 to 57 points.

The solving of the square matrix (equation 6) constituted the major portion of the computational time. Each additional parameter substantially increased this time, with the eight parameter function requiring six to eight minutes per iteration. For this reason a four parameter polynomial was fitted separately to the baseline data points. The boundaries selected by the peak detection routines were used as guidelines, and all points within these boundaries were excluded from the baseline calculation.

Using the basic fitting program, the polynomial approximation of the baseline was determined. Only the constant parameter was initially approximated, with all others being initially set to zero. No more than three iterations were ever necessary to obtain the best possible fit, and each iteration required approximately one minute.

The calculated baseline was then extended through the peak and subtracted from the original digital data. The result was an estimate of the pure photopeak shape, resting on a flat, zero baseline. The data was positive throughout the peak area and oscillated about zero in the regions of pure baseline. The first negative value on either side of the central peak was therefore used to determine the boundaries for the peak fit. All data within, but not including, these boundaries

were used to evaluate the eight parameters of the fitting function.

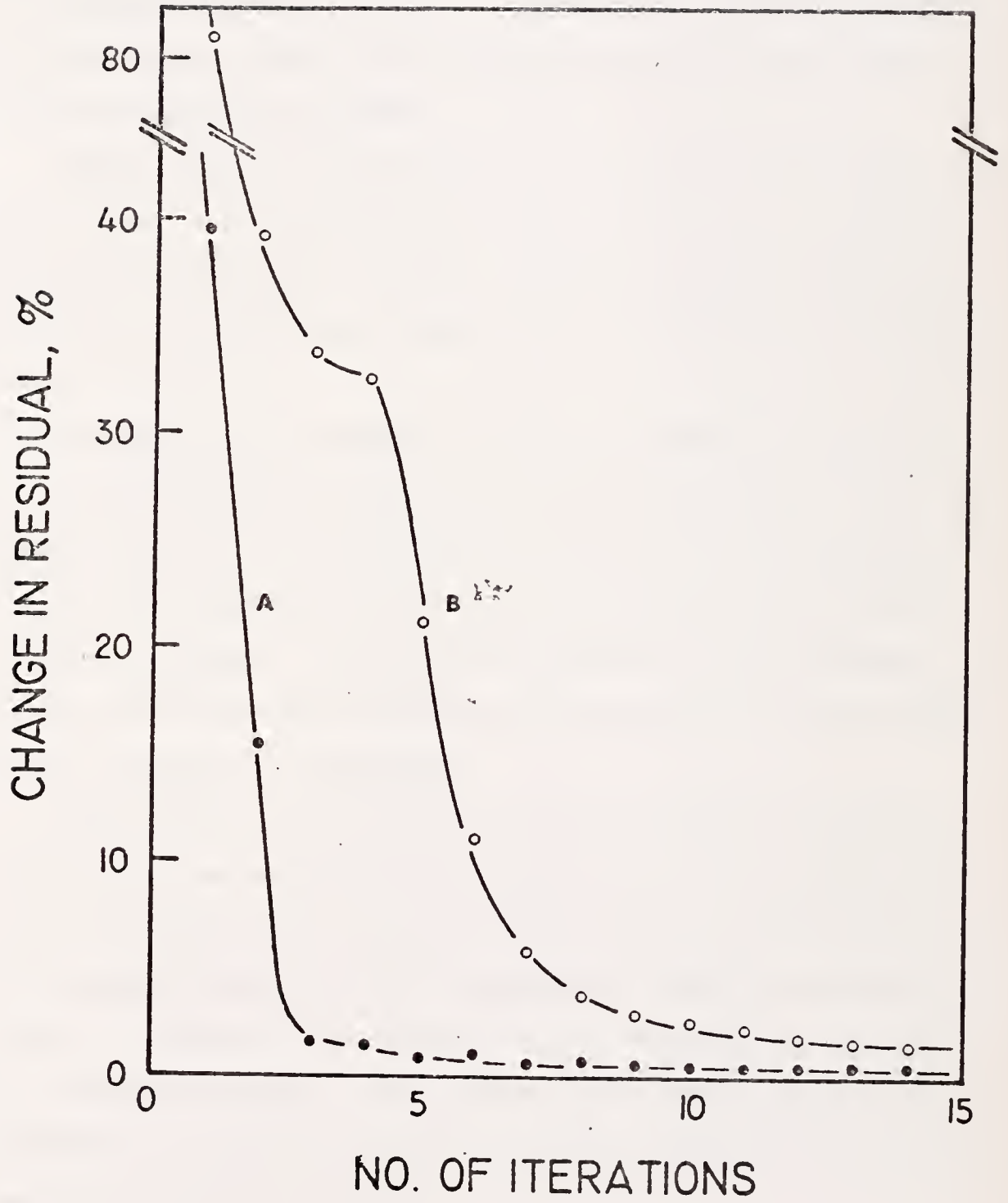
The original estimate of P_1 was obtained directly from the data. The initial values of P_2 , P_3 , P_4 , P_5 , and P_8 were normally set to 3.0, -1.5, 0, 1.0, and -1.5 respectively. The estimates of P_6 and P_7 depended upon the actual shape of the peak, but were between zero and one.

The abscissa values were expressed in sigma units, the standard deviation of the central Gaussian. To determine the X_1 values in the fitting function, the right side of the peak was assumed to be pure Gaussian in shape. The number of abscissa points from the peak maximum to the right boundary was therefore assumed to be equal to three sigma units. With this estimate the values of the increment (IN) and the initial abscissa value in the fitting interval (X_0) were determined.

A measure of the improvement in the fit following each iteration was determined by the percent change in the calculated residual sum of squares. Figure 31 shows a plot of this percent change versus the number of iterations performed for two of the peaks fit. These curves illustrate that a sharp decrease in the early iterations was followed by a gradual change in the latter calculations. The shoulder on curve B in Figure 31 indicated that the fitting process passed through a local minimum in the residual sum of squares. A point was quickly reached, however, where the improvement gained by the iteration was not worth the time involved for the computation.

For the fitting program used in this research this crossover point was judged to be either ten iterations or a percent change of less than 5% in the residual sum of squares. The absolute values of the residuals were not used in this consideration because they were

Figure 31. Plot of the percent change in the residual sum of squares vs. the number of iterations performed in the curve fitting process



found to be dependent upon the peak size, the amount of scatter present, the number of points in the fitting interval, and the values of the initial parameter estimates. In Figure 31, curve A had initial and final residual values of 3300 and 1552, respectively, while curve B fell from 4,415,190 to 126,069.

Table IV lists the percent change in the residual sum of squares for the first, tenth, and final iteration for each peak fit. Table IV shows the large reduction in the first iteration and the fact that the majority of the peaks showed a change of less than 5% within ten iterations.

To demonstrate the validity of the fitting procedure, 35 peaks of all sizes and shapes were chosen from the eleven sample spectra. The digital data were fit as described above, and the curve was evaluated at each point by adding the contribution from the peak to that of the background polynomial. The spectral data displayed in the following figures are the raw curves and the fitted functions with the latter offset for the purpose of illustration.

Table V lists the location, size, and background shape for each of the peaks. The peak heights were taken from the final P_1 values of the fitted functions while the average noise heights were calculated from the baseline region of the fitting interval immediately preceding the peak. The peak-to-noise ratios (P/N) were calculated from these two values and represent a dynamic range of 500. The descriptions of the baselines pertained to the relative shape and slope of the baseline immediately surrounding the peaks.

Table VI lists the complete fitting information for each of the peaks. The calculation of the increment, in sigma units, was discussed

TABLE IV

PERCENT CHANGE IN THE RESIDUAL OF THE CURVE FITTING FUNCTION

<u>PEAK</u>	<u>ITERATION</u>		
	<u>FIRST</u>	<u>TENTH</u>	<u>FINAL (#)</u>
1	72.1	4.0	4.0 (10)
2	81.1	2.5	0.2 (39)
3	47.9	7.8	1.1 (23)
4	82.0	3.7	3.7 (10)
5	89.8	0.9	0.9 (10)
6	18.1	1.3	1.3 (10)
7	19.9	1.6	1.6 (10)
8	62.6	5.7	5.7 (10)
9	23.4	6.2	6.2 (10)
10	82.8	0.3	0.3 (10)
11	33.9	0.4	0.4 (10)
12	13.0	-	3.8 (5)
13	17.3	1.3	0.7 (15)
14	73.3	-	1.1 (6)
15	22.8	11.4	0.0 (60)
16	32.6	-	1.3 (6)
17	60.0	3.5	3.5 (10)
18	57.1	-	1.7 (8)
19	46.2	9.7	9.7 (10)
20	30.9	1.5	1.5 (10)
21	51.7	-	0.6 (9)
22	29.6	-	1.1 (8)
23	19.0	-	0.2 (6)
24	2.0	-	2.0 (1)
25	7.0	-	0.6 (3)
26	43.2	-	3.9 (7)
27	39.5	0.5	0.4 (16)
28	15.3	0.0	0.0 (31)
29	40.2	0.0	0.0 (10)
30	53.6	0.6	0.6 (10)
31	50.4	-	1.2 (7)
32	50.7	-	0.2 (7)
33	54.6	0.2	0.2 (10)
34	86.0	0.8	0.8 (10)
35	57.9	0.1	0.0 (19)

TABLE V

DESCRIPTION OF PEAKS SELECTED FOR CURVE FITTING

PEAK	SPECTRUM		ISOTOPE	ENERGY (KeV)	PEAK HEIGHT ^a (COUNTS)	P/N ^b	BASELINE ^c
	NUMBER	CHANNEL					
1	2	1657	Zn - 65	1115.51	9329	944	Flat
2	1	1315	Ag - 110m	884.50	6120	323	Flat
3	9	1875	Ag - 110m	884.50	3588	159	Flat
4	1	1393	Ag - 110m	937.30	2835	154	Flat
5	9	1987	Ag - 110m	937.30	1538	87	Flat
6	11	1745	Ag - 110m	834.50	1734	97	Flat
7	7	1946	Cr - 51	320.08	1641	77	Flat
8	3	1633	Fe - 59	1099.27	9863	319	Steep Neg.
9	4	1393	Ag - 110m	937.30	1469	58	Steep Neg.
10	4	1315	Ag - 110m	884.50	3491	78	Steep Pos.
11	7	729	Se - ^d 75	121.13	2882	67	Slight Pos.
12	8	1063	- ^d	511.00	289	19	Flat
13	1	1216	Ag - 110m	817.90	715	15	Slight Neg.
14	9	1734	Ag - 110m	817.90	366	23	Slight Neg.
15	1	665	Ag - 110m	446.20	895	18	Steep Pos.
16	10	1716	Se - 75	400.64	645	20	Slight Pos.
17	4	1216	Ag - 110m	817.90	355	8	Slight Pos.
18	10	1917	Ag - 110m	446.20	240	9	Slight Pos.
19	9	1316	Ag - 110m	620.10	218	7	Slight Pos.
20	7	580	Se - 75	96.73	560	17	Compton Edge
21	10	410	Se - 75	96.73	343	8	Compton Edge
22	11	1459	Ag - 110m	817.90	175	14	Flat
23	11	613	Ag - 110m	620.10	112	5	Flat
24	7	1846	Se - 75	303.89	90	4	Flat
25	10	1301	Se - 75	303.89	65	2	Flat
26	6	1742	Co - 60	1173.20	24	4	Steep Neg.
27	5	1743	Co - 60	1173.20	163	8	Steep Neg.
28	11	1143	Ag - 110m	744.20	149	7	Slight Neg.
29	6	978	Ag - 110m	657.60	199	6	Slight Pos.
30	3	1743	Co - 60	1173.20	201	9	Steep Neg.
31	3	1743	Co - 60	1173.20	194	8	Steep Neg.
32	8	1959	Ag - 110m	657.60	52	3	Flat
33	6	1315	Ag - 110m	884.50	129	3	Steep Pos.
34	1	1008	Ag - 110m	677.50	1410	45	Steep Neg.
35	1	1022	Ag - 110m	686.80	862	27	Steep Neg.

^aObtained from the final P_1 value of the fitting function.

^bPeak-to-noise ratio.

^cGeneral description of the baseline shape and slope.

^dAnnihilation peak.

TABLE VI
INITIAL AND FINAL VALUES FROM THE CURVE FITTING CALCULATIONS

PEAK	INCREMENT	NUMBER OF		P_1	P_2	P_3	P_4	P_5	P_6	P_7	P_8
		POINTS	ITERATION								
1	0.375	46	0	10225	3.00	-1.50	0	1.00	0.50	0.50	-1.50
			10	9329	0.49	-1.67	0.032	0.67	0.65	0.48	-1.51
2	0.43	34	0	6440	3.00	-1.50	0	1.00	0.50	0.50	-1.50
			39	6120	0.67	-1.82	0.059	0.71	0.71	0.52	-1.39
3	0.30	30	0	3600	3.00	-1.50	0	1.00	0.20	0.50	-1.50
			23	3583	1.20	-1.30	0.169	0.76	0.42	0.46	-1.30
4	0.43	25	0	2778	3.00	-1.50	0	0.80	0.30	0.50	-1.50
			10	2835	1.16	-1.55	0.151	0.79	0.42	0.42	-1.31
5	0.333	29	0	1560	3.00	-1.50	0	1.00	0.25	0.25	-1.50
			10	1538	1.22	-1.21	-0.148	0.88	0.34	0.32	-1.88
6	0.167	57	0	1844	3.00	-1.50	0	1.00	0.25	0.50	-1.50
			10	1734	0.70	-1.31	-0.019	0.93	0.36	0.34	-1.81
7	0.17	52	0	1682	3.00	-1.50	0	1.00	0.01	0.10	-1.50
			10	1641	0.88	-0.004	0.020	1.05	0.03	1.08	-3.49
8	0.33	34	0	9880	3.00	-1.50	0	0.75	0.30	0.50	-1.50
			10	9863	1.19	-1.49	0.038	0.56	0.44	0.53	-1.30
9	0.43	21	0	1468	3.00	-1.50	0	1.00	0.10	0.25	-1.50
			10	1469	1.99	-1.12	0.042	0.86	0.20	0.34	-1.92
10	0.50	21	0	3411	3.00	-1.50	0	1.00	0.25	0.25	-1.50
			10	3491	1.28	-1.35	-0.069	1.00	0.28	0.30	-1.83
11	0.20	48	0	2963	3.00	-1.50	0	1.10	0.10	0.50	-1.50
			10	2882	0.11	-3.02	-0.018	1.15	0.07	0.16	-0.44
12	0.12	46	0	300	3.00	-1.50	0	1.10	0.10	0.10	-1.50
			5	289	1.35	-0.40	0.004	1.24	0.08	3.01	-2.37
13	0.50	16	0	750	3.00	-1.50	0	1.00	0.10	0.10	-1.50
			15	715	1.23	-1.37	0.046	0.92	0.22	0.27	-2.12
14	0.333	26	0	385	3.00	-1.50	0	1.00	0.10	0.10	-1.50
			6	366	0.99	-0.73	-0.152	0.86	0.13	0.27	-2.63
15	0.75	10	0	910	3.00	-1.50	0	1.00	0.25	0.50	-1.50
			60	895	6.25	-1.56	-0.034	1.26	0.29	0.70	-2.05
16	0.20	34	0	650	3.00	-1.50	0	1.00	0.10	0.25	-1.50
			6	645	14.21	-1.91	0.040	1.00	0.13	0.39	-1.87
17	0.30	19	0	370	3.00	-1.50	0	0.75	0.01	0.10	-1.50
			10	355	8.57	-1.36	-0.107	0.43	0.09	0.13	-4.24

Table VI continued

PEAK	INCREMENT	NUMBER		P_1	P_2	P_3	P_4	P_5	P_6	P_7	P_8
		OF POINTS	ITERATION								
18	0.20	19	0	225	3.00	-1.50	0	1.00	0.001	1.00	-1.50
			8	240	27.89	-1.22	-0.228	0.77	0.19	0.96	-1.70
19	0.60	11	0	202	3.00	-0.50	0	1.00	0.50	0.10	-0.50
			10	218	2.06	-1.62	-0.450	1.50	0.48	0.12	-0.90
20	0.20	28	0	565	3.00	-1.50	0	1.00	0.10	0.30	-1.50
			10	560	8.74	-1.42	-0.083	0.98	0.16	0.65	-1.51
21	0.333	20	0	350	3.00	-1.50	0	1.00	0.15	0.25	-1.50
			9	343	7.62	-0.67	-0.114	1.21	0.17	0.47	-2.00
22	0.20	40	0	185	3.00	-1.50	0	1.00	0.25	0.25	-1.50
			8	175	1.35	-1.29	-0.045	1.19	0.31	0.31	-2.13
23	0.30	20	0	120	3.00	-1.50	0	1.00	0.25	0.25	-1.50
			6	112	4.03	-1.36	-0.031	1.14	0.33	0.10	-0.90
24	0.20	30	0	92	3.00	-0.70	0	1.40	0.010	0.001	-0.40
			1	90	1.50	-0.35	0.014	1.46	0.008	0.0005	-0.20
25	0.30	17	0	70	3.00	-0.75	-0.112	1.15	0.05	0.05	-0.05
			3	65	85.14	-0.09	-0.141	1.50	0.03	0.01	-0.01
26	0.60	14	0	25	3.00	-1.50	0	1.00	0.05	0.10	-1.50
			7	24	12.72	-0.85	0.006	1.78	0.10	0.43	-3.61
27	0.50	16	0	160	3.00	-1.50	0	1.00	0.30	0.20	-1.50
			16	163	1.75	-1.28	0.027	0.83	0.53	0.24	-1.35
28	0.20	32	0	160	3.00	-1.50	0	1.00	0.25	0.25	-1.50
			15	149	126.14	-1.61	-0.028	1.40	0.15	0.43	-1.53
			31	149	126.14	-1.61	-0.027	1.40	0.15	0.44	-1.54
29	0.50	10	0	206	3.00	-1.50	0	1.00	0.10	0.10	-1.50
			10	199	8.29	-1.51	0.071	0.84	0.26	0.30	-1.66
30	0.50	19	0	196	3.00	-1.50	0	1.00	0.50	0.50	-1.50
			10	201	2.99	-0.85	0.189	0.83	0.68	0.27	-0.92
31	0.50	18	0	190	3.00	-0.85	0.200	0.90	0.70	0.30	-0.90
			7	194	2.01	-0.78	0.219	0.90	0.79	0.25	-0.68
32	0.15	35	0	55	3.00	-1.50	0	1.00	0.15	0.50	-1.50
			7	52	7.56	-1.34	-0.062	0.85	0.25	0.47	-1.42
33	0.50	12	0	127	3.00	-1.50	0	0.90	0.20	0.25	-1.50
			10	129	29.06	-1.79	-0.143	0.56	0.33	0.57	-2.44
34	0.50	18	0	1423	3.00	-1.50	0	1.00	0.30	0.60	-1.50
			10	1410	0.71	-1.71	-0.131	0.89	0.36	0.34	-1.49
35	0.60	12	0	853	3.00	-1.50	0	1.00	0.30	0.20	-1.50
			19	862	3.16	-0.85	-0.073	0.98	0.34	0.21	-1.75

earlier. The number of points in the fitting interval ranged from ten to fifty-seven. The original and final parameter estimates are listed, along with the number of iterations actually computed. Peak 28 illustrates that once the fitting process converged to a minimum residual sum of squares, further iterations did not significantly change any of the parameter estimates.

Table VII lists some of the information obtained from the eight parameter estimates shown in Table VI. The initial and final residual values were calculated from the initial and final parameter estimates. The raw sum was obtained by summing the digital data, following the polynomial baseline subtraction, over the total peak fitting interval. The fitted sums were obtained by evaluating and summing the fitted functions, using both the initial and final parameter estimates, at each channel location in the peak fitting interval.

The percentage ratio of the final fitted sum to the raw sum was calculated for each of the 35 peaks, using the values shown in Table VII. These ratios had a range of 97.70% to 100.86%, a mean of 99.80%, and a standard deviation of only 0.74%. This demonstrated that the fitted curves were truly representative of the actual areas encompassed by the raw data. Since the raw data, in this case, had no background contribution, the fitted curves were representative of the quantitative areas enclosed by the photopeaks.

The seven peaks shown in Figures 32-38 were examples of large peaks which rested on relatively flat baselines. The large peak-to-noise ratios (greater than 75) indicated that there was little scatter associated with the data in the central region of the peak. The peaks in Figures 37 and 38 were taken from spectra with increased ADC

TABLE VII

INITIAL AND FINAL VALUES FROM THE CURVE FITTING CALCULATIONS

<u>PEAK</u>	<u>NUMBER OF ITERATIONS</u>	<u>INITIAL RESIDUAL</u>	<u>FINAL RESIDUAL</u>	<u>RAW SUM</u>	<u>INITIAL FITTED SUM</u>	<u>FINAL FITTED SUM</u>
1	10	13,414,000	504,028	72,545	82,167	72,196
2	39	4,415,190	108,796	39,593	45,049	39,254
3	23	555,058	31,779	31,879	32,449	31,881
4	10	354,854	19,789	17,613	16,438	17,635
5	10	418,561	12,432	14,137	13,907	14,227
6	10	451,891	26,523	32,405	30,456	32,457
7	10	51,315	23,898	26,366	25,442	26,276
8	10	4,419,770	376,740	68,284	74,108	68,047
9	10	53,310	7,473	9,403	9,158	9,466
10	10	502,123	44,171	21,532	20,343	21,588
11	10	217,715	89,223	41,079	40,423	41,059
12	5	12,334	8,887	6,959	6,824	7,005
13	15	16,859	6,346	4,214	4,118	4,219
14	6	24,654	5,903	3,035	3,227	3,050
15	60	40,345	2,400	3,729	3,338	3,723
16	6	23,609	13,298	8,466	8,589	8,495
17	10	55,389	13,811	2,208	2,690	2,158
18	8	29,023	7,070	2,690	2,531	2,713
19	10	10,815	2,011	1,403	1,296	1,399
20	10	32,788	16,009	7,290	7,315	7,246
21	9	38,778	9,830	3,226	2,852	3,219
22	8	9,506	3,673	3,010	2,703	2,981
23	6	3,458	2,067	1,207	1,127	1,201
24	1	3,819	3,741	1,348	1,357	1,347
25	3	2,827	2,500	663	636	660
26	7	286	105	143	110	143
27	16	3,300	1,540	1,084	978	1,078
28	31	7,943	6,376	2,264	2,274	2,273
29	10	1,929	521	990	1,047	972
30	10	9,705	1,674	1,444	1,182	1,452
31	7	1,848	387	1,458	1,340	1,465
32	7	571	226	875	951	872
33	10	3,483	617	620	666	607
34	10	154,939	10,455	8,119	7,855	8,118
35	19	106,251	4,836	4,844	4,300	4,822

Figure 32. Raw data and fitted curve (offset) for the 1115.51 KeV Zn - 65 peak taken from spectrum 2

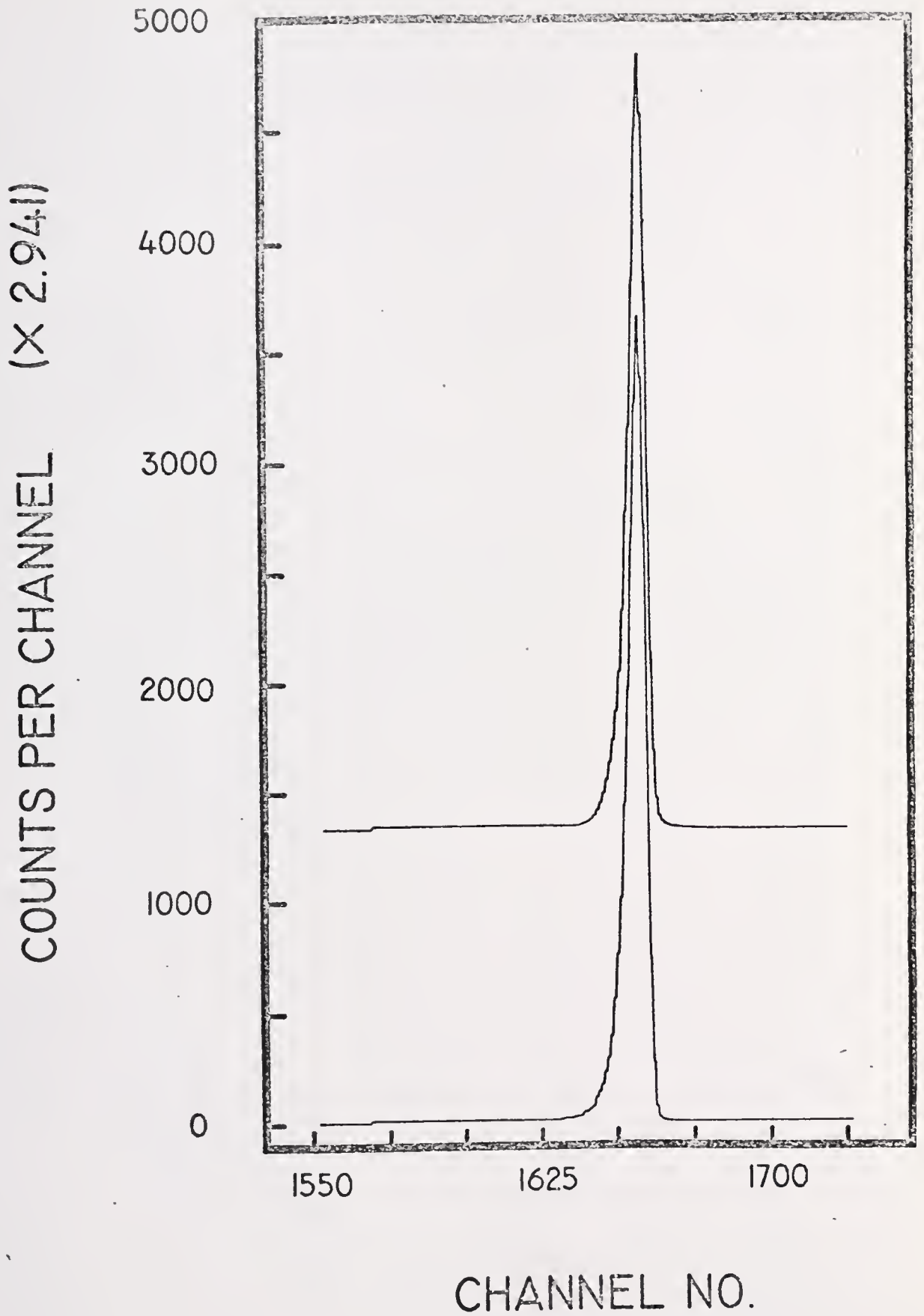
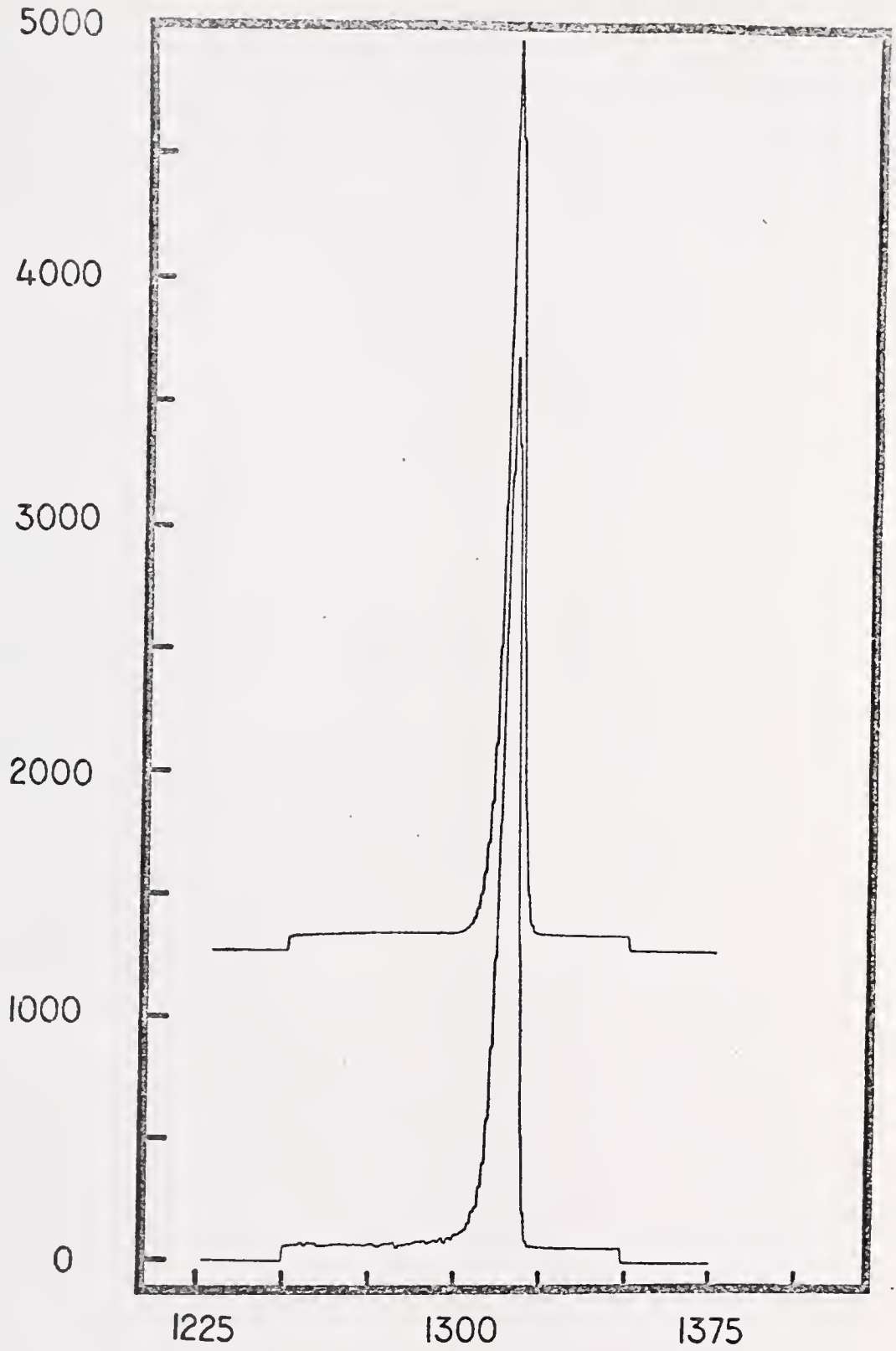


Figure 33. Raw data and fitted curve (offset) for the
884.5 KeV Ag - 110m peak taken from
spectrum 1

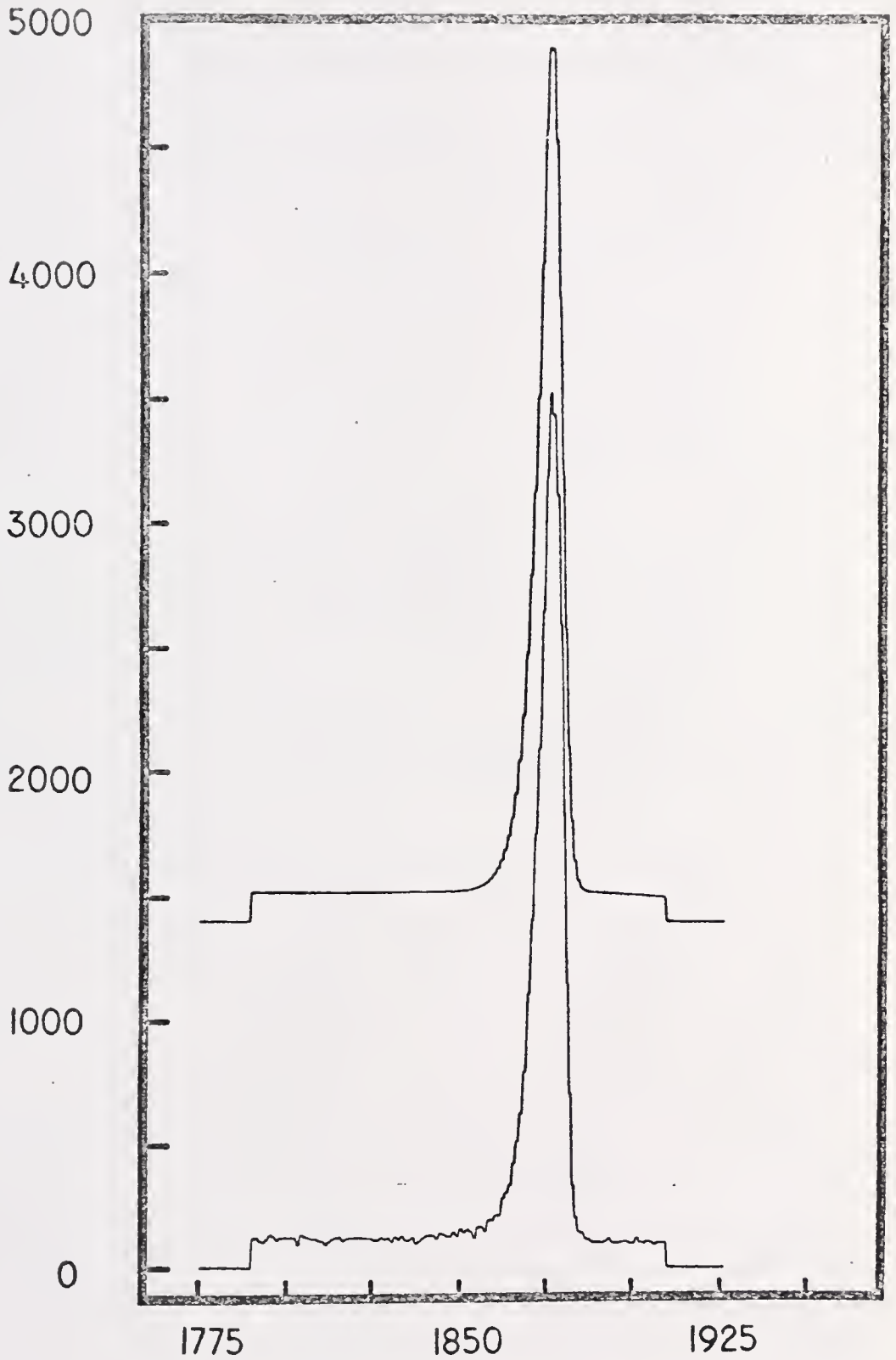
COUNTS PER CHANNEL (X 1.880)



CHANNEL NO.

Figure 34. Raw data and fitted curve (offset) for the 884.5 KeV Ag - 110m peak taken from spectrum 9

COUNTS PER CHANNEL (X 1.066)



CHANNEL NO.

Figure 35. Raw data and fitted curve (offset) for the 937.3 KeV Ag - 110m peak taken from spectrum 1

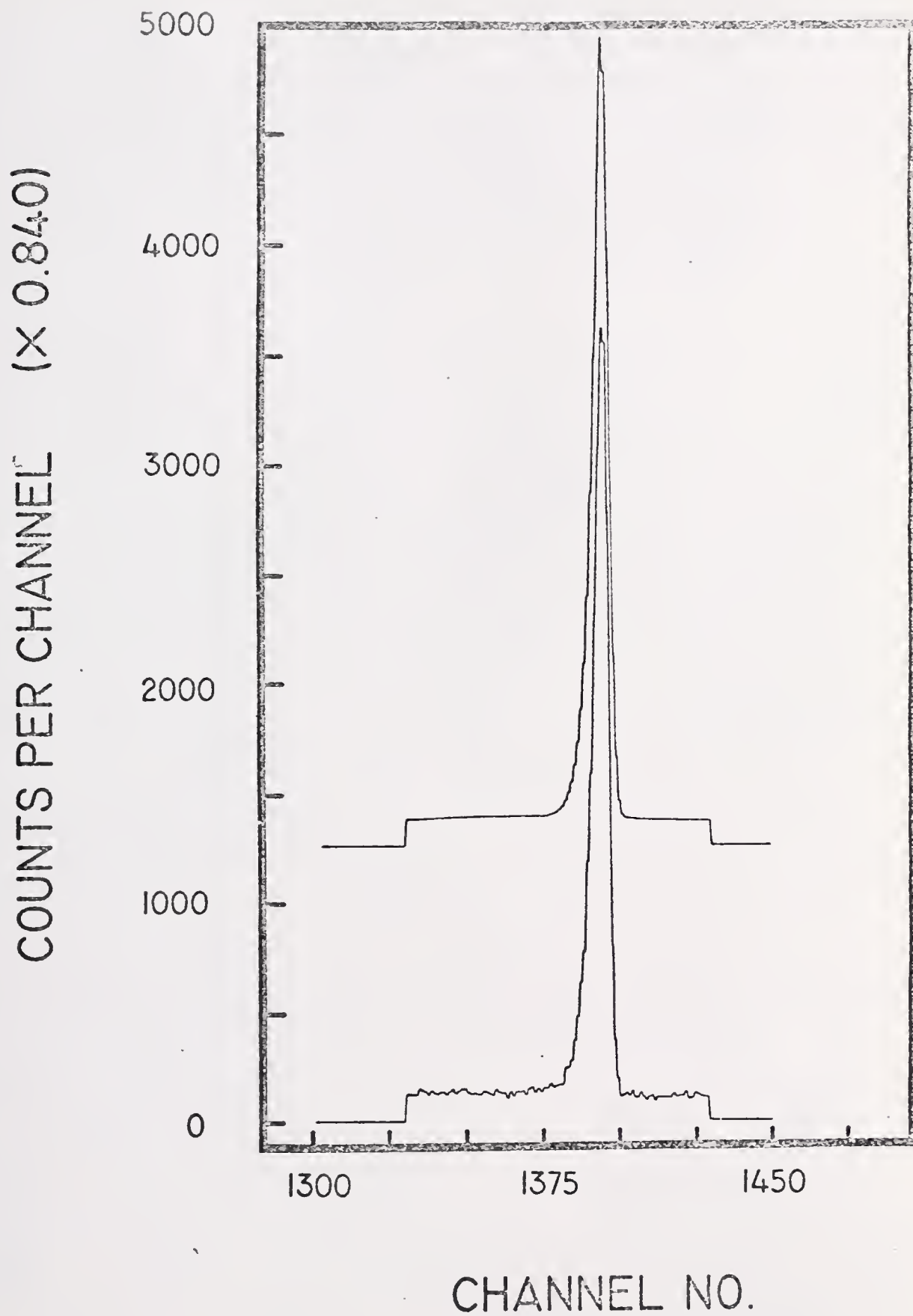
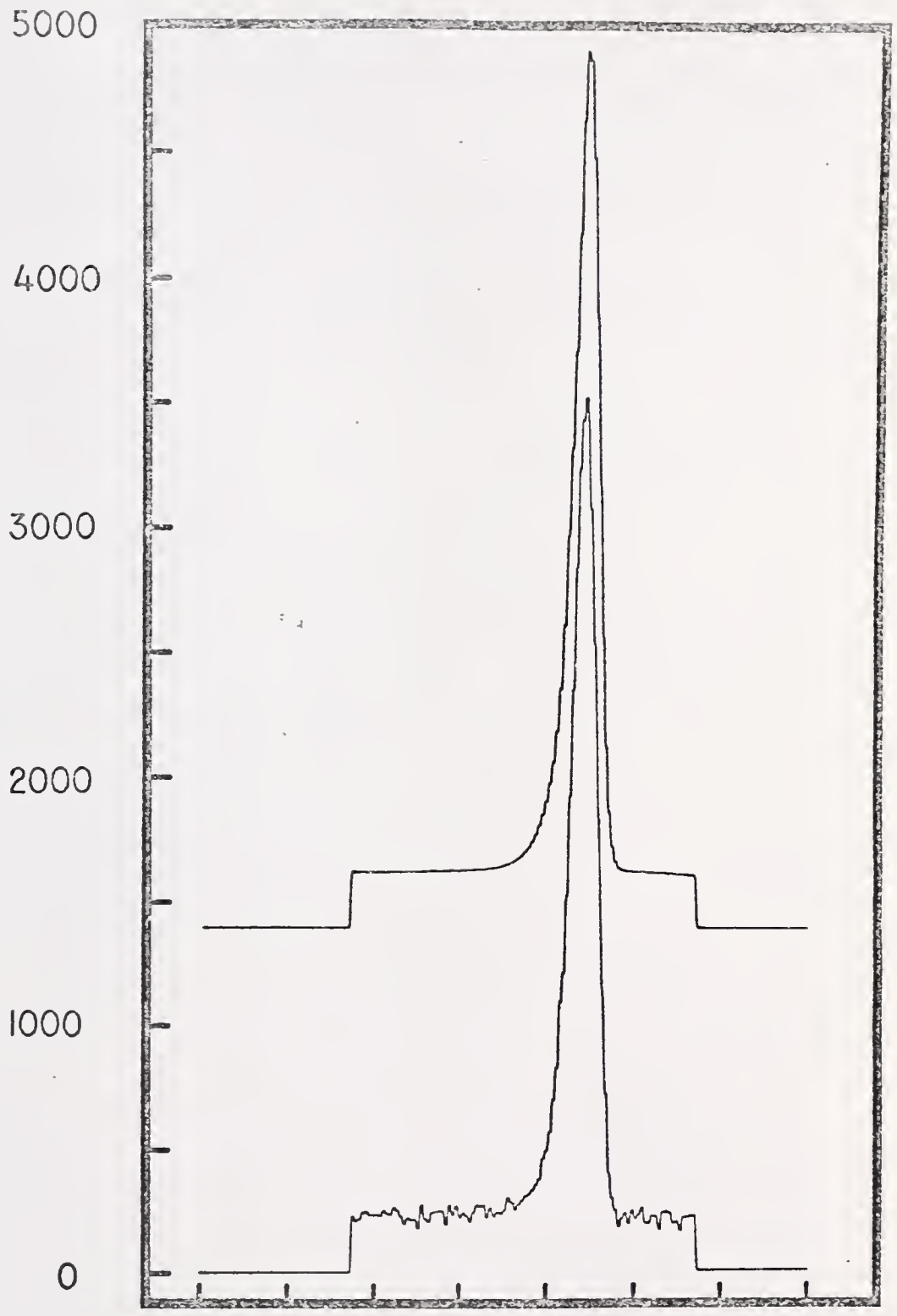


Figure 36. Raw data and fitted curve (offset) for the
937.3 KeV Ag - 110m peak taken from
spectrum 9

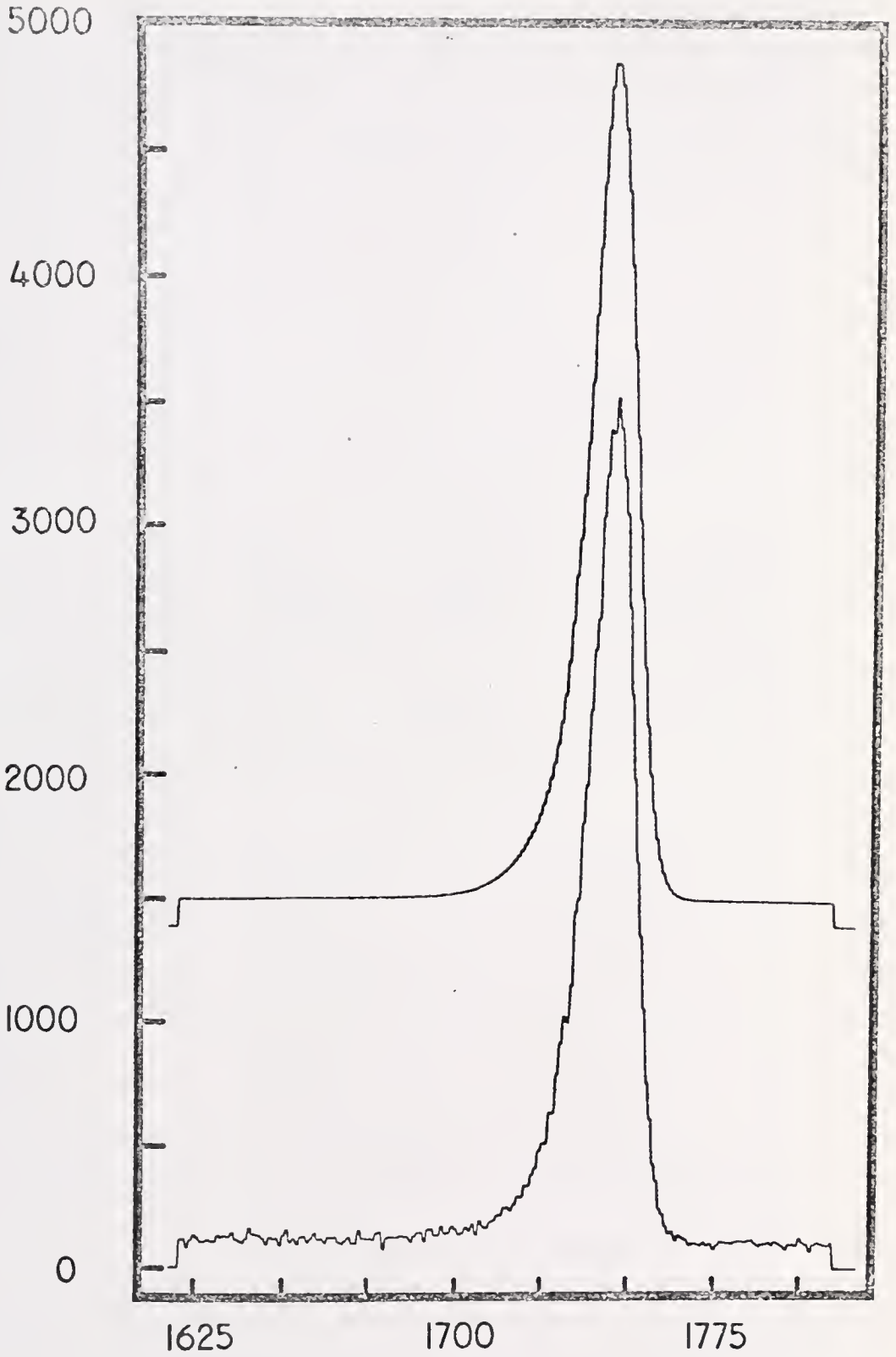
COUNTS PER CHANNEL (X 0.478)



CHANNEL NO.

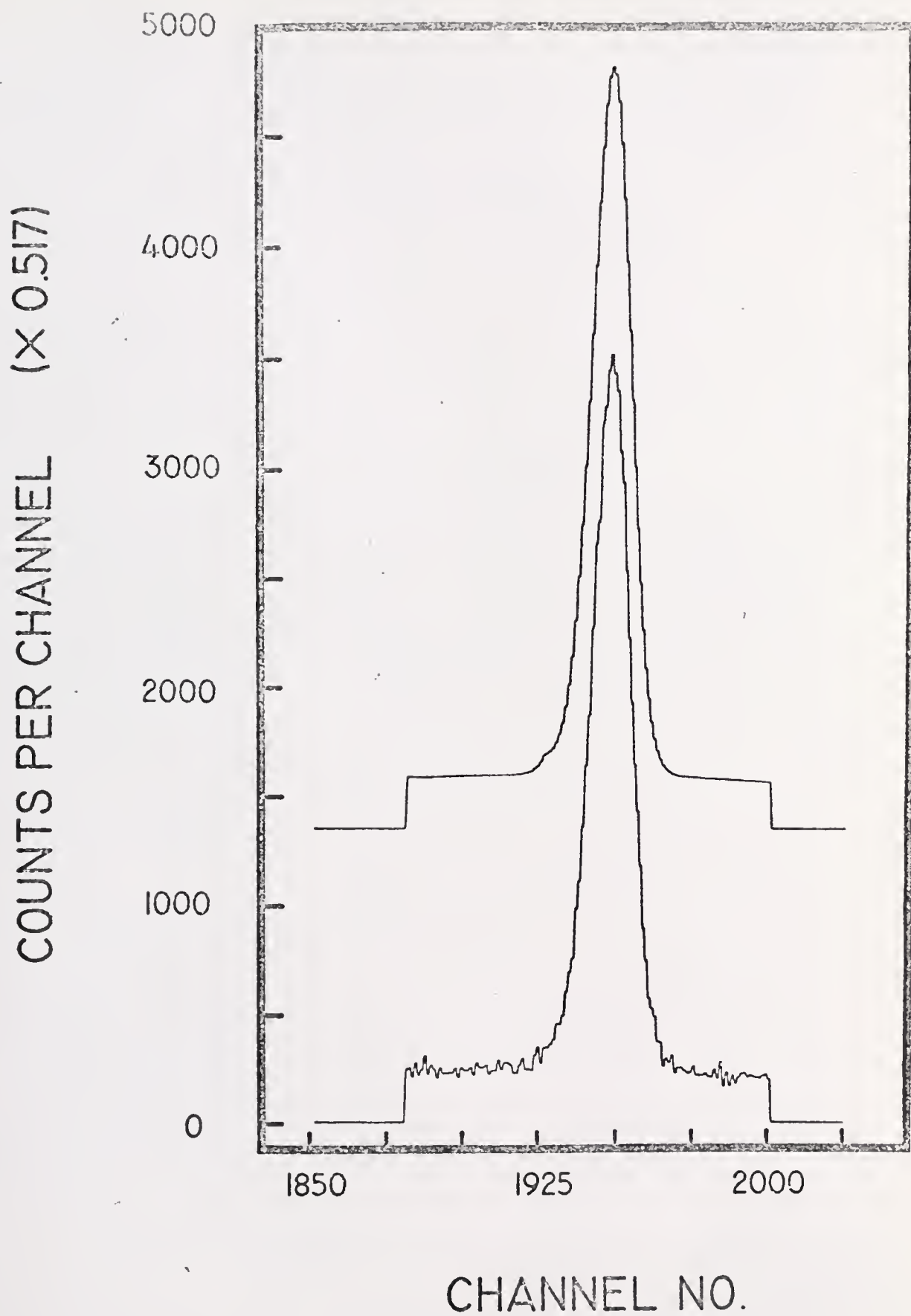
Figure 37. Raw data and fitted curve (offset) for the
884.5 KeV Ag - 110m peak taken from
spectrum 11

COUNTS PER CHANNEL (X 0.544)



CHANNEL NO.

Figure 38. Raw data and fitted curve (offset) for the
320.08 KeV Cr - 51 peak taken from
spectrum 7



resolution and therefore had a greater number of data points in the peak fitting interval. For all of these peaks the initial parameter estimates were easy to make, and the fits, as shown by the comparison curves, were excellent.

The peaks shown in Figures 39-42 were again large, but were located on sloping baselines. The slopes were the result of Compton edges from higher energy peaks, and the degree of the slope depended upon the intensity of the higher energy peak. The cubic polynomial easily approximated the sloping backgrounds so that, following the polynomial subtraction, all skew associated with background was removed. Again the comparison curves clearly illustrate the excellent simulation achieved by the fitted function.

Figure 43 shows a smaller peak (less than 1000 counts at the peak maximum) which was located on a flat background. The apparent negative slope of the baseline to the right of the peak was the result of too few points used to estimate this region. However the simulation agreed with the apparent slope of the raw data for this narrow region.

The peaks shown in Figures 44-50 also had less than 100 counts at the peak maxima. Again, the baselines were sloped due to a Compton edge present in the spectrum. The fitted peaks shown in Figures 47-49, however, displayed some form of complex behavior on the left side of the peaks. Figures 47 and 49 show a small shoulder which was real and was caused by the irregularity of the raw data. The best fit obtainable in these cases did not have a smooth joining of the Gaussian and exponential parts of the fitting function. It is significant to note, however, that the fitting function characterized the shoulders

Figure 39. Raw data and fitted curve (offset) for the
1099.27 KeV Fe - 59 peak taken from
spectrum 3

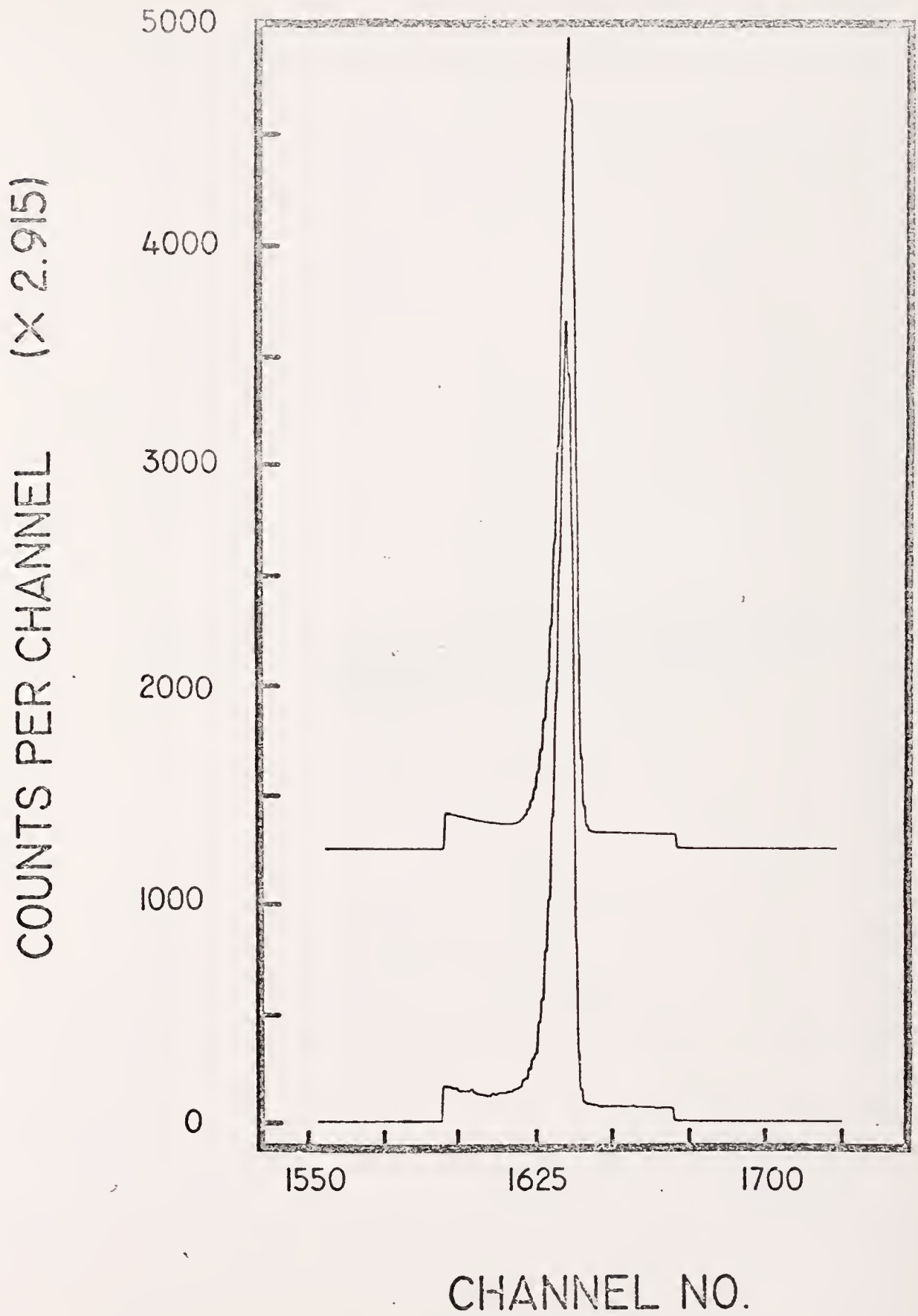


Figure 40. Raw data and fitted curve (offset) for the
937.3 KeV Ag - 110m peak taken from
spectrum 4

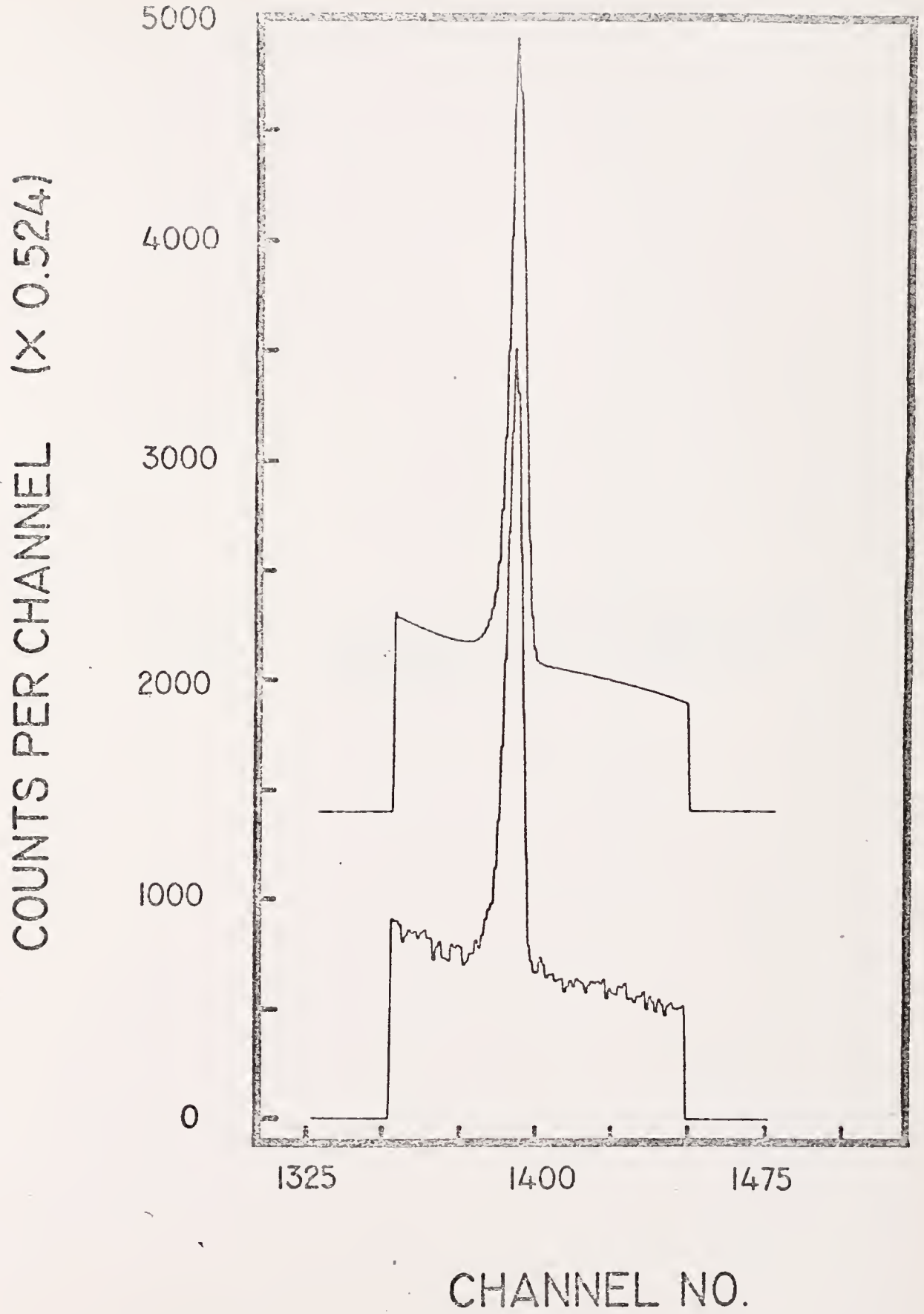
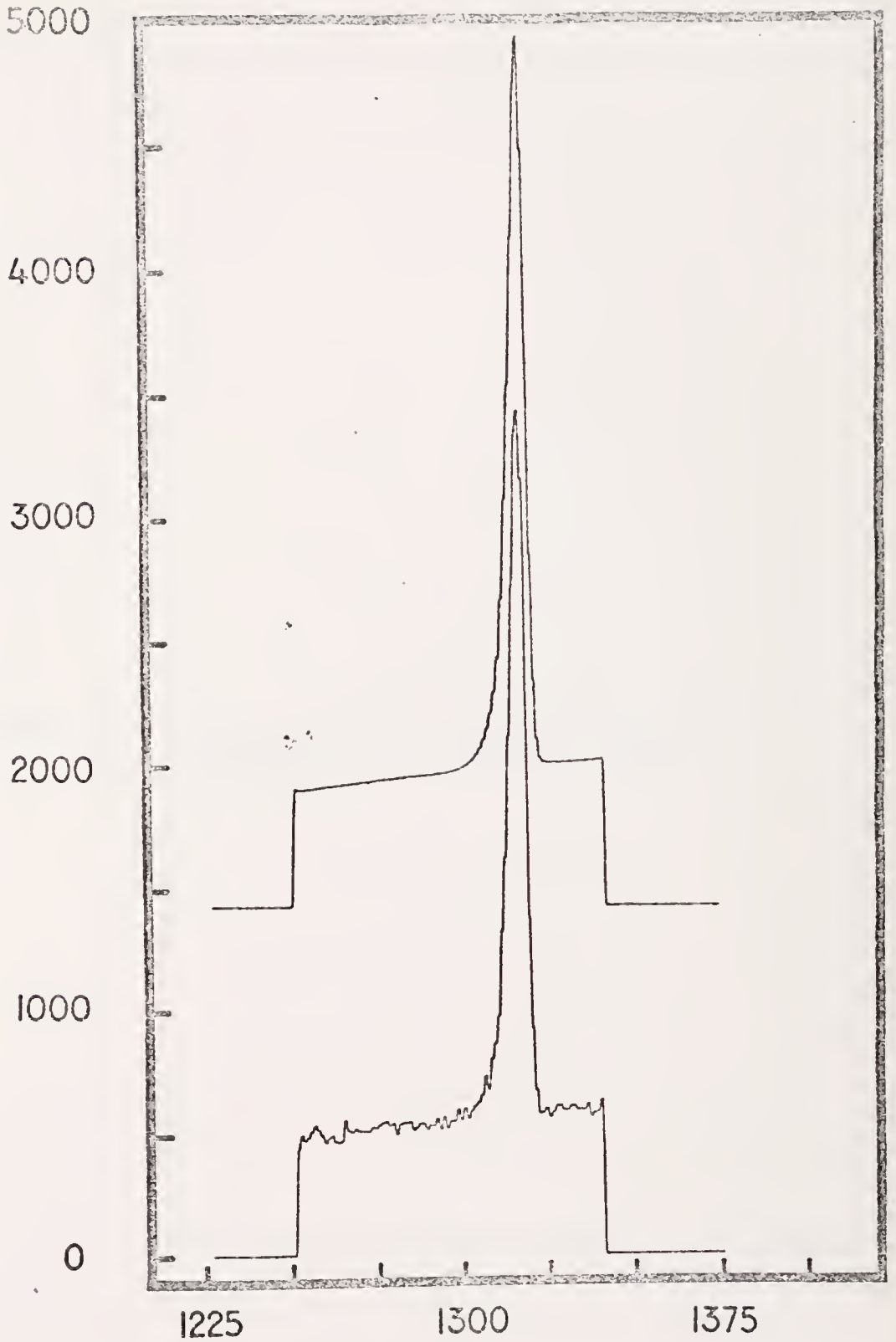


Figure 41. Raw data and fitted curve (offset) for the
884.5 KeV Ag - 110m peak taken from
spectrum 4

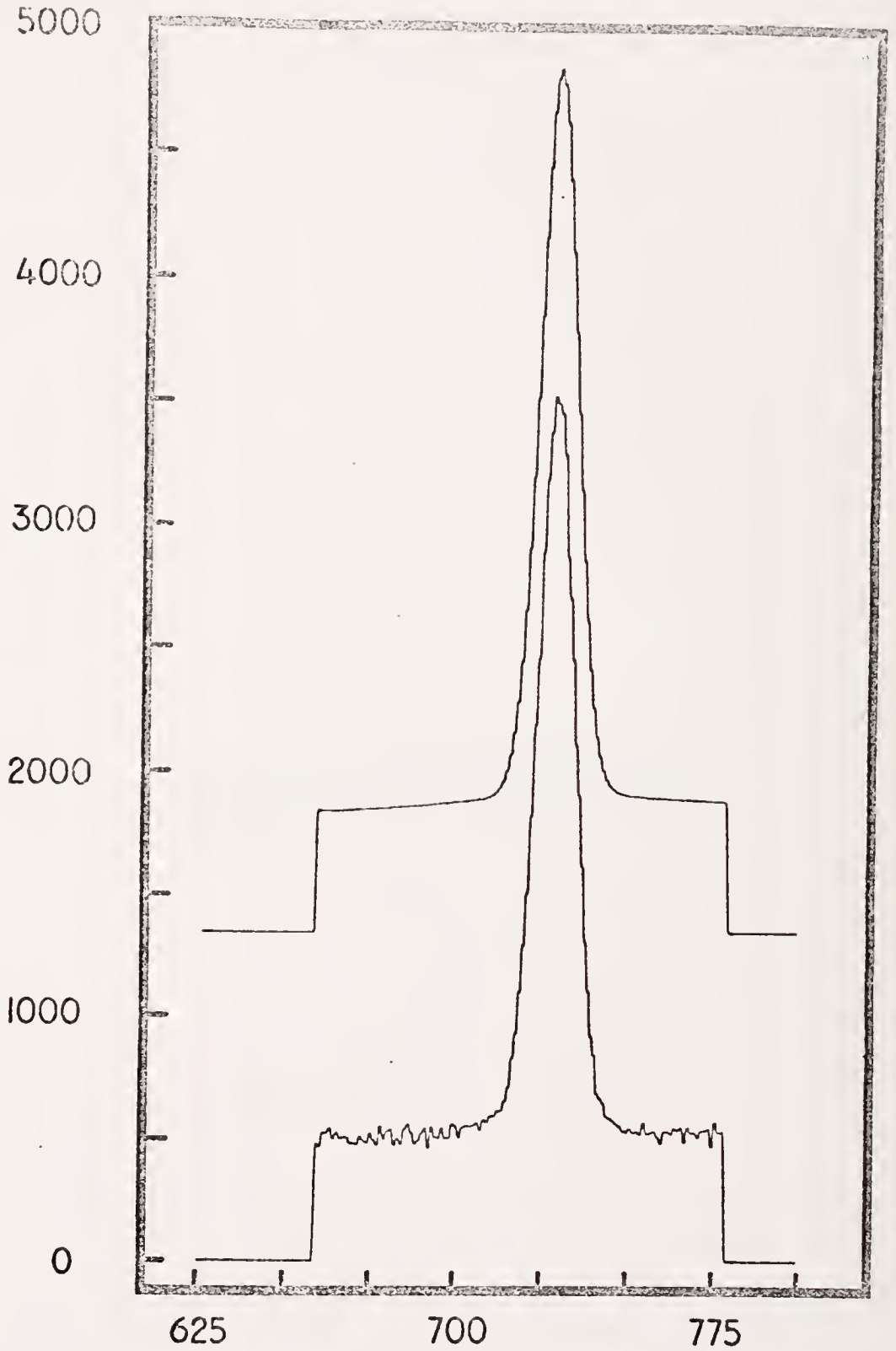
COUNTS PER CHANNEL (X 1.199)



CHANNEL NO.

Figure 42. Raw data and fitted curve (offset) for the
121.13 KeV Se - 75 peak taken from
spectrum 7

COUNTS PER CHANNEL (× 0.9994)



CHANNEL NO.

Figure 43. Raw data and fitted curve (offset) for the
511 KeV annihilation peak taken from
spectrum 8

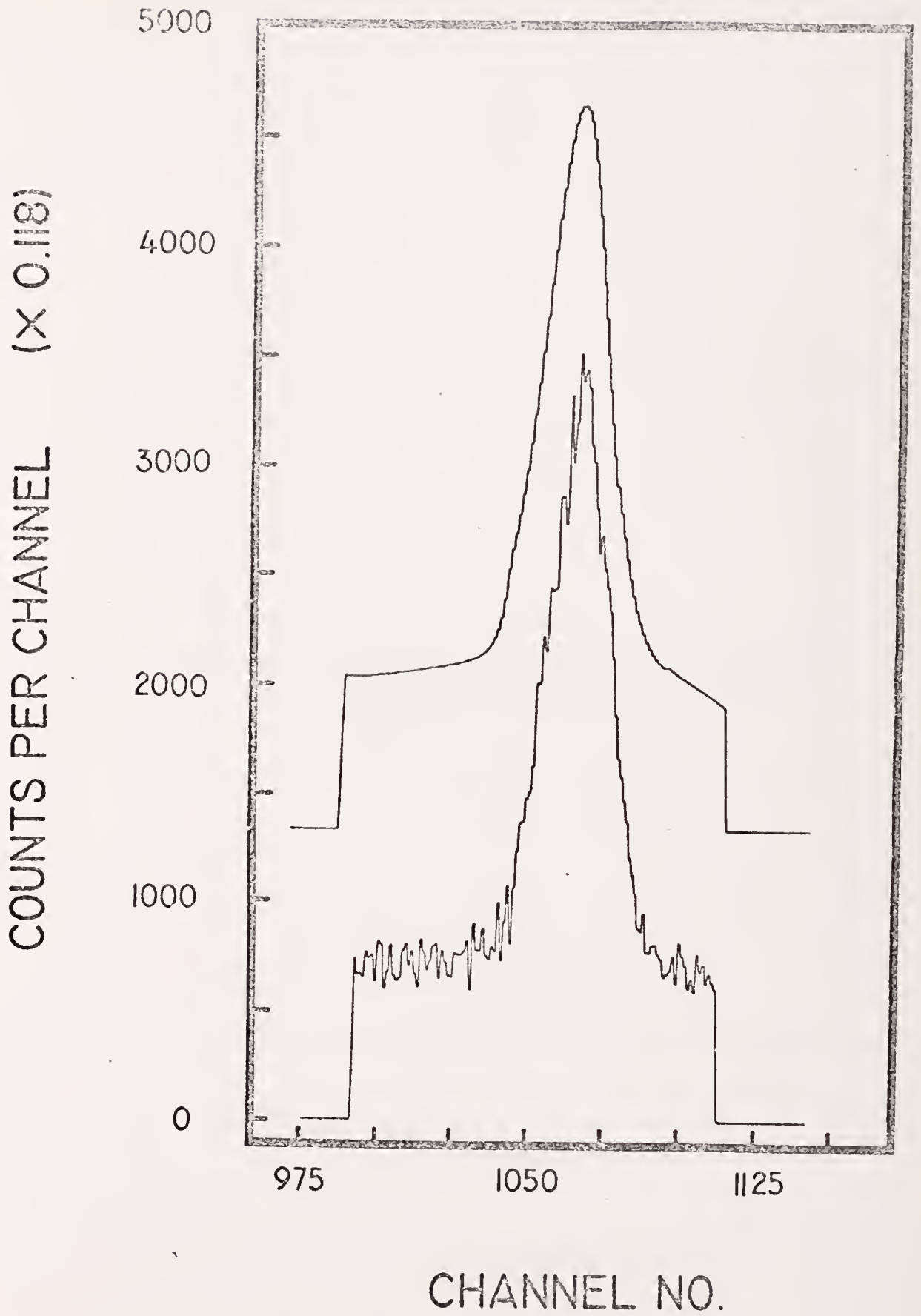
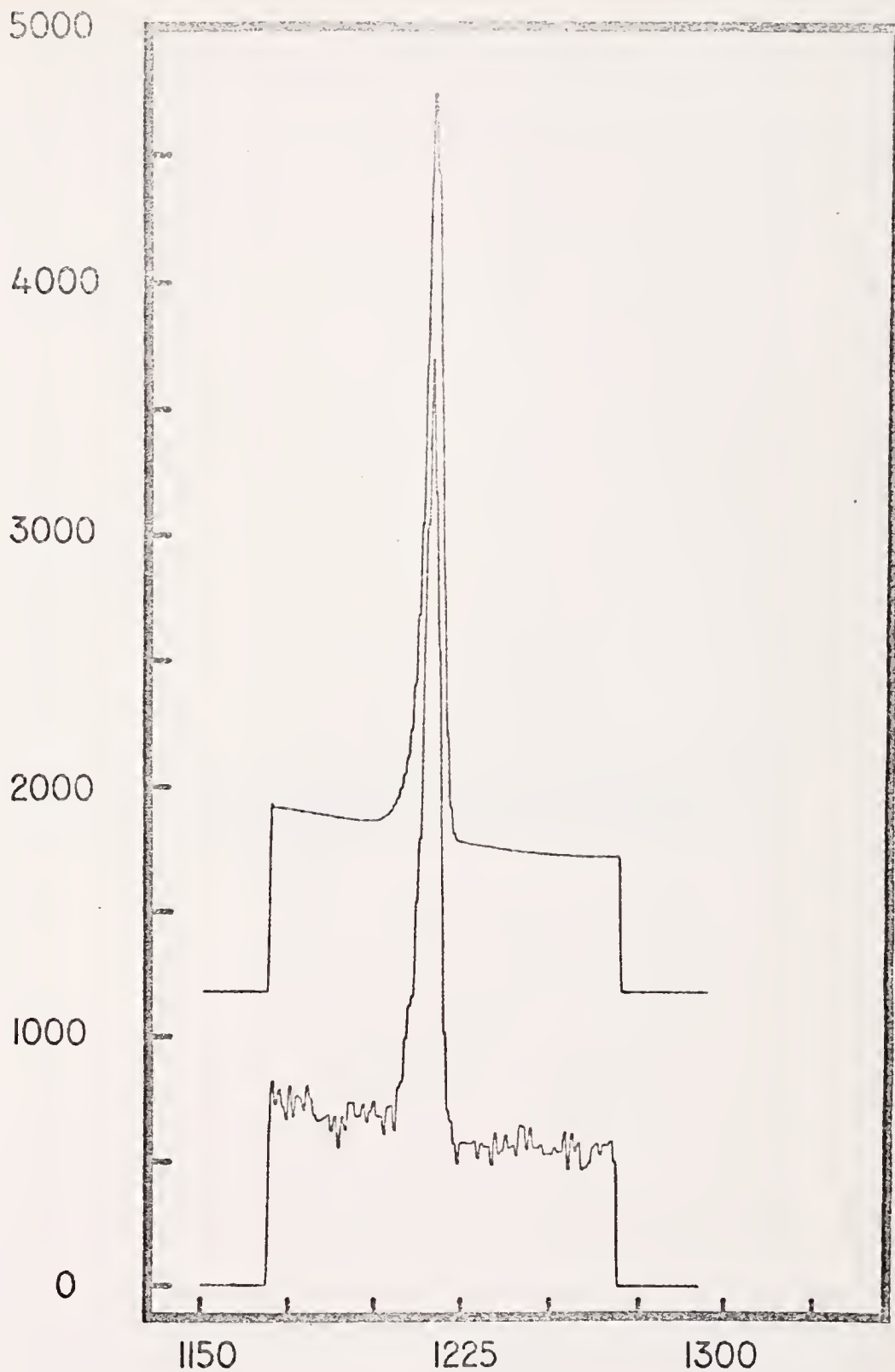


Figure 44. Raw data and fitted curve (offset) for the
817.9 KeV Ag - 110m peak taken from
spectrum 1

COUNTS PER CHANNEL (X 0.258)



CHANNEL NO.

Figure 45. Raw data and fitted curve (offset) for the
817.9 KeV Ag - 110m peak taken from
spectrum 9

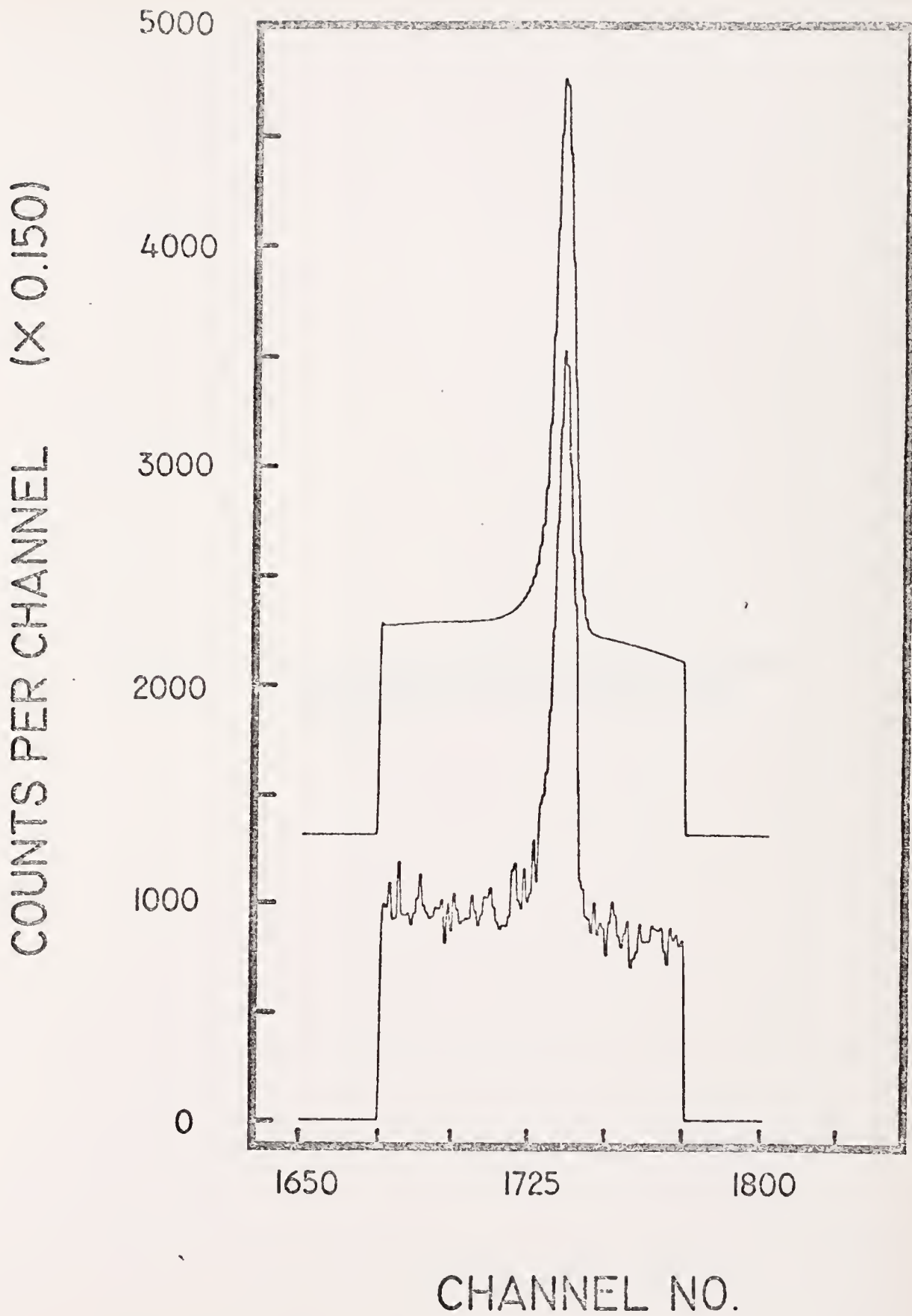


Figure 46. Raw data and fitted curve (offset) for the
446.2 KeV Ag - 110m peak taken from
spectrum 1

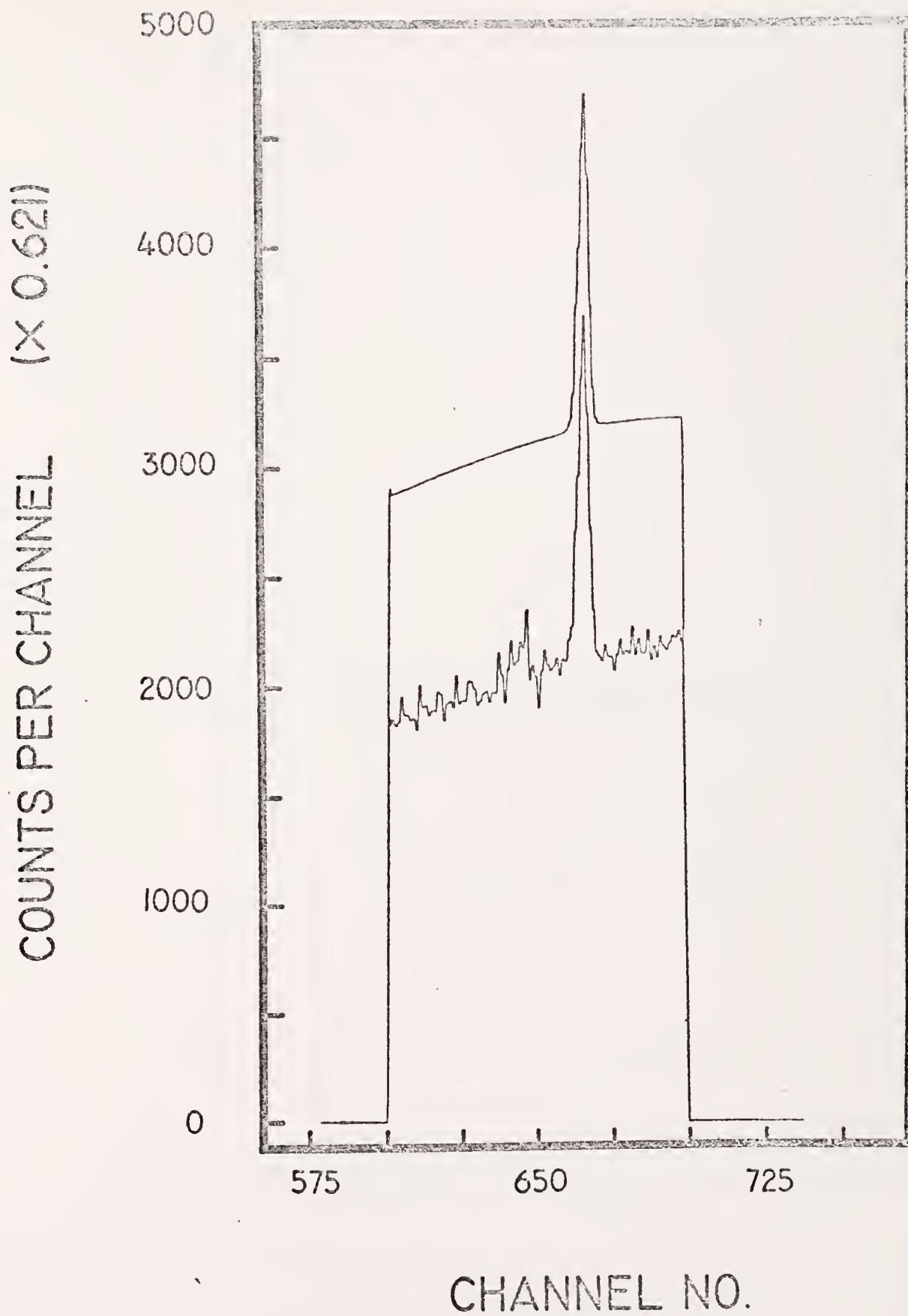
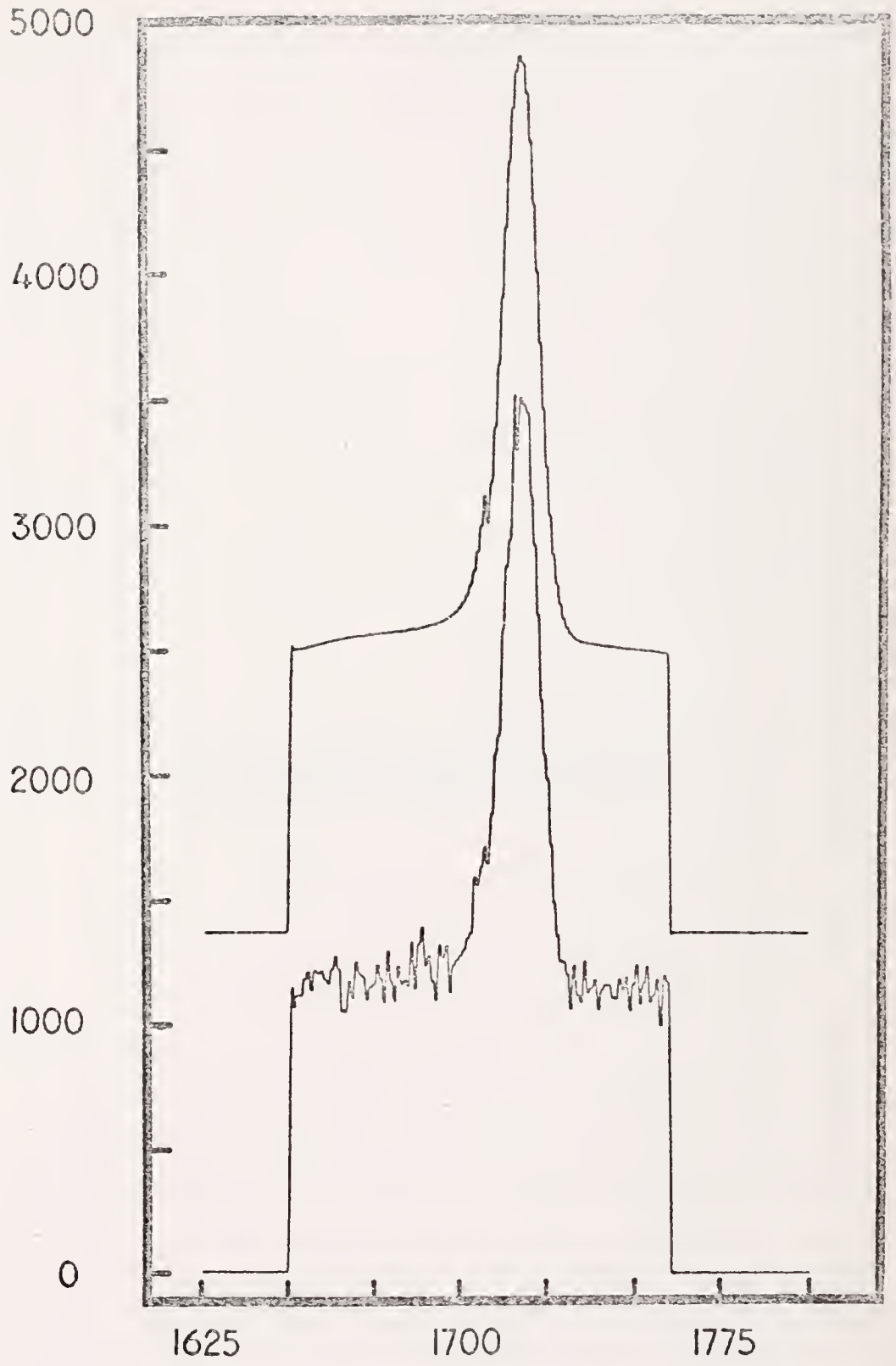


Figure 47. Raw data and fitted curve (offset) for the
400.64 KeV Se - 75 peak taken from
spectrum 10

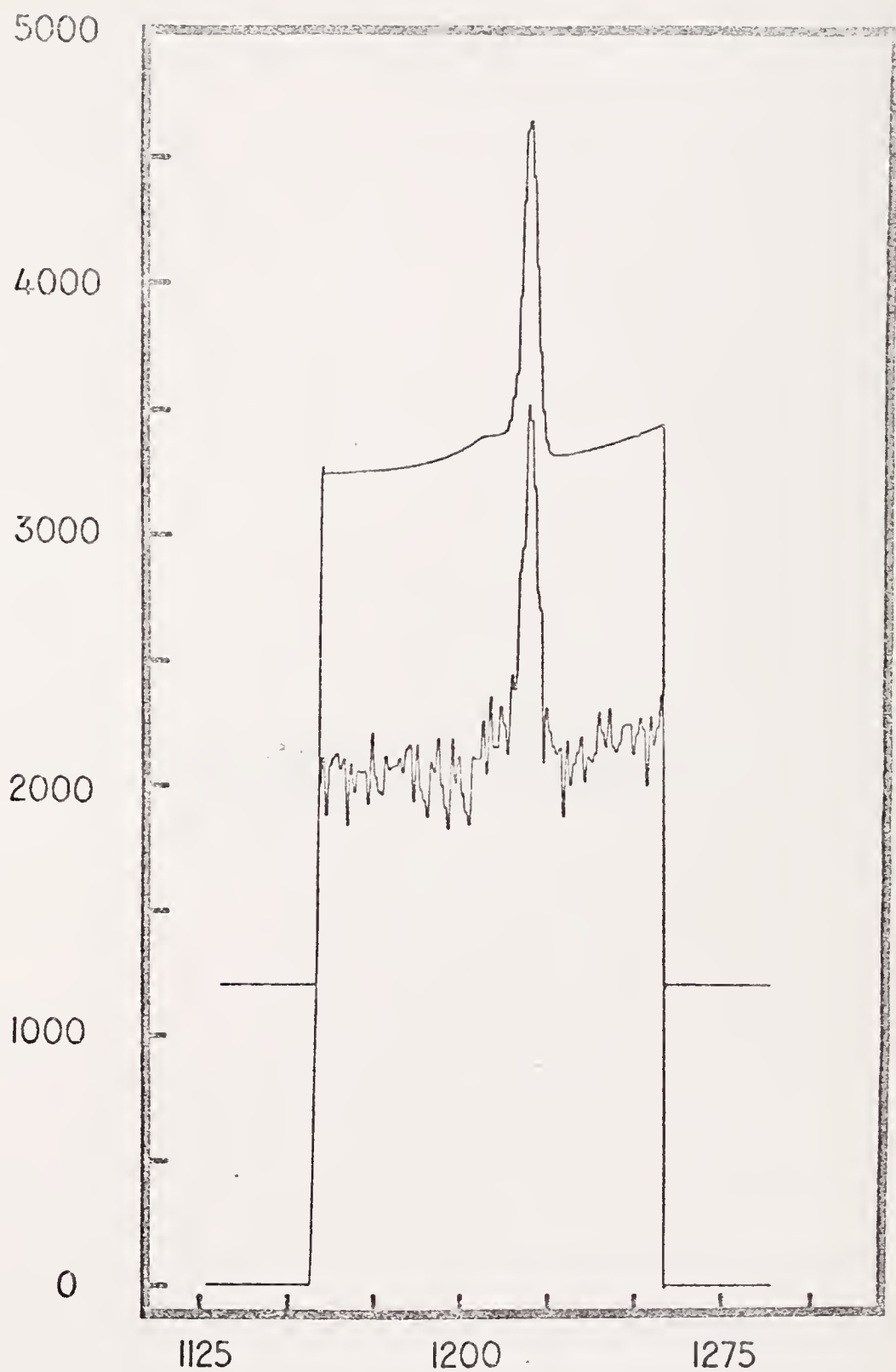
COUNTS PER CHANNEL (X 0.280)



CHANNEL NO.

Figure 48. Raw data and fitted curve (offset) for the
817.9 KeV Ag - 110m peak taken from
spectrum 4

COUNTS PER CHANNEL (X 0.260)



CHANNEL NO.

Figure 49. Raw data and fitted curve (offset) for the
446.2 KeV Ag - 110m peak taken from
spectrum 10

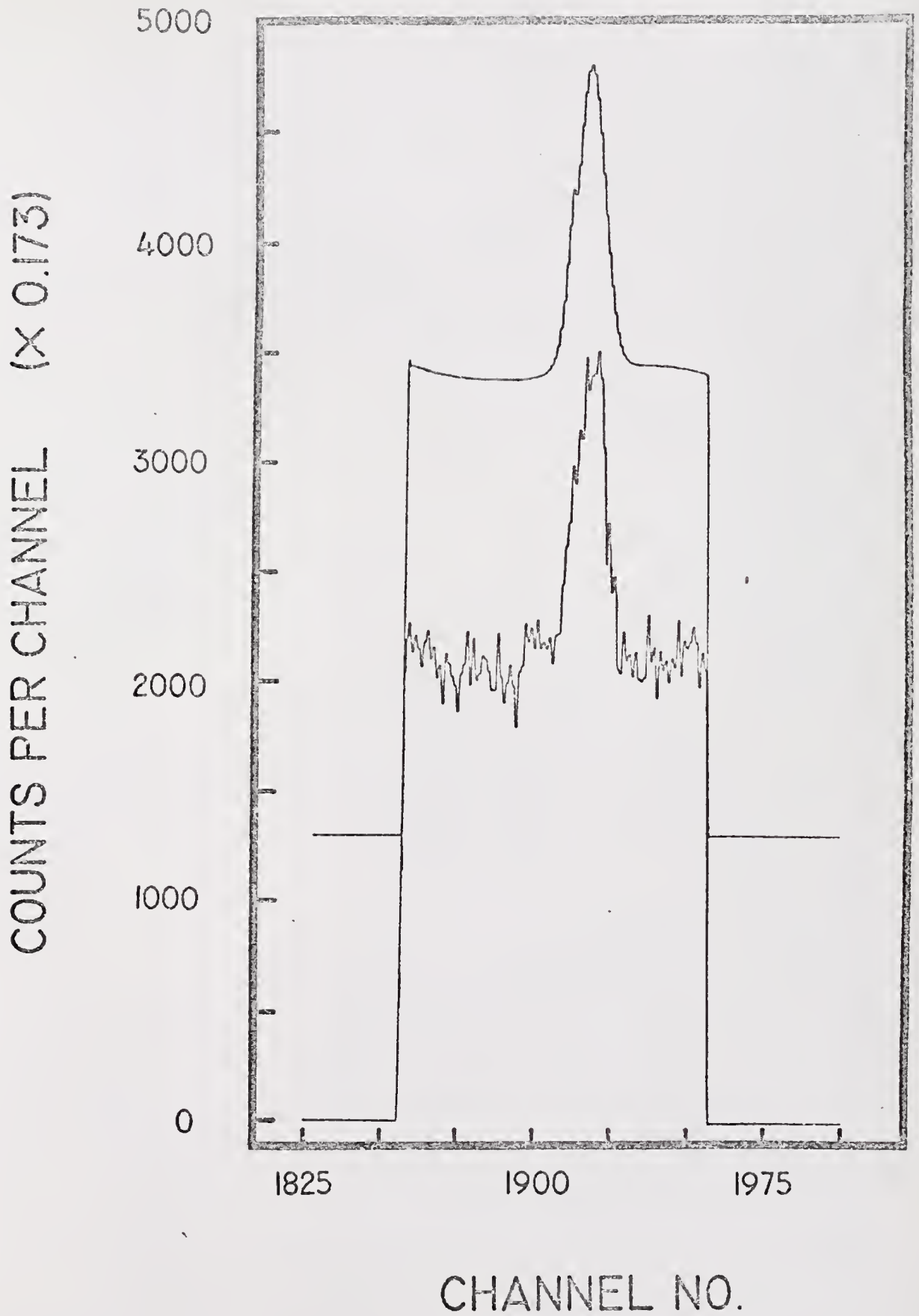
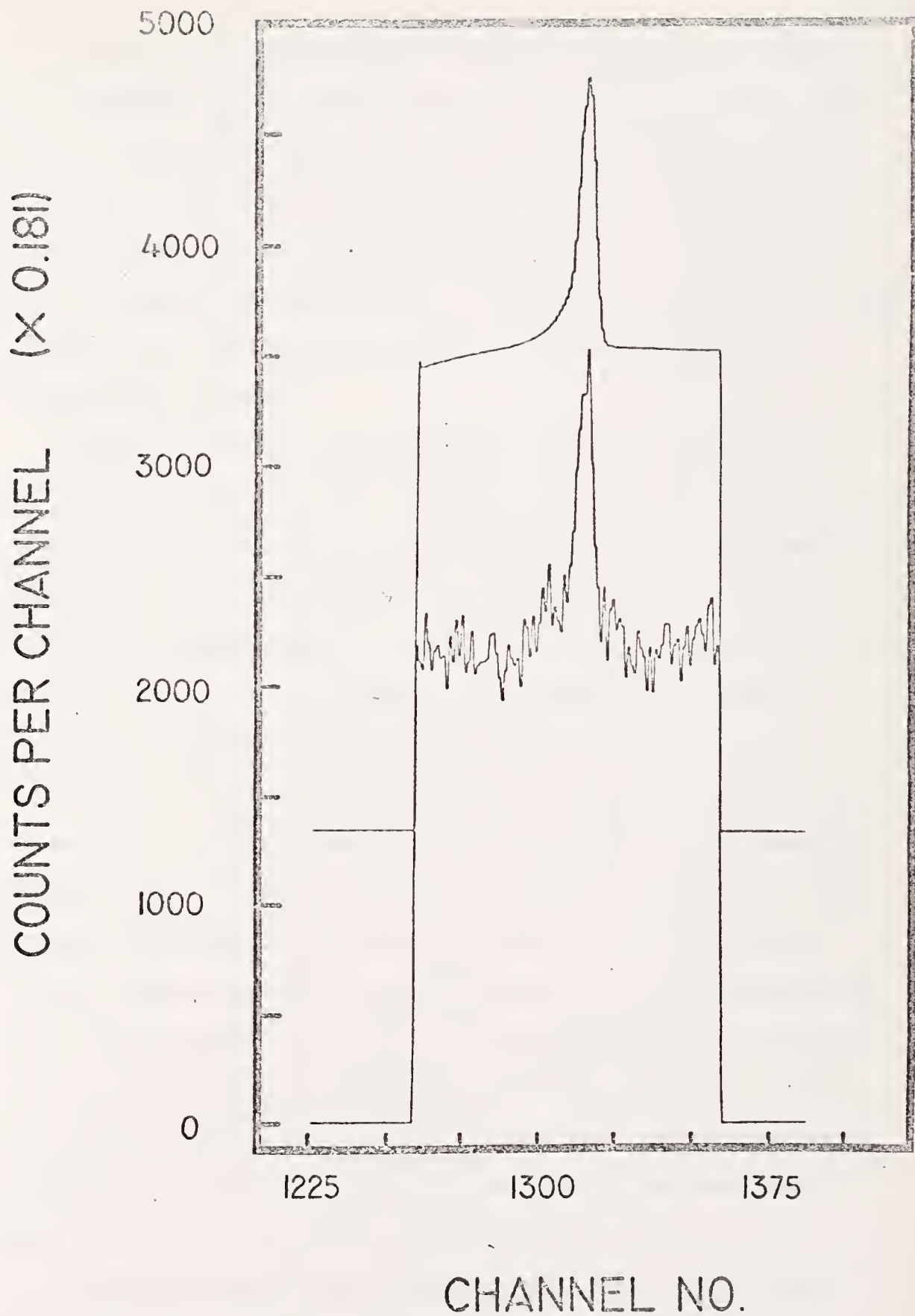


Figure 50. Raw data and fitted curve (offset) for the
620.1 KeV Ag - 110m peak taken from
spectrum 9



very effectively and was sensitive to their presence. As seen from the comparative curves, the fits were accurate representations of the raw data. Figure 48 shows a high baseline near the left edge of the fitted peak. This high baseline was due to both the extreme scatter in the raw data and the method of choosing the fitting interval. If more data points (including negative points) from the left side had been included in the fit, the rate of decrease of the exponential tail would have been greater.

Figures 51 and 52 show two different examples of the 96.73 KeV Se^{75} peak, taken from spectra 7 (Figure 28) and 10. The peak, shown at channel 580 of Figure 28, was located directly on top of a Compton edge from a higher energy Se^{75} peak. Since the Compton edge was caused by a photopeak from the same Se^{75} isotope, the peaks from both spectra were very similar in shape but, as indicated in Table V, differed in height and peak-to-noise ratio by a factor of two.

Due to the Compton edge, the slope of the baseline was positive to the left of each peak and negative to the right. As the curves in Figures 51 and 52 show, however, the cubic polynomial correctly simulated the baseline over the entire fitting interval. Although the fitting function simulated a slight shoulder on the low energy side of the peak in Figure 51, this was, as in the examples above, the result of the best fit of the chosen function to the available data. Since the purpose of the fitting function was just that, the final shape of the fitted curve was an accurate representation of the experimental data.

The above examples clearly demonstrate that the chosen function and fitting technique were applicable to the major photopeaks in a

Figure 51. Raw data and fitted curve (offset) for the
96.73 KeV Sc - 75 peak taken from
spectrum 7

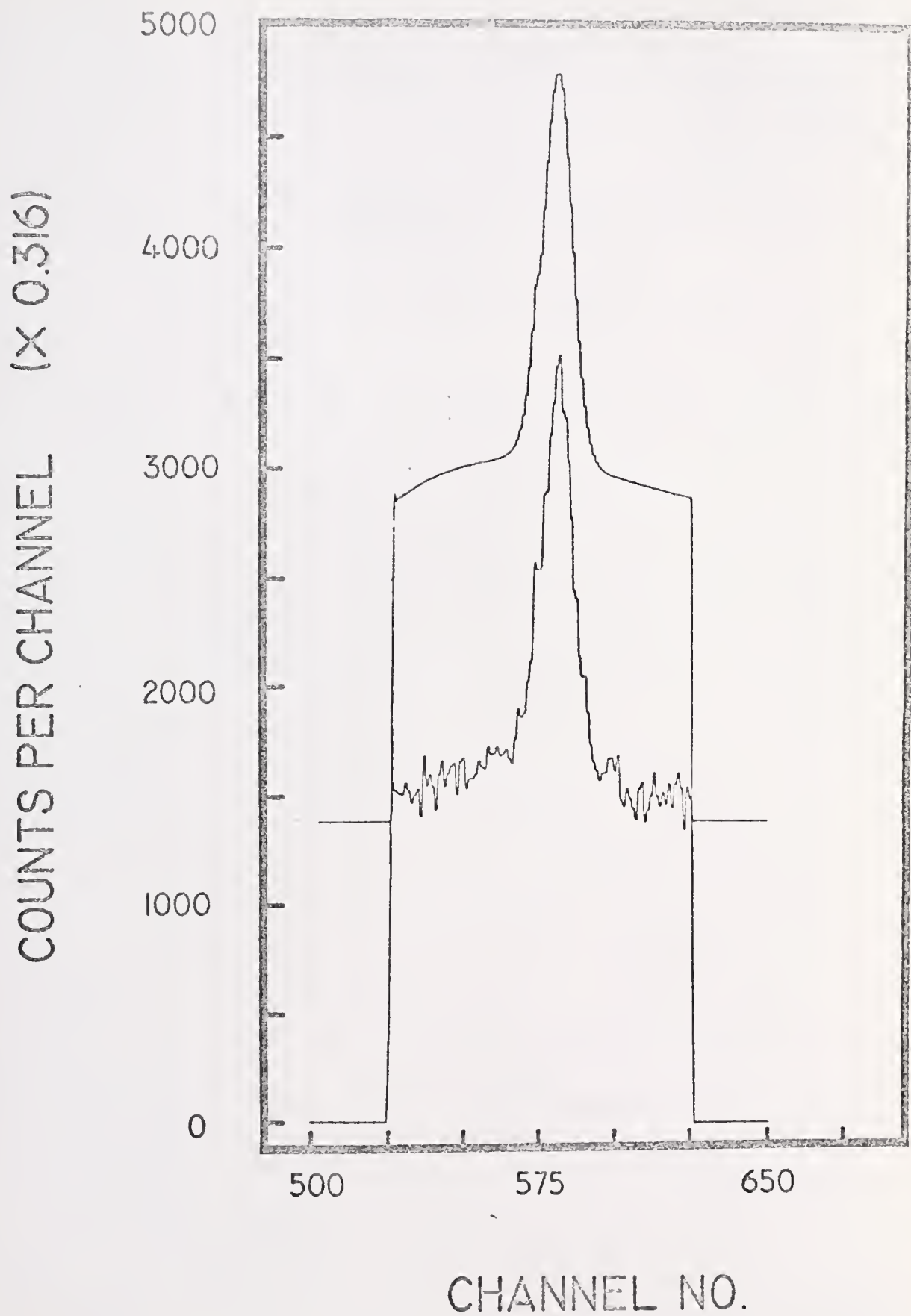
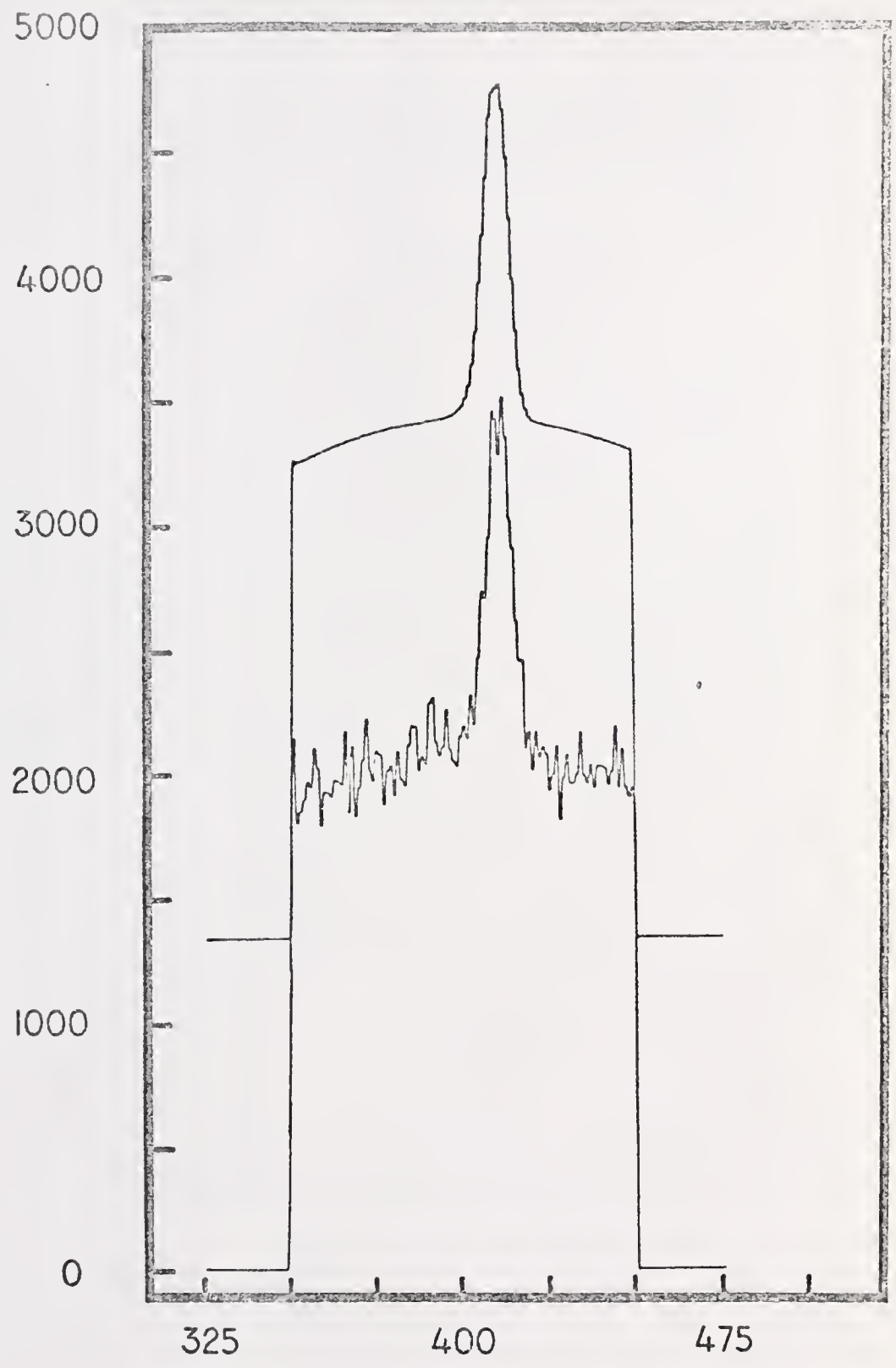


Figure 52. Raw data and fitted curve (offset) for the
96.73 KeV Se - 75 peak taken from
spectrum 10

COUNTS PER CHANNEL (X 0.253)



CHANNEL NO.

Ge(Li) spectrum. The remaining peaks will demonstrate the applicability of the technique to small peaks (less than 200 counts at the peak maximum) which, because of their small peak-to-noise ratios, had excessive scatter superimposed on the peak shapes.

The peaks shown in Figures 53-56 were located on essentially flat baselines. Although the raw data showed considerable scatter throughout the region of the peak, the fitted curves were representative of the basic peak shapes. Even the apparent sloping baseline in Figure 54 was truly representative of the raw data over the narrow region immediately surrounding the peak.

The peaks in Figures 57-60 were typical of small peaks which occurred at energies which coincided with large Compton edges from higher energy peaks. Although the baselines were high and sharply sloping, the polynomial approximation and subtraction easily removed this strong interaction, leaving only the basic peak shapes. As the figures show, these composite curves clearly approximated the original raw data.

In all of the above examples the original, unsmoothed data were utilized. In a few cases, however, the scatter altered the basic photopeak to such an extent that the fitting function was no longer able to simulate the resultant shape. In these cases the data were smoothed once and then fitted. This was not always successful, but a few examples of successful applications are discussed below.

Figures 61 and 62 show the results of two fits to the same peak. Figure 61 shows the result of the fit to the raw, unsmoothed data, while Figure 62 shows the outcome when the data were smoothed first. In both figures the unsmoothed peak is compared to the final, fitted

Figure 53. Raw data and fitted curve (offset) for the
817.9 KeV Ag - 110m peak taken from
spectrum 11

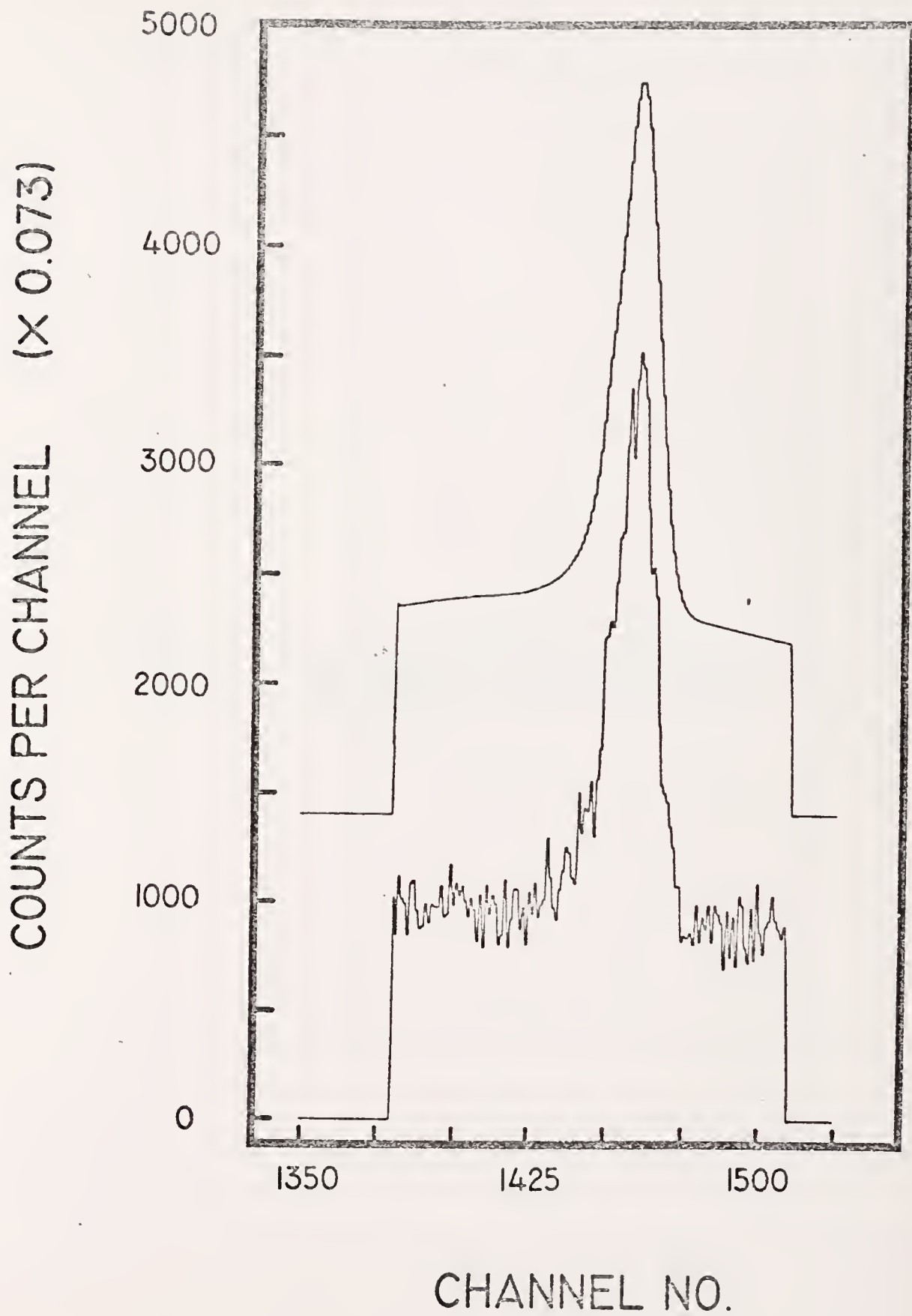


Figure 54. Raw data and fitted curve (offset) for the
620.1 KeV Ag - 110m peak taken from
spectrum 11

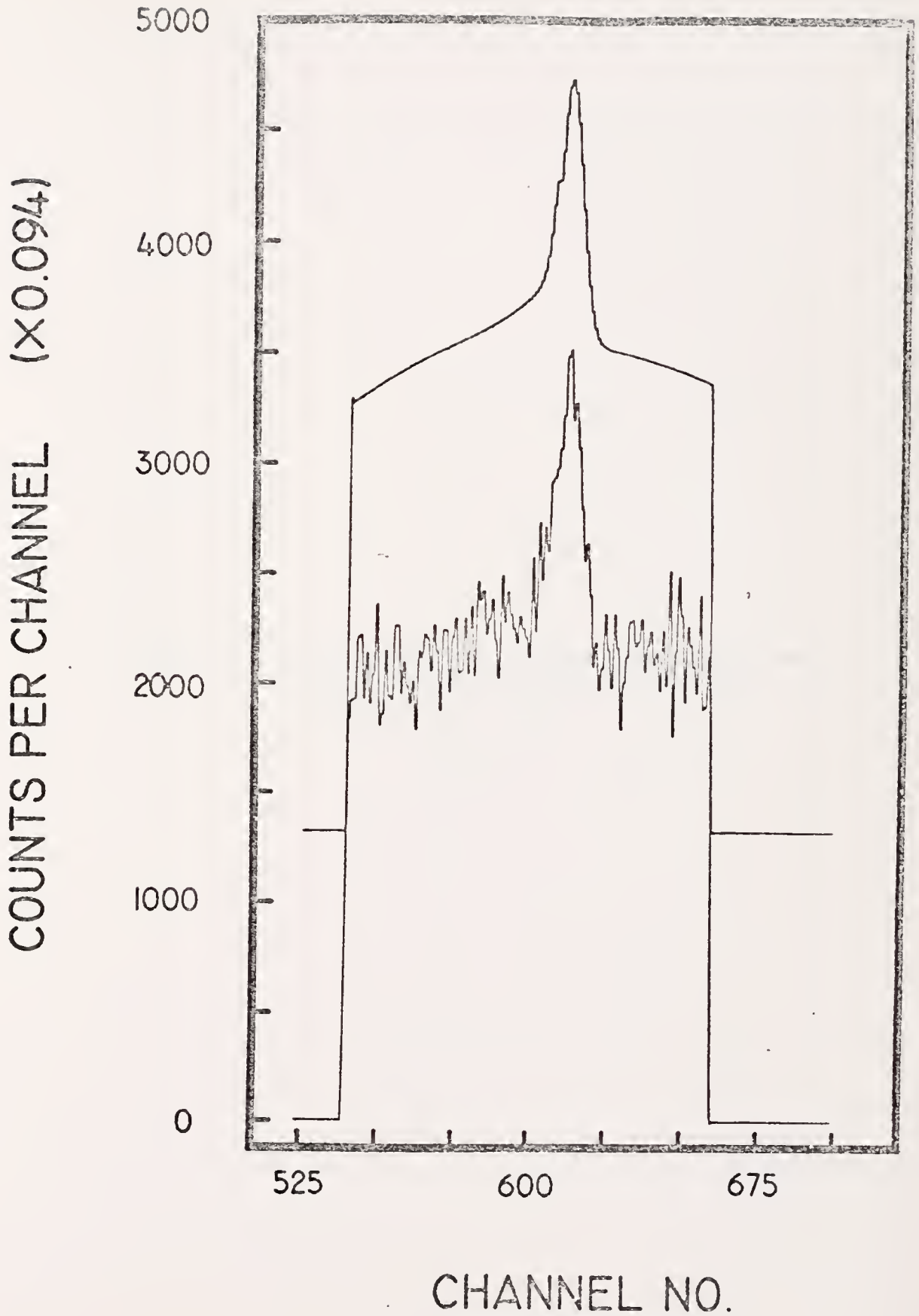


Figure 55. Raw data and fitted curve (offset) for the
303.89 KeV Se - 75 peak taken from
spectrum 7

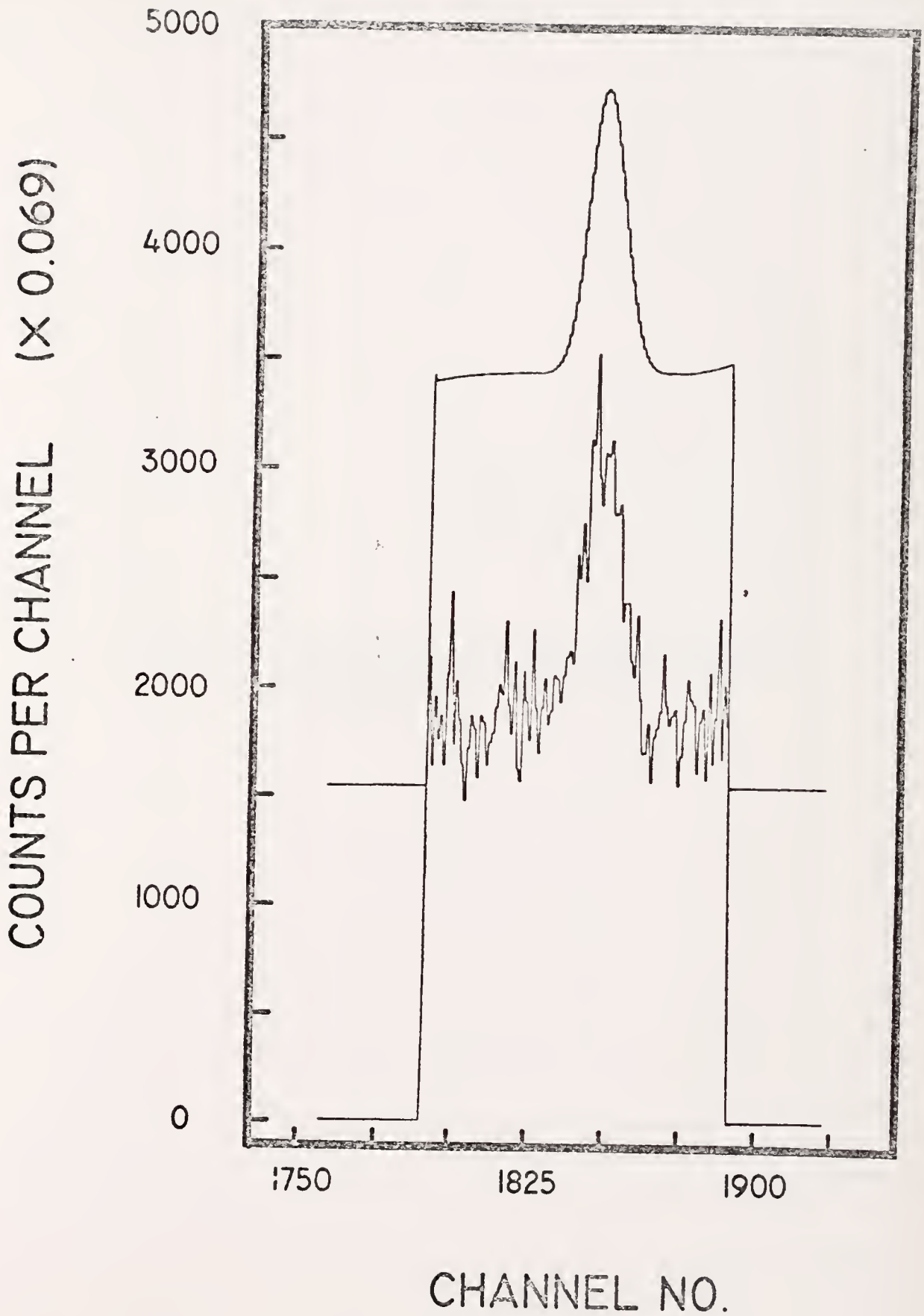


Figure 56. Raw data and fitted curve (offset) for the
303.89 KeV Se - 75 peak taken from
spectrum 10

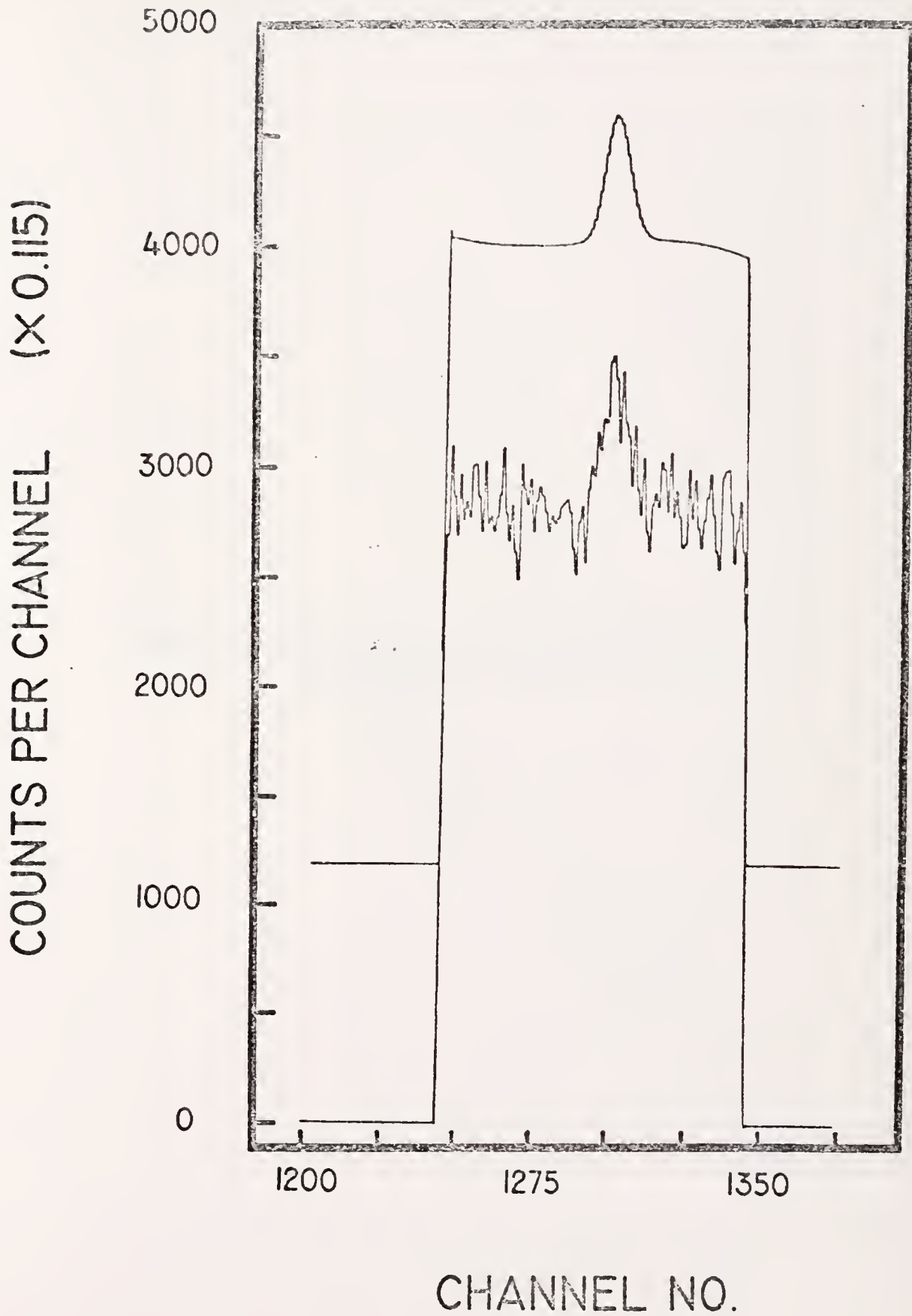
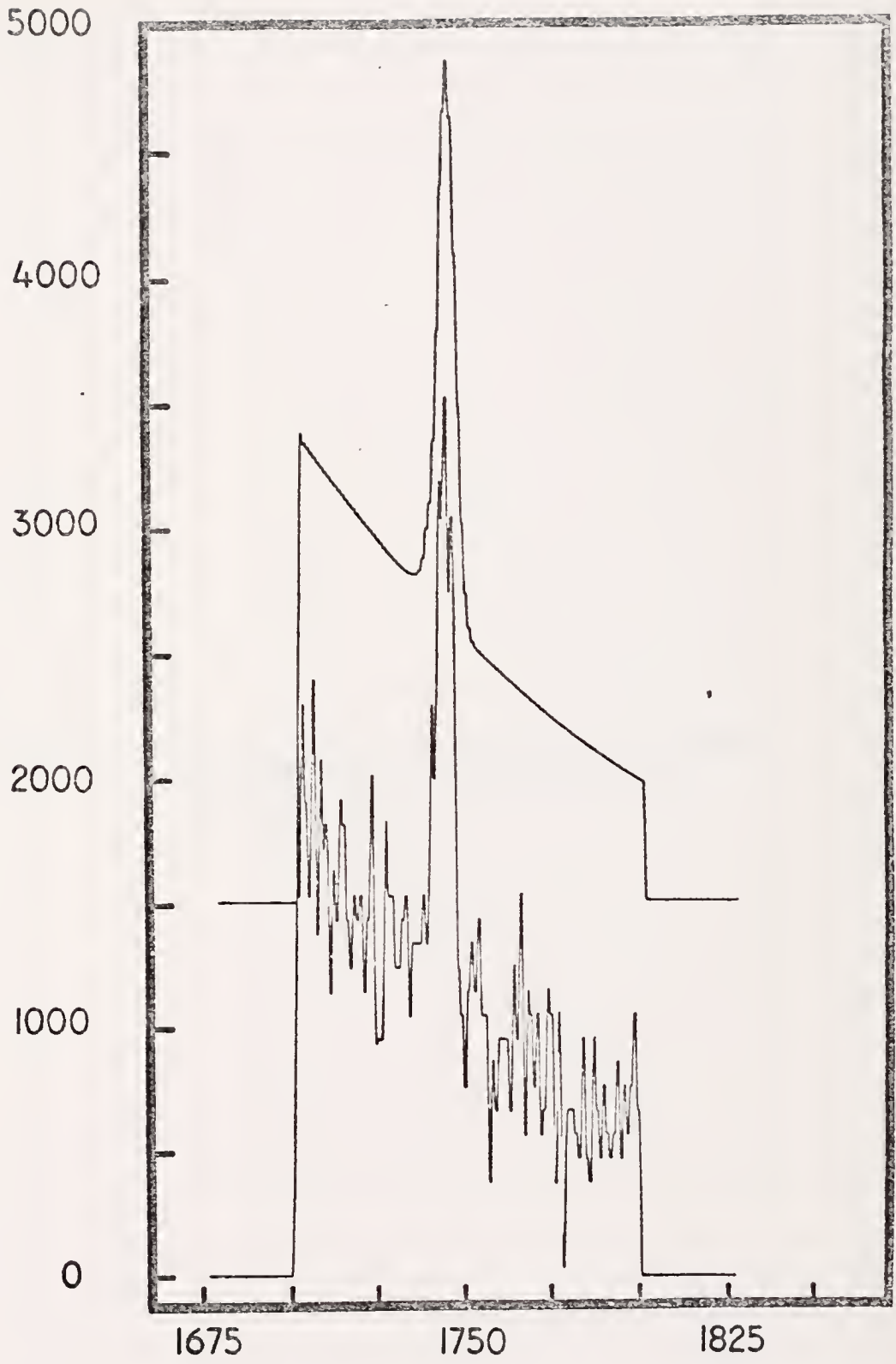


Figure 57. Raw data and fitted curve (offset) for the
1173.2 KeV Co - 60 peak taken from
spectrum 6

COUNTS PER CHANNEL
(X 0.011)



CHANNEL NO.

Figure 58. Raw data and fitted curve (offset) for the
1173.2 KeV Co - 60 peak taken from
spectrum 5

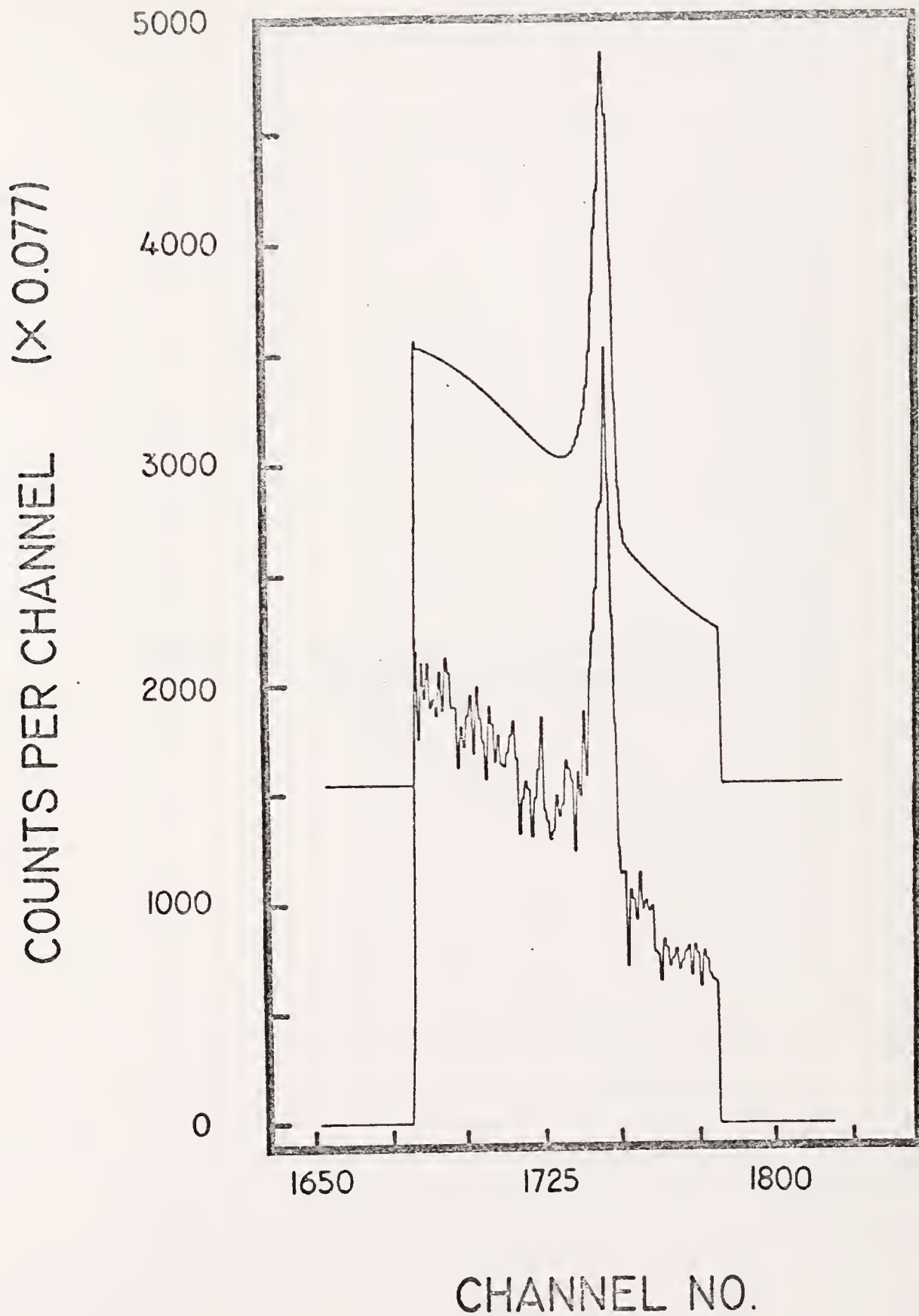


Figure 59. Raw data and fitted curve (offset) for the
744.2 KeV Ag - 110m peak taken from
spectrum 11

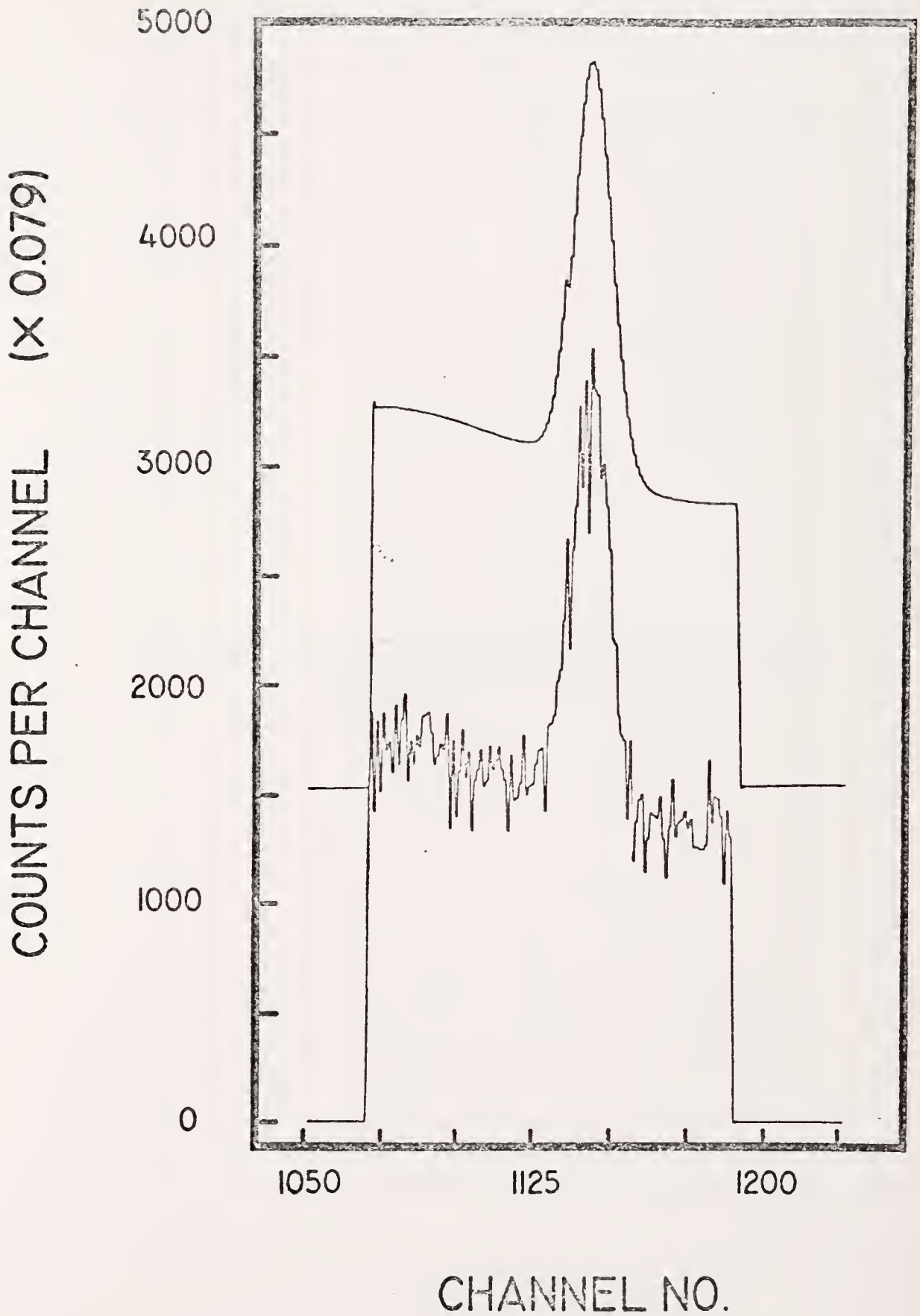


Figure 60. Raw data and fitted curve (offset) for the 657.6 KeV Ag - 110m peak taken from spectrum 6

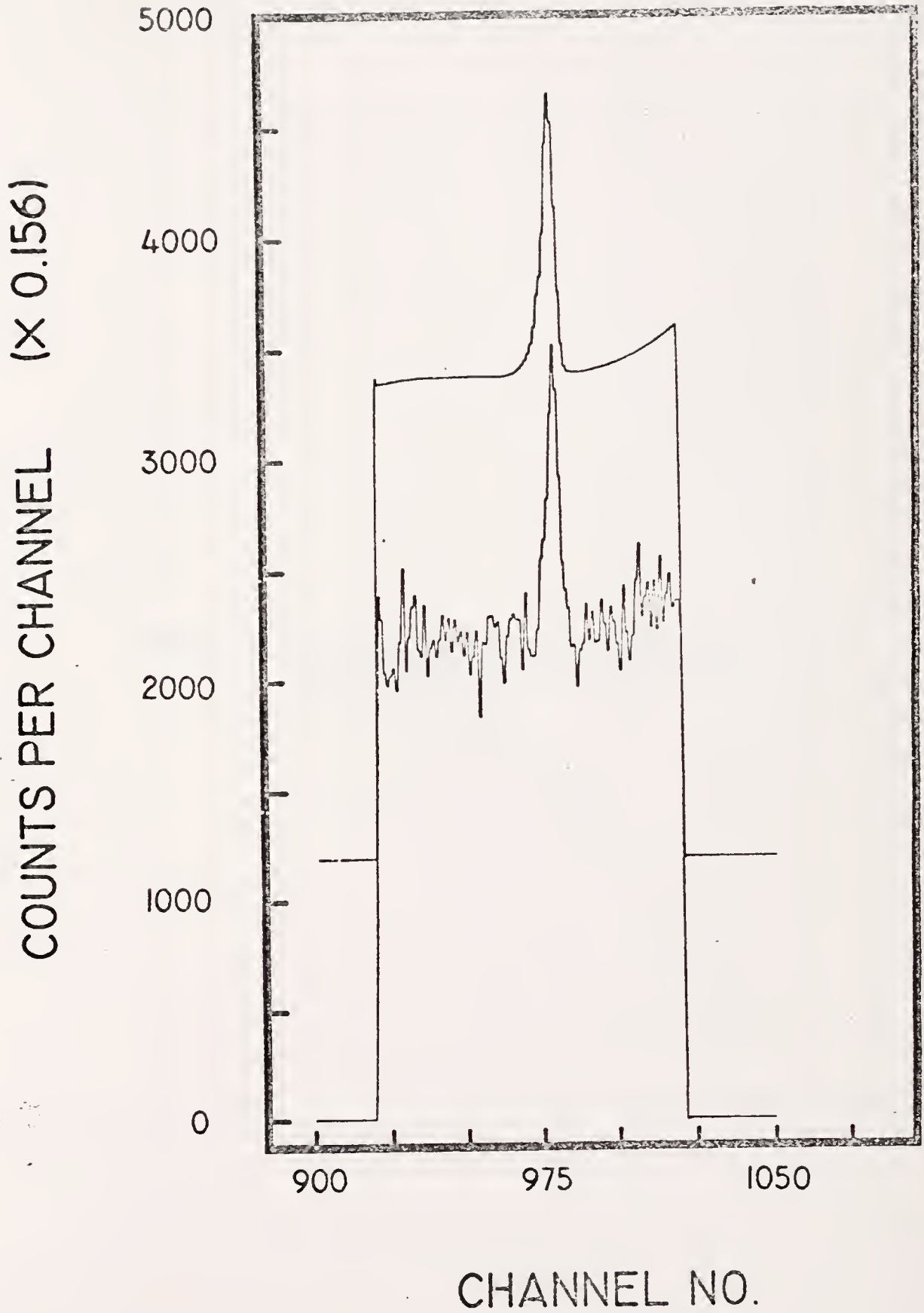


Figure 61. Raw data and fitted curve (offset) for the
1173.2 KeV Co - 60 peak taken from
spectrum 3

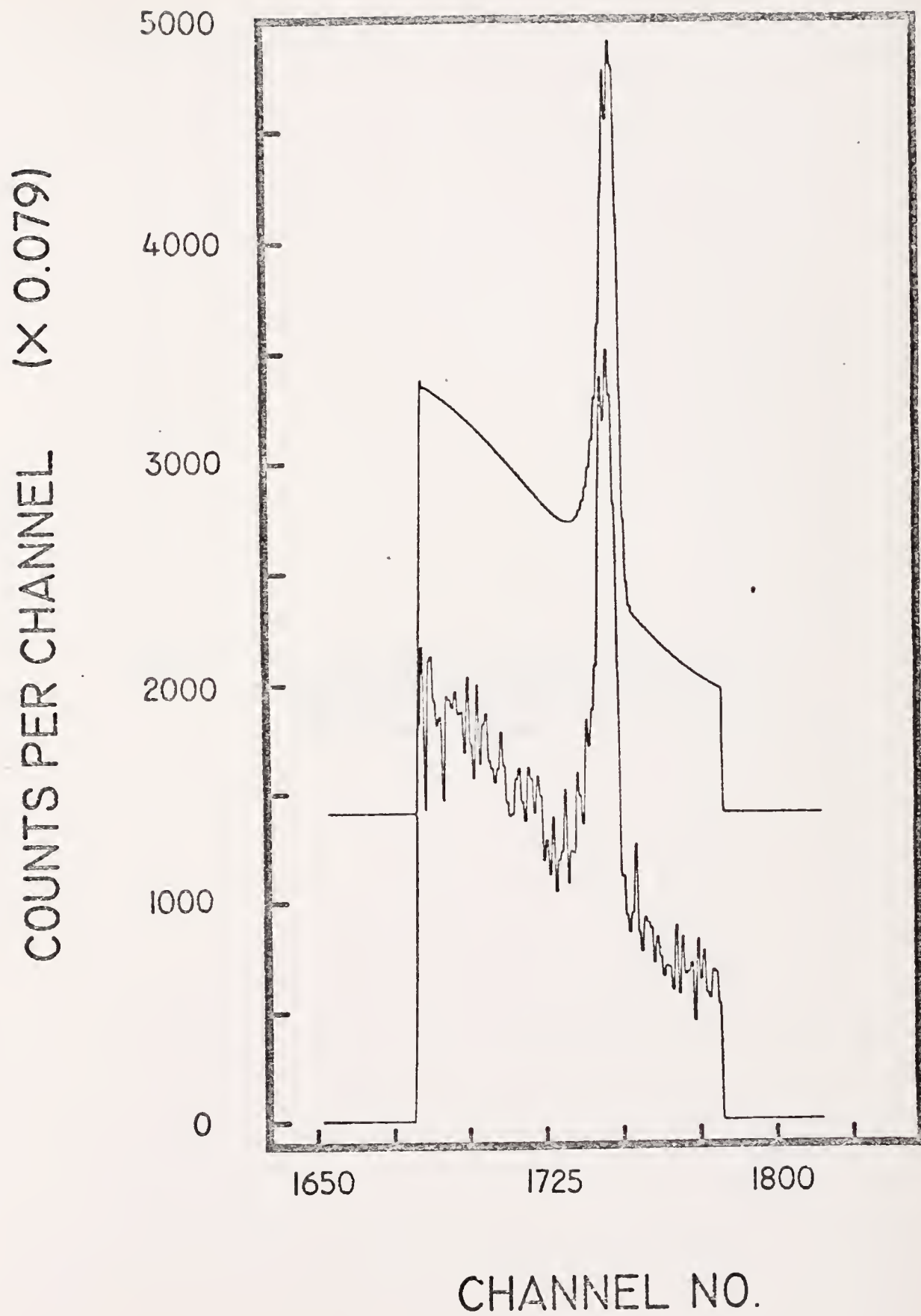
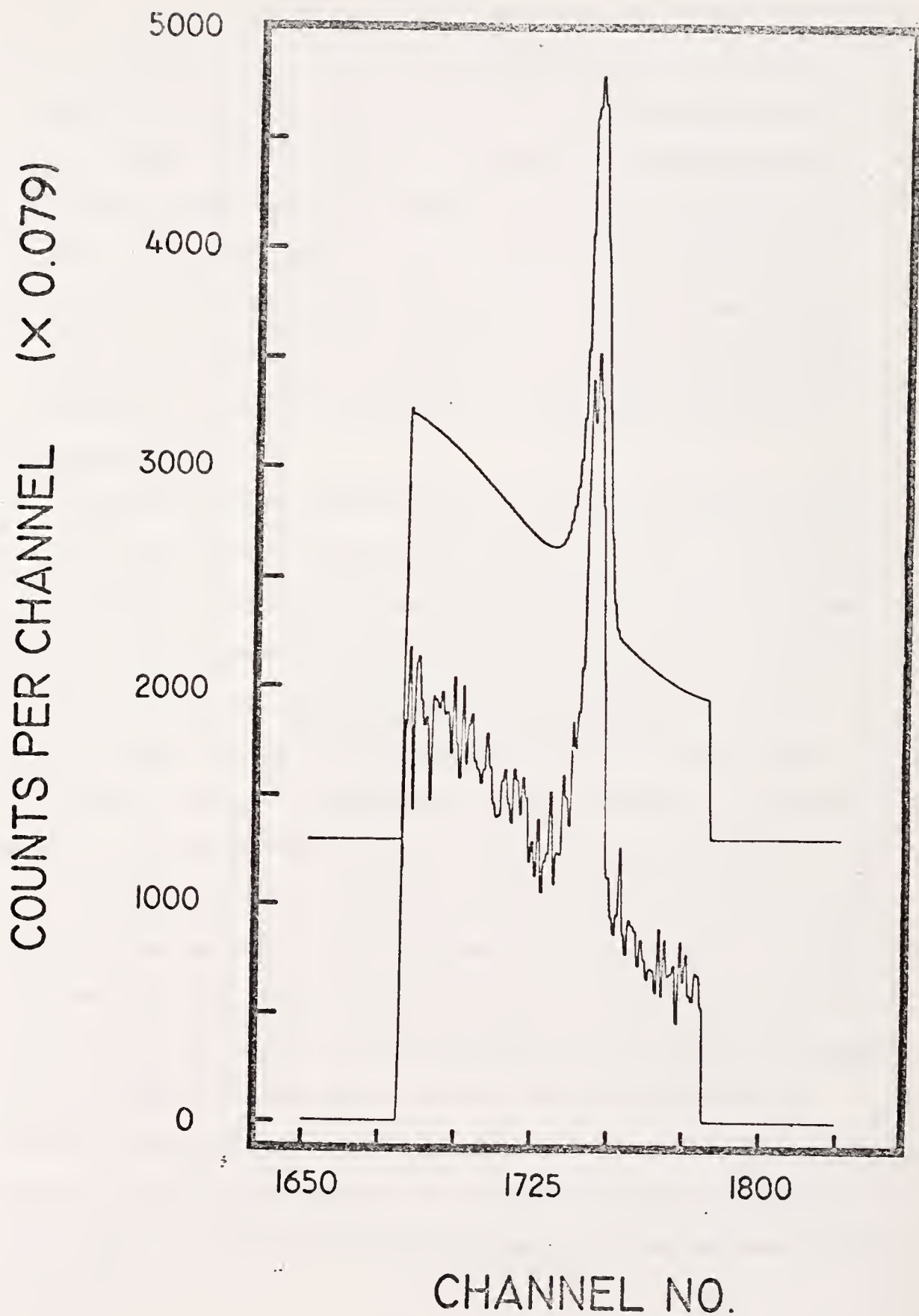


Figure 62. Raw data and fitted curve (offset) for the 1173.2 KeV Co - 60 peak taken from spectrum 3. The data was smoothed before the fit was obtained.



curve. The basic difference occurred at the top of the peaks in the two fitted functions. The sharp minimum in the raw data was best approximated by a separation of the Gaussian and exponential parts of the fitting function, as shown in Figure 61. The smoothing reduced this minimum to such an extent that the fitted function failed to show it, although there is still a slight shoulder on the final curve near the top of the peak in Figure 62. Since the two fitting intervals were not exact, the sums in Table VII were not comparable, although the ratios between the fitted and raw sums in each case were nearly exact.

Figures 63 and 64 show examples of peaks whose shapes were distorted to such an extent that pre-smoothing was necessary to obtain any valid fit. In both cases the best fit showed a distinct shoulder on the leading edge of the peak. Because the peak in Figure 64 was located near the top of a large Compton edge, the number of data points included in the polynomial baseline fit was limited on the right side of the peak. Enough points were included on the left, however, to accurately establish a correct baseline approximation.

The eight parameters utilized in the fitting function were, for practical purposes, the upper limit for the PDP-8/L computer. Since each new parameter expanded the square matrix which was the heart of the least squares procedure, the computational time greatly increased with the number of parameters. For this reason the simultaneous fitting of two overlapping peaks was impractical. Overlapping peaks presented few problems, however, due to the tremendous resolution of the system. A simple expansion of the energy scale solved most of the problems.

Figure 63. Raw data and fitted curve (offset) for the 657.6 KeV Ag - 110m peak taken from spectrum 8. The data was smoothed before the fit was obtained.

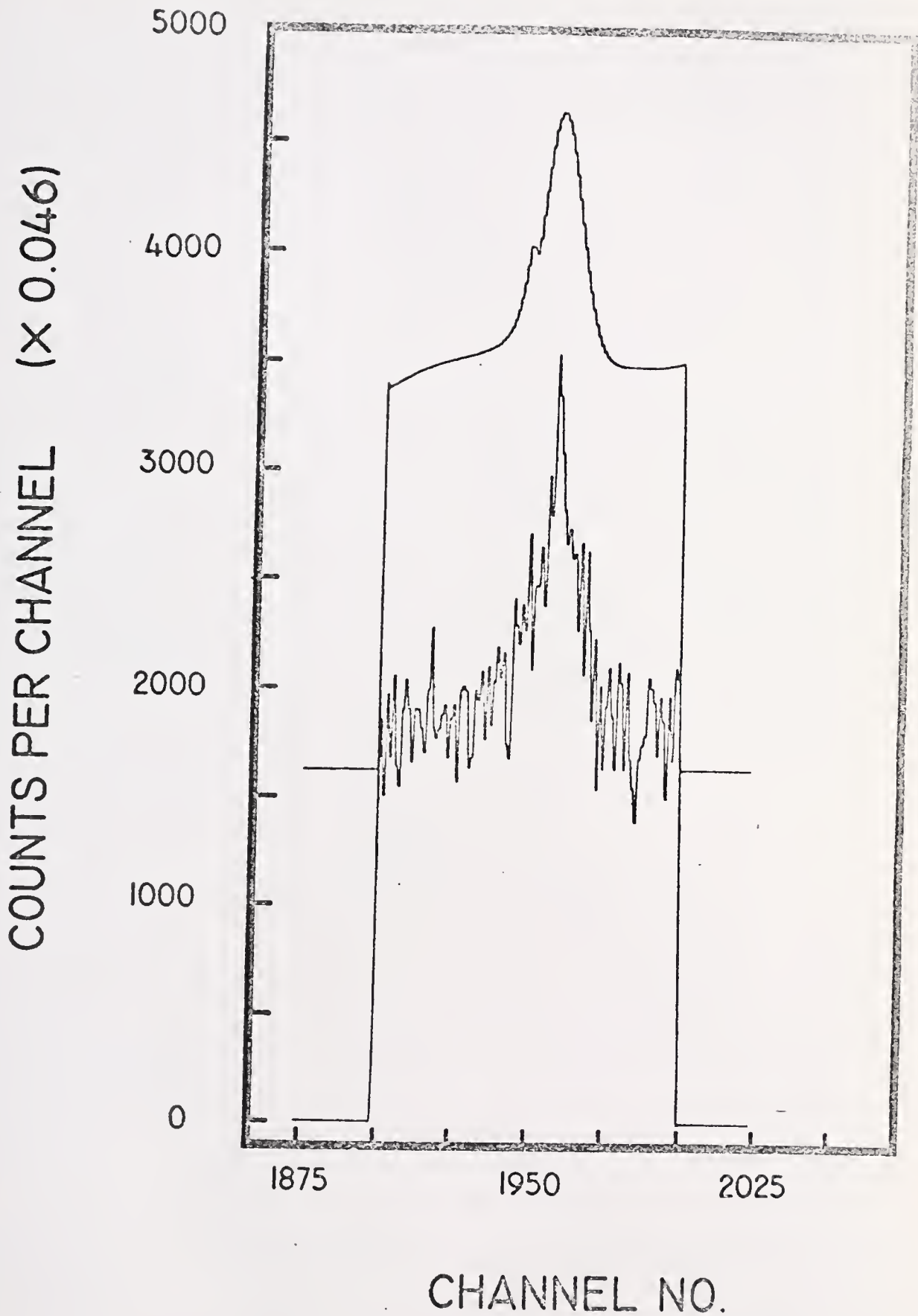
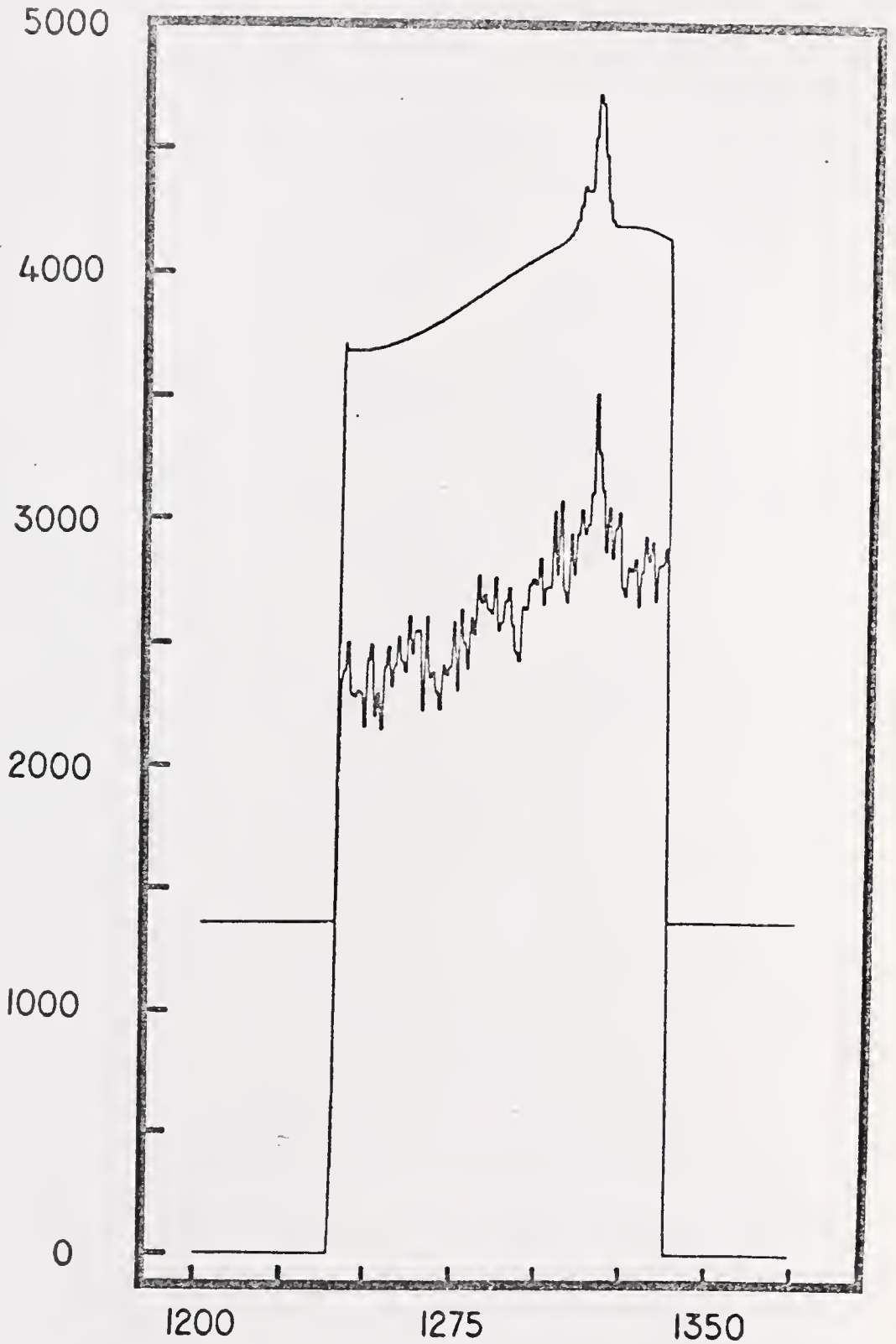


Figure 64. Raw data and fitted curve (offset) for the 884.5 KeV Ag - 110m peak taken from spectrum 6. The data was smoothed before the fit was obtained.

COUNTS PER CHANNEL (X 0.231)



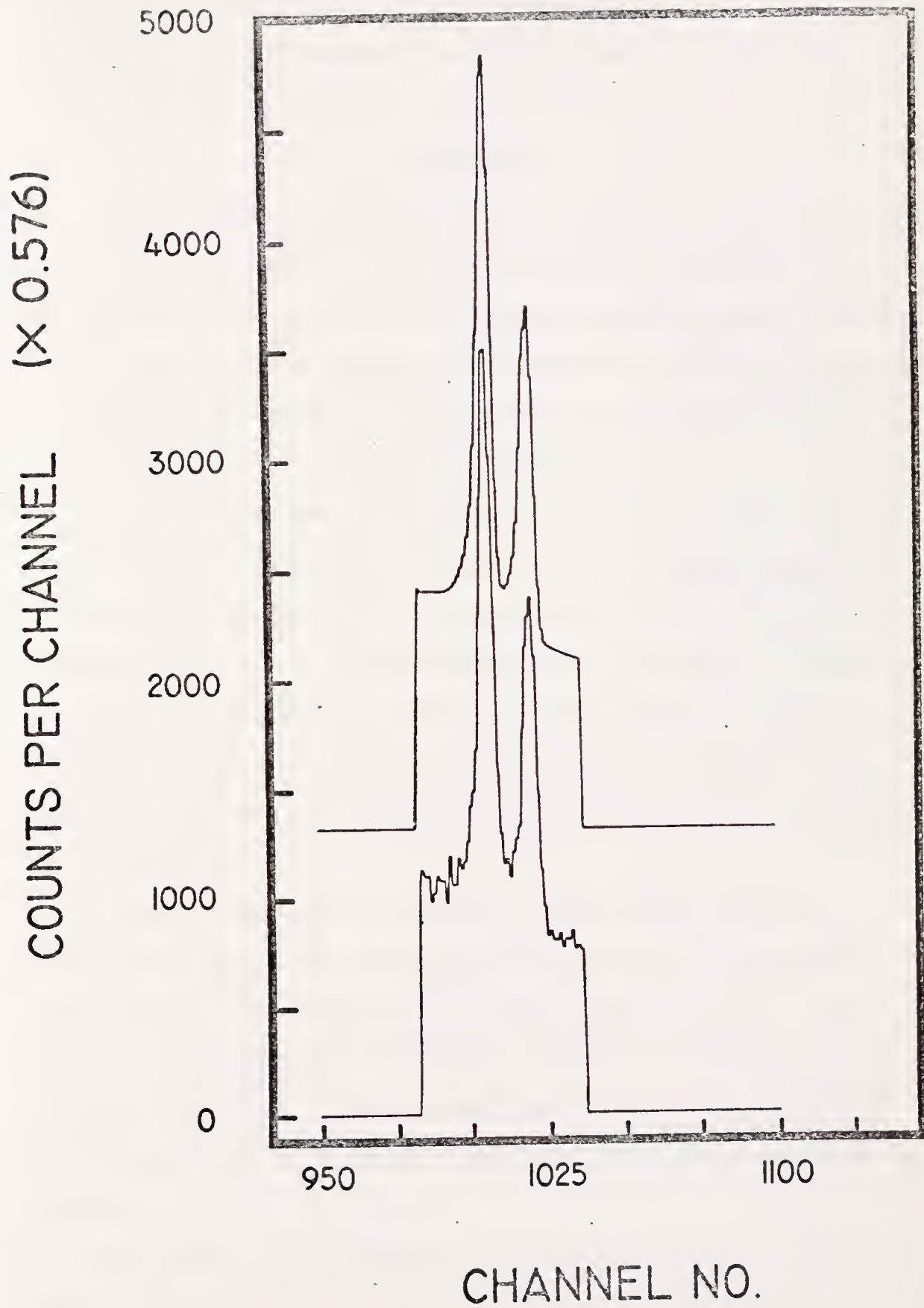
CHANNEL NO.

In a few cases, however, there was a small amount of overlap between two major peaks which did not prevent the detection routines from locating the peak boundaries, but affected the final quantitative results. Such a case resulted when the low energy tail of one peak extended below the base of another. The tail was usually treated as a positively sloped baseline and approximated by the polynomial. This approach, however, did not solve the area problem of the higher energy peak.

A more accurate solution involved the individual fitting of each peak. The peaks in Figure 65 illustrate such a case. The basic fitting function assumed that the photopeaks were pure Gaussian on the high energy side. It was therefore assumed that the data to the right of the separating minimum did not include any overlap contribution. Since enough of the higher energy peak shape was represented to allow a valid fit, the functional form for this peak was calculated. This function was then subtracted from the lower energy peak, leaving a new set of data from which a second function was calculated. Each set of parameters was then used to calculate the individual peak areas. The total curve was obtained by adding the contribution from each peak to the background.

The results of the above procedure were used to verify the original Gaussian assumption. The total peak area was determined for each of the fitting intervals by adding the contribution from each of the individual peaks. When the total areas were compared to the individual contributions, it was found that the second peak in Figure 65 contributed over 4% of the total peak area to the left of the separating minimum while the first peak was responsible for less than 0.1% of the

Figure 65. Raw data and fitted curve (offset) for the
677.5 and 686.8 KeV Ag - 110m peaks taken from
spectrum 1



areas to the right. This verified the assumption that the right side of the first peak was Gaussian and did not contribute significantly to the shape of the second peak.

Peak Areas

The curve fitting results were used to obtain the true peak areas of the 35 fitted peaks. The areas were obtained by numerically integrating the fitted functions by the trapezoid method, using an interval of 0.1 channel. The fitted sums were calculated by adding the functional values at each channel. The boundaries of the original data blocks were used to fix the limits for these calculations.

The fitted sums were calculated as a percentage of the total integrated areas to determine the necessity for the lengthy integration procedure. The 35 values had a narrow range of 99.7% to 100.8% and averaged 100.0 ± 0.3 %. These results indicated that the simplified summation technique was as accurate as the more complicated numerical integration process. However, in order to maintain as high a degree of accuracy as possible the integrated areas were utilized in the remainder of this research.

Because of the nature of the least squares method, the curve fitting approach offered the most accurate technique for determining the peak areas. The complications and time involved, however, often offset the increased accuracy achieved. Therefore the peak detection routines, together with the more simplified methods for approximating the peak areas directly from the digital data, were used for routine analysis.

There were two major sources of error associated with the simplified peak area methods. The first involved the correct location of

the peak boundaries, and the second involved the method of choice for calculating the peak area.

To test the boundary selections obtained from the peak detection routines the fitted functions were reevaluated. With the limits for the integration of the fitted functions fixed by the boundary channels selected by the search routines from smoothed data, the partial integrated areas were calculated. The boundaries selected by method two were given precedence whenever conflict arose.

The partial integrated areas were then compared to the total integrated areas previously calculated. Table VIII lists both of these areas and the comparison values. The low results from peaks 17, 23, 32, and 33 were understandable in view of the earlier curve fitting discussion regarding these peaks. The high exponential tail of peak 17 and the unusual separation of the exponential tail from the Gaussian in the three other cases were all indications of severe scatter in the region of the peak, which led to an increased chance of a poor boundary selection. The comparison values for all 35 peaks averaged $95.3 \pm 7.0\%$. When the above four peaks were excluded from consideration the remaining 31 values averaged $97.4 \pm 3.4\%$. These results clearly indicated that the majority of the peak area was included within the peak boundaries selected by the peak detection routines.

In a similar study the peak areas determined by the total peak area (TPA) method on smoothed data were compared to the total integrated areas. Table IX lists these results. The comparison values for all 35 peaks had an average of $93.8 \pm 16.5\%$, while removal of the same four values raised this average to $97.7 \pm 11.5\%$. These results indicated that the TPA method also produced the majority of the total available

TABLE VIII

CURVE FITTING RESULTS

<u>PEAK</u>	<u>TOTAL INTEGRATED AREA (COUNTS)</u>	<u>PARTIAL INTEGRATED AREA (COUNTS)</u>	<u>PERCENTAGE (PARTIAL*100/TOTAL)</u>
1	72341.9	72235.6	99.8530
2	39290.6	39267.4	99.9409
3	31973.4	31919.8	99.8323
4	17656.4	17594.6	99.6500
5	14337.1	14243.1	99.3443
6	32724.9	32615.3	99.6651
7	26289.2	26280.2	99.9657
8	68018.0	67996.0	99.9677
9	9533.95	9481.54	99.4503
10	21722.5	21624.4	99.5484
11	42070.2	40942.8	97.3202
12	7101.57	7091.12	99.8528
13	4360.07	4318.65	99.0500
14	3099.44	2967.26	95.7353
15	3771.99	3767.94	99.8926
16	8623.54	8488.35	98.4323
17	2687.95	2022.88	75.2573
18	2866.65	2840.25	99.0790
19	1708.67	1505.49	88.1089
20	7336.80	7311.71	99.6580
21	3266.39	3242.64	99.2729
22	3057.08	2973.21	97.2565
23	1538.70	1264.37	82.1713
24	1396.69	1377.22	98.6060
25	761.712	684.913	89.9175
26	146.218	143.535	98.1651
27	1151.00	1019.02	88.5334
28	2332.64	2295.22	98.3958
29	1098.28	1042.07	94.8820
30	1480.54	1403.56	94.8005
31	1516.16	1423.51	93.8892
32	899.946	752.137	83.5758
33	614.963	451.014	73.3400
34	8178.49	8075.90	98.7456
35	5216.33	4873.82	93.4339
		MEAN	95.2739
		± STANDARD DEVIATION	± 7.0420
		MEAN (OMIT 17,23,32,33)	97.4271
		± STANDARD DEVIATION	± 3.4254

TABLE IX

CURVE FITTING RESULTS

<u>PEAK</u>	<u>TOTAL INTEGRATED AREA (COUNTS)</u>	<u>TPA QUANTITATIVE AREA (COUNTS)</u>	<u>PERCENTAGE (TPA*100/TOTAL)</u>
1	72341.9	71688	99.0961
2	39290.6	39039	99.3596
3	31973.4	31915	99.8173
4	17656.4	17336	98.1854
5	14337.1	14185	98.9391
6	32724.9	32159	98.2707
7	26289.2	26351	100.235
8	68018.0	67881	99.7986
9	9533.95	9517	99.8222
10	21722.5	21368	98.3680
11	42070.2	40215	95.5902
12	7101.57	7390	104.061
13	4360.07	4420	101.375
14	3099.44	2859	92.2424
15	3771.99	3986	105.674
16	8623.54	8514	98.7297
17	2687.95	1667	62.0175
18	2866.65	2765	96.4540
19	1708.67	1320	77.2531
20	7336.80	7173	97.7674
21	3266.39	3238	99.1308
22	3057.08	3010	98.4600
23	1538.70	1366	88.7762
24	1396.69	1782	127.587
25	761.712	936	122.881
26	146.218	160	109.426
27	1151.00	869	75.4996
28	2332.64	2177	93.3278
29	1098.28	1219	110.992
30	1480.54	1248	84.2936
31	1516.16	1248	82.3132
32	899.946	489	54.3366
33	614.963	290	47.1573
34	8178.49	7438	90.9459
35	5216.33	3866	74.1134
		MEAN	93.7798
		± STANDARD DEVIATION	± 16.4712
	MEAN (OMIT 17,23,32,33)		97.7421
	± STANDARD DEVIATION		± 11.5100

area, but with a greater margin for error and with less precision. This, however, was to be expected since the original data included an uncertainty in not only the boundary channel locations, but the contents of these channels as well.

The accuracy of the TPA method was verified by comparing the TPA peak areas to the partial integrated areas, which were calculated from the same boundaries. The 35 values, listed in Table X, had an average of $100.0 \pm 13.9\%$. Removal of the four problem values led to an average of $100.3 \pm 11.4\%$. These results indicated that the TPA peak areas determined from the smoothed digital data were representative of the true area enclosed by the chosen boundaries, within the limits of the uncertainty created by the scatter present in the digital data.

All of the above results indicated that the peak search routines utilized in this research, together with the TPA method of quantitation, offered a fast, accurate method for the data reduction of Ge(Li) spectra. The curve fitting technique provided an excellent means for obtaining more accuracy when desired and time permitted. For routine analysis, however, the direct reduction of the digital data yielded rapid, accurate results.

Liver Analysis

The application of the proposed system to the analysis of biological materials was demonstrated by the quantitative determination of four elements of bovine liver. The sample was Standard Reference Material 1577, obtained from the National Bureau of Standards in the form of a dry powder. The method of standard addition was chosen to insure a constant matrix effect in all of the samples.

TABLE X
CURVE FITTING RESULTS

PEAK	PARTIAL INTEGRATED AREA (COUNTS)	TPA QUANTITATIVE AREA (COUNTS)	PERCENTAGE (TPA*100/PARTIAL)
1	72235.6	71688	99.2419
2	39267.4	39039	99.4184
3	31919.8	31915	99.9850
4	17594.6	17336	98.5302
5	14243.1	14185	99.5921
6	32615.3	32159	98.6010
7	26280.2	26351	100.269
8	67996.0	67881	99.8309
9	9481.54	9517	100.374
10	21624.4	21368	98.8143
11	40942.8	40215	98.2224
12	7091.12	7390	104.214
13	4318.65	4420	102.347
14	2967.26	2859	96.3515
15	3767.94	3986	105.787
16	8488.35	8514	100.302
17	2022.88	1667	82.4072
18	2840.25	2765	97.3506
19	1505.49	1320	87.6791
20	7311.71	7173	98.1029
21	3242.64	3238	99.8569
22	2973.21	3010	101.237
23	1264.37	1366	108.038
24	1377.22	1782	129.391
25	684.913	936	136.660
26	143.535	160	111.471
27	1019.02	869	85.2780
28	2295.22	2177	94.8493
29	1042.07	1219	116.979
30	1403.56	1248	88.9167
31	1423.51	1248	87.6706
32	752.137	489	65.0147
33	451.014	290	64.2995
34	8075.90	7438	92.1012
35	4873.82	3866	79.3217
		MEAN	97.9572
		± STANDARD DEVIATION	± 13.9399
		MEAN (OMIT 12, 23, 32, 33)	100.282
		± STANDARD DEVIATION	± 11.3695

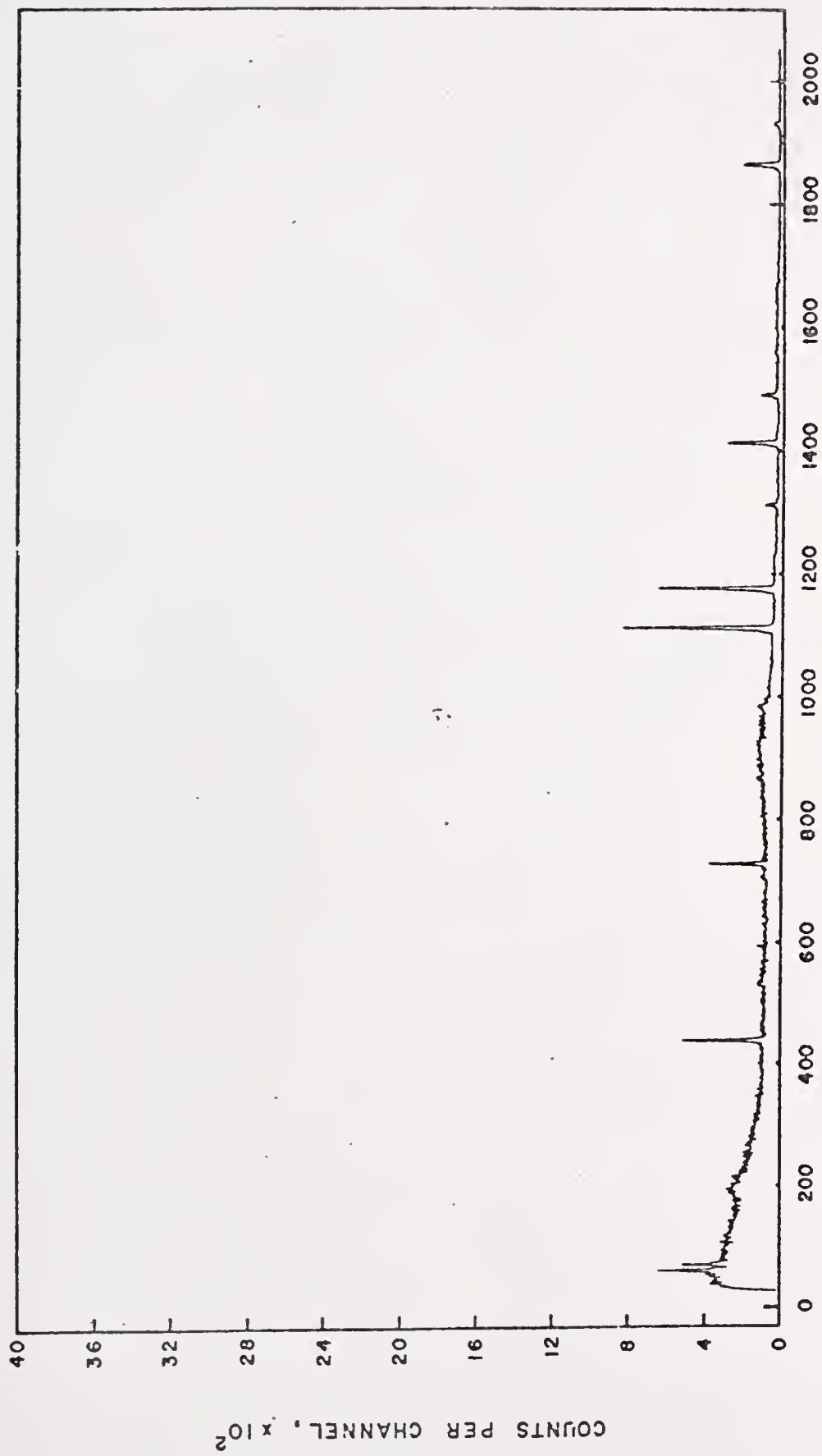
Two samples of pure liver were initially irradiated for five minutes and one hour, respectively, at a neutron flux of approximately 10^{12} neutrons/cm²/sec. Since the longer irradiation time did not produce any new peaks upon immediate analysis, the shorter time was chosen for the experiment to reduce the total activity and allow immediate handling of the samples.

Figures 66 and 67 show two views of an irradiated liver sample, and Table XI lists the significant peaks. Both spectra had a full scale energy range of 2.383 MeV. Figure 66 is a plot of the untreated data and has a full scale ordinate value of 4095 counts. Figure 67 shows the same spectrum after the contents of each channel had been multiplied by a factor of 4.8. This was done to highlight the regions of low activity and still keep the largest peak on scale.

All samples were counted directly in the irradiation vials, which were made of Nalgene and supplied by the Nalge Company. Blank spectra contained only the 1.294 MeV Ar⁴¹ peak, produced from the air trapped inside the vials during irradiation. Since, as Figure 67 shows, this Ar⁴¹ photopeak was completely resolved, no blank correction was performed on any of the sample spectra.

Standard aqueous solutions of Cl⁻, Mn⁺⁺, K⁺, and Na⁺ were prepared from high purity LiCl, metallic Mn, K₂CO₃, and Na₂CO₃, obtained from the Alpha Products division of the Ventron Corporation. Because of the limited size of the reactor port only two irradiation vials could be placed side by side in the reactor. Therefore in order to maintain the assumption of a constant neutron flux, only six samples could be irradiated simultaneously. From a knowledge of the total activity of the previously irradiated samples the experimental sample size was

Figure 66. Plot of an irradiated liver spectrum, unattenuated. The full energy range of the spectrum is 2.383 MeV (1.164 KeV/channel)



CHANNEL NO.

Figure 67. Plot of an irradiated liver spectrum, attenuated by a factor of (x 0.208). The full energy range of the spectrum is 2.383 MeV (1.164 KeV/channel)

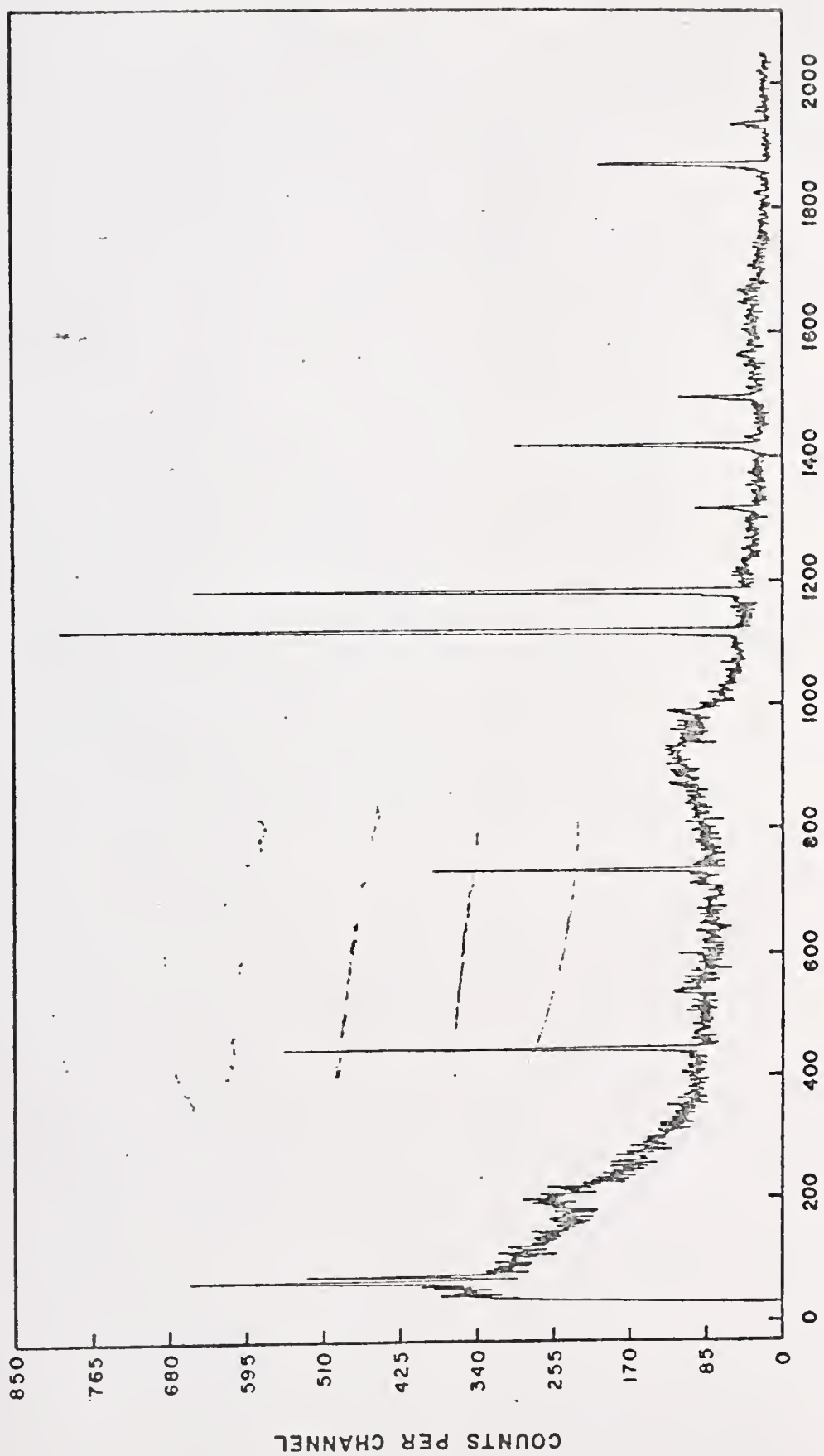


TABLE XI
SIGNIFICANT PEAKS IN AN IRRADIATED LIVER SAMPLE

<u>CHANNEL</u>	<u>ENERGY (KeV)</u>	<u>ISOTOPE</u>	<u>HALF-LIFE (MINUTES)</u>
442	511.0	- ^a	-
730	846.7	Mn - 56	154.56
1113	1293.8	Ar - 41	110
1177	1368.4	Na - 24	900
1311	1524.7	K - 42	744
1412	1642.7	Cl - 38	37.3
1424	1656.6 ^b	Cl - 38	37.3
1489	1732.1 ^c	Na - 24	900
1556	1811.2	Mn - 56	154.56
1862	2167.6	Cl - 38	37.3
1927	2244	-	-

^a Annihilation peak

^b Single escape peak

^c Double escape peak

chosen to be 0.1-0.2 grams. This ensured that the total activity of the irradiated samples did not prevent immediate handling of the samples.

Four samples were used in each of the chlorine and manganese experiments, five for potassium, and six for sodium. Because of the dilute nature of the manganese standard a pure sample was included as a check against error. Two pure samples were included in each of the potassium and sodium runs to demonstrate the precision of the overall technique.

The dry liver was weighed directly into the irradiation vials. The samples were ordered according to their weight, and the larger samples received the least amount of standard in an attempt to equalize the final peak areas. When two pure samples were included the largest and smallest were chosen to further demonstrate the reproducibility of the technique. All vials were then heat sealed to prevent spillage. The exact experimental conditions are listed in Table XII.

The samples were counted directly in the irradiation vials to eliminate transfer errors. Chlorine samples were counted for three minutes live time and all others for five minutes live time. All samples were counted at a distance of at least six inches from the face of the detector to eliminate any errors due to surface effects. This distance was varied for each run to insure a maximum dead time of 5% for any sample.

Peak detection method two was used on smoothed data to obtain the peak boundaries. Both a total peak area and a nine-point Wasson area were calculated. The quantitative areas and the values of standard

TABLE XII

EXPERIMENTAL CONDITIONS FOR THE LIVER ANALYSIS

<u>ELEMENT</u>	<u>SPECTRUM ENERGY RANGE (KeV)</u>	<u>SAMPLE NUMBER</u>	<u>SAMPLE WEIGHT (gm)</u>	<u>AMOUNT OF STANDARD ADDED (ug)</u>	<u>RELATIVE DECAY TIME^a (MINUTES)</u>
Cl	0-2383	1	0.1973	330.80	8.258
		2	0.1895	661.61	13.850
		3	0.1747	926.25	22.625
		4	0.1729	1190.89	34.242
Mn	0-1883	1	0.1934	0	10.375
		2	0.1434	0.9945	17.533
		3	0.1402	2.9835	32.275
		4	0.1377	3.9780	40.150
K	0-1598	1	0.1141	0	2.616
		2	0.2022	0	10.166
		3	0.1641	712.17	18.383
		4	0.1578	1424.34	25.858
		5	0.1520	2670.64	33.833
Na	0-1598	1	0.1050	0	2.575
		2	0.1859	0	9.808
		3	0.1366	152.32	16.941
		4	0.1360	380.80	24.166
		5	0.1352	533.12	32.791
		6	0.1278	685.44	40.741

^aThe midpoint of the count time relative to the starting time of the first count.

added were corrected for decay and varying sample size according to the equations introduced in the theory section. The final experimental results are listed in Tables XIII and XIV and are displayed in Figures 68-73.

The actual concentrations of manganese, potassium, and sodium were certified by the National Bureau of Standards (NBS), based on the results of six to twelve determinations by two independent methods. In the case of potassium and sodium the results included a homogeneity test performed on 28 samples. Both sodium and potassium were analyzed by flame emission spectrometry (homogeneity test) and neutron activation analysis (NAA), while manganese was analyzed by atomic absorption spectrometry and NAA. A value for chlorine, based on NAA results alone, was reported but not certified.

Reduction of activation analysis data at the National Bureau of Standards was performed on a Univac 1108 computer, using the computer program ALSPIS written by Yule (88). The reduction algorithm located peak boundaries by using the first derivative values determined by the Savitsky and Golay (41) convolution technique. The constants for both a quadratic and cubic polynomial were used, and several checks were performed on the peaks to insure that complete resolution had been achieved. After locating the peak boundaries the total peak area method was used to determine the peak area.

The final NBS certified concentrations were obtained by giving approximately equal weight to the experimental results of the two independent methods of analysis. Table XV lists the NBS results from each of the reported methods, the final certified concentrations, and the experimental results obtained in this research for each of the

TABLE XIII
RESULTS OF THE LIVER ANALYSIS

<u>ELEMENT</u>	<u>SAMPLE NUMBER</u>	<u>ADJUSTED STANDARD ADDED ($\mu\text{g}/\text{gm}$)</u>	<u>ADJUSTED TPA AREA (COUNTS)</u>	<u>ADJUSTED WASSON AREA (COUNTS)</u>
C1(PK 1)	1	1676.64	14725.4	13992.7
	2	3491.35	22273.3	21037.8
	3	5301.95	28195.3	26033.8
	4	6887.74	33626.7	31484.7
C1(PK 2)	1	1676.64	14902.7	13951.3
	2	3491.35	23181.2	19228.9
	3	5301.95	30234.8	25807.2
	4	6887.74	33943.6	30370.0
Mn(PK 1)	1	0	24305.6	23157.2
	2	6.9351	42359.3	40624.2
	3	21.2803	78379.4	74669.8
	4	28.8889	98321.9	94965.7
Mn(PK 2)	1	0	2648.9	2432.2
	2	6.9351	5831.5	4692.3
	3	21.2803	9661.4	7823.1
	4	28.8889	11981.6	10242.6
K	1	0	11711.2	9347.9
	2	0	11388.3	9446.1
	3	4339.8	16669.4	14351.0
	4	9026.2	21435.4	18209.1
	5	17570.0	31904.4	27851.0
Na	1	0	95799	81313
	2	0	93588	79897
	3	1115.08	141312	120374
	4	2800.00	212746	179981
	5	3943.20	256675	214908
	6	5363.38	321762	258413

TABLE XIV
RESULTS OF THE LIVER ANALYSIS

<u>ELEMENT</u>	<u># DATA POINTS</u>	<u>SLOPE</u>	<u>Y-INTERCEPT (COUNTS)</u>	<u>X-INTERCEPT ($\mu\text{g}/\text{gm}$)</u>	<u>ESTIMATED ERROR ($\mu\text{g}/\text{gm}$)</u>
C1(PK 1)					
TPA	4	3.59360	9111.03	- 2535.35	\pm 153.004
WASSON	4	3.29550	8836.71	- 2681.45	\pm 179.314
C1(PK 2)					
TPA	4	3.69397	9535.88	- 2581.47	\pm 360.955
WASSON	4	3.20263	8441.81	- 2635.90	\pm 128.851
Mn(PK 1)					
TPA	4	2552.04	24408.4	- 9.56427	\pm 0.13087
WASSON	4	2463.83	23180.4	- 9.40825	\pm 0.33764
Mn(PK 2)					
TPA	4	311.618	3082.15	- 9.89078	\pm 1.67827
WASSON	4	260.047	2585.10	- 9.94090	\pm 1.28762
K					
TPA	5	1.15026	11504.9	- 10002.0	\pm 286.646
WASSON	5	1.03823	9417.2	- 9070.5	\pm 416.687
Na					
TPA	6	41.9956	94438.4	- 2248.77	\pm 51.5370
WASSON	6	33.4440	82116.8	- 2455.35	\pm 87.9728

Figure 63. Plot of the total peak area (open circles) and Wasson area (closed circles) vs. the amount of standard added to the liver samples for the analysis of chlorine. The peak areas were obtained from the 1.643 MeV Cl - 38 peak

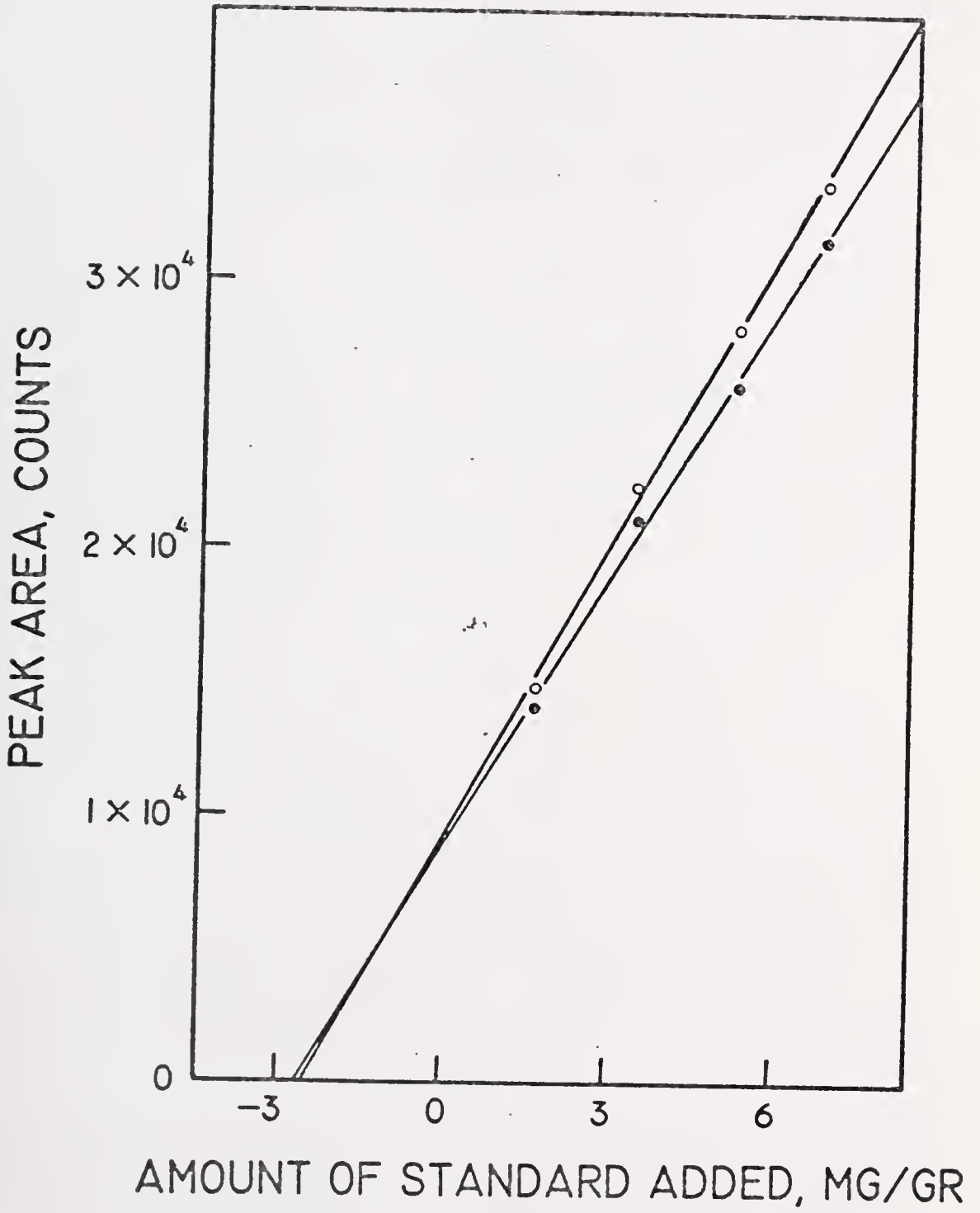


Figure 69. Plot of the total peak area (open circles) and
Wasson area (closed circles) vs. the amount
of standard added to the liver samples for
the analysis of chlorine. The peak areas
were obtained from the 2.168 MeV Cl - 38 peak

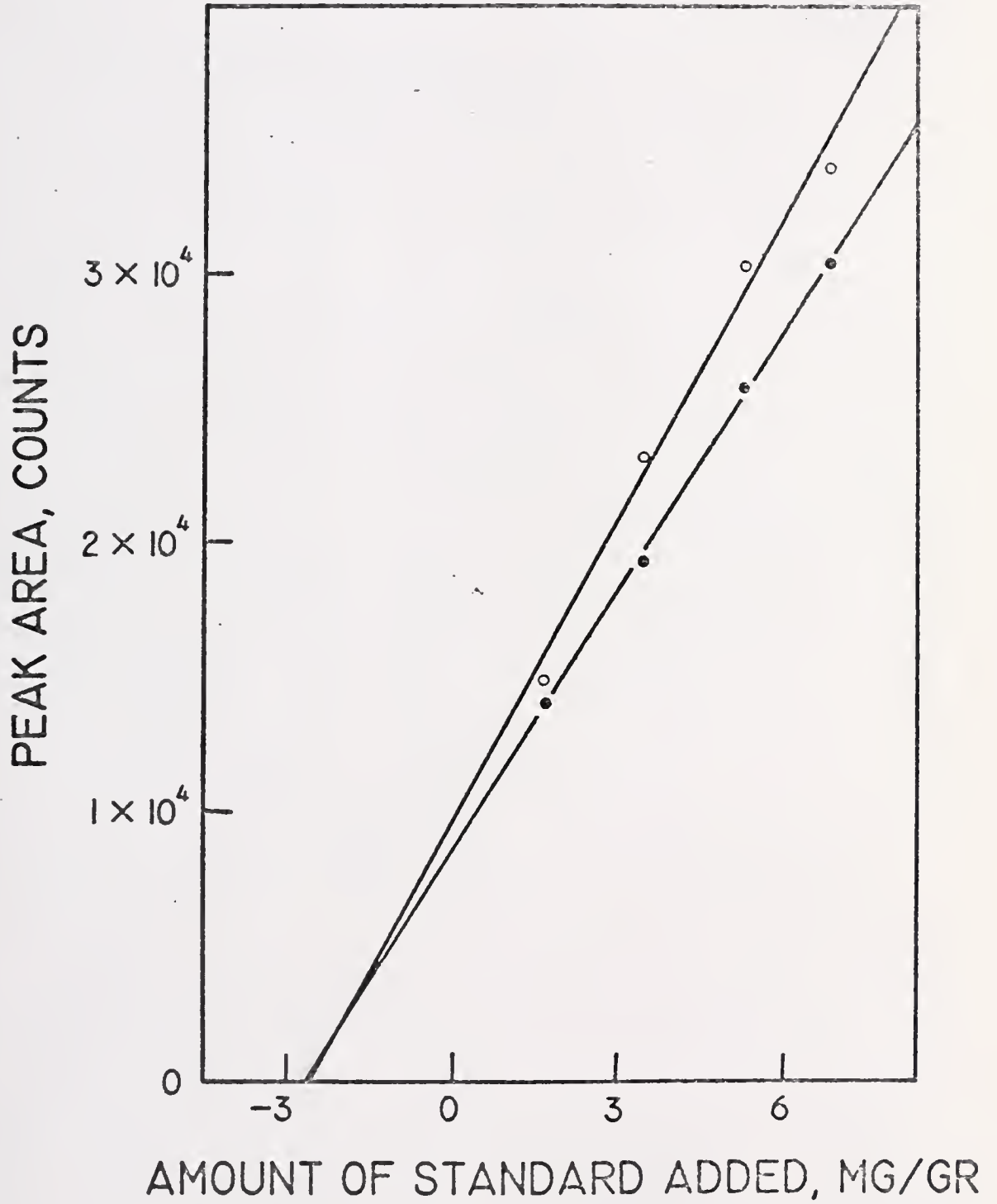


Figure 70. Plot of the total peak area (open circles) and
Wasson area (closed circles) vs. the amount
of standard added to the liver samples for
the analysis of manganese. The peak areas
were obtained from the 0.847 MeV Mn - 56 peak

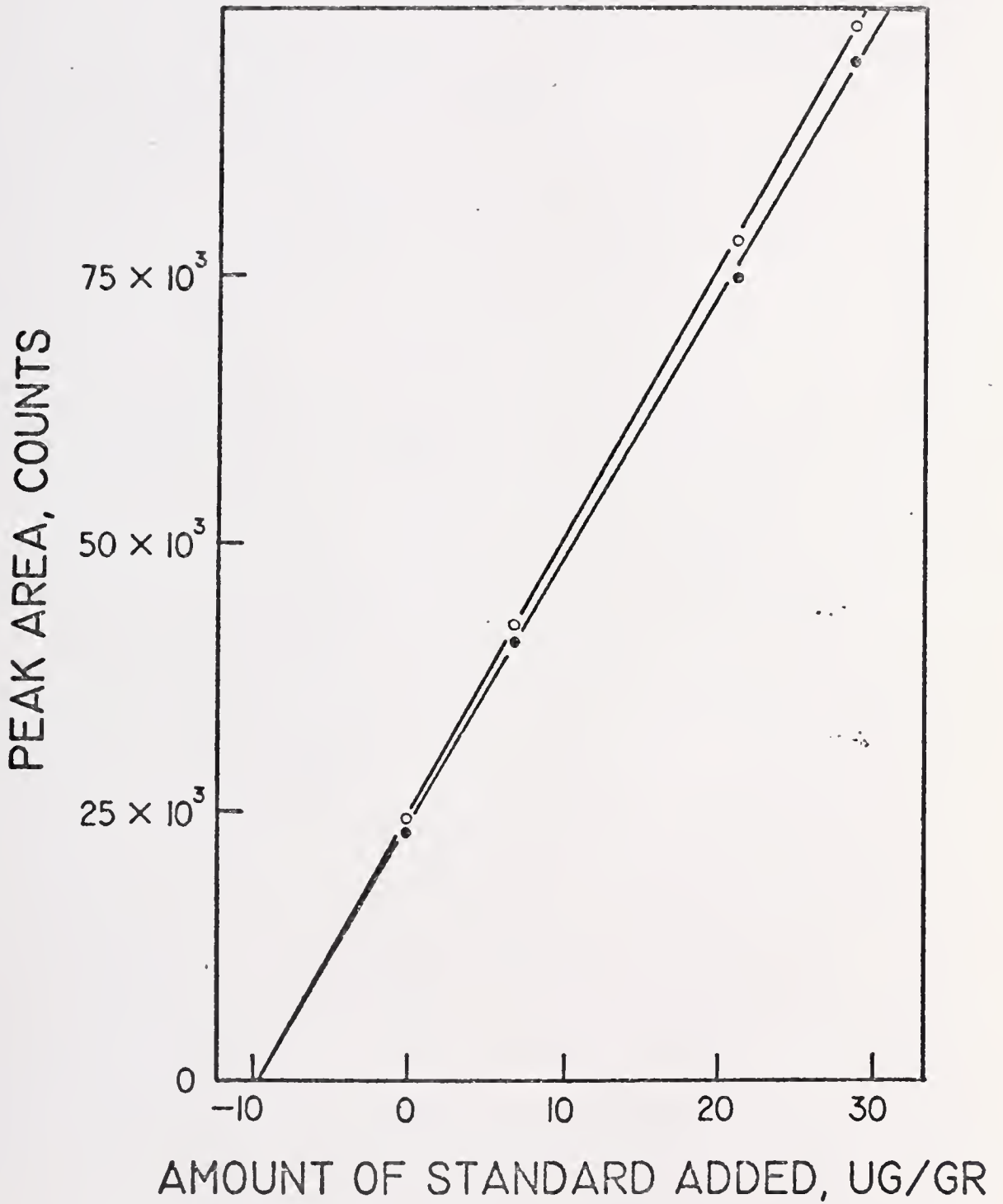


Figure 71. Plot of the total peak area (open circles) and Wasson area (closed circles) vs. the amount of standard added to the liver samples for the analysis of manganese. The peak areas were obtained from the 1.811 MeV Mn - 56 peak

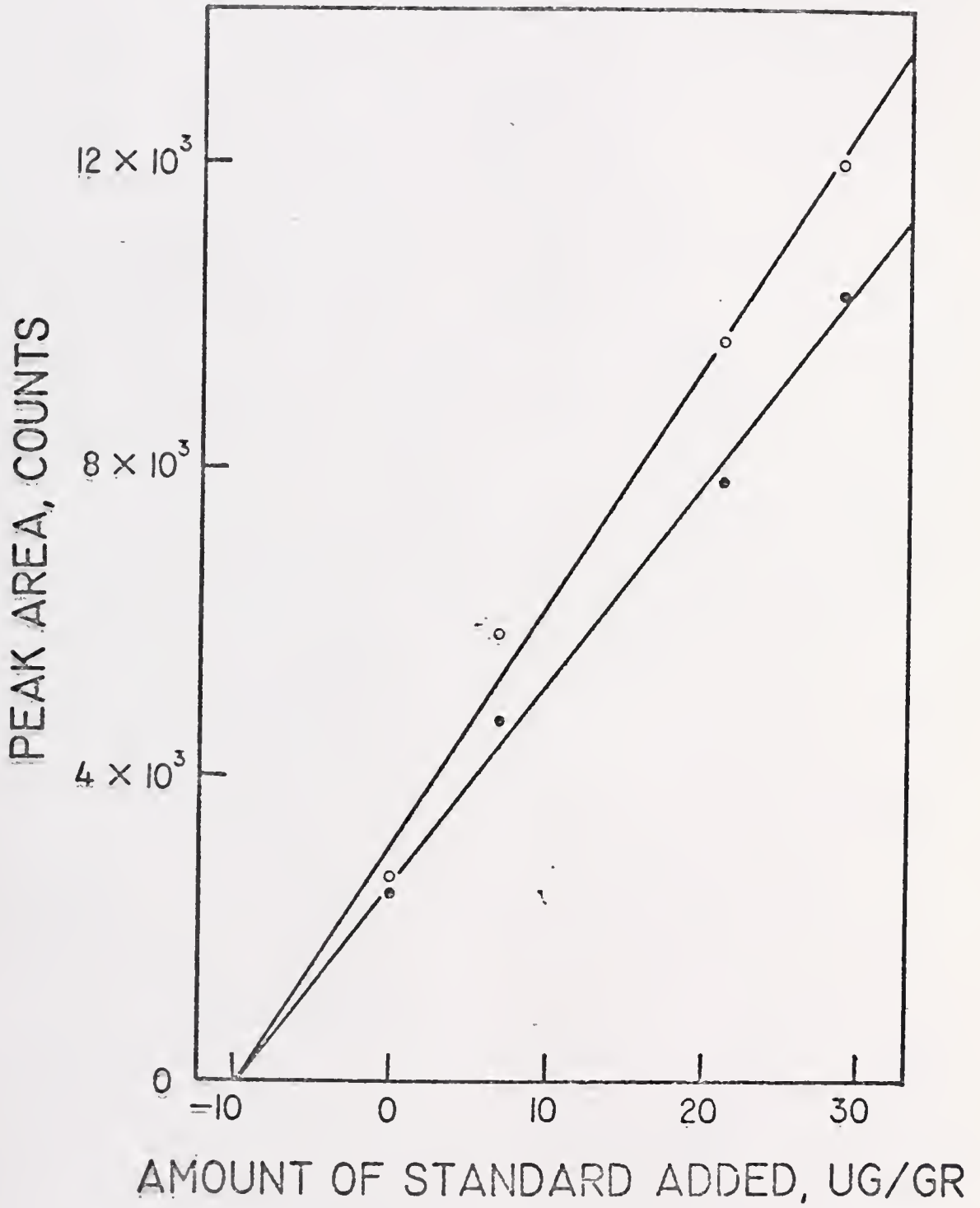


Figure 72. Plot of the total peak area (open circles) and
Wasson area (closed circles) vs. the amount
of standard added to the liver samples for
the analysis of potassium. The peak areas
were obtained from the 1.525 MeV K - 42 peak

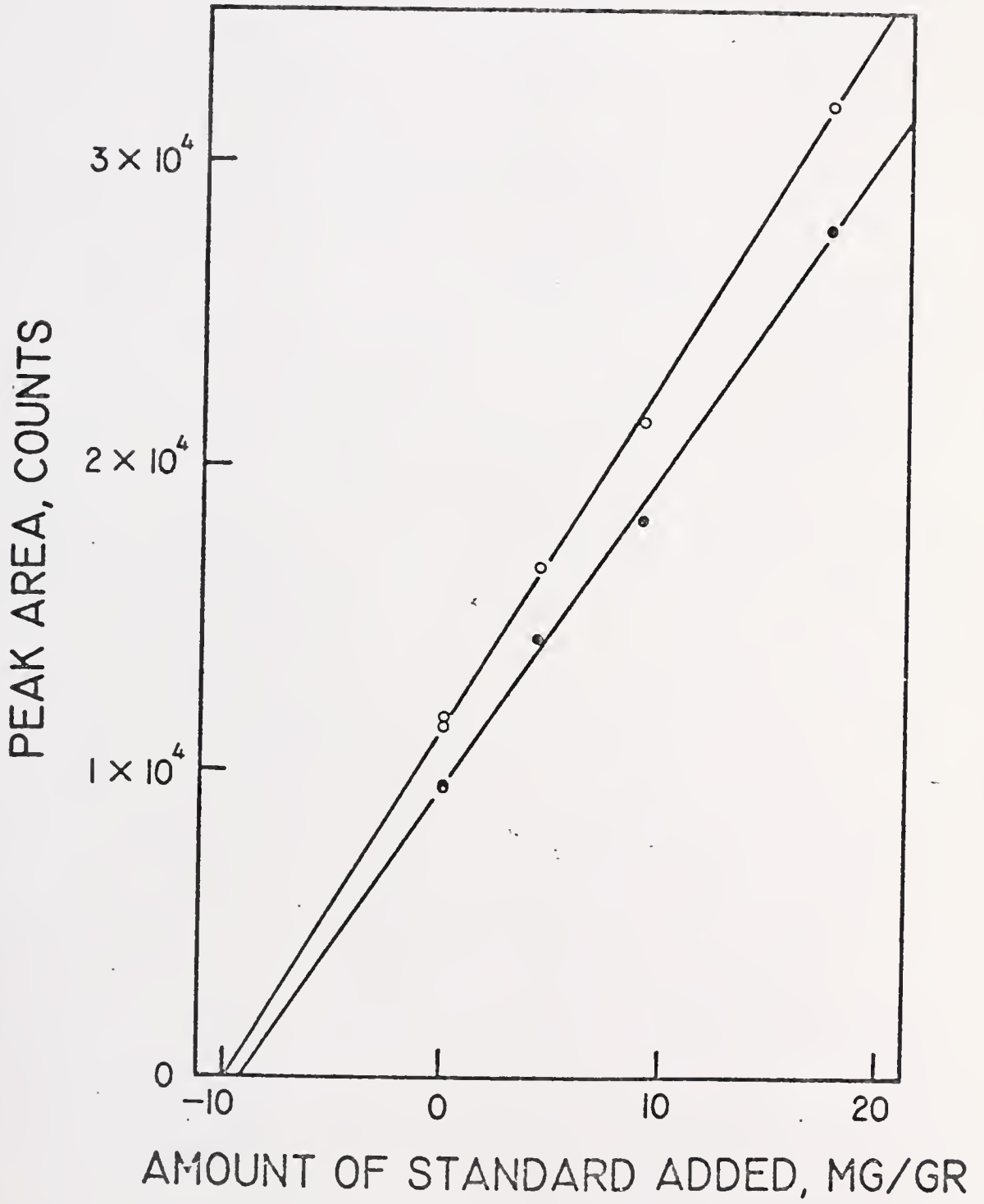


Figure 73. Plot of the total peak area (open circles) and Wasson area (closed circles) vs. the amount of standard added to the liver samples for the analysis of sodium. The peak areas were obtained from the 1.368 MeV Na - 24 peak

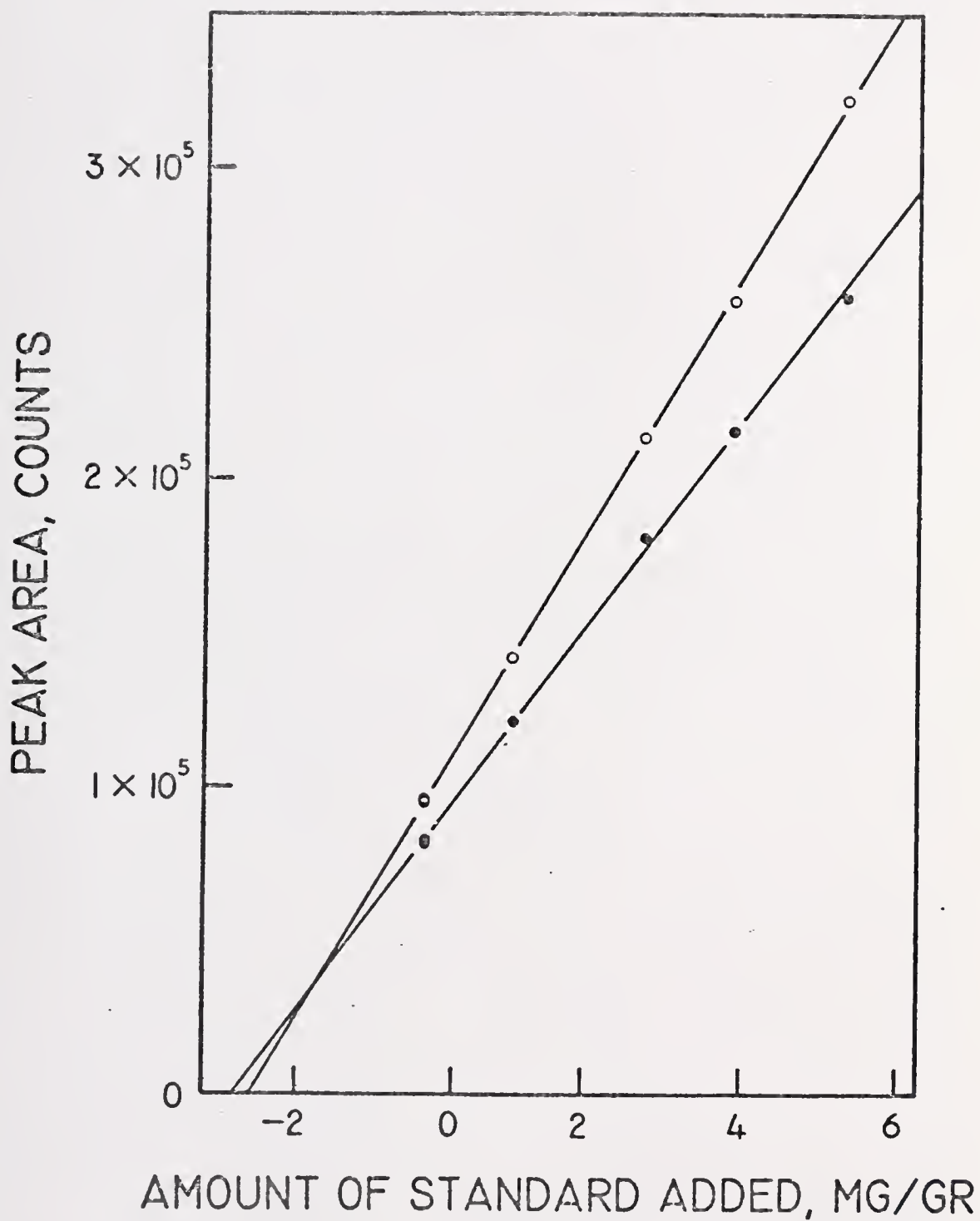


TABLE XV

EXPERIMENTAL AND NATIONAL BUREAU OF STANDARDS
RESULTS OF THE ANALYSIS OF STANDARD REFERENCE
MATERIAL 1577 (BOVINE LIVER)

ELEMENT	NATIONAL BUREAU OF STANDARDS RESULTS ($\mu\text{g}/\text{gm}$)			EXPERIMENTAL RESULTS ($\mu\text{g}/\text{gm}$)	
	METHOD 1 ^a	NAA ^b	CERTIFIED ^c	METHOD ^d	VALUE
Cl	-	2610 \pm 90	-	T-1	2540 \pm 150
				W-1	2680 \pm 180
				T-2	2580 \pm 360
				W-2	2640 \pm 130
				Mean	2610 \pm 110
Mn	11.2 \pm 0.4	9.96 \pm 0.85	10.3 \pm 1.0	T-1	9.56 \pm 0.13
				W-1	9.41 \pm 0.34
				T-2	9.89 \pm 1.68
				W-2	9.94 \pm 1.29
				Mean	9.70 \pm 0.54
K	9820 \pm 300	9600 \pm 600	9700 \pm 600	T-1	10000 \pm 290
				W-1	9070 \pm 420
				Mean	9540 \pm 250
Na	2400 \pm 100	2460 \pm 70	2430 \pm 130	T-1	2250 \pm 50
				W-1	2460 \pm 90
				Mean	2350 \pm 50

^aAtomic absorption spectrometry for Mn and flame emission spectrometry for K and Na

^bNeutron activation analysis

^cBased on the combined results of method 1 and NAA

^dT-1 = total peak area method, first peak
W-1 = Wasson method, first peak
T-2 = total peak area method, second peak
W-2 = Wasson method, second peak

four elements examined. Since the reduction algorithm used by NBS was similar to that used in this research, the lower NAA results reported by NBS for both manganese and potassium could have resulted from the problem illustrated by peak B in Figure 26, which was earlier discussed in detail. The experimental values from this research were means of all results obtained by both the TPA and Wasson method. The means were calculated from four values for chlorine and manganese and from two values for potassium and sodium. The approximate error limits on the mean results were calculated by assuming that the variance of each individual result could be obtained from the mean square deviation calculated by the linear least squares method.

Both the 1646.7 and 2167.6 KeV chlorine peaks were analyzed, and the peak areas were found to be approximately equal. For both peaks the TPA method yielded results smaller than the reported NBS concentration while the Wasson method yielded results that were larger. However each of the four experimental results fell within the reported uncertainty of the NBS value, and the experimental mean, as shown in Table XV, agreed with the NBS value to the three significant figures reported.

In the manganese determination both the 846.7 and 1811.2 KeV peaks were analyzed, but the higher energy peak, as seen from Figure 67 (channel 1556), was much smaller and was nearly buried in the baseline scatter. All four experimental results were smaller than the certified NBS value, but all fell within the reported uncertainty of this concentration. The results obtained from the smaller peak were larger in value, and the estimated error ranges were considerably larger due to the small peak-to-noise ratio of this peak. The exper-

imental mean was well within the uncertainty limits of the NBS certified concentration and was 5.8% smaller in absolute value. When compared to the NBS value obtained from NAA results, however, the experimental mean was only 2.6% smaller in absolute value.

The two potassium results straddled the NBS certified value. The TPA value was large but fell within the reported uncertainty limits. The Wasson value was small, had a greater uncertainty, and fell outside the error range of the certified concentration. From the plot in Figure 72 it is apparent that the major deviation from the linear least squares fit occurred in the three points which were obtained from spiked samples. The two experimental points from pure samples were close in absolute value and showed little deviation from the fitted line. This suggested that some of the apparent error in the results may have been introduced by the experimental technique used to add the standard solution to the samples. While the experimental mean was 1.6% smaller than the certified NBS concentration it was only 0.6% smaller than the NBS value obtained from NAA results.

In the sodium determination the certified value again fell between the two experimental results. In this case, however, the Wasson value was large but within the reported uncertainty limits. The TPA result was small and fell outside of the uncertainty limits of the NBS certified concentration.

Figure 73 and Table XII show that the two pure samples had little difference in their adjusted peak areas and showed little deviation from the fitted curves. The deviation from the fitted curves by the spiked samples, however, supported the possibility that the spiking technique may have introduced much of the error found in the final ex-

perimental results. As before, the mean value fell within the reported uncertainty of the NBS concentration and was only 3.3% smaller than this certified value.

APPENDICES

APPENDIX I

CORE RESIDENT SOFTWARE

The following is a computer printout of the software used in this research. The programs are written in assembly language and the printout includes a listing of the location and octal value of each instruction.

PAGE 0002

CKSUM,
 CNT,
 COUNT,
 0034 0000 LOC34, 0
 FINAL,
 LSECSW,
 NPEAKS,
 0035 0000 LOC35, 0
 INDEX,
 NDAIPT,
 PEAKST,
 0036 0000 LOC36, 0
 INDX,
 LINE,
 MPTSP1,
 MRIGHT,
 OBLCT,
 0037 0000 LOC37, 0

*65

LEFT,
 NLINES,
 PKLEFT,
 NPTS,
 STRTM1,
 0065 0000 LOC65, 0
 LINDEX,
 MAX,
 PINDEX,
 PKMX,
 PTEMP,
 TEMP1,
 0066 0000 LOC66, 0
 PKRT,
 RIGHT,
 0067 0000 LOC67, 0
 OUTTAP,
 0070 0000 LOC70, 0
 LDPTMS,
 TAPEN,
 0071 0000 LOC71, 0

/LOCATIONS 70 & 71 ARE
 /RESERVED EXCLUSIVELY
 /FOR THE LIB. GEN.

PAGE 0003

/CONSTANTS & POINTERS (PAGE 0)

0072	3600	AREA,	PKAREA	/PEAK AREA CALCULATION
0073	0001	C1,	1	
0074	0013	C13,	13	
0075	0027	C27,	27	
0076	0003	C3,	3	
0077	0004	C4,	4	
0100	0007	C7,	7	
0101	4400	CHKPKS,	PKSRCH	/2ND PEAK SEARCH ROUTINE
0102	2251	DIFF,	DIF	/MOVING POINT DIFFERENTIAL
0103	2400	DNOISE,	SNOISE	/NOISE DETERMINATION
0104	6600	DNORM,	6600	/F.P. NORMALIZATION
0105	2471	FIX,	FFIX	/FLOATING TO FIXED
0106	2333	FLOAT,	FFLOAT	/FIXED TO FLOATING
0107	3357	FPSTOR,	FSTORE	/STORE F(AC) IN CORE
0110	2310	GET,	GGET	/DATA FETCH & FLOAT
0111	4466	GNOISE,	NWNOIS	/SETUP, NOISE DETERMINATION
0112	4200	MAGTPE,	SETUP	/SETUP, MAG. TAPE OUTPUT
0113	7660	MSPECF,	-120	/RANGE FOR DNOISE
0114	7777	M1,	-1	
0115	7773	M5,	-5	
0116	2132	PKTEST,	PKTST	/TEST FOR VALID PEAK
0117	1600	SCDSY,	SSCDYS	/DISPLAY
0120	0236	SER,	SR	/STORAGE ROUTINE
0121	1000	SICON,	1000	/S.P. DECIMAL INPUT
0122	3200	SMOOTH,	SMOTH	/LEAST SQUARES SMOOTH
0123	2231	SPPRNT,	SPPRT	/S.P. OUTPUT THROUGH F.P.
0124	2553	START,	CFP+3	/LOC FOR PK. SER. STRING
0125	0214	STRTCH,	214	/1ST CHANNEL IN PK. SEARCH
0126	2070	STORPK,	SAVEPK	/STORE PEAK BOUNDARIES
0127	2270	SUBTRC,	SUBTR	/D.P. SUBTRACTION
0130	0253	TER,	TR	/TERMINATING ROUTINE
0131	2105	TEST,	COMPAR	/PK. HT. COMPARISON TEST
0132	1120	TYCR,	TTYCR	/TYPE C.R./L.F.
0133	0600	TYPST,	600	/MESSAGE STRING PRINT
0134	1127	TYSP,	TTYSP	/TYPE A SPACE

/INTERRUPT CONTROL ROUTINE

0135	6201	INTRUP,	CDF	
0136	7420		SNL	/IS LINK ZERO?
0137	5530		JMP I TER	/YES, GO TO TERM. ROUTINE
0140	6001		ION	/NO, TURN INTERRUPT ON
0141	6534		6534	/CLEAR ADC
0142	5520		JMP I SER	/GO TO STORAGE ROUTINE

PAGE 0004

```

/CLEAR CORE, DECIDE ON PRINTOUT,
/& BEGIN DATA STORAGE

```

```

                                +200
0200 7340 ADC,      CLL CLA CMA      /REMOVE CONFLICTING
0201 3010          DCA IR10         /INTERRUPT REQUEST
0202 6676          6676             /AND CLEAR CORE
0203 3034          DCA CNT
0204 6211          CDF+10
0205 3410          DCA I IR10
0206 2034          ISZ CNT
0207 5205          JMP.-2
0210 6201          CDF
0211 1367          TAD MAG1         /"PRINTOUT?"
0212 4533          JMS I TYPST
0213 6031          KSF
0214 5213          JMP.-1
0215 6036          KRB             /INPUT Y OR N?
0216 6046          TLS             /ECHO
0217 6041          TSF
0220 5217          JMP.-1
0221 0073          AND C1
0222 7650          SNA CLA
0223 5233          JMP NOPRT
0224 1363          TAD CTR         /SET INTERRUPT EXIT
0225 3130          DCA TER         /ADDRESS FOR NO PRINTOUT
0226 4773          JMS I STPRT     /INIT. PRINTOUT PARAMETERS
0227 1370 COLECT, TAD MAG2        /"START TIMER TO"
0230 4533          JMS I TYPST     /" STORE DATA"
0231 6001          IOV            /WAIT FOR TIMER
0232 7320          CLA STL         /SET LINK FOR INTERRUPT
0233 1362 VOPRT,  TAD CHLT        /SET INTERRUPT EXIT
0234 3130          DCA TER         /ADDRESS FOR PRINTOUT
0235 5227          JMP COLECT

```

```

/STORAGE ROUTINE

```

```

0236 7100 SR,      CLL            /CLEAR LINK FOR INTERRUPT
0237 6211          CDF+10
0240 6531          6531           /CHECK ADC FLAG
0241 5240          JMP.-1
0242 6536          6536           /READ ADC INTO AC, THEN
0243 7004          HAL            /CLEAR ADC FLAG
0244 3037          DCA LOC37
0245 2437          ISZ I LOC37     /INCREMENT PROPER CHANNEL
0246 5237          JMP SR+1        /NO OVERFLOW
0247 2037          ISZ LOC37       /OVERFLOW OCCURRED
0250 2437          ISZ I LOC37     /INCREMENT FOR OVERFLOW
0251 5237          JMP SR+1
0252 5237          JMP SR+1

```

PAGE 0005

/INITIAL SETUP FOR DATA PRINTOUT

0253	7300	TR,	CLL CLA	/INIT. # PER LINE &
0254	1034		TAD CNT	/LINE COUNTERS
0255	1364		TAD C5	
0256	7420		SVL	
0257	5255		JMP.-2	
0260	1371		TAD M4	
0261	7440		SZA	
0262	1364		TAD C5	
0263	3036		DCA INDEX	
0264	1036		TAD INDEX	
0265	7041		CIA	
0266	1034		TAD CNT	
0267	1115		TAD M5	
0270	3037		DCA LINE	

/NEW PAGE SETUP

0271	1366	PAGER,	TAD YAGDSH	/6 CR/LF'S, 10 DASHES
0272	4533		JMS I TYPSI	
0273	4765		JMS I HEADER	/PRINT PAGE HEADER
0274	1372		TAD M62	/INIT. # LINES PER PAGE
0275	3065		DCA NLINES	

/NEW LINE SETUP

0276	1036	PPRINT,	TAD INDEX	/RE-INIT. # PER LINE CNTA
0277	1115		TAD M5	
0300	3036		DCA INDEX	
0301	1037		TAD LINE	/DETERMINE NEXT LINE #
0302	1364		TAD C5	
0303	3037		DCA LINE	
0304	1077		TAD C4	/4 DIGIT OUTPUT FORMAT
0305	3062		DCA 62	
0306	1037		TAD LINE	/PRINT LINE #
0307	4523		JMS I SPPRNT	
0310	4534		JMS I TYSP	
0311	4534		JMS I TYSP	

PAGE 0006

/DATA PRINTOUT THROUGH FLOATING POINT OUTPUT

0312	1034	PRDATA, TAD CNT	/PRINT DATA IN
0313	7104	CLL RAL	/CURRENT CHANNEL
0314	3066	DCA PTEMP	
0315	6211	CDF+10	
0316	1466	TAD I PTEMP	
0317	3046	DCA 46	
0320	2066	ISZ PTEMP	
0321	1466	TAD I PTEMP	
0322	3045	DCA 45	
0323	6201	CDF	
0324	1075	TAD C27	
0325	3044	DCA 44	
0326	4407	JMS I FP	
0327	7000	FNOR	
0330	0000	FEXT	
0331	1100	TAD C7	/7 DIGIT OUTPUT FORMAT
0332	3062	DCA 62	
0333	4406	JMS I OUTPUT	/PRINT DATA
0334	2034	ISZ CNT	/INCREMENT TO NEXT CHANNEL
0335	1034	TAD CNT	/PASSED CHANNEL 2047(10)?
0336	7510	SPA	
0337	5351	JMP LASTPG	/YES
0340	1035	TAD FINAL	/NO, PASSED FINAL CHANNEL?
0341	7740	SYA SZA CLA	
0342	5351	JMP LASTPG	/YES
0343	2036	ISZ INDEX	/NO, FINISHED LINE?
0344	5312	JMP PRDATA	/NO
0345	4532	JMS I TYCH	/YES
0346	2065	ISZ NLINES	/FINISHED PAGE?
0347	5276	JMP PPRINT	/NO
0350	5271	JMP PAGEK	/YES

/OUTPUT FOR LAST PAGE

0351	7300	LASTPG, CLL CLA	/SKIP 50(10) LINES
0352	1372	TAD M62	
0353	3066	DCA LINDEK	
0354	4532	JMS I TYCH	/TYPE C.R./L.F.
0355	2066	ISZ LINDEK	
0356	5354	JMP.-2	
0357	7402	CEND, HLT	/TERMINATE PROGRAM

/DATA PRINTOUT WITHOUT STORAGE

0360	4773	PTONLY, JMS I STPRT	/INITIALIZE PARAMETERS &
0361	5253	JMP TR	/BEGIN DATA PRINTOUT

PAGE 0007

/VARIABLES

```

0362 0357 CHLT,   CEND           /ADDRESS OF HLT COMMAND
0363 0253 CTR,    TR
0364 0005 C5,     5
0365 0434 HEADER, HEDEH
0366 0557 MAGDSH, ADC5
0367 0474 MAG1,   ADC1
0370 0505 MAG2,   ADC2
0371 7774 M4,     -4
0372 7716 M62,    -62
0373 0400 STPRT,  STPT

```

/INITIALIZE DATA PRINTOUT AND HEADER PARAMETERS

```

                                *400
0400 0000 STPT,   0000
0401 7300        CLL CLA
0402 1255        TAD MAG3           /"INITIAL CHANNEL = "
0403 4533        JMS I TYPST
0404 4521        JMS I SICOV
0405 3034        DCA CNT
0406 1256        TAD MAG4           /"FINAL CHANNEL = "
0407 4533        JMS I TYPST
0410 4521        JMS I SICOV
0411 7041        CIA
0412 3035        DCA FIVAL
0413 4223        JMS INITAL
0414 1411 HDRGET, TAD I IR11       /PRINT HEADER MESSAGE
0415 4533        JMS I TYPST
0416 4521        JMS I SICOV       /READ IN APPROPRIATE #
0417 3412        DCA I IR12       /STORE #'S IN STRING
0420 2066        ISZ PIVDEX       /FINISHED?
0421 5214        JMP HDRGET       /NO
0422 5600        JMP I STPT       /YES, EXIT
0423 0000 INITAL, 0000           /INITIALIZE CNTR'S
0424 7300        CLL CLA         /FOR HEADER
0425 1115        TAD M5
0426 3066        DCA PIVDEX
0427 1257        TAD START1
0430 3011        DCA IR11
0431 1266        TAD START2
0432 3012        DCA IR12
0433 5623        JMP I INITAL     /EXIT

```

PAGE 0008

/PRINT HEADER

0434	0000	HEADER,	0000	/PRINT HEADER, WITH #'S
0435	7326		CLA SIL RTL	/2 DIGIT OUTPUT FORMAT
0436	3062		DCA 62	
0437	4223		JMS INITAL	
0440	1411	PRT,	TAD I IR11	/PRINT HEADER MESSAGE
0441	4533		JMS I TYPST	
0442	1412		TAD I IR12	/PRINT APPROP. HEADER #
0443	3045		DCA 45	/THROUGH F.P. OUTPUT
0444	3046		DCA 46	
0445	1074		TAD C13	
0446	3044		DCA 44	
0447	4406		JMS I OUTPUT	
0450	2066		ISZ PINDEX	/FINISHED?
0451	5240		JMP PRT	/NO
0452	1411		TAD I IR11	/YES, PRINT LAST
0453	4533		JMS I TYPST	/HEADER MESSAGE
0454	5634		JMP I HEADER	/EXIT

/VARIABLES

0455	0530	MAG3,	ADC3
0456	0544	MAG4,	ADC4
0457	0457	START1,	.
0460	1150		HEADER1
0461	1164		HEADER2
0462	0760		HEADER3
0463	0766		HEADER4
0464	0766		HEADER4
0465	0770		HEADERS
0466	0466	START2,	.
0467	0000		0
0470	0000		0
0471	0000		0
0472	0000		0
0473	0000		0

PAGE 0009

/MESSAGE STRINGS FOR ADC MONITOR

0474	0015	ADC1,	0015	/C.R.
0475	0012		0012	/L.F. TWICE
0476	0012		0012	
0477	2022		2022	/"PRINTOUT? "
0500	1116		1116	
0501	2417		2417	
0502	2524		2524	
0503	7740		7740	
0504	0001		0001	/END MESSAGE
0505	0015	ADC2,	0015	/C.R.
0506	0012		0012	/L.F. TWICE
0507	0012		0012	
0510	2324		2324	/"START TIMER TO"
0511	0122		0122	/" STORE DATA"
0512	2440		2440	
0513	2411		2411	
0514	1505		1505	
0515	2240		2240	
0516	2417		2417	
0517	4023		4023	
0520	2417		2417	
0521	2205		2205	
0522	4004		4004	
0523	0124		0124	
0524	0100		0100	
0525	1500		1500	/C.R.
0526	1200		1200	/L.F.
0527	0100		0100	/END MESSAGE
0530	0015	ADC3,	0015	/C.R.
0531	0012		0012	/L.F.
0532	1116		1116	/"INITIAL CHANNEL = "
0533	1124		1124	
0534	1101		1101	
0535	1440		1440	
0536	0310		0310	
0537	0116		0116	
0540	1605		1605	
0541	1440		1440	
0542	7540		7540	
0543	0001		0001	/END MESSAGE
0544	0015	ADC4,	0015	/C.R.
0545	0012		0012	/L.F.
0546	0611		0611	/"FINAL CHANVEL = "
0547	1601		1601	
0550	1440		1440	
0551	0310		0310	
0552	0116		0116	
0553	1605		1605	
0554	1440		1440	
0555	7540		7540	
0556	0001		0001	/END MESSAGE

```

PAGE 0010
0557 0015 ADC5, 0015 /C.R.
0560 0012 0012 /L.F. 8 TIMES
0561 0012 0012
0562 0012 0012
0563 0012 0012
0564 0012 0012
0565 0012 0012
0566 0012 0012
0567 0012 0012
0570 5555 5555 /"-----"
0571 5555 5555
0572 5555 5555
0573 5555 5555
0574 5555 5555
0575 0001 0001 /END MESSAGE

```

/MESSAGE STRINGS FOR HEADER

```

*1150
1150 0015 HEDER1, 0015 /C.R.
1151 0012 0012 /L.F. 4 TIMES
1152 0012 0012
1153 0012 0012
1154 0012 0012
1155 2320 2320 /"SPECTRUM = "
1156 0503 0503
1157 2422 2422
1160 2515 2515
1161 4075 4075
1162 4000 4000
1163 0100 0100 /END MESSAGE
1164 4040 HEDER2, 4040 /" TAPE = "
1165 4024 4024
1166 0120 0120
1167 0540 0540
1170 7540 7540
1171 0001 0001 /END MESSAGE

*760
0760 4040 HEDER3, 4040 /" DATE : "
0761 4004 4004
0762 0124 0124
0763 0540 0540
0764 7240 7240
0765 0001 0001 /END MESSAGE
0766 5700 HEDER4, 5700 /"/"
0767 0100 0100 /END MESSAGE
0770 0015 HEDER5, 0015 /C.R.
0771 0012 0012 /L.F. 4 TIMES
0772 0012 0012
0773 0012 0012
0774 0012 0012
0775 0001 0001 /END MESSAGE

```

PAGE 0011

/DIGITAL 8-20-U (MODIFIED)
/CHARACTER STRING TYPE-OUT

/MODIFIED FOR USE WITH DEC'S ADC MONITOR

/CALL WITH STRING ADDRESS IN AC;
/ALL CODES MAY BE DEVELOPED
/RETURN FOLLOWING THE JMS

```

                                *600
0600 0000 TYPSTG, 0000
0601 3262          DCA TEMQ          /STORE INITIAL ADDRESS
0602 3264          DCA FLAG          /CLEAR FLAG

                                /PROCESS THE STRING

0603 1662 TSCC1,  TAD I TEMQ        /PICK UP DATA
0604 7012          RTR              /ROTATE 6 BITS RIGHT
0605 7012          RTR
0606 7012          RTR
0607 4214          JMS TSCC2        /TYPE FIRST CHARACTER
0610 1662          TAD I TEMQ        /PICK UP DATA
0611 4214          JMS TSCC2        /TYPE SECOND CHARACTER
0612 2262          ISZ TEMQ         /INCREMENT STORAGE ADDRESS
0613 5203          JMP TSCC1        /GO BACK FOR MORE

                                /CHECK FOR OUTPUT CODES & OUTPUT A CHARACTER

0614 0000 TSCC2,  0000
0615 0265          AND K77          /MASK OFF 6 BITS
0616 3263          DCA TEMR         /SAVE CHARACTER
0617 1264          TAD FLAG         /TEST "SPECIAL" FLAG
0620 7640          SZA CLA
0621 5231          JMP TYPSP        /SET: TYPE SPECIAL
0622 1263          TAD TEMR         /NO: REGULAR CHARACTER
0623 7450          SNA              /IS IT ZERO?
0624 5227          JMP .+3          /YES: SET FLAG
0625 4250 TYPAT,  JMS TYPE         /NO: PRINT IT
0626 5614          JMP I TSCC2      /RETURN
0627 2264          ISZ FLAG         /SET "SPECIAL" FLAG
0630 5614          JMP I TSCC2      /RETURN

```

PAGE 0012

/SPECIAL CHARACTER ROUTINE

```

0631 3264 TYPSP,   DCA FLAG           /CLEAR "SPECIAL" FLAG
0632 1263         TAD TEMR           /TEST FOR "0"
0633 7041         CIA
0634 7453         SNA
0635 5225         JMP TYPAT           /0: TYPE "0"
0636 7001         IAC                 /TEST FOR 01
0637 7650         SNA CLA
0640 5273         JMP MODIFY          /YES: EXIT
0641 1271         TAD SKIPMA          /ALTER INSTRUCTION
0642 3252         DCA SWITCH          /TO BE "SMA"
0643 1263         TAD TEMR           /TYPE CHARACTER
0644 4250         JMS TYPE
0645 1272         TAD SKIPPA          /ALTER INSTRUCTION
0646 3252         DCA SWITCH          /TO BE "SPA"
0647 5614         JMP I TSCC2         /RETURN

```

/TYPE A CHARACTER

```

0650 0000 TYPE,   0000
0651 1266         TAD M40             /COMPARE WITH 40
0652 7510 SWITCH, SPA                /OR SMA FOR SPECIAL CODES
0653 1267         TAD C100
0654 1270         TAD C240
0655 6046         TLS
0656 6041         TSF
0657 5256         JMP .-1
0660 7200         CLA
0661 5650         JMP I TYPE          /RETURN

```

/CONSTANTS AND TEMPORARY REGISTERS

```

0662 0000 TEMO,   0                   /CONTAINS STRING ADDRESS
0663 0000 TEMR,   0                   /CONTAINS 6 BIT CHARACTER
0664 0000 FLAG,   0                   /"SPECIAL" FLAG
0665 0077 K77,    77
0666 7740 M40,    -40
0667 0100 C100,   100
0670 0240 C240,   240
0671 7500 SKIPMA, SMA
0672 7510 SKIPPA, SPA

```

/MODIFICATION FOR USE WITH INTERRUPT

```

0673 6042 MODIFY, TCF                 /CLEAR TTY/PUNCH FLAG
0674 5600         JMP I TYPSTG        /EXIT

```

PAGE 0013

/DIGITAL 8-28-U-ASCII (MODIFIED)
/SINGLE PRECISION DECIMAL INPUT FROM KEYBOARD

/MODIFIED FOR USE WITH DBC'S ADC MONITOR

/CALLING SEQUENCE: JMS SICONV
/ACC IGNORED, RETURN WITH BINARY WORD IN ACC

```

                                *1000
1000 0000 SICONV, 0000
1001 7300          CLA CLL
1002 1276          TAD S1SET1 +1   /INITIALIZE SWITCHES
1003 3232          DCA SICTRL
1004 1276          TAD S1SET1 +1
1005 3224          DCA SIXSW1
1006 3312          DCA SIHOLD
1007 3313          DCA S1NEG1     /CLEAR NEGATIVE SWITCH
1010 5257          JMP S1NPUT     /BEGIN INPUT

                                /PROCESS THE CHARACTER
1011 3311 S1PROC, DCA S1SAVE
1012 1311          TAD S1SAVE     /SAVE IT BEFORE PROCESSING
1013 1303          TAD S1RBT
1014 7450          SNA             /IS IT A "BACK-ARROW"?
1015 5201          JMP SICONV +1  /YES, REINITIALIZE
1016 1304          TAD S1M260
1017 7510          SPA             /IS IT LESS THAN 260?
1020 5232          JMP SICTRL     /YES, SEE WHAT IT IS
1021 1305          TAD S1M271
1022 7740          SMA SZA CLA     /IS IT GREATER THAN 271?
1023 5232          JMP SICTRL     /YES, SEE WHAT IT IS
1024 7300 SIXSW1, CLA CLL         /NO, 1ST CHAR. WAS DECIMAL
1025 1231          TAD .+4        /CLOSE SWITCH TO "S1NMBR"
1026 3224          DCA .-2
1027 1245          TAD S1NMBR -1  /SET TER. CHAR. SWITCH
1030 3232          DCA SICTEL
1031 5246          JMP S1NMBR
1032 7300 SICTRL, CLA CLL        /CONTINUE CHECKING
1033 1311          TAD S1SAVE
1034 1306          TAD S1MSPC
1035 7450          SNA             /IS IT A SPACE?
1036 5276          JMP S1SET1 +1  /YES
1037 1307          TAD S1MPLS
1040 7450          SNA             /IS IT A "PLUS"?
1041 5276          JMP S1SET1 +1  /YES
1042 1310          TAD S1MNS
1043 7650          SNA CLA        /IS IT A MINUS?
1044 5275          JMP S1SET1     /YES
1045 5266          JMP S1END      /NO, IT WAS A TER. CHAR.

```

PAGE 0014

/UPDATE THE CURRENT ASSEMBLED NUMBER

1046	1312	SINMBR,	TAD SIHOLD	/MULTIPLY CURRENT
1047	7106		CLL RTL	/ASSEMBLED # BY 10
1050	1312		TAD SIHOLD	
1051	7004		RAL	
1052	3312		DCA SIHOLD	
1053	1311		TAD SISAVE	/PICK UP CURRENT DIGIT
1054	0302		AND SIMASK	/MASK OFF THE H.O. BIT
1055	1312		TAD SIHOLD	/ADD TO ASSEMBLED #
1056	3312		DCA SIHOLD	/STORE BACK IN SIHOLD

/INPUT & ECHO ROUTINE

1057	6031	SINPUT,	KSF	/READ TTY KEYBOARD
1060	5257		JMP .-1	
1061	6036		KRB	
1062	6046		TLS	/ECHO INPUT
1063	6041		TSF	
1064	5263		JMP.-1	
1065	5211		JMP SIPROC	

/TERMINATING ROUTINE

1066	7300	SIEND,	CLA CLL	
1067	1313		TAD SINEG1	
1070	7010		RAR	/PUT NEG. SWITCH INTO LINK
1071	1312		TAD SIHOLD	
1072	7430		SZL	/NEGATIVE #?
1073	7041		CMA IAC	/YES, COMPLEMENT
1074	5600		JMP I SICONV	/NO, EXIT

/ROUTINE TO SET NEGATIVE & TERMINATING SWITCHES

1075	2313	SISSET1,	ISZ SINEG1	/SET NEGATIVE SWITCH
1076	7300		CLA CLL	
1077	1245		TAD SINMBR -1	/SET TER. CHAR. SWITCH
1100	3232		DCA SICTRL	
1101	5257		JMP SINPUT	

/CONSTANTS AND VARIABLES

1102	0017	SIMASK,	17	
1103	7441	SIRBUT,	-337	/CODE FOR ERASE
1104	0057	SIM260,	57	/# TO GEN. CODE "260"
1105	7767	SIM271,	-11	/# TO GEN. CODE "271"
1106	7540	SIMSPC,	-240	/CODE FOR SPACE
1107	7765	SIMPLS,	-13	/# TO GEN. CODE "253" (+)
1110	7776	SIMMNS,	-2	/# TO GEN. CODE "255" (-)
1111	0000	SISAVE,	0	
1112	0000	SIHOLD,	0	
1113	0000	SINEG1,	0	

PAGE 0015

/DIGITAL 8-19-U (MODIFIED)
 /TELETYPE OUTPUT PACKAGE (PORTIONS)
 /MODIFIED FOR USE WITH DEC'S ADC MONITOR
 /TYPE C.R./L.F.

*1120
 1120 0000 TTYCR, 0
 1121 7300 CLL CLA
 1122 1343 TAD C0215 /GET ASCII FOR C.R.
 1123 4334 JMS OTY /TYPE THIS
 1124 1342 TAD C0212 /GET ASCII FOR L.F.
 1125 4334 JMS OTY /TYPE THIS
 1126 5720 JMP I TTYCR /RETURN

/TYPE A SPACE

1127 0000 TTYSP, 0
 1130 7300 CLL CLA
 1131 1344 TAD C0240 /GET ASCII FOR A SPACE
 1132 4334 JMS OTY /TYPE THIS
 1133 5727 JMP I TTYSP /RETURN

/OUTPUT A TELETYPE CHARACTER

1134 0000 OTY, 0
 1135 6046 TLS
 1136 6041 TSF
 1137 5336 JMP.-1
 1140 7300 CLL CLA
 1141 5734 JMP I OTY /RETURN
 1142 0212 C0212, 212
 1143 0215 C0215, 215
 1144 0240 C0240, 240

/CORRECTIONS TO DEC'S FLOATING POINT PACKAGE
 /TO REPLACE + WITH A SPACE, AND TO MAKE PRINT
 /LOOP COMPATIBLE WITH DEC'S ADC MONITOR

*7333
 7333 0240 240 /REPLACE + WITH SPACE
 7334 0015 15 /CORRECTION FOR - SIGN

*7352
 7352 6046 TLS /REVERSE PRINT LOOP
 7353 6041 TSF
 7354 5353 JMP.-1

PAGE 0016

/ROTATE UPPER CORE ONCE TO LEFT (MULTIPLY BY 2).
 /ROUTINE ENDS AT A HLT. PRESS CONTINUE TO LEVEL
 /AND PLOT ROTATED DATA. LOAD ADDRESS AND
 /RESTART TO ROTATE AGAIN.

```

*1200
1200 7301 ROTUP,  CLL CLA IAC
1201 3031          DCA LOC31
1202 3032          DCA LOC32
1203 6211          CDF+10
1204 1432 REPET,  TAD I LOC32      /ROTATE & RESTORE
1205 7134          CLL BAL        /L.O. WORD
1206 3432          DCA I LOC32
1207 1431          TAD I LOC31      /ROTATE & RESTORE
1210 7034          BAL            /H.O. WORD
1211 3431          DCA I LOC31
1212 2031          ISZ LOC31
1213 2031          ISZ LOC31
1214 2032          ISZ LOC32
1215 2032          ISZ LOC32      /FINISHED ALL DATA?
1216 5204          JMP REPET       /NO
1217 6201          CDF            /YES
1220 7402          HLT            /WAIT FOR PROGRAMMER

```

/LEVEL DOUBLE PRECISION DATA IN UPPER CORE BY
 /PUTTING A 7777(8) IN THE L.O. WORD OF EACH
 /DATA POINT THAT EXCEEDS SINGLE PRECISION.

```

1221 7301 LEVEL,  CLL CLA IAC
1222 3034          DCA COUNT
1223 6211 REPET1, CDF+10
1224 1434          TAD I COUNT      /IS (H.O. WORD)>0?
1225 7450          SNA
1226 5234          JMP.+6         /NO, LEAVE DATA AS IS
1227 7340          CLL CLA CMA     /YES, PUT 7777(8)
1230 1034          TAD COUNT       /IN L.O. WORD
1231 3032          DCA LOC32
1232 7340          CLL CLA CMA
1233 3432          DCA I LOC32
1234 6201          CDF
1235 2034          ISZ COUNT       /FINISHED ALL DATA?
1236 7410          SKP            /NO
1237 5642          JMP I PLOT      /YES, PLOT IT
1240 2034          ISZ COUNT
1241 5223          JMP REPET1
1242 1411 PLOT,   BOUNDS

```

PAGE 0017

/ROTATE UPPER CORE ONCE TO RIGHT (DIVIDE BY 2).
 /ROUTINE ENDS AT A HLT. PRESS CONTINUE TO LEVEL
 /AND PLOT ROTATED DATA. LOAD ADDRESS AND
 /RESTART TO ROTATE AGAIN.

1243 4646 ROTDWN, JMS I ROTDN /ROTATE UPPER CORE DOWN
 1244 7402 HLT /WAIT FOR PROGRAMMER
 1245 5221 JMP LEVEL
 1246 1443 ROTDN, ROTAT

/ROUTINE TO ADJUST PLOTTER OUTPUT FOR LOWEST
 /AND HIGHEST DESIRED SETTINGS. BY PRESSING
 /CONTINUE THE CONTENTS OF "PENLW" & "PENHGH"
 /WILL ALTERNATELY BE DISPLAYED ON THE PLOTTER.

1247 7300 PENLOW, CLL CLA
 1250 1260 TAD PENLW /ZERO PLOTTER PEN
 1251 6562 6562
 1252 7402 HLT /WAIT FOR PROGRAMMER
 1253 7300 PENHI, CLL CLA
 1254 1261 TAD PENHGH /FULL SCALE PLOTTER PEN
 1255 6562 6562
 1256 7402 HLT /WAIT FOR PROGRAMMER
 1257 5247 JMP PENLOW /REPEAT
 1260 0000 PENLW, J
 1261 7777 PENHGH, 7777

PAGE 0018

/ROUTINE TO ROTATE UPPER CORE FROM
 /DOUBLE TO SINGLE PRECISION TO
 /ALLOW DISPLAY ON A SCOPE OR PLOTTER

/CHECK HIGH-ORDER PARTS OF DATA LOCATIONS
 /IN UPPER CORE AND ROTATE ENTIRE CORE
 /UNTIL ALL DATA IS SINGLE PRECISION

```

                                *1400
1400 7300 ROTATE, CLL CLA
1401 3015      DCA IR15
1402 6211      CDF+10
1403 1415 FETCH, TAD I IR15      /IS H.O. WORD=0?
1404 7440      SZA
1405 5235      JMP ROT          /NO, ROTATE UPPER CORE
1406 2015      ISZ IR15         /YES, FINISHED ALL DATA?
1407 5203      JMP FETCH        /NO
1410 6201      CDF              /YES, READY FOR SCDSY!

```

/INITIALIZATION OF BOUNDRY
 /CHANNELS FOR SCOPE DISPLAY

```

1411 1266 BOUNDS, TAD MAG6      /"DISPLAY FROM "
1412 4533      JMS I TYPST
1413 4521      JMS I SICDN      /INPUT 1ST CHANNEL
1414 7104      CLL RAL
1415 7430      SZL              /ABOVE LIMITS OF CORE?
1416 5237      JMP ERROR        /YES, TYPE ERROR MESSAGE
1417 3231      DCA FIRST        /NO, STORE FOR SCDSY
1420 1267      TAD MAG7        /" TO "
1421 4533      JMS I TYPST
1422 4521      JMS I SICDN      /INPUT FINAL CHANNEL
1423 7104      CLL RAL
1424 7430      SZL              /ABOVE LIMITS OF CORE?
1425 5237      JMP ERROR        /YES, TYPE ERROR MESSAGE
1426 3232      DCA LAST        /NO, STORE FOR SCDSY
1427 4532      JMS I TYCN      /TYPE C.R./L.F.
1430 4517      JMS I SCDSY     /JUMP TO DISPLAY
1431 0000 FIRST, 0              /FIRST LOCATION FOR DISPLAY
1432 0000 LAST, 0              /LAST LOCATION FOR DISPLAY
1433 0002 INCMNT, 2            /INCREMENT FOR SCDSY
1434 7402      HLT
1435 4243 ROT, JMS ROTAT
1436 5200      JMP ROTATE
1437 7300 ERROR, CLL CLA
1440 1270      TAD MAG8        /"EXCEEDS CORE LIMITS, "
1441 4533      JMS I TYPST     /"TRY AGAIN"
1442 5211      JMP BOUNDS

```

PAGE 0019

/SUBROUTINE TO ROTATE ENTIRE UPPER CORE OF
/DOUBLE PRECISION PACKED DATA ONCE TO RIGHT

1443	0000	ROTAT,	0000	
1444	7301		CLL CLA IAC	
1445	3264		DCA HIGH	
1446	3265		DCA LOW	
1447	6211		CDF+10	
1450	1664	REP1,	TAD I HIGH	/ROTATE & RESTORE
1451	7110		CLL BAR	/H.O. WORD
1452	3664		DCA I HIGH	
1453	1665		TAD I LOW	/ROTATE & RESTORE
1454	7010		BAR	/L.O. WORD
1455	3665		DCA I LOW	
1456	2264		ISZ HIGH	
1457	2264		ISZ HIGH	
1460	2265		ISZ LOW	
1461	2265		ISZ LOW	/FINISHED ALL DATA?
1462	5250		JMP REP1	/NO
1463	5643		JMP I ROTAT	/YES, EXIT

/VARIABLES

1464	0000	HIGH,	0
1465	0000	LOW,	0
1466	1471	MAG6,	HOT1
1467	1504	MAG7,	HOT2
1470	1510	MAG8,	HOT3

PAGE 0020

/MESSAGE STRINGS FOR SCLSY

1471	0015	ROT1,	0015	/C.R.
1472	0012		0012	/L.F. TWICE
1473	0012		0012	
1474	0411		0411	/"DISPLAY FROM "
1475	2320		2320	
1476	1401		1401	
1477	3140		3140	
1500	0622		0622	
1501	1715		1715	
1502	4040		4040	
1503	0001		0001	/END MESSAGE
1504	4040	ROT2,	4040	/" TO "
1505	2417		2417	
1506	4040		4040	
1507	0001		0001	/END MESSAGE
1510	0015	ROT3,	0015	/C.R.
1511	0012		0012	/L.F. TWICE
1512	0012		0012	
1513	0530		0530	/"EXCEEDS CORE LIMITS, "
1514	0305		0305	/"TRY AGAIN"
1515	0504		0504	
1516	2340		2340	
1517	0317		0317	
1520	2205		2205	
1521	4014		4014	
1522	1115		1115	
1523	1124		1124	
1524	2354		2354	
1525	4024		4024	
1526	2231		2231	
1527	4001		4001	
1530	0701		0701	
1531	1116		1116	
1532	0001		0001	/END MESSAGE

PAGE 0021

/DISPLAY ROUTINE FOR EITHER SCOPE OR PLOTTER.
 /THIS IS A SPECIFIC VERSION, WHICH IGNORES THE
 /INCREMENT SPECIFIED IN THE CALLING COMMAND
 /AND EXECUTES A FIXED INCREMENT OF TWO.

/SET BIT 11 OF THE SWITCH REGISTER TO 0 FOR A
 /SCOPE ADAPTABLE DISPLAY AND TO 1 FOR A PLOTTER.

/THIS ROUTINE SHOULD BE ENTERED WITH THE FIRST
 /LOCATION, LAST LOCATION, AND INCREMENT IN THE
 /FIRST, SECOND, AND THIRD POSITIONS AFTER THE
 /CALLING COMMAND. THE INCREMENT WILL BE IGNORED,
 /BUT THIS FORMAT WILL MAKE THE CALLING COMMAND
 /COMPATIBLE WITH THE GENERALIZED SSCDSY ROUTINE.
 /TO EXIT FROM THE ROUTINE, SET BIT 0 ON THE
 /SWITCH REGISTER TO 1 (APPLICABLE ONLY TO SCOPE).

/THE DELAY TIME FOR THE PLOTTER DISPLAY (TO
 /GIVE THE PEN TIME TO RESPOND) IS CONTROLLED
 /BY TWO DELAY LOOPS. THE INNER LOOP DELAYS
 /ABOUT 20 MILLISECONDS BETWEEN POINTS. THE
 /OUTER LOOP CONTROLS THE NUMBER OF TIMES
 /THE INNER LOOP IS EXECUTED. THE VARIABLE
 /"COUNT1", FOUND IN LOCATION 161 OF THE
 /APPROPRIATE PAGE, IS THE NEGATIVE OF THE
 /NUMBER OF TIMES THE INNER LOOP IS EXECUTED.

/DECISION SECTION FOR SCOPE OR PLOTTER

```

                *1600
1600 0000 SSCDSY, 0000
1601 7300     CLA CLL
1602 7404     OSR           /CHECK BIT 11
1603 0262     AND C0001
1604 7650     SVA CLA       /SCOPE(S) OR PLOTTER(P)?
1605 5215     JMP.+10
1606 1267     TAD VJMP      /PLOTTER, MAKE THE
1607 3244     DCA CHANG1    /APPROPRIATE CHANGES
1610 1251     TAD CHANG2+2
1611 3247     DCA CHANG2
1612 1270     TAD VNOP
1613 3256     DCA CHANG3
1614 5223     JMP.+7        /BEGIN REGULAR PROGRAM
1615 1201     TAD SSCDSY+1  /SCOPE, MAKE THE
1616 3244     DCA CHANG1    /APPROPRIATE CHANGES
1617 1202     TAD SSCDSY+2
1620 3247     DCA CHANG2
1621 1263     TAD C6561
1622 3256     DCA CHANG3

```

PAGE 0022

/BASIC SSCDSY ROUTINE

1623	1600	TAD I SSCDSY	/GET FIRST ADDRESS
1624	7041	CIA	
1625	7040	CMA	
1626	3265	DCA FLOC	
1627	2200	ISZ SSCDSY	
1630	1600	TAD I SSCDSY	/GET FINAL ADDRESS
1631	7041	CIA	/CALCULATE # OF LOCATIONS
1632	1265	TAD FLOC	
1633	7130	STL KAR	/DIV. BY 2 & SAVE
1634	3266	DCA NPNTS	
1635	2200	ISZ SSCDSY	/IGNOR SPECIFIED INCREMENT
1636	2200	ISZ SSCDSY	/INCREMENT FOR RETURN
1637	6211	CDF+10	
1640	5252	JMP IDSPY	
1641	2017	DSPLY, ISZ ADPNTR	/SKIP UNDESIRIED LOCATION
1642	1417	TAD I ADPNTR	
1643	6562	6562	/DISPLAY A DATA POINT
1644	0000	CHANG1, 0	/"CLA"(S) OR "JMP DELAY"(P)
1645	2264	ISZ CNTR	/FINISHED?
1646	5241	JMP DSPLY	/NO
1647	0000	CHANG2, 0	/YES, "OSR"(S) OR
1650	7710	SPA CLA	/"JMP EXIT"(P)
1651	5260	JMP EXIT	
1652	1265	IDSPY, TAD FLOC	/REINITIATE DISPLAY
1653	3017	DCA ADPNTR	
1654	1266	TAD NPNTS	
1655	3264	DCA CNTR	
1656	0000	CHANG3, 0	/"6561"(S) OR "NOP"(P)
1657	5242	JMP DSPLY+1	
1660	6201	EXIT, CDF	
1661	5600	JMP I SSCDSY	/EXIT

PAGE 0023

/VARIABLES

```

1662 0001 C0001, 1
1663 6561 C6561, 6561
1664 0000 CVTR, 0
1665 0000 FLOC, 0
1666 0000 NPNTS, 0
1667 5271 VJMP, JMP DELAY
1670 7000 VNOP, NOP

```

/DELAY SECTION FOR PLOTTER OUTPUT

```

1671 7300 DELAY, CLL CLA
1672 1303 TAD OUTER
1673 3301 DCA COUNT1
1674 2302 ISZ COUNT2 /RDN THROUGH INNER LOOP
1675 5274 JMP.-1
1676 2301 ISZ COUNT1 /FINISHED OUTER LOOP?
1677 5274 JMP.-3 /NO
1700 5245 JMP DSPLY+4 /YES, RETURN TO SCDSY
1701 0000 COUNT1, 0
1702 0000 COUNT2, 0
1703 7774 OUTER, -4

```

PAGE 0024

/1ST PEAK SEARCH ROUTINE

/PROGRAM TO SEARCH FOR PEAKS IN A
 /SPECTRUM AND DETERMINE THE #,
 /MAXIMUM, AND BOUNDRIES USING A
 /MOVING POINT DIFFERENTIAL. THIS
 /SEARCH USES A MINIMUM HEIGHT
 /CRITERIA ON THE FIRST MAX.

/INITIALIZATION OF VARIABLES

```

                *2000
2000 7300 PKSER,  CLL CLA
2001 1356          TAD CJMP          /SET PEAK PRINTOUT TO EXIT
2002 3757          DCA I CHANG4     /TO 2ND PEAK SEARCH
2003 3035          DCA NPEAKS
2004 3037          DCA MRIGHT
2005 1124          TAD START
2006 3036          DCA PEAKST
2007 1036          TAD PEAKST
2010 3012          DCA IHPK
2011 1125          TAD STATCH
2012 3034          DCA COUNT

```

/DETECTION OF A POSSIBLE LEFT BOUNDARY

```

2013 4502 LFTDET, JMS I DIFF      /GET DIFFERENTIAL
2014 7750          SPA SVA CLA     /IS IT>0?
2015 5213          JMP.-2         /NO
2016 1034          TAD COUNT       /YES, SAVE LEFT BOUNDARY
2017 3065          DCA LEFT

```

/DETECTION OF A POSSIBLE PEAK MAXIMUM

```

2020 4502 PKMAX,  JMS I DIFF      /GET DIFFERENTIAL
2021 7700          SMA CLA         /IS IT NEGATIVE?
2022 5220          JMP.-2         /NO
2023 1034          TAD COUNT       /YES, STORE PEAK MAX
2024 3066          DCA MAX
2025 1360          TAD MINHT      /SET GNOISE TO FIND
2026 4506          JMS I FLOAT    /MINHT*NOISE
2027 0031          FPTEMP
2030 4511          JMS I GNOISE   /DETERMINE NOISE VALUE
2031 1065          TAD LEFT       /SET TEST FOR (MAX-LEFT)
2032 3307          DCA MINEND
2033 1066          TAD MAX
2034 3310          DCA SUBTRA
2035 4531          JMS I TEST     /((MAX-LEFT)>NOISE?
2036 5213          JMP LFTDET     /NO, REJECT AS A PEAK

```

PAGE 0025

/DETECTION OF A POSSIBLE RIGHT BOUNDARY

2037	4502	RTDET,	JMS I DIFF	/YES, GET DIFFERENTIAL
2040	7710		SPA CLA	/POSITIVE YET?
2041	5237		JMP.-2	/NO
2042	1034		TAD COUNT	/YES, SAVE POSSIBLE
2043	3067		DCA RIGHT	/RIGHT BOUNDARY
2044	1067		TAD RIGHT	/SET TEST FOR (RIGHT-LEFT)
2045	3310		DCA SUBTRA	
2046	4531		JMS I TEST	/(RIGHT-LEFT)>NOISE?
2047	5321		JMP PKCHCK	/NO, TEST FOR VALID PEAK
2050	4502		JMS I DIFF	/YES, RIGHT BOUNDARY
2051	7700		SMA CLA	/NOT RETURNED TO BASELINE,
2052	5250		JMP.-2	/FIND NEXT MAX
2053	1034		TAD COUNT	/SAVE THIS POSSIBLE MAX
2054	3261		DCA NEWMAX	
2055	1066		TAD MAX	/SET UP COMPARISON OF MAX'S
2056	3260		DCA OLDMAX	
2057	4527		JMS I SUBTRC	/(NEWMAX-OLDMAX)
2060	0000	OLDMAX,	J	
2061	0000	NEWMAX,	0	
2062	1021		TAD FPA+1	/KEEP LARGER OF 2
2063	7750		SPA SVA CLA	/AS PEAK MAX
2064	5237		JMP RTDET	
2065	1261		TAD NEWMAX	
2066	3066		DCA MAX	
2067	5237		JMP RTDET	

/SUBROUTINE TO SAVE VALID PEAK BOUNDARIES

2070	0000	SAVEPK,	0000	
2071	1065		TAD LEFT	/STORE LEFT BOUNDARY
2072	3412		DCA I IRPK	
2073	1066		TAD MAX	/STORE PEAK MAX
2074	3412		DCA I IRPK	
2075	2035		ISZ NPEAKS	/INCREMENT # OF PEAKS
2076	1067		TAD RIGHT	/STORE RIGHT BOUNDARY
2077	3412		DCA I IRPK	
2100	1067		TAD RIGHT	/SAVE LAST VALID RIGHT
2101	7110		CLL RAR	/BOUNDARY FOR COMPARISON
2102	7041		CIA	
2103	3037		DCA MRIGHT	
2104	5670		JMP I SAVEPK	/EXIT

PAGE 0026

/SUBROUTINE TO COMPARE HEIGHT OF EITHER PEAK
/MAXIMUM OR RIGHT BOUNDARY (RELATIVE TO LEFT
/BOUNDARY) WITH APPROPRIATE NOISE VALUE.

```

2105 0000 COMPAR, 0000
2106 4527     JMS I SUBTRC     /DETERMINE DESIRED HEIGHT
2107 0000 MINEND, 0
2110 0000 SUBTRA, 0           /EITHER MAX OR RIGHT
2111 4407     JMS I FP
2112 5020     FGET FPA
2113 2026     FSUB FPC        /HEIGHT-(NOISE OR N*NOISE)
2114 0000     FEXT
2115 1045     TAD 45
2116 7700     SMA CLA        /HEIGHT>NOISE?
2117 2305     ISZ COMPAR     /YES, INCREMENT FOR EXIT
2120 5705     JMP I COMPAR   /NO, EXIT

```

/ROUTINE TO DETERMINE IF PSEUDO-PEAK MEETS
/ALL REQUIREMENTS FOR A VALID PEAK. THE
/REQUIREMENTS ARE:
/ 1. # CHANNELS IN PEAK>NCH
/ 2. (MAX-RIGHT)>N*NOISE
/ 3. (MAX-LEFT)>N*NOISE
/THE VALUE OF NCH IS 2*(# CHANNELS) BECAUSE
/THE VALUES OF LEFT & RIGHT ARE LOCATIONS.
/THE VALUES OF NCH AND N MAY BE CHANGED
/TO GIVE FLEXIBILITY TO THE PEAK SEARCH.

```

2121 1065 PKCHCK, TAD LEFT     /DETERMINE (RIGHT-LEFT-NCH)
2122 1362     TAD NCH
2123 7041     CIA
2124 1067     TAD RIGHT
2125 7750     SPA SVA CLA     /ENOUGH CHANNELS IN PEAK?
2126 5216     JMP LFTDET+3    /NO, REJECT
2127 4516     JMS I PKTEST   /YES, LARGE ENOUGH?
2130 4526     JMS I STORPK   /YES, STORE AS VALID PEAK
2131 5216     JMP LFTDET+3    /NO, REJECT

```

PAGE 0027

```

/SUBROUTINE TO DETERMINE IF PSEUDO-PEAK MEETS
/HEIGHT REQUIREMENTS OF:
/      1. (MAX-RIGHT)>N*NOISE
/      2. (MAX-LEFT)>N*NOISE

```

```

2132 0000 PKTST, 0000
2133 1361      TAD N           /CALC. N*NOISE
2134 4506      JMS I FLOAT     /FLOAT N & STORE IN FPA
2135 0020      FPA
2136 4437      JMS I FP
2137 5032      FGET FPD       /REPLACE NOISE WITH N*NOISE
2140 3023      FMPY FPA
2141 6026      FPUT FPC
2142 0003      FEXT
2143 1066      TAD MAX        /SET TEST FOR (MAX-RIGHT)
2144 3310      DCA SUBTRA
2145 1067      TAD RIGHT
2146 3307      DCA MINEND
2147 4531      JMS I TEST     /((MAX-RIGHT)>N*NOISE)?
2150 5354      JMP REJECT     /NO, REJECT
2151 1065      TAD LEFT       /YES, SET TEST FOR
2152 3337      DCA MINEND     /((MAX-LEFT)
2153 4531      JMS I TEST     /((MAX-LEFT)>N*NOISE)?
2154 2332 REJECT, ILZ PKTST  /NO, REJECT
2155 5732      JMP I PKTST    /YES, EXIT

```

```

/VARIABLES

```

```

2156 5531 CJMP,   JMP I CHKPKS /EXIT TO 2ND PK SEARCH
2157 2230 CHANG4, CHOICE /LOCATION OF PRINTOUT EXIT
2160 0001 MINHT, 1 /1ST MAX. IN PSEUDO-PK.
/      MUST BE > MINHT*NOISE
2161 0002 N,      2 /VALUE OF N IN N*NOISE
2162 0010 NCH,   10 /2*(# CH'S) IN VALID
/      PEAK WIDTH

```

PAGE 0028

/ROUTINE TO TYPE OUT PEAK
/MAXIMA AND BOUNDARIES

/TYPE # OF PEAKS & INITIALIZE COUNTERS

```

*2200
2200 1350 PRINT, TAD MAG9          /"NUMBER OF PEAKS : "
2201 4533      JMS I TYPST
2202 1076      TAD C3             /3 DIGIT OUTPUT FORMAT
2203 3062      DCA 62
2204 1035      TAD NPEAKS        /PRINT # OF PEAKS
2205 4231      JMS SPPRT
2206 1036      TAD PEAKST
2207 3010      DCA IR10
2210 1035      TAD NPEAKS
2211 7450      SVA                /ANY PEAKS AT ALL?
2212 5230      JMP CHOICE        /NO
2213 7041      CIA                /YES
2214 3037      DCA INDX

```

/LOOP TO PRINT PEAK PARAMETERS AND AREAS

```

2215 1351      TAD MAG10         /PRINT HEADING
2216 4533      JMS I TYPST
2217 4532 REP3, JMS I TYCR
2220 1077      TAD C4            /4 DIGIT OUTPUT FORMAT
2221 3062      DCA 62
2222 4243      JMS PRNUM        /PRINT LEFT BOUNDARY
2223 4243      JMS PRNUM        /PRINT PEAK MAX
2224 4243      JMS PRNUM        /PRINT RIGHT BOUNDARY
2225 4472      JMS I AREA       /CALC. & PRINT PK AREAS
2226 2037      ISZ INDX         /FINISHED ALL PEAKS?
2227 5217      JMP REP3        /NO
2230 7402 CHOICE, HLT          /YES (OR "JMP I CHKPKS")

```

/SUBROUTINE TO OUTPUT A S.P. NUMBER. CALL
/WITH THE NUMBER IN THE AC AND LOCATION 62
/CONTAINING THE DESIRED FORMAT OF THE OUTPUT.

```

2231 0000 SPPRT, 0000
2232 3045      DCA 45            /STORE # IN H.O. OF F(AC)
2233 3046      DCA 46            /CLEAR L.O.
2234 1074      TAD C13          /PUT 11(10) IN EXP
2235 3044      DCA 44
2236 4407      JMS I FP
2237 7000      FNOR             /NORMALIZE F(AC)
2240 0000      FEXT
2241 4406      JMS I OUTPUT     /OUTPUT NUMBER THROUGH FP
2242 5631      JMP I SPPRT     /EXIT

```

PAGE 0029

/SUBROUTINE TO OUTPUT PEAK PARAMETERS

```

2243 0000 PRTNUM, 0000
2244 1410      TAD I IR10      /GET LOCATION OF PARAMETER
2245 7110      CLL RAK        /DECODE LOCATION TO CHANNEL
2246 4231      JMS SPPRT      /OUTPUT PARAMETER
2247 4534      JMS I TYSP
2250 5643      JMP I PRTNUM    /EXIT

```

/MOVING POINT DIFFERENTIATION SUBROUTINE

```

2251 0000 DIF,      0000
2252 2034      ISZ COUNT
2253 2034      ISZ COUNT      /FINISHED ALL DATA?
2254 5256      JMP.+2        /NO
2255 5200      JMP PRINT      /YES
2256 7326      CLL CLA CML RTL /INCREMENT FOR MINUEND
2257 1034      TAD COUNT      /STORE L.O. LOCATION
2260 3265      DCA DIF2      /OF MINUEND
2261 1034      TAD COUNT      /STORE L.O. LOCATION
2262 3264      DCA DIF1      /OF SUBTRAHEND
2263 4527      JMS I SUBTRC   /GET DIFFERENTIAL
2264 0000 DIF1,      0
2265 0000 DIF2,      0
2266 1021      TAD FPA+1     /GET H.O. WORD OF DIFF.
2267 5651      JMP I DIF      /EXIT

```

/DOUBLE PRECISION SUBTRACTION SUBROUTINE.
 /DATA IS LOCATED IN UPPER CORE (D.P.).
 /CALL WITH JMS FOLLOWED BY LOCATION
 /OF LOW-ORDER WORD OF SUBTRAHEND AND
 /THEN LOCATION OF LOW-ORDER WORD OF
 /MINUEND. FINAL DIFFERENCE WILL BE
 /STORED AS A NORMALIZED FLOATING POINT
 /WORD IN LOCATIONS 20-22, PAGE 0

```

2270 0000 SUBTR, 0000
2271 7300      CLL CLA
2272 1670      TAD I SUBTR
2273 4510      JMS I GET      /FLOAT SUBTRAHEND
2274 0020      FPA
2275 2270      ISZ SUBTR
2276 1670      TAD I SUBTR
2277 4510      JMS I GET      /FLOAT MINUEND
2300 0023      FPB
2301 4407      JMS I FP
2302 5023      FGET FPB
2303 2020      FSUB FPA
2304 6020      FPUT FPA      /MINUEND-SUBTRAHEND
2305 0000      FEXT
2306 2270      ISZ SUBTR
2307 5670      JMP I SUBTR    /EXIT

```

PAGE 0030

/SPECIAL SUBROUTINE TO FETCH DOUBLE
 /PRECISION DATA FROM UPPER CORE,
 /CONVERT IT TO FLOATING POINT, AND
 /STORE IT IN THE DESIGNATED LOCATIONS.
 /THE ROUTINE IS CALLED BY A JMS,
 /FOLLOWED BY THE FIRST LOCATION OF
 /THE DESIRED STORAGE SPACE. THE
 /CONTENTS OF THE AC SHOULD CONTAIN
 /THE LOCATION OF L.O. WORD OF DATA

2310	0000	GGET,	0000	
2311	1114		TAD M1	
2312	3011		DCA 11LOC	
2313	1710		TAD I GGET	
2314	3352		DCA STORE	
2315	1075		TAD C27	/SET F(AC) EXP TO 27(8)
2316	3044		DCA 44	
2317	6211		CDF+10	
2320	1411		TAD I 11LOC	/STORE LOW-ORDER WORD
2321	3046		DCA 46	/IN F(AC) L.O. MANTISSA
2322	1411		TAD I 11LOC	/STORE HIGH-ORDER WORD
2323	3045		DCA 45	/IN F(AC) H.O. MANTISSA
2324	6201		CDF	
2325	4407		JMS I FP	
2326	7000		FNOR	/NORMALIZE F(AC)
2327	6752		FPUT I STORE	/STORE NORMALIZED DATA
2330	0000		FEXT	
2331	2310		ISZ GGET	
2332	5710		JMP I GGET	/EXIT

/FIXED TO FLOATING POINT CONVERSION.
 /CALL WITH 12 BIT, UNSIGNED INTEGER
 /IN THE AC. FOLLOW THE JMS WITH THE
 /DESIRED STORAGE LOCATION FOR THE
 /NORMALIZED F.P. DATA.

2333	0000	FFLOAT,	0000	
2334	3046		DCA 46	/PUT INTEGER IN L.O. MANTISSA
2335	3045		DCA 45	/CLEAR H.O. MANTISSA
2336	1075		TAD C27	/PUT 27(8) IN EXP
2337	3044		DCA 44	
2340	1733		TAD I FFLOAT	
2341	3352		DCA STORE	
2342	4407		JMS I FP	
2343	7000		FNOR	/NORMALIZE F(AC)
2344	6752		FPUT I STORE	/STORE WHERE DESIRED
2345	0000		FEXT	
2346	2333		ISZ FFLOAT	
2347	5733		JMP I FFLOAT	/EXIT

PAGE 0031

/VARIABLES

```
2350 2353 MAG9, PRINT1
2351 4670 MAG10, PRINT2
2352 0000 STORE, 0
```

/MESSAGE STRING FOR PEAK PRINTOUT

```
2353 0015 PRINT1, 0015 /C.R.
2354 0012 0012 /L.F. TWICE
2355 0012 0012
2356 1625 1625 /"NUMBER OF PEAKS : "
2357 1502 1502
2360 0522 0522
2361 4017 4017
2362 0640 0640
2363 2005 2005
2364 0113 0113
2365 2340 2340
2366 7240 7240
2367 0001 0001 /END MESSAGE
```

PAGE 0032

/DETERMINATION OF RANDOM STATISTICAL NOISE--
 /SUBROUTINE DETERMINES THE AVERAGE PEAK TO
 /PEAK NOISE BETWEEN TWO SPECIFIC CHANNELS. THE
 /STARTING CHANNEL IS DETERMINED BY THE PEAK
 /DETECTION ROUTINE, AND THE DETERMINATION IS
 /OVER A FIXED RANGE OF CHANNELS.

```

                *2400
2400 0000 SNOISE, 0000
2401 7300      CLL CLA
2402 3333      DCA NMAX
2403 3002      DCA FPD
2404 3003      DCA FPD+1
2405 3004      DCA FPD+2
2406 3331      DCA DIVISR
2407 1113      TAD MSPECF      /SET FIXED RANGE FOR
2410 3335      DCA NUM          /NOISE DETERMINATION
2411 4243      JMS FDIFF        /GET DIFFERENTIAL
2412 7700      SMA CLA          /NEG YET?
2413 5211      JMP.-2           /NO
  
```

/DETERMINE NOISE MINIMUM

```

2414 4243 MINDET, JMS FDIFF      /YES, GET DIFF.
2415 7710      SPA CLA          /POS YET?
2416 5214      JMP.-2           /NO
2417 1034      TAD COUNT        /YES, SAVE LOCATION OF MIN
2420 3334      DCA VMIN
2421 4250      JMS DTPKPK       /DETERMINE PK-PK NOISE
  
```

/DETERMINE NOISE MAXIMUM

```

2422 4243 MAXDET, JMS FDIFF      /GET DIFF.
2423 7700      SMA CLA          /NEG YET?
2424 5222      JMP.-2           /NO
2425 1034      TAD COUNT        /YES, SAVE LOCATION OF MAX
2426 3333      DCA NMAX
2427 4250      JMS DTPKPK       /DETERMINE PK-PK NOISE
2430 5214      JMP MINDET       /REPEAT
  
```

PAGE 0033

/CALCULATE AVERAGE PEAK TO PEAK NOISE

```

2431 7300 AVER,   CLL CLA
2432 1331      TAD DIVISR   /FLOAT DIVISOR & STORE
2433 4506      JMS I FLOAT
2434 0023      FPB
2435 4407      JMS I FP
2436 5002      FGET FPD     /GET TOTAL PK-PK NOISE
2437 4023      FDIV FPB     /DIVIDE BY DIVISOR
2440 6002      FPUT FPD     /STORE NOISE IN FPD
2441 0000      FEXT
2442 5600      JMP I SNOISE  /EXIT

```

```

/SUBROUTINE TO FETCH DIFFERENTIAL
/AND ALSO DETERMINE WHEN FINISHED

```

```

2443 0000 FDIFF, 0000
2444 4502      JMS I DIFF   /GET DIFFERENTIAL
2445 2335      ISZ NUM      /FINISHED YET?
2446 5643      JMP I FDIFF  /NO, EXIT
2447 5231      JMP AVER     /YES, CALCULATE AVERAGE NOISE

```

```

/CALCULATION OF TOTAL PEAK TO PEAK NOISE.
/PEAK MINIMUM IS SUBTRACTED FROM PEAK
/MAXIMUM AND DIFFERENCE IS SUBTOTALLED

```

```

2450 0000 DTPKPK, 0000
2451 1333      TAD NMAX
2452 7450      SNA
2453 5650      JMP I DTPKPK
2454 3262      DCA DTPK2
2455 1334      TAD NMIN
2456 3261      DCA DTPK1
2457 2331      ISZ DIVISR
2460 4527      JMS I SUBTRC  /SUBTRACT MIN. FROM MAX.
2461 0000 DTPK1, 0
2462 0000 DTPK2, 0
2463 4407      JMS I FP
2464 5002      FGET FPD     /GET PREVIOUS TOTAL NOISE
2465 1020      FADD FPA     /ADD LATEST DIFFERENCE
2466 6002      FPUT FPD     /SAVE NEW TOTAL NOISE
2467 0000      FEXT
2470 5650      JMP I DTPKPK  /EXIT

```

PAGE 0034

/FLOATING TO FIXED (D.P.) CONVERSION.
 /CALL WITH JMS FOLLOWED BY LOCATION
 /OF F.P. WORD. EXIT WITH D.P. INTEGER
 /IN LOCATIONS 46 (L.O.) & 45 (H.O.).
 /SET INTEGER TO 0 IF THE F.P. WORD IS NEG.

2471	0000	FFIX,	0000	
2472	7300		CLL CLA	
2473	1671		TAD I FFIX	/SAVE DATA LOCATION
2474	3336		DCA STOR	
2475	4407		JMS I FP	
2476	5736		FGET I STOR	
2477	7000		FNOR	/NORMALIZE F.P. WORD
2500	0000		FEXT	
2501	2271		ISZ FFIX	
2502	1044		TAD 44	/IS THE #<1?
2503	7540		SZA SMA	
2504	5311		JMP.+5	/NO
2505	7300	ZERO,	CLL CLA	/YES, SET IT TO 0
2506	3045		DCA 45	
2507	3046		DCA 46	
2510	5671		JMP I FFIX	/EXIT
2511	1332		TAD M27	/SET BIN. PT 23(10) PLACES
2512	7450		SVA	/TO RIGHT OF CURRENT PT
2513	5671		JMP I FFIX	/IT'S ALREADY THERE, EXIT
2514	3044		DCA 44	
2515	7100	REP2,	CLL	
2516	1045		TAD 45	/GET H.O. MANTISSA
2517	7510		SPA	/IS IT NEGATIVE?
2520	5305		JMP ZERO	/YES
2521	7010		RAK	/NO, ROTATE & RESTORE
2522	3045		DCA 45	
2523	1046		TAD 46	/GET L.O. MANTISSA
2524	7010		RAK	/ROTATE & RESTORE
2525	3046		DCA 46	
2526	2044		ISZ 44	/ROTATED ENOUGH?
2527	5315		JMP REP2	/NO
2530	5671		JMP I FFIX	/YES, EXIT

/VARIABLES

2531	0000	DIVISR,	0
2532	7751	M27,	-27
2533	0000	VMAX,	0
2534	0000	VMIN,	0
2535	0000	NUM,	0
2536	0000	STOR,	0

PAGE 0035

/SUBROUTINE TO RUN A SAVITZKY & GOLAY
 /LEAST SQUARES SMOOTH ON A 2048(10)
 /CHANNEL SPECTRUM WHICH IS STORED
 /IN DOUBLE PRECISION IN UPPER CORE

/INPUT REQUIRED INFORMATION

```

*3200
3200 0000 SMOTH, 0000
3201 7300 CLL CLA
3202 1366 TAD MAG19 /"# PTS IN SMOOTH = "
3203 4533 JMS I TYPST
3204 4521 JMS I SICON /INPUT #
3205 3065 DCA NPTS
3206 1065 TAD NPTS /DETERMINE POINTER FOR
3207 1065 TAD NPTS /STORAGE OF LAST DATA
3210 1065 TAD NPTS /POINT IN STRING
3211 1365 TAD CSTART
3212 3314 DCA ENDSTG
3213 7325 CLA STL IAC RAL /CALC. CONSTANTS POINTER
3214 1314 TAD ENDSTG /AS ENDSTG+3
3215 3032 DCA CNSTPT
3216 1367 TAD MAG20 /"DIVISOR = "
3217 4533 JMS I TYPST
3220 4405 JMS I INPUT /INPUT # THROUGH F.P.
3221 1365 TAD CSTART
3222 4507 JMS I FPSTOR
3223 1065 TAD NPTS
3224 7041 CIA
3225 3036 DCA INDEX
3226 1370 INPTCS, TAD MAG21 /"CONSTANT = "
3227 4533 JMS I TYPST
3230 4405 JMS I INPUT /INPUT # THROUGH F.P.
3231 1032 TAD CNSTPT
3232 4507 JMS I FPSTOR
3233 2032 ISZ CNSTPT
3234 2032 ISZ CNSTPT
3235 2032 ISZ CNSTPT
3236 2036 ISZ INDEX /INPUT ALL CONSTANTS?
3237 5226 JMP INPTCS /NO

```

PAGE 0036

/INITIALIZE VARIABLES & POINTERS

```

3240 1065      TAD NPTS          /YES, CALC. -(# PTS)+1
3241 7041      CIA
3242 7001      IAC
3243 3037      DCA MPTSP1
3244 1037      TAD MPTSP1
3245 3036      DCA INDEX
3246 1037      TAD MPTSP1      /INITIALIZE I.R. TO
3247 7001      IAC              /RESTORE SMOOTHED DATA
3250 7041      CIA              /AT (# PTS)-2
3251 3014      DCA IRSTOR
3252 3031      DCA CNTER      /INIT. RAW DATA POINTER
3253 7330      CLA STL RAR      /INIT. TOTAL PTS COUNTER
3254 1037      TAD MPTSP1      /AT 2048(10)-MPTSP1
3255 3034      DCA CNT
3256 7327      CLA STL IAC RTL /SET LOCATION POINTER FOR
3257 1365      TAD CSTART      /STRING AT 2606(8)
3260 3264      DCA CFPX

```

/INITIALIZE STRING OF RAW DATA POINTS

```

3261 1031 REP4,  TAD CNTER
3262 7104      CLL RAL
3263 4510      JMS I GET        /FETCH, FLOAT, 2
3264 2606 CFPX, 2606          /STORE RAW DATA
3265 2264      ISZ CFPX
3266 2264      ISZ CFPX
3267 2264      ISZ CFPX
3270 2031      ISZ CNTER
3271 2036      ISZ INDEX      /FINISHED STRING?
3272 5261      JMP REP4       /NO

```

/MOVE STRING UP ONE DATA POINT

```

3273 7326 RELOC, CLA STL RTL
3274 1365      TAD CSTART
3275 3013      DCA IRPUT
3276 7325      CLA STL IAC RAL
3277 1013      TAD IRPUT
3300 3010      DCA IRGET
3301 1037      TAD MPTSP1      /INIT. INDEX FOR (# PTS-1)
3302 1037      TAD MPTSP1      /F.P. STORAGE LOCATIONS
3303 1037      TAD MPTSP1
3304 3036      DCA INDEX
3305 1410      TAD I IRGET      /GET DATA WORD
3306 3413      DCA I IRPUT      /MOVE IT BACK ONE F.P. LOC.
3307 2036      ISZ INDEX      /FINISHED STRING?
3310 5305      JMP.-3         /NO
3311 1031      TAD CNTER      /YES, GET NEW FINAL
3312 7104      CLL RAL        /DATA POINT
3313 4510      JMS I GET      /FETCH, FLOAT, & STORE
3314 0000 ENDSTG, 0         /AT END OF STRING

```

PAGE 0037

/CALCULATE SMOOTHED DATA & TRANSFER IT
/TO IT'S PROPER PLACE IN THE SPECTRUM

3315	4337	JMS AVERAG	/CALC. WEIGHTED AVERAGE
3316	4407	JMS I FP	
3317	5020	FGET FPA	/GET WEIGHTED AVERAGE
3320	4765	FDIV I CSTART	/DIVIDE BY DIVISOR
3321	6020	FPUT FPA	/SAVE SMOOTHED DATA POINT
3322	0000	FEXT	
3323	4505	JMS I FIX	/INTEGERIZE SMOOTHED DATA
3324	0020	FPA	
3325	6211	CDF+10	
3326	1046	TAD 46	/TRANSFER SMOOTHED DATA TO
3327	3414	DCA I IRSTOR	/CORRECT PLACE IN SPECTRUM
3330	1045	TAD 45	
3331	3414	DCA I IRSTOR	
3332	6201	CDF	
3333	2031	ISZ CNTER	
3334	2034	ISZ CNT	/FINISHED ALL DATA?
3335	5273	JMP RELOC	/NO
3336	5600	JMP I SMOTH	/YES, EXIT

/CALCULATE THE TOTAL WEIGHTED AVERAGE

3337	0000	AVERAG, 0000	
3340	7340	CLL CLA CMA	
3341	1037	TAD MPTSP1	
3342	3036	DCA INDEX	
3343	3020	DCA FPA	
3344	3021	DCA FPA+1	
3345	3022	DCA FPA+2	
3346	1365	TAD CSTART	
3347	3033	DCA GETDAT	
3350	7325	CLA STL IAC HAL	
3351	1314	TAD ENDSIG	
3352	3032	DCA CVSTPT	
3353	4771	JMS I SUBTOT	/FIND SUBTOTAL
3354	2036	ISZ INDEX	/FINISHED ALL POINTS?
3355	5353	JMP.-2	/NO
3356	5737	JMP I AVERAG	/YES, EXIT

/SUBROUTINE TO STORE A F.P. # WHICH
/HAS BEEN INPUT THROUGH THE F.P.
/PACKAGE. CALL WITH THE DESIRED
/STORAGE LOCATION IN THE AC.

3357	0000	FSTORE, 0000	
3360	3066	DCA PTEMP	
3361	4407	JMS I FP	
3362	6466	FPUT I PTEMP	/STORE F.P. #
3363	0000	FEXT	
3364	5757	JMP I FSTORE	/EXIT

PAGE 0038

/VARIABLES

```

3365 2600 CSTART, 2600           /START OF STORAGE SPACE
3366 4540 MAG19, SMOTH1
3367 4555 MAG20, SMOTH2
3370 4565 MAG21, SMOTH3
3371 4520 SUBTOT, SBTOT

```

```

/SUBROUTINE TO FIND A SUBTOTAL
/FOR A WEIGHTED AVERAGE SMOOTH

```

```

                                *4520
4520 0000 SBTOT, 0000
4521 2033          ISZ GETDAT
4522 2033          ISZ GETDAT
4523 2033          ISZ GETDAT
4524 4407          JMS I FP
4525 5433          FGET I GETDAT   /GET FAW DATA POINT
4526 3432          FMPY I CNSTPT  /MULTIPLY BY WEIGHTING
4527 6026          FPUT FPC       /CONSTANT & SAVE PRODUCT
4530 5020          FGET FPA       /GET SUBTOTAL
4531 1026          FADD FPC       /ADD PRODUCT
4532 6020          FPUT FPA       /STORE AS NEW SUBTOTAL
4533 0000          FEXT
4534 2032          ISZ CNSTPT
4535 2032          ISZ CNSTPT
4536 2032          ISZ CNSTPT
4537 5720          JMP I SBTOT     /EXIT

```

PAGE 0039

/MESSAGE STRINGS FOR L.S. SMOOTH

4540	0015	SMOOTH1,	0015	/C.F.
4541	0012		0012	/L.F. TWICE
4542	0012		0012	
4543	4340		4340	/"# PTS IN SMOOTH = "
4544	2024		2024	
4545	2340		2340	
4546	1116		1116	
4547	4023		4023	
4550	1517		1517	
4551	1724		1724	
4552	1040		1040	
4553	7540		7540	
4554	0001		0001	/END MESSAGE
4555	0015	SMOOTH2,	0015	/C.F.
4556	0012		0012	/L.F.
4557	0411		0411	/"DIVISOR = "
4560	2611		2611	
4561	2317		2317	
4562	2240		2240	
4563	7540		7540	
4564	0001		0001	/END MESSAGE
4565	0015	SMOOTH3,	0015	/C.F.
4566	0012		0012	/L.F.
4567	0317		0317	/"CONSTANT = "
4570	1623		1623	
4571	2401		2401	
4572	1624		1624	
4573	4075		4075	
4574	4000		4000	
4575	0100		0100	/END MESSAGE

PAGE 0040

/SUBROUTINE TO DETERMINE THE QUANTITATIVE
 /AREA IN A GAMMA-RAY PHOTOPEAK----
 /CALCULATION USES TOTAL PEAK AREA---
 /TOTAL AREA IS CALCULATED BY SUMMATION
 /OF DATA OVER ALL CHANNELS IN PEAK, THEN
 /THE TRAPEZOIDAL AREA DETERMINED BY THE
 /TWO BOUNDARY CHANNELS IS SUBTRACTED TO
 /YIELD THE QUANTITATIVE AREA DESIRED.

```

                                *3600
3600 0000 PKAREA, 0000
3601 7346          CLL CLA CMA RTL /(-3)
3602 1010          TAD IR10          /RESET REGISTER FOR
3603 3010          DCA IR10          /PROPER PEAK
3604 7040          CMA              /SET DECISION POINTER
3605 3374          DCA ONETWO
3606 1410 GETPK,   TAD I IR10        /GET LEFT BOUNDARY
3607 7110          CLL RAR
3610 3065          DCA PKLEFT
3611 1410          TAD I IR10        /GET PEAK MAX
3612 7110          CLL RAR
3613 3066          DCA PKMX
3614 1410          TAD I IR10        /GET RIGHT BOUNDARY
3615 7110          CLL RAR
3616 3067          DCA PKRT
3617 1065          TAD PKLEFT        /FLOAT & STORE
3620 7104          CLL RAL          /LEFT BOUNDARY
3621 4510          JMS I GET
3622 0002          FPD
3623 1067          TAD PKRT          /FLOAT & STORE
3624 7104          CLL RAL          /RIGHT BOUNDARY
3625 4510          JMS I GET
3626 0031          FPTEMP
3627 1065 CALC,   TAD PKLEFT        /FLOAT & STORE #
3630 7041          CIA              /CHANNELS IN PEAK
3631 1067          TAD PKRT
3632 7001          IAC
3633 4506          JMS I FLOAT
3634 0026          FPC              /# CHANNELS=(RIGHT-LEFT)+1
3635 4407          JMS I FP
3636 5031          FGET FPTEMP      /CAL. TRAPEZOID AREA AS
3637 1002          FADD FPD         /<V*(LEFT+RIGHT)/2>
3640 3026          FMPY FPC
3641 4370          FDIV FP2
3642 6023          FPUT FPB        /STORE TRAPEZOID AREA
3643 0000          FEXT
3644 1067 TOTAL, TAD PKRT          /CALC. TOTAL AREA
3645 7041          CIA              /BY SUMMATION
3646 3375          DCA MPKRT
3647 3020          DCA FPA
3650 3021          DCA FPA+1
3651 3022          DCA FPA+2
3652 1065          TAD PKLEFT
3653 3034          DCA CNT
  
```

```

PAGE 0041
3654 1034 LOOP,   TAD CNT           /ADD CURRENT CHANNEL
3655 7104         CLL RAL           /TO SUBTOTAL
3656 4510         JMS I GET
3657 0026         FPC
3660 4407         JMS I FP
3661 5026         FGET FPC
3662 1020         FADD FPA
3663 6020         FPUT FPA           /STORE SUBTOT. IN FPA
3664 0000         FEXT
3665 2034         ISZ CNT
3666 1034         TAD CNT           /PASSED RIGHT BOUNDARY?
3667 1375         TAD MPKRT
3670 7750         SPA SVA CLA
3671 5254         JMP LOOP         /NO
3672 4407         JMS I FP         /YES
3673 5020         FGET FPA         /GET TOTAL AREA
3674 2023         FSUB FPB         /SUBTRACT TRAP. AREA
3675 6026         FPUT FPC         /STORE QUAN. AREA IN FPC
3676 0000         FEXT
3677 1367         TAD FPSTRT        /"FGET FPA-3"
3700 3766         DCA I CCFP        /INIT. FETCH LOC. FOR LOOP
3701 4776         JMS I PNT         /PRINT TOTAL AREA
3702 4776         JMS I PNT         /PRINT TRAPEZOID AREA
3703 4776         JMS I PNT         /PRINT QUANTITATIVE AREA
3704 2374         ISZ ONETWO        /FINISHED BOTH METHODS?
3705 5600         JMP I PKAREA       /YES, EXIT

```

```

/ CALCULATION OF PEAK AREA USING WASSON'S METHOD---
/ THE ORIGINAL LEFT (X1) & RIGHT (X4) BOUNDARIES
/ ARE USED TO CALCULATE THE SLOPE OF THE BASELINE
/ AND THEN THE WASSON LEFT (X2) & RIGHT (X3)
/ BOUNDARIES ARE USED TO CALCULATE THE AREAS USING
/ THE SAME METHOD AS WITH THE TOTAL PEAK METHOD.

```

```

3706 1065 WASSON, TAD PKLEFT       /NO, CALC. (X4-X1)
3707 7041         CIA              /AS (LEFT-RIGHT)
3710 1067         TAD PKRT
3711 4506         JMS I FLOAT
3712 0026         FPC
3713 1067         TAD PKRT         /IS (X4-MAX)>OR=NWASON?
3714 7041         CIA
3715 1066         TAD PKMX
3716 1373         TAD NWASON
3717 7540         SMA SZA
3720 5600         JMP I PKAREA       /NO, EXIT
3721 1067         TAD PKRT         /YES, FIND WASSON'S PKRT
3722 3067         DCA PKRT
3723 1065         TAD PKLEFT       /CALC. (X3-X1)
3724 7041         CIA
3725 1067         TAD PKRT
3726 4506         JMS I FLOAT
3727 0023         FPB

```

```

PAGE 0042
3730 1373      TAD  NWASON      /IS (MAX-X1)>OR=NWASON?
3731 1065      TAD  PKLEFT
3732 7041      CIA
3733 1066      TAD  PKYX
3734 7510      SPA
3735 5600      JMP  I PKAREA    /NO, EXIT
3736 1065      TAD  PKLEFT    /YES, FIND WASSON'S PKLEFT
3737 3375      DCA  PKTEMP    /PUT IN TEMP. STORAGE
3740 1065      TAD  PKLEFT    /CALC. (X2-X1)
3741 7041      CIA
3742 1375      TAD  PKTEMP
3743 4506      JMS  I FLOAT
3744 0020      FPA
3745 1375      TAD  PKTEMP    /CHANGE PKLEFT TO X2
3746 3065      DCA  PKLEFT
3747 4407      JMS  I FP
3750 5031      FGET  FPTEMP
3751 2002      FSUB  FPD
3752 4026      FDIV  FPC
3753 6026      FPUT  FPC      /SLOPE=(Y4-Y1)/(X4-X1)
3754 5026      FGET  FPC
3755 3023      FMPY  FPB
3756 1002      FADD  FPD
3757 6031      FPUT  FPTEMP    /Y3=SLOPE*(X3-X1)+Y1
3760 5026      FGET  FPC
3761 3020      FMPY  FPA
3762 1002      FADD  FPD
3763 6002      FPUT  FPD      /Y2=SLOPE*(X2-X1)+Y1
3764 0000      FEAT
3765 5227      JMP  CALC      /CALCULATE THE AREAS

```

/VARIABLES

```

3766 2550  CCFP,   CFP
3767 5015  FPSTRT, 5015      / (FGET FPA-3)
3770 0002  FP2,    0002      /2.0
3771 2000                2000
3772 0000                0000
3773 0004  NWASON,  4
3774 0000  ONETWO,  0
                MPKRT,
3775 0000  PKTEMP,  0
3776 2540  PNT,    PPNT

```

PAGE 0043

/SUBROUTINE TO PRINT AREAS

```

                *2540
2540 0000 PPNT,  0000
2541 4534      JMS I TYSP
2542 1100      TAD C7           /7 DIGIT OUTPUT FORMAT
2543 3062      DCA 62
2544 7325      CLA STL IAC HAL /(+3)
2545 1350      TAD CFP         /INCREMENT FETCH LOC. FOR
2546 3350      DCA CFP         /PROPER AREA
2547 4407      JMS I FP
2550 0000 CFP,  0           /"FGET FPX"
2551 0000      FEXT
2552 4406      JMS I OUTPUT   /OUTPUT AREA
2553 5740      JMP I PPNT     /EXIT

```

/MESSAGE STRING FOR HEADING FOR PEAK PRINTOUT

```

                *4670
4670 0012 PRINT2, 0012      /L.F. TWICE
4671 0012      0012
4672 4040      4040      /"   TOTAL PEAK METHOD   "
4673 4024      4024      /"           WASSON'S METHOD"
4674 1724      1724
4675 0114      0114
4676 4020      4020
4677 0501      0501
4700 1340      1340
4701 1505      1505
4702 2410      2410
4703 1704      1704
4704 4040      4040
4705 4040      4040
4706 4040      4040
4707 4040      4040
4710 4040      4040
4711 4027      4027
4712 0123      0123
4713 2317      2317
4714 1647      1647
4715 2340      2340
4716 1505      1505
4717 2410      2410
4720 1704      1704

```

PAGE 0044

/MESSAGE STRING FOR HEADING
/FOR PEAK PRINTOUT (CONT.)

4721	0015	0015	/C. R.		
4722	0012	0012	/L. F.		
4723	4014	4014	/" LEFT	MAX RIGHT	"
4724	0506	0506	/" TOTAL	TRAP	"
4725	2440	2440	/" QUAN	TOTAL	"
4726	4040	4040	/"TRAP	QUAN"	
4727	1501	1501			
4730	3040	3040			
4731	2211	2211			
4732	0710	0710			
4733	2440	2440			
4734	4040	4040			
4735	4040	4040			
4736	2417	2417			
4737	2401	2401			
4740	1440	1440			
4741	4040	4040			
4742	4040	4040			
4743	2422	2422			
4744	0120	0120			
4745	4040	4040			
4746	4040	4040			
4747	4021	4021			
4750	2501	2501			
4751	1640	1640			
4752	4040	4040			
4753	4024	4024			
4754	1724	1724			
4755	0114	0114			
4756	4040	4040			
4757	4040	4040			
4760	4024	4024			
4761	2201	2201			
4762	2040	2040			
4763	4040	4040			
4764	4040	4040			
4765	2125	2125			
4766	0116	0116			
4767	0015	0015	/C. R.		
4770	0012	0012	/L. F.		
4771	0001	0001	/END MESSAGE		

PAGE 0045

/LIBRARY GENERATOR ROUTINE---SUBROUTINE WILL
 /READ THROUGH PREVIOUSLY RECORDED PROGRAMS
 /AND THEN STORE A PROGRAM WHICH IS CONTAINED
 /IN UPPER CORE IN A FORMAT COMPATIBLE WITH
 /TRI-DATA'S LIBRARY GENERATOR ROUTINE. WHEN
 /THE PROGRAM # IS 0, TAPE WILL NOT REWIND &
 /PROGRAM WILL BE STORED IMMEDIATELY ONTO TAPE.

/INPUT TAPE AND PROGRAM #'S

```

                                *4000
4000 0000 LIEGEN, 0000
4001 7300 CLL CLA
4002 1367 TAD MAG12 /"PROGRAM = "
4003 4533 JMS I TYPST
4004 4521 JMS I SIC0V
4005 7450 SNA /RESET TAPE PARAMETERS?
4006 5263 JMP DWRITE /NO, STORE PROG. IMMED.
4007 3371 DCA PROGNO
4010 1366 TAD MAG11 /"TAPE # = "
4011 4533 JMS I TYPST
4012 4521 JMS I SIC0V
4013 7041 CIA
4014 3371 DCA TAPEN
4015 7107 CLL IAC RTL /(+4)
4016 1071 TAD TAPEN /MAKE SURE IT'S<5
4017 7710 SPA CLA
4020 5201 JMP LIEGEN+1 /ITS NOT, ASK AGAIN

```

/SET UP APPROPRIATE MAG TAPE VARIABLES

```

4021 7320 CLA STL /GENERATE INPUT TAPE #
4022 7010 MAGTAP, RAR / (BITS 8-11)
4023 2071 ISZ TAPEN
4024 5222 JMP MAG1AP
4025 3365 DCA INTAPE
4026 1365 TAD INTAPE /GENERATE OUTPUT TAPE #
4027 7012 RTR / (BITS 4-7)
4030 7012 RTR
4031 3070 DCA OUTTAP
4032 1070 TAD OUTTAP /GENERATE LOAD PT MASK
4033 7012 RTR
4034 7012 RTR
4035 3071 DCA LDPTMS

```

PAGE 0046

/SKIP OVER PREVIOUSLY RECORDED PROGRAMS

4036	1071		TAD LDPTMS	
4037	6314		ACMD	/GO TO LOAD PT.
4040	7326		CLA STL RTL	/(+2) TO ALLOW FOR LOADERS
4041	1371		TAD PROGNO	/INITIALIZE PROG. COUNTER
4042	7041		CIA	
4043	3371		DCA PROGNO	
4044	1365	PROG,	TAD INTAPE	/START READING A PROGRAM
4045	6314	READ,	ACMD	/INITIATE READ ACTION
4046	6332		SRWC	/IS READ WORD FLAG SET?
4047	5245		JMP READ	/NO
4050	6335		RTB	/YES, READ A WORD
4051	3066		DCA TEMPI	/STORE LAST WORD READ
4052	6305		L TSA	/IS READ READY FLAG SET?
4053	0365		AND INTAPE	
4054	7650		SVA CLA	
4055	5245		JMP READ	/NO, READ ANOTHER WORD
4056	1066		TAD TEMPI	/YES, END OF PROGRAM?
4057	0076		AND C3	
4060	7650		SVA CLA	
4061	2371		ISZ PROGNO	/YES, LAST PROGRAM?
4062	5244		JMP PROG	/NO, READ ANOTHER PROGRAM
4063	1065	DWRITE,	TAD STRTMI	/(STARTING ADDRESS-1)
4064	3016		DCA IADATA	
4065	3035		DCA LSECSW	/CLEAR LAST SECTION SWITCH
4066	6211	REP6,	CDR+10	
4067	6324		LTB	/RESET WRITE FLAG
4070	1115		TAD M5	/SET COUNTER TO LIMIT #
4071	3066		DCA TEMPI	/BLOCKS IN A SECTION TO 5
4072	3034		DCA CKSUM	/CLEAR CHECK SUM
4073	1036	REP7,	TAD VDATPT	/(# DATA PTS LEFT IN PROG.)
4074	7550		SPA SVA	/4000(8) DATA PTS LEFT?
4075	5303		JMP D1	/YES
4076	1370		TAD M777	/NO, ARE THERE 777(8)?
4077	7540		SMA SZA	
4100	5304		JMP D2	/YES
4101	2035		ISZ LSECSW	/NO, SET LAST SECTION SWITCH
4102	5305		JMP D3	
4103	1370	D1,	TAD M777	/(# DATA PTS IN BLOCK)
4104	3036	D2,	DCA VDATPT	/RECALC. # DATA PTS LEFT
4105	1362	D3,	TAD C777	/SET UP OUTPUT BLOCK COUNT
4106	3037		DCA OBLCT	
4107	1037		TAD OBLCT	/WRITE BLOCK COUNT &
4110	1364		TAD DATAFD	/FIELD IN THE FIRST WORD
4111	4772		JMS I SWRITE	/OF THE SECTION
4112	1037		TAD OBLCT	/INITIALIZE OUTPUT COUNTER
4113	7041		CIA	
4114	3037		DCA OBLCT	
4115	1016		TAD IADATA	/WRITE DATA OUTPUT
4116	7001		IAC	/ADDRESS IN THE 2ND
4117	4772		JMS I SWRITE	/WORD OF THE SECTION

PAGE 0047			
4120 1416	WRTDAT,	TAD I IRDATA	/WRITE A DATA WORD
4121 4772		JMS I SWRITE	
4122 2037		ISZ OBLCT	/FINISHED BLOCK?
4123 5320		JMP WRTDAT	/NO
4124 2066		ISZ TEMP1	/YES, FINISHED A SECTION?
4125 7410		SKP	
4126 5332		JMP ENDSEC	/YES
4127 1035		TAD LSECSW	/NO, LAST SECTION FINISHED?
4130 7650		SNA CLA	
4131 5273		JMP REP7	/NO, REPEAT
4132 6201	ENDSEC,	CDF	/YES, END A SECTION
4133 1034		TAD CKSUM	/LAST 3 WORDS OF SECTION
4134 1361		TAD C200	/ARE CONFUSING. 1ST ONE
4135 7041		CIA	/CONTAINS CONTROL TRANSFER
4136 3066		DCA TEMP1	/FIELD # 2 LAST 2 BITS
4137 1066		TAD TEMP1	/OF CHECK SUM. 2ND ONE
4140 0076		AND C3	/HAS CONTROL TRANSFER
4141 4772		JMS I SWRITE	/ADDRESS. 3RD ONE HAS
4142 1361		TAD C200	/1ST 10 BITS OF CHECK
4143 4772		JMS I SWRITE	/SUM & LAST 2 BITS ARE
4144 1066		TAD TEMP1	/LAST SECTION SWITCH
4145 0363		AND C7774	/(00 IF LAST SECTION).
4146 3066		DCA TEMP1	
4147 1035		TAD LSECSW	/LAST SECTION?
4150 7650		SNA CLA	
4151 7001		IAC	/NO, INDICATE MORE TO COME
4152 1066		TAD TEMP1	/YES
4153 4772		JMS I SWRITE	
4154 4773		JMS I SWRSTP	/PUT A WRITE STOP ON TAPE
4155 1035		TAD LSECSW	/LAST SECTION?
4156 7650		SNA CLA	
4157 5266		JMP REP6	/NO, REPEAT
4160 5600		JMP I LIRGEN	/YES, EXIT

/VARIABLES

4161 0200	C200,	200
4162 0777	C777,	777
4163 7774	C7774,	7774
4164 1000	DATAFD,	1000
4165 0000	INTAPE,	J
4166 4304	MAG11,	MGTP2
4167 4274	MAG12,	MGTP1
4170 7001	M777,	-777
4171 0000	PROGNO,	0
4172 4240	SWRITE,	WRITE
4173 4265	SWRSTP,	WRSTOP

PAGE 0048

/ROUTINE TO SET UP STARTING DATA LOCATION
 /AND # DATA WORDS IN THE PROGRAM FOR
 /THE LIBRARY GENERATOR SUBROUTINE

```

*4200
4200 7300 SETUP,  CLL CLA
4201 1231          TAD MAG14          /"STARTING CHANNEL = "
4202 4533          JMS I TYPST
4203 4521          JMS I SICOV
4204 7510          SPA                /LESS THAN 2047(10)?
4205 5233          JMP MAGERR         /NO, TRY AGAIN
4206 7104          CLL RAL
4207 1114          TAD M1
4210 3065          DCA STRTM1
4211 1232          TAD MAG15          /"FINAL CHANNEL = "
4212 4533          JMS I TYPST
4213 4521          JMS I SICOV
4214 7510          SPA                /LESS THAN 2047(10)?
4215 5233          JMP MAGERR         /NO, TRY AGAIN
4216 7104          CLL RAL
4217 7001          IAC                /INCREMENT FOR H.O. WORD
4220 3227          DCA CLAST
4221 1065          TAD STRTM1        /CALC. # DATA WORDS
4222 7041          CIA
4223 1227          TAD CLAST
4224 3036          DCA VDATPT
4225 4630          JMS I LBGEN
4226 7402          HLT
4227 0000 CLAST,  0
4230 4000 LEGEN,  4000
4231 4325 MAG14,  MGTP4
4232 4343 MAG15,  MGTP5

```

/ERROR MESSAGE FOR EXCESSIVELY LARGE CHANNEL #

```

4233 7300 MAGERR, CLL CLA
4234 1237          TAD MAG16          /"TOO LARGE, START OVER"
4235 4533          JMS I TYPST
4236 5200          JMP SETUP
4237 4356 MAG16,  MGTP6

```

PAGE 0049

/SUBROUTINE TO WRITE A DATA WORD ON MAG TAPE

```

4240 0000 WRITE, 0000
4241 3257 DCA WORD /SAVE THE DATA WORD
4242 1070 TAD OUTTAP /ACTIVATE WRITE
4243 6314 ACMD /IF NECESSARY
4244 6321 SWWC /SKIP WHEN WRITE WORD
4245 5243 JMP.-2 /FLAG IS SET
4246 6305 LTSA /CHECK TAPE UNIT STATUS
4247 0071 AND LDPTMS /AT LOAD POINT?
4250 7640 SZA CLA
4251 5260 JMP LDPTMG /YES, PRINT ERROR MESSAGE
4252 1257 TAD WORD /NO, WRITE WORD
4253 6324 LTB
4254 1034 TAD CKSUM /UPDATE CHECK SUM
4255 3034 DCA CKSUM
4256 5640 JMP I WRITE /EXIT
4257 0000 WORD, 0

```

/WRITE ERROR MESSAGE WHEN TAPE IS AT LOAD POINT

```

4260 6201 LDPTMG, CDF
4261 1264 TAD MAG13 /"AT LOAD POINT"
4262 4533 JMS I TYPST
4263 7402 HLT
4264 4313 MAG13, MGTP3

```

/ROUTINE TO PUT A WRITE STOP ON TAPE

```

4265 0000 WRSTOP, 0000
4266 6321 SWWC /SKIP WHEN WRITE WORD
4267 5266 JMP.-1 /FLAG IS SET
4270 6312 WSPC /INIT. WRITE STOP ACTION
4271 6321 SWWC /SKIP WHEN WRITE WORD
4272 5271 JMP.-1 /FLAG IS SET
4273 5665 JMP I WRSTOP /EXIT

```

PAGE 0050

/MESSAGE STRINGS FOR LIBRARY GENERATOR

4274	0015	MGTP1,	0015	/C.R.
4275	0012		0012	/L.F.
4276	2022		2022	/"PROGRAM = "
4277	1707		1707	
4300	2201		2201	
4301	1540		1540	
4302	7540		7540	
4303	0001		0001	/END MESSAGE
4304	4040	MGTP2,	4040	/" TAPE # = "
4305	2401		2401	
4306	2005		2005	
4307	4043		4043	
4310	4075		4075	
4311	4000		4000	
4312	0100		0100	/END MESSAGE
4313	0015	MGTP3,	0015	/C.R.
4314	0012		0012	/L.F.
4315	0124		0124	/"AT LOAD POINT!"
4316	4014		4014	
4317	1701		1701	
4320	0440		0440	
4321	2017		2017	
4322	1116		1116	
4323	2441		2441	
4324	0001		0001	/END MESSAGE
4325	0015	MGTP4,	0015	/C.R.
4326	0012		0012	/L.F. TWICE
4327	0012		0012	
4330	2324		2324	/"STARTING CHANNEL = "
4331	0122		0122	
4332	2411		2411	
4333	1607		1607	
4334	4003		4003	
4335	1001		1001	
4336	1616		1616	
4337	0514		0514	
4340	4075		4075	
4341	4000		4000	
4342	0100		0100	/END MESSAGE

PAGE 0051		
4343 0015	MGTP5,	0015
4344 0012		0012
4345 0611		0611
4346 1601		1601
4347 1440		1440
4350 0310		0310
4351 0116		0116
4352 1605		1605
4353 1440		1440
4354 7540		7540
4355 0001		0001
		/END MESSAGE
4356 0015	MGTP6,	0015
4357 0012		0012
4360 0012		0012
4361 2417		2417
4362 1740		1740
4363 1401		1401
4364 2207		2207
4365 0554		0554
4366 4023		4023
4367 2401		2401
4370 2224		2224
4371 4017		4017
4372 2605		2605
4373 2200		2200
4374 0100		0100
		/END MESSAGE

PAGE 0052

```

/PROGRAM TO SEARCH FOR PEAKS IN A
/SPECTRUM AND DETERMINE THE #,
/MAXIMUM, AND BOUNDRIES USING A
/MOVING POINT DIFFFERENTIAL. THIS
/SEARCH USES A MINIMUM SERIES OF
/POS. & NEG. DER.'S AS CRITERIA.

```

```

/INITIALIZATION OF VARIABLES

```

```

                                *4400
4400 7300 PKSEARCH, CLL CLA
4401 1311 TAD CHALT           /SET PEAK PRINTOUT TO HALT
4402 3712 DCA I CHANGS
4403 3035 DCA NPEAKS
4404 3037 DCA MRIGHT
4405 1124 TAD START
4406 3036 DCA PEAKST
4407 1036 TAD PEAKST
4410 3012 DCA IIRPK
4411 1125 TAD STRTCH
4412 3034 DCA COUNT
4413 7040 CMA                /SET CHECK FOR FIRST
4414 3000 DCA                /IN A SERIES
4415 1314 TAD MNUM
4416 3315 DCA NUMBER

```

```

/ROUTINE TO SEARCH FOR A MINIMUM
/SERIES OF POSITIVE NUMBERS

```

```

4417 4502 SEARCH, JMS I DIFF   /GET DIFFERENTIAL
4420 7710 SPA CLA             /IS IT POSITIVE?
4421 5213 JMP SEARCH-4        /NO
4422 2313 ISZ CHECK          /YES, FIRST IN SERIES?
4423 5226 JMP.+3             /NO
4424 1034 TAD COUNT          /YES, SAVE LEFT BOUNDRY
4425 3065 DCA LEFT
4426 2315 ISZ NUMBER         /MIN POS SERIES COMPLETED?
4427 5217 JMP SEARCH           /NO

```

PAGE 0053

/PEAK DETECTION ROUTINE

4430	4502	PKDET,	JMS I DIFF	/YES, GET DIFFERENTIAL
4431	7700		SMA CLA	/IS IT NEGATIVE?
4432	5230		JMP.-2	/NO
4433	1034		TAD COUNT	/YES, STORE PEAK MAX
4434	3066		DCA MAX	

/DETECTION OF VALID RIGHT BOUNDARY

4435	1314	RTBN DY,	TAD XNUM	/RESET SERIES INDEX FOR NEG
4436	7001		IAC	/INCREMENT FOR LAST DATA
4437	3315		DCA NUMBER	
4440	4502		JMS I DIFF	/GET DIFFERENTIAL
4441	7700		SMA CLA	/POSITIVE YET?
4442	5246		JMP DONE	/YES, RUN CHECKS
4443	2315		ISZ NUMBER	/NO
4444	5240		JMP.-4	
4445	5240		JMP.-5	

/ROUTINE TO VERIFY FOR VALID PEAKS

4446	1315	DONE,	TAD NUMBER	/MINIMUM NEG SERIES
4447	7710		SPA CLA	/COMPLETED?
4450	5261		JMP NEXTPK	/NO, REJECT
4451	1034		TAD COUNT	/YES, SAVE RIGHT BOUNDARY
4452	3067		DCA RIGHT	
4453	1073		TAD CI	/SET GNOISE TO FIND 1*NOISE
4454	4506		JMS I FLOAT	
4455	0031		FPTEMP	
4456	4511		JMS I GNOISE	/CALC. STATISTICAL NOISE
4457	4516		JMS I PKTEST	/VALID PEAK?
4460	4526		JMS I STORPK	/YES, STORE BOUNDARIES
4461	1034	NEXTPK,	TAD COUNT	/NO, SAVE POSSIBLE
4462	3065		DCA LEFT	/LEFT BOUNDARY
4463	3313		DCA CHECK	
4464	7001		IAC	/INCREMENT FOR LAST DATA
4465	5215		JMP SEARCH-2	/BEGIN SEARCH FOR NEW PEAK

PAGE 0054

/SUBROUTINE TO DETERMINE BOUNDARIES FOR
/CALCULATION OF RANDOM STATISTICAL NOISE

4466	0000	N&NOIS, 0000	
4467	1034	TAD COUNT	/SAVE PRESENT LOC COUNTER
4470	3316	DCA SAVE	
4471	1065	TAD LEFT	/MOVE BACK SPECIFIED
4472	1113	TAD MSPECF	/# OF LOCATIONS
4473	3034	DCA COUNT	/RESET LOCATION COUNTER
4474	1034	TAD COUNT	
4475	7110	CLL RAR	
4476	1037	TAD MRIGHT	/ARE WE BELOW LAST
4477	7700	SMA CLA	/RIGHT BOUNDARY?
4500	4503	JMS I DNOISE	/NO, DETERMINE NEW NOISE
4501	4407	JMS I FP	/YES, USE LAST NOISE VALUE
4502	5002	FGET FPD	/RETAIN ACTUAL NOISE
4503	3031	FMPY FPTEMP	/VALUE IN PERMAVENT
4504	6026	FPUT FPC	/STORAGE (FPD), PUT
4505	0000	FEXT	/FPTEMP+NOISE IN FPC
4506	1316	TAD SAVE	/RESTORE LOCATION COUNTER
4507	3034	DCA COUNT	
4510	5666	JMP I N&NOIS	/EXIT

/VARIABLES

4511	7402	CHALT, HLT	
4512	2230	CHANG5, CHOICE	/LOCATION OF PRINTOUT EXIT
4513	0000	CHECK, 0	
4514	7776	XNUM, -2	/MIN. # POS. OR NEG. DER.'S
4515	0000	NUMBER, 0	
4516	0000	SAVE, 0	

PAGE 0055

/ROUTINE TO FLOAT & STORE SPECTRAL
 /DATA IN FNEW LOCATIONS FOR PEAK
 /FITTING USING FOCAL PROGRAMMING

```

                                *4600
4600 7340 RELCTE,  CLL CLA CMA
4601 1264          TAD FNEW
4602 3015          DCA IR15
4603 1265          TAD MAG17          /"STARTING CHANNEL = "
4604 4533          JMS I TYPST
4605 4521          JMS I SICON
4606 7104          CLL RAL
4607 3033          DCA LFTBDY
4610 1266          TAD MAG18          /"FINAL CHANNEL ="
4611 4533          JMS I TYPST
4612 4521          JMS I SICON
4613 7105          CLL IAC RAL
4614 7041          CIA
4615 1033          TAD LFTBDY
4616 3031          DCA CNTER

```

/RELOCATE BLOCK OF DATA TO BEGIN AT LOCATION 0

```

4617 7340 MOVE0,  CLL CLA CMA
4620 3012          DCA IR12
4621 7140          CLL CMA
4622 1033          TAD LFTBDY
4623 3010          DCA IR10
4624 1031          TAD CNTER
4625 3032          DCA LOC32
4626 6211          CDF+10
4627 1410          TAD I IR10          /GET DATA
4630 3412          DCA I IR12          /RELOCATE IT
4631 2032          ISZ LOC32          /FINISHED ALL DATA?
4632 5227          JMP.-3           /NO
4633 7340          CLL CLA CMA          /YES
4634 3012          DCA IR12

```

PAGE 0356

/FLOAT DATA & STORE IN THE EVEN FNEW
/LOCATION, BEGINNING WITH FNEW(152)

4635	1412	MVFNEW,	TAD I IR12	/PUT DATA IN F(AC)
4636	3046		DCA 46	
4637	1412		TAD I IR12	
4640	3045		DCA 45	
4641	6201		CDF	
4642	1075		TAD C27	/SET EXP. TO 23(10)
4643	3044		DCA 44	
4644	4504		JMS I DVORM	/NORMALIZE F(AC)
4645	6211		CDF+10	
4646	1044		TAD 44	/STORE F.P. DATA IN FNEW
4647	3415		DCA I IR15	
4650	1045		TAD 45	
4651	3415		DCA I IR15	
4652	1046		TAD 46	
4653	3415		DCA I IR15	
4654	3415		DCA I IR15	/SET ODD FNEW'S TO 0
4655	3415		DCA I IR15	
4656	3415		DCA I IR15	
4657	2031		ISZ CNTER	/FINISHED ALL DATA?
4660	2031		ISZ CNTER	
4661	5235		JMP MVFNEW	/NO
4662	6201		CDF	/YES
4663	5512		JMP I MAGTPE	/STORE ON MAG. TAPE

/VARIABLES

4664	3710	FNEW,	3710
4665	4325	MAG17,	MGTP4
4666	4343	MAG18,	MGIP5

ADC	0200	ADC1	0474	ADC2	0505	ADC3	0530
ADC4	0544	ADC5	0557	ADPNTR	0017	ARFA	0072
AVER	2431	AVERAGE	3337	BOUNDS	1411	CALC	3627
CCFP	3766	CEND	0357	CFP	2553	CFPK	3264
CHALT	4511	CHANG1	1644	CPANG2	1647	CHANG3	1656
CHANG4	2157	CHANG5	4512	CHECK	4513	CHKPKB	0101
CHLT	0362	CHOICE	2230	CJMP	2156	CKSUM	0034
CLAST	4227	CNSTPT	0032	CNT	0534	CNTFR	0031
CNTA	1664	COLECT	0227	COMPAL	2105	CJUNT	0034
COUNT1	1701	COUNT2	1702	CSTAF1	3365	CTA	0363
C0001	1662	C0212	1142	C0215	1143	C0240	1144
C1	0073	C100	0667	C13	0074	C200	4161
C240	0670	C27	0075	C3	0076	C4	0077
C5	0364	C6561	1663	C7	0103	C777	4162
C7774	4163	DATAFD	4164	DELAY	1671	DIF	2251
DIFF	0102	DIF1	2264	DIF2	2265	DIVISH	2531
DNOISE	0103	DNOVM	0104	DOVE	4446	DSPLY	1641
DTPKPK	2450	DTPK1	2461	DTPK2	2462	DWRITE	4063
D1	4103	D2	4104	D3	4105	ENDSEC	4132
ENDSTG	3314	ERROR	1437	EXIT	1660	FDIFF	2443
FETCH	1403	FFIX	2471	FFLOAT	2333	FINAL	0035
FIRST	1431	FIX	0105	FLAG	0664	FLOAT	0106
FLOC	1665	FNEW	4664	FP	0007	FPA	0020
FPB	0023	FPC	0026	FPD	0002	FPSTOR	0107
FPSTRI	3767	FPTEMP	0031	FP2	3770	FSTORE	3357
GET	0110	GETDAT	0033	GETPK	3600	GGFI	2310
GNOISE	0111	HDRGET	0414	HEADER	0365	HEDEK	0434
HEDEK1	1150	HEDEK2	1164	HEDEK3	0760	HEDEK4	0766
HEDEK5	0770	HIGH	1464	IDSPLY	1652	INCMNT	1433
INDEX	0036	INDX	0037	INITAL	0423	INPTCS	3226
INPUT	0005	INTAPE	4165	INTRUP	0135	IRDATA	0016
IRGET	0010	IRLOC	0011	IRPK	0012	IRPUT	0013
IRSTOR	0014	IR10	0010	IR11	0011	IR12	0012
IR15	0015	K77	0665	LAST	1432	LASTPG	0351
LRGEN	4230	LDPTMG	4260	LDPTMS	0071	LEFT	0065
LEVEL	1221	LFTBDY	0033	LFTDET	2013	LIBGEN	4000
LINDEX	0066	LINE	0037	LOC31	0031	LOC32	0032
LOC33	0033	LOC34	0034	LOC35	0035	LOC36	0036
LOC37	0037	LOC65	0065	LOC66	0066	LOC67	0067
LOC70	0070	LOC71	0071	LOOP	3654	LOW	1465
LSECSW	0035	MAGDSH	0366	MAGERR	4233	MAGTAP	4022
MAGTPE	0112	MAG1	0367	MAG10	2351	MAG11	4166
MAG12	4167	MAG13	4264	MAG14	4231	MAG15	4232
MAG16	4237	MAG17	4665	MAG18	4666	MAG19	3366
MAG2	0370	MAG20	3367	MAG21	3370	MAG3	0455
MAG4	0456	MAG6	1466	MAG7	1467	MAG8	1470
MAG9	2350	MAX	0066	MAXDET	2422	MGTP1	4274
MGTP2	4304	MGTP3	4313	MGTP4	4325	MGTP5	4343
MGTP6	4356	MINDET	2414	MINEND	2107	MINHT	2160
MNUM	4514	MODIFY	0673	MOVE0	4617	MPKRT	3775
MPTSP1	0037	MRIGHT	0037	MSPCF	0113	MVFNEW	4635
M1	0114	M27	2532	M4	3371	M40	0666

M5	0115	M62	0372	M777	4170	V	2161
NCH	2162	NDATPT	0036	NERMAX	2061	VEKTPK	4461
NLINES	0065	NMAX	2533	NMIN	2534	NOPT	0233
NPEAKS	0035	NPNTS	1666	NPTS	0065	NUM	2535
NUMBER	4515	NWASOV	3773	NWJIS	4466	OBLCT	0037
OLDMAX	2060	OVETWO	3774	OY	1134	OUTER	1703
OUTPUT	0006	OUTTAP	0070	PAGER	0271	PEAKST	0036
PENHGH	1261	PENHI	1253	PENLOW	1247	PENLW	1260
PINDEX	0066	PKAREA	3600	PKCHCK	2121	PKDET	4430
PKLEFT	0065	PKMAX	2020	PKXX	0066	PKRT	0067
PKSER	2000	PKSRCH	4400	PKTEMP	3775	PKTEST	0116
PKTST	2132	PLOT	1242	PNT	3776	PPNT	2540
PPRINT	0276	PRDATA	0312	PRINT	2200	PRINT1	2353
PRINT2	4670	PROG	4044	PROGNO	4171	PRT	0440
PRTNUM	2243	PTEMP	0066	PTONLY	0360	READ	4045
REJECT	2154	RELCTE	4600	RELOC	3273	REPET	1204
REPET1	1223	REP1	1450	REP2	2515	REP3	2217
REP4	3261	REP6	4066	REP7	4073	EIGHT	0067
ROT	1435	ROTAT	1443	ROTATE	1400	ROTDN	1246
ROTDW	1243	ROTUP	1200	ROT1	1471	ROT2	1504
ROT3	1510	RTBNDY	4435	RTDET	2037	SAVE	4516
SAVEPK	2070	SBTOT	4520	SCDSY	0117	SEARCH	4417
SER	0120	SETUP	4200	SICOV	0121	SICOVV	1000
SICTRL	1032	SIEND	1066	SIHOLD	1112	SIMASK	1102
SIMMNS	1110	SIMPLS	1107	SIMSPC	1106	SIM260	1104
SIM271	1105	SINEG1	1113	SINMNR	1046	SINPUT	1057
SIPROC	1011	SIRBUT	1103	SISAVE	1111	SISSET1	1075
SIXSW1	1024	SKIPMA	0671	SKIPPA	0672	SMOOTH	0122
SMOTH	3200	SMOTH1	4540	SMOTH2	4555	SMOTH3	4565
SNOISE	2400	SPPRNT	0123	SPPRT	2231	SK	0236
SSCDY	1600	START	0124	START1	0457	START2	0466
STOR	2536	STORE	2352	STORPK	0126	STPRT	0373
STPT	0400	STRTCH	0125	STATM1	0065	SUBTOT	3371
SUBTR	2270	SUBTRA	2110	SUBTRC	0127	SWITCH	0652
SWRITE	4172	SWRSTP	4173	TAPEN	0071	TEMP1	0066
TEM0	0662	TEMR	0663	TER	0130	TEST	0131
TOTAL	3644	TR	0253	TSCC1	0603	TSCC2	0614
TTYCH	1120	TTYSP	1127	TYCH	0132	TYPAT	0625
TYPE	0650	TYPSP	0631	TYPST	0133	TYPSTG	0600
TYSP	0134	VJMP	1667	VNOP	1670	WASSON	3706
WORD	4257	WRITE	4240	WRSTOP	4265	WRTDAT	4120
ZERO	2505						

APPENDIX II

FOCAL PROGRAMS

All computer programs listed in this appendix were run on an 8K Digital Equipment Corporation PDP-8/L computer with a Model ASR 33 Teletype input and output. All programs were written in FOCAL (FOrmula CALculator) conversational language. The following new functions were user defined: common storage functions FNEW(1,...,...) and FNEW(2,...,...), and integer scaling function FNEW(3,...,...), and an oscilloscope display function FNEW(4,...,...).

Program 1

Photopeak Fitting Routine

This program performs the nonlinear least squares iterative fit of an eight parameter function, described in the theory section, to the digital data stored in the even FNEW locations, beginning with FNEW(150). The original parameter estimates, the value of the increment, the number of points in the fit, and the initial abscissa value are input through the Teletype. New values of the parameter estimates, the residual sum of squares, and the raw and fitted sums are printed following each iteration.

PS = number of parameters

C(V) = parameter estimate

IN = abscissa increment, in sigma units

NP = number of points in the fitting interval

XO = initial abscissa value, in sigma units

C-8K FOCAL @1969

```

01.01 E
01.02 T %8.05
01.03 F V=1,150;S Z=FNEW(1,V,0)
01.04 A ?PS?,!!
01.05 F V=1,PS;A ?C(V)?,!
01.07 T !;A ?IN?,?NP?,?X0?;!
01.10 S I=0;S X=X0;S U=75;S SM=0
01.15 S S1=C(2)*(X-C(3));S S2=(X-C(4))/2*C(5)
01.20 S S3=C(8)-X;S S4=FSQT(S3+2)
01.25 S S5=FEEXP(S1);S S6=FEEXP(-S1);S S7=S5+S6
01.30 S Q1=FEEXP(-S2*(X-C(4)))
01.35 S Q2=.5*(1-(S5-S6)/S7)
01.40 S Q3=C(6)*FEEXP(-C(7)*(S4+S3))
01.45 S D(1)=Q1+Q2+Q3
01.50 S Y=C(1)*D(1)
01.55 S S8=C(1)*Q3;S S9=S8*Q2
01.60 S U=U+1;S Z=FNEW(1,2*U-1,Y)
01.65 S D(3)=2*S8+C(2)/S7+2
01.70 S D(2)=D(3)*((C(3)-X)/C(2))
01.75 S D(4)=2*C(1)+S2*Q1
01.80 S D(5)=S2*D(4)
01.85 S D(6)=S9/C(6)
01.90 S D(7)=-S9*(S4+S3)
01.95 S D(8)=D(7)*C(7)/S4

02.40 S RS=FNEW(2,2*U,W)-FNEW(2,2*U-1,W);S SM=SM+RS+2
02.45 F J=1,PS;S Z=FNEW(2,J+PS+2,W)+D(J)*RS;S Z1=FNEW(1,
    J+PS+2,Z)
02.50 F J=1,PS;F K=1,J;D 4
02.55 S X=X+IV;S I=I+1;I (I-NP)1.15;
02.85 T !;T ?SM?,!;G 8.1
02.90 T "GG";S Z=FNEW(4,150,650)

03.05 S IT=IT+1
03.10 S L=PS;S N=L-1;S I=-1
03.15 F K=0,N;S R(K)=K+1
03.20 S M=1E-6
03.25 F J=0,N;F K=0,N;D 5
03.30 S R(P)=0
03.35 F K=0,L;S Z=FNEW(2,P+L*K+1,W)/M;S Z1=FNEW(1,P+L*K+
    1,Z)
03.40 F J=0,N;D 6
03.45 S I=I+1;I (I-N)3.2,3.5,3.2
03.50 F J=0,N;F K=0,N;D 7
03.55 T !!!"# OF ITERATIONS",%2,IT
03.60 T !;F K=0,N;T ! %2"X(",K+1,") ",%8.05,X(K)
03.65 T !!!;F V=1,PS;S C(V)=C(V)+X(V-1);T C(V),!
03.70 F V=1,2;D 3.9
03.74 F V=5,7;D 3.9
03.78 F V=3,5,8;D 3.95
03.80 D 1.03

```

```

03.85 G 1.1
03.90 I (-C(V))3.99;S C(V)=(C(V)-X(V-1))/2;T "C(",Z1 V,"
)"%8.05 C(V),!
03.95 I (C(V)-C(4))3.99;S C(V)=(C(V)-X(V-1))/2;T "C(",Z1
V,")"%8.05 C(V),!
03.99 R

04.10 S V=J+K*PS-PS
04.15 S Z=FNEW(2,V,W)+D(J)*D(K)
04.20 S Z1=FNEW(1,V,Z)

05.10 I (R(J))0,5.3,5.15
05.15 I (FABS(FNEW(2,J+K*L+1,W))-FABS(M))5.3;
05.20 S M=FNEW(2,J+K*L+1,W)
05.25 S P=J;S Q=K
05.30 R

06.10 I (J-P)6.15,6.25,6.15
06.15 S D=FNEW(2,J+L*Q+1,W)
06.20 F K=0,L;S V=J+K*L+1;S V1=V-J+P;D 6.3
06.25 R
06.30 S Z=FNEW(2,V,W)-FNEW(2,V1,W)*D;S Z1=FNEW(1,V,Z)

07.10 I (1E-6-FABS(FNEW(2,J+K*L+1,W)))7.2;R
07.20 S X(K)=FNEW(2,J+L*L+1,W)

08.10 S R=0;S S=0
08.15 F I=76,(NP-1)+76;D 9
08.20 T !"RAW SUM",R;T " SMOOTH SUM",S,!
08.25 G 2.9

09.10 S R=R+FNEW(2,2*I,W)
09.20 S S=S+FNEW(2,2*I-1,W)
09.30 R
*
```

Program 2

Baseline Fitting Routine

This program performs the nonlinear least squares iterative fit of a cubic polynomial to up to five separate segments of the digital data stored in the even FNEW locations, beginning with FNEW(150). The original parameter estimates, the value of the increment, the number of points in the fit, the initial abscissa value, the number of baseline segments, and the first and last channel location of each segment are input through the Teletype. New values of the parameter estimates, the residual sum of squares, and the raw and fitted sums are printed following each iteration.

PS = number of parameters

C(V) = parameter estimate

IN = abscissa increment, in channels

NP = number of points in the fitting interval

XO = initial abscissa value, in channels

SS = number of baseline segments in the fit

N(J) = first or last channel location of a baseline
segment

C-8K FOCAL @1969

```

01.01 E
01.03 F V=1,150;S Z=FNEW(1,V,0)
01.04 A ?PS?,!!
01.05 F V=1,PS;A ?C(V)?,!
01.07 T !;A ?IN?,?NP?,?X0?,!!
01.08 T "# SECTIONS";A SS;T " ";F J=1,2*(SS-1);A ?N(J
    )?
01.10 S I=0;S X=X0;S U=75;S SM=0
01.15 S B=1;S Y=C(1);S D(1)=1
01.20 F II=2,PS;DO 5.9
01.60 S U=U+1;S Z=FNEW(1,2*U-1,Y)
01.65 I (I-N(1))2.4;
01.70 I (I-N(2)+1)2.55;
01.75 I (I-N(3))2.4;
01.80 I (I-N(4)+1)2.55;
01.85 I (I-N(5))2.4;
01.90 I (I-N(6)+1)2.55;
01.95 I (I-N(7))2.4;

02.05 I (I-N(8)+1)2.55;
02.10 I (I-N(9))2.4;
02.15 I (I-N(10)+1)2.55;
02.40 S RS=FNEW(2,2*U,W)-FNEW(2,2*U-1,W);S SM=SM+RS*2
02.45 F J=1,PS;S Z=FNEW(2,J+PS*2,W)+D(J)*RS;S Z1=FNEW(1,
    J+PS*2,Z)
02.50 F J=1,PS;F K=1,PS;D 4
02.55 S X=X+IN;S I=I+1;I (I-NP)1.15;
02.85 T !;T ?SM?,!;G 8.1
02.90 T "GG";S Z=FNEW(4,150,650)

03.05 S IT=IT+1
03.10 S L=PS;S N=L-1;S I=-1
03.15 F K=0,N;S R(K)=K+1
03.20 S M=1E-6
03.25 F J=0,N;F K=0,N;D 5
03.30 S R(P)=0
03.35 F K=0,L;S Z=FNEW(2,P+L*K+1,W)/M;S Z1=FNEW(1,P+L*K+
    1,Z)
03.40 F J=0,N;D 6
03.45 S I=I+1;I (I-N)3.2,3.5,3.2
03.50 F J=0,N;F K=0,N;D 7
03.55 T !!!"# OF ITERATIONS",%2,IT
03.60 T !;F K=0,N;T ! %2"X(",K+1,") ",%8.05,X(X)
03.65 T !;F V=1,PS;S C(V)=C(V)+X(V-1);T C(V),!
03.70 I (-C(1))3.8;S C(1)=(C(1)-X(0))/2;T "C(1)",C(1),!
03.80 D 1.03
03.85 G 1.1

04.10 S V=J+K*PS-PS
04.15 S Z=FNEW(2,V,W)+D(J)*D(K)
04.20 S Z1=FNEW(1,V,Z)

```

```

05.10 I (R(J))0,5.3,5.15
05.15 I (FABS(FNEW(2,J+K*L+1,W))-FABS(M))5.3;
05.20 S M=FNEW(2,J+K*L+1,W)
05.25 S P=J;S Q=K
05.30 R
05.90 S B=B*X;S Y=Y+C(II)*B;S D(II)=B

06.10 I (J-P)6.15,6.25,6.15
06.15 S D=FNEW(2,J+L*Q+1,W)
06.20 F K=0,L;S V=J+K*L+1;S V1=V-J+P;D 6.3
06.25 R
06.30 S Z=FNEW(2,V,W)-FNEW(2,V1,W)*D;S Z1=FNEW(1,V,Z)

07.10 I (1E-6-FABS(FNEW(2,J+K*L+1,W)))7.2;R
07.20 S X(K)=FNEW(2,J+L+L+1,W)

08.10 S R=0;S S=0
08.15 F I=76,(NP-1)+76;D 9
08.20 T !"RAW SUM",R;T "    SMOOTH SUM",S,!
08.25 G 2.9

09.02 S J=I-76
09.05 I (J-N(1))9.6;
09.10 I (J-N(2)+1)9.7;
09.15 I (J-N(3))9.6;
09.20 I (J-N(4)+1)9.7;
09.25 I (J-N(5))9.6;
09.30 I (J-N(6)+1)9.7;
09.35 I (J-N(7))9.6;
09.40 I (J-N(8)+1)9.7;
09.45 I (J-N(9))9.6;
09.50 I (J-N(10)+1)9.7;
09.60 S R=R+FNEW(2,2*I,W)
09.65 S S=S+FNEW(2,2*I-1,W)
09.70 R
*
```

Program 3

Calculation of the Total Fitted Curve

This program uses the final parameter estimates from Programs 1 and 2 to calculate the total fitted curve. The total curve is obtained by adding the polynomial baseline contribution to the fitted peak function. The calculated values are stored in the odd FNEW locations, beginning with FNEW(151). The program assumes that the original raw data are stored in the even FNEW locations, beginning with FNEW(150). The residual sum of squares and the raw and fitted sums are calculated, and the raw and fitted spectra are simultaneously displayed on an oscilloscope.

PS = number of parameters

C(V) = final calculated parameter estimates

IN = abscissa increment, in sigma units

NP = number of points in the fitting interval

XO = initial abscissa value, in sigma units

C-8K FOCAL @1969

```

01.01 E
01.02 T 28.05
01.04 A ?PS?,!!
01.05 F V=1,PS;A ?C(V)?,!
01.07 T !;A ?IV?,?NP?,?X0?;!
01.10 S I=0;S X=X0;S U=75;S SM=0
01.15 S S1=C(2)*(X-C(3));S S2=(X-C(4))/2+C(5)
01.20 S S3=C(8)-X;S S4=FSQI(S3+2)
01.25 S S5=FEXP(S1);S S6=FEXP(-S1);S S7=S5+S6
01.30 S Q1=FEXP(-S2*(X-C(4)))
01.35 S Q2=.5*(1-(S5-S6)/S7)
01.40 S Q3=C(6)*FEXP(-C(7)*(S4+S3))
01.45 S D(1)=Q1+Q2*Q3
01.50 S Y=C(1)*D(1)
01.52 S JJ=I+1;S B=1;S Y=Y+C(9)
01.55 F II=10,PS;S B=B*JJ;S Y=Y+C(11)*B
01.60 S U=U+1;S Z=FNEW(1,2*U-1,Y)

02.40 S RS=FNEW(2,2*U,W)-FNEW(2,2*U-1,W);S SM=SM+RS+2
02.55 S X=X+IN;S I=I+1;I (I-NP)1.15;
02.60 T !"RESIDUAL SUM OF SQUARES",SM,!
02.65 S R=0;S S=0
02.70 F I=76,NP+75;D 3
02.75 T !"RAW SUM",R;T " SMOOTH SUM",S,!
02.90 T "GG";S Z=FNEW(4,150,450)
02.95 Q

03.10 S R=h+FNEW(2,2*I,W)
03.20 S S=S+FNEW(2,2*I-1,W)
03.30 R

```

*

Program 4

Numerical Integration by the Trapezoid Method

This program performs the numerical integration of the eight parameter fitting function, using the trapezoid method and an increment of 0.1 channel. The final parameter estimates from Program 1, the abscissa increment used with the fitting function, and the channel locations of the peak boundaries are input through the Teletype. The integrated area is printed and the process is repeated.

C(V) = final calculated parameter estimates

IF = abscissa increment, in sigma units,
used with the fitting function

C-8K FOCAL 01969

```

01.01 E
01.02 T 78.06,!!!!
01.05 T "PEAK";A PK,!!
01.07 F V=1,8;A ?C(V)?,!
01.08 A !"FITTING INCREMENT",IF
01.10 A !! "LEFT BOUNDARY",LB;A " PEAK MAX",MX;A " RIGH
    T BOUNDARY",RB
01.15 S HH=0.1;S X0=(LB-MX)*IF;S XF=(RB-MX)*IF;S H=IF*HH
01.20 S N=((RB-LB)*IF/H)+1;T !!! "# POINTS",N;T " X0",X0
01.25 S S=0;S X=X0
01.30 F I=1,N+.4;D 2
01.35 S A=S*HH/2;T !!! "AREA",A
01.40 A !!! "CONTINUE?",CC;I (20-CC)1.5;
01.45 T !!!!!;Q
01.50 T !;G 1.1

02.10 S S1=C(2)*(X-C(3));S S2=(X-C(4))/(2*C(5))
02.15 S S3=C(8)-X;S S4=FSQT(S3+2)
02.20 S S5=FEXP(S1);S S6=FEXP(-S1);S S7=S5+S6
02.25 S Q1=FEXP(-S2*(X-C(4)))
02.30 S Q2=0.5*(1-(S5-S6)/S7)
02.35 S Q3=C(6)*FEXP(-C(7)*(S4+S3))
02.40 S Y=C(1)*(Q1+Q2*Q3)
02.50 I (I-2)2.6;I (N-I-1)2.6;
02.55 S Y=2*Y
02.60 S S=S+Y;S X=X+H;S Z=Z+HH
02.65 S W=W+H
02.70 R
*
```

Program 5

Linear Least Squares

This program performs the least squares fit of a straight line to a set of data points. The abscissa and ordinate values are input through the Teletype. The program calculates and prints the Y-intercept, slope, mean square deviation, and X-intercept.

L1 = number of data points to be fit

X(J1) = abscissa value, J1 = 1, ..., L1

Y(J1) = ordinate value, J1 = 1, ..., L1

C-8K FOCAL @1969

```

01.06 E
01.07 T !!!;S NA=2;S NB=2;A L1
01.08 F J1=1,L1;T !;A X(J1),Y(J1)
01.10 T !!!"DATA POINTS:",!," NO.          X
      Y",!
01.11 F J1=1,L1;T %2,J1,"          ",%6.06,X(J1),"          ",Y(J1)
      ),!
01.15 F L=VA,NB;DO 2
01.17 S XX=-(B(1)/B(2));T "X-INTERCEPT",XX
01.20 G 1.07

02.17 S N2=2*L-1
02.20 F J1=1,N2;S SX(J1)=0
02.22 F J1=1,L;S YX(J1)=0
02.25 F J2=1,N2;F J1=1,L1;S SX(J2)=SX(J2)+X(J1)+(J2-1)
02.27 F J2=1,L;F J1=1,L1;S YX(J2)=YX(J2)+Y(J1)*(X(J1)+(J2-1))
02.30 F J2=1,L;F J1=1,L;S A(J2+J1*L)=SX(J1+(J2-1))
02.35 D 15.0
02.78 T !;F K=1,L; T !"B(",%2,K,")          ",%6.06,B(K)
02.80 F J1=1,L;S YX(J1)=0
02.82 S SD=0
02.84 T !!!" NO.          Y OBS.          Y CALC.          DFIFF.",!
02.85 F J1=1,L1;S YX=0;D 8.0
02.86 S SD=FSQT(SD/(L1-L))
02.88 T !!!"MEAN SQUARE DEVIATION",%6.06,SD,!!!;R

08.10 F J2=1,L;S YK=YK+B(J2)*(X(J1)+(J2-1))
08.15 S D=Y(J1)-YX;S SD=SD+D*D
08.17 R
08.20 T %2,J1,"          ",%6.06,Y(J1),"          ",YX,"          ",D,!!;R

14.05 S N=K+1; S DD=A(N+II*L)/A(II+II*L)
14.10 F J=II,L; S A(N+J*L)=A(N+J*L)-A(II+J*L)*DD
14.15 S YX(N)=YX(N)-YX(II)*DD; R

15.05 S MM=L-1
15.10 F II=1,MM;F K=II,MM; D 14.0
15.15 S B(L)=YX(L)/A(L+L*L)
15.20 F M=2,L;S N=L+1-M;S KK=N+1;S B(N)=YX(N)/A(N+N*L);D
      15.25
15.21 G 15.30
15.25 F K=KK,L; S B(N)=B(N)-A(N+K*L)*B(K)/A(N+N*L)
15.30 R
*
```

BIBLIOGRAPHY

1. W. S. Lyon, "Guide to Activation Analysis," D. Van Nostrand Company, Inc., New York, 1964.
2. G. Hevesy and H. Levi, Det. Kgl. Danske Videnskabernes Selskab. Matematisk-Fysiske Meddelelser. 14(5), 3 (1936).
3. G. Hevesy and H. Levi, Det. Kgl. Danske Videnskabernes Selskab. Matematisk-Fysiske Meddelelser. 15(11), 14 (1938).
4. G. T. Seaborg and J. J. Livingood, J. Am. Chem. Soc. 60, 1784 (1938).
5. R. E. Connally and M. B. Leboeuf, Anal. Chem. 25, 1095 (1953).
6. G. H. Morrison and J. F. Cosgrove, Anal. Chem. 27, 810 (1955).
7. G. H. Morrison and J. F. Cosgrove, Anal. Chem. 28, 320 (1956).
8. A. K. De and W. W. Meinke, Anal. Chem. 30, 1474 (1958).
9. V. P. Guinn and C. D. Wagner, Anal. Chem. 32, 317 (1960).
10. L. E. Fite, E. L. Steele, and R. E. Wainerdi, Texas Eng. Exp. Sta. Rept. TEES-2671-2, November 1, 1962, p 440.
11. F. S. Goulding, Nucl. Instr. Meth. 43, 1 (1966).
12. D. F. Covell, Anal. Chem. 31, 1785 (1959).
13. V. P. Guinn and J. E. Lasch, Nat. Acad. Sci. Rept. NAS-NS-3107, 1963, p 243.
14. B. R. Kowalski and T. L. Isenhour, Anal. Chem. 40, 1186 (1968).
15. B. L. Robinson, Nat. Acad. Sci. Rept. NAS-NS-3107, 1963, p 67.
16. H. P. Yule, Anal. Chem. 38, 103 (1966).
17. S. C. Choy and R. A. Schmitt, Nature 205, 758 (1965)
18. J. Pauly, G. Guzzi, F. Girardi, and A. Borella, Nucl. Instr. Meth. 42, 15 (1966).
19. R. L. Heath, Nucl. Instr. Meth. 43, 209 (1966).
20. W. Lee, Anal. Chem. 31, 800 (1959).

21. O. U. Anders and W. H. Beamer, Anal. Chem. 33, 226 (1961).
22. A. K. Furr, E. L. Robinson, and C. H. Robins, Nucl. Instr. Meth. 63, 205 (1968).
23. K. G. Heinen and G. B. Larrabee, Anal. Chem. 38, 1853 (1966).
24. J. A. Blackburn, Anal. Chem. 37, 1000 (1965).
25. E. Schonfeld, Nucl. Instr. Meth. 42, 213 (1966).
26. L. Salmon, Nat. Acad. Sci. Rept. NAS-NS-3107, 1963, p 165.
27. P. J. M. Korthoven, M. A. Wechter, and A. F. Voigt, Anal. Chem. 39, 1595 (1967).
28. J. S. Elridge and A. A. Brooks, Nucleonics 24(4), 54 (1966).
29. D. E. Hull and J. T. Gilmore, Anal. Chem. 36, 2072 (1964).
30. B. T. Watson, J. Nucl. Med. 4, 306 (1963).
31. N. E. Scofield, Nat. Acad. Sci. Rept. NAS-NS-3107, 1963, p 108.
32. L. E. Fite, D. Gibbons, and R. E. Wainerdi, Texas Eng. Exp. Sta. Rept. TEES-2671-1, Category No. UC-23, May, 1961, 100p.
33. K. Liebscher and H. Smith, Anal. Chem. 40, 1999 (1968).
34. M. Ciampi, L. Daddi, and V. D. D'Angelo, Nucl. Instr. Meth. 66, 102 (1968).
35. J. M. Hollander, Nucl. Instr. Meth. 43, 66 (1966).
36. F. Lamb, S. G. Prussin, J. A. Harris, and J. M. Hollander, Anal. Chem. 38, 813 (1966).
37. S. G. Prussin, J. A. Harris, and J. M. Hollander, Anal. Chem. 37, 1127 (1965).
38. T. Inouye, T. Harper, and N. C. Rasmussen, Nucl. Instr. Meth. 67, 125 (1969).
39. J. A. Blackburn, Nucl. Instr. Meth. 63, 66 (1968).
40. Z. Kosina, Nucl. Instr. Meth. 88, 163 (1970).
41. A. Savitsky and M. J. E. Golay, Anal. Chem. 36, 1627 (1964).
42. H. P. Yule, Nucl. Instr. Meth. 54, 61 (1967).
43. H. Tominaga, M. Dojyo, and M. Tanaka, Nucl. Instr. Meth. 98, 69 (1972).

44. H. P. Yule, Anal. Chem. 44, 1245 (1972).
45. A. L. Connelly and W. W. Black, Nucl. Instr. Meth. 82, 141 (1970).
46. W. W. Black, Nucl. Instr. Meth. 71, 317 (1969).
47. J. A. Dooley, J. H. Gorrell, and P. Polishuk, "Modern Trends in Activation Analysis," Nat. Bur. Stand. (U.S.), Spec. Publ. 312, 1969, p 1090.
48. R. Gunnink and J. B. Niday, "Modern Trends in Activation Analysis," Nat. Bur. Stand. (U.S.), Spec. Publ. 312, 1969, p 1244.
49. H. R. Ralston and G. E. Wilcox, "Modern Trends in Activation Analysis," Nat. Bur. Stand. (U.S.), Spec. Publ. 312, 1969, p 1238.
50. J. R. Morrey, Anal. Chem. 40, 905 (1968).
51. H. P. Yule, Anal. Chem. 40, 1480 (1968).
52. H. P. Yule, "Modern Trends in Activation Analysis," Nat. Bur. Stand. (U.S.), Spec. Publ. 312, 1969, p 1256.
53. V. Barnes, IEEE Trans. Nucl. Sci. NS-15, 1968, p 437.
54. S. J. Mills, Nucl. Instr. Meth. 81, 217 (1970).
55. M. A. Mariscotti, Nucl. Instr. Meth. 50, 309 (1967).
56. J. T. Routti and S. G. Prussin, Nucl. Instr. Meth. 72, 125 (1969).
57. O. U. Anders, Anal. Chem. 41, 428 (1969).
58. S. Sterlinski, Anal. Chem. 40, 1995 (1968).
59. S. Sterlinski, Anal. Chem. 42, 151 (1970).
60. P. Quittner, Nucl. Instr. Meth. 76, 115 (1969).
61. P. Quittner, Anal. Chem. 41, 1504 (1969).
62. P. A. Baedeker, Anal. Chem. 43, 405 (1971).
63. S. M. Roberts, D. H. Wilkinson, and L. R. Walker, Anal. Chem. 42, 886 (1970).
64. C. Gunther and D. Parsignault, Phys. Rev. 153, 1297 (1967).
65. R. G. Helmer, R. L. Heath, M. Putnam, and D. H. Lipson, Nucl. Instr. Meth. 57, 46 (1967).
66. W. M. Sanders and D. M. Holm, Los Alamos Sci. Lab. Rept. LA-4030, July, 1968, 100p.

67. L. Varnell and J. Trischuk, Nucl. Instr. Meth. 75, 109 (1969).
68. J. H. Head, Nucl. Instr. Meth. 98, 419 (1972).
69. J. Kern, Nucl. Instr. Meth. 79, 233 (1970).
70. T. A. E. C. Pratt and M. L. Luther, Nucl. Instr. Meth. 92, 317 (1971).
71. D. C. Robinson, Nucl. Instr. Meth. 78, 120 (1970).
72. C. J. Thompson, "Modern Trends in Activation Analysis," Nat. Bur. Stand. (U.S.), Spec. Publ. 312, 1969, p 1121.
73. E. E. Maslin, S. H. Terry, and L. A. Wraight, Nucl. Instr. Meth. 71, 13 (1969).
74. R. K. Webster, "Activation Analysis in Geochemistry and Cosmochemistry," Universitetsforlaget, Oslo, 1971, p 183.
75. R. K. Hobbie and R. W. Goodwin, Nucl. Instr. Meth. 52, 119 (1967).
76. T. B. Pierce, R. K. Webster, R. Hallett, and D. Mapper, "Modern Trends in Activation Analysis," Nat. Bur. Stand. (U.S.), Spec. Publ. 312, 1969, p 1116.
77. E. DerMateosian, Nucl. Instr. Meth. 73, 77 (1969).
78. E. Norbeck and M. D. Mancusi, Nucl. Instr. Meth. 56, 293 (1967).
79. K. Samsahl, P. O. Webster, and O. Landstrom, Anal. Chem. 40, 181 (1968).
80. G. H. Morrison and N. M. Potter, Anal. Chem. 44, 839 (1972).
81. S. Meloni, A. Bromdone, and V. Maxia, Int. J. Appl. Radiat. Isot. 20, 757 (1969).
82. T. F. Budinger, J. R. Farwell, A. R. Smith, and H. Bichsel, Int. J. Appl. Radiat. Isot. 23, 49 (1972).
83. D. M. Linekin, J. F. Balcius, R. D. Cooper, and G. L. Brownell, "Modern Trends in Activation Analysis," Nat. Bur. Stand. (U.S.), Spec. Publ. 312, 1969, p 110.
84. S. N. Chesler and S. P. Cram, Anal. Chem., in press.
85. R. H. Filby, A. I. Davis, K. R. Shah, G. G. Wainscott, W. A. Haller, and W. A. Cassatt, "Gamma-Ray Energy Tables for Neutron Activation Analysis," Washington State University Report WSUNRC-97(2), 1970.

- 86. "Handbook of Chemistry and Physics," R. C. Weast, Ed., Chemical Rubber Co., Cleveland, 1969, p B-265.
- 87. G. Friedlander, J. W. Kennedy, and J. M. Miller, "Nuclear and Radiochemistry," John Wiley and Sons, Inc., New York, 1966, p 535.
- 88. H. P. Yule, private communication.

BIOGRAPHICAL SKETCH

David Baldwin Cottrell was born on September 17, 1946, at Covington, Virginia. He was educated in the public school systems of Fishersville and Newport News, Virginia. He graduated from Ferguson High School, Newport News, Virginia, in June, 1964, where he was elected to the National Honor Society.

In September, 1964, he began his undergraduate studies at the University of Virginia, Charlottesville, Virginia. In June, 1968, he received the degree of Bachelor of Science, With Distinction, in Chemistry and was named the outstanding graduate in analytical chemistry.

He entered graduate school in September, 1968, at the University of Florida, Gainesville, Florida, majoring in analytical chemistry. He held teaching and research assistantships until September, 1971, when he was awarded a Traineeship from the National Science Foundation.

He married the former Elizabeth Neil Blackwell of Newport News, Virginia, on May 27, 1967. He has been a member of the American Chemical Society and the Society of Sigma Xi.

I certify that I have read this study and that in my opinion it conforms to acceptable standards of scholarly presentation and is fully adequate, in scope and quality, as a dissertation for the degree of Doctor of Philosophy.



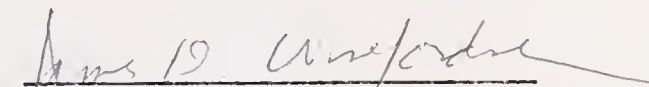
Stuart P. Cram, Chairman,
Assistant Professor of Chemistry

I certify that I have read this study and that in my opinion it conforms to acceptable standards of scholarly presentation and is fully adequate, in scope and quality, as a dissertation for the degree of Doctor of Philosophy.



Roger G. Bates,
Professor of Chemistry

I certify that I have read this study and that in my opinion it conforms to acceptable standards of scholarly presentation and is fully adequate in scope and quality, as a dissertation for the degree of Doctor of Philosophy.



James D. Winefordner,
Professor of Chemistry

I certify that I have read this study and that in my opinion it conforms to acceptable standards of scholarly presentation and is fully adequate, in scope and quality, as a dissertation for the degree of Doctor of Philosophy.

William H. Ellis

William H. Ellis,
Associate Professor of Nuclear
Engineering

I certify that I have read this study and that in my opinion it conforms to acceptable standards of scholarly presentation and is fully adequate, in scope and quality, as a dissertation for the degree of Doctor of Philosophy.

Frank G. Martin

Frank G. Martin,
Associate Professor of Statistics

This dissertation was submitted to the Department of Chemistry in the College of Arts and Sciences and to the Graduate Council, and was accepted as partial fulfillment of the requirements for the degree of Doctor of Philosophy.

March, 1973

Dean, Graduate School

